

**Pharmacology of novel approaches designed to target picornaviral
infections**



Osamah Hasan

A thesis submitted for the degree of Doctor of Philosophy in molecular
medicine

Department of Biological Sciences

University of Essex

October 2019

Acknowledgement

Being grateful to Al-Mighty God (Allah) is my first concern for only He has been my first support in completing this thesis.

My gratitude should also be to the School of Life Sciences including Emma Revill and the University of Essex, for their support. Sincere warm thanks go also to Iraqi Cultural Attaché/ Embassy of the Republic of Iraq and the Ministry of Higher Education of Iraq, also University of Kirkuk and Kirkuk Health Department for their generosity and support.

Whatever I say, it will not be enough to express respect and sincere gratefulness to Professor Glyn Stanway and Dr. Sinan Battah for their kind supervision, judicious advice, rigorous efforts, unlimited support and valuable guidance during my study. I guess that something would be missing if Dr. Brandon Reeder's brilliant notice and feedback were not there in my work. As such, I hereby thank him for that and for offering me to use his HPLC. Special thanks go to Hannah Adams and Elizabeth Welbourn for always being around to help.

I would also like to express my thanks to lab colleagues Dr. Ali Khrid, Dr. Marina Ioannou, Dr. Ashjan Shami and Dr. Cheryl Eno-Ibanga for showing me the excitement and joy of lab work. I wish also to expand my deepest thanks to Dr. Muslim Mohsin for generously providing the cells I needed for the project.

Now, my chance for dedicating something comes. I really feel proud to dedicate my success to those who prayed for my success. I would proudly dedicate this thesis to my actual and spiritual parents, the most loving people in my life for their support, they encouraged and inspired me before and during my study, my wife for her love and patience, my brothers for their help, my sister for her wishes and my children who understand my business through the study.

Abstract

Many Picornaviridae family members infect humans. Enterovirus (EV), the largest genus, causes diseases ranging from the common cold to fatal heart disease and paralysis. Human parechoviruses (HPeV) are at least as prevalent as EVs. Currently, no antipicornavirus drugs are used clinically and the large number of viruses precludes vaccination. New drugs are therefore required. Picornavirus infection exploits viral and host proteins, lipids and cellular systems, all potentially targetable by inhibitors. In addition to compounds with a known target, natural products are potential sources of new drugs. Plant material such as berries are cheap, and some extracts have proven antiviral activity. The aim of this project was to repurpose known drugs, approved and used for several years for various medical indications, as well as identify new compounds from natural sources. Coxsackievirus A9 (CAV9) was used as a typical enterovirus and a plaque reduction assay was used to assess antiviral activity. Both approaches gave promising agents. Fluoxetine and dibucaine caused a complete CAV9 inhibition at low concentrations. All drug resistant mutants (DRM) against these compounds had a protein 2C I227V mutation, suggesting this protein is targeted, in accord with previous work on coxsackievirus B3. The identification of DRMs with a single mutation suggests that drug resistance could be problematical if dibucaine and fluoxetine are used clinically. A previously observed interaction between lipid droplets (LDs) and CAV9 and HPeV1 led to studies of LD targeting agents. DGAT inhibitors A922500 and betulonic acid were the most active compounds, in addition to promising results from aspirin and metformin. Redcurrant extract showed antiviral activity, in addition to antioxidant and photodynamic activity. Some microalgae extracts also showed antiviral effects. Although much work remains to be done to fully develop these novel approaches, they have great potential to combat the serious effect of picornavirus infections.

Contents

Table of Figures	ix
List of Tables	xii
Abbreviations.....	xiii
Appendices	xvi
Chapter 1: Introduction.....	17
1.1 Introduction to viruses	18
1.1.1 Importance of viruses	18
1.1.2 History of virus classification.....	18
1.1.3 The ICTV Nomenclature of virus taxa.....	20
1.2 Picornaviridae	21
1.2.1 <i>Picornaviridae</i> classification.....	21
1.2.2 Significance of picornaviruses.....	21
1.2.3 Examples of clinically important picornaviruses	22
1.2.3.1 Poliovirus.....	22
1.2.3.2 Coxsackievirus	22
1.2.3.3 Enterovirus 71	24
1.2.3.4 Enterovirus 70	25
1.2.3.5 Enterovirus 68	26
1.2.3.6 Rhinoviruses	26
1.2.3.7 Parechoviruses.....	27
1.2.3.8 Hepatitis A virus.....	28
1.2.3.9 Foot-and-Mouth Disease Virus	29
1.2.3.10 Aichi virus	30
1.2.3.11 Other picornaviruses.....	31
1.2.4 Picornavirus particle and replication	32
1.3 The importance of receptors in picornavirus infection	37
1.3.1 Receptors in infection and disease.....	37
1.3.2 The main receptor types of picornaviruses	38
1.3.3 The role of canyon in some viral infection.....	39
1.3.4 Virus movement and entry across the host cell membrane	39
1.3.5 Endocytosis, the principle pathway of entry.....	42
1.4 Virus replication within the host cell	43

1.5	Functions and interactions of untranslated regions.....	44
1.5.1	5'-untranslated region (5'-UTR).....	44
1.5.1.1	The cloverleaf structure.....	46
1.5.1.2	The internal ribosome entry site.....	46
1.5.2	The role of the 3'-untranslated region in virus replication.....	47
1.5.2.1	The importance of poly (A) tail in viral replication.....	47
1.5.3	Cis-acting replication element (cre).....	48
1.6	Protein roles during viral infection.....	48
1.6.1	Capsid proteins (Structural proteins).....	49
1.6.2	Non-structural proteins.....	49
1.6.2.1	2A protein.....	49
1.6.2.2	Leader protein.....	50
1.6.2.3	2BC and 2B proteins.....	50
1.6.2.4	2C protein.....	51
1.6.2.5	3AB and 3A.....	52
1.6.2.6	Viral genome-linked protein (VPg).....	53
1.6.2.7	3C ^{pro}	53
1.6.2.8	3D ^{pol}	54
1.7	Lipids as important host factors mediating infection.....	57
1.8	Lipid droplets.....	58
1.9	Antiviral agents with their therapeutic targets.....	61
1.10	G-protein-coupled receptors Inhibitors.....	65
1.11	Lipids, lipid droplets and lipoproteins targeting agents.....	66
1.12	Some aspects of using antiviral compounds.....	67
1.13	Naturally occurring antiviral agents.....	68
1.14	Berries.....	69
1.15	Microalgae.....	70
1.16	Oxidative stress and its relationship to viral replication.....	71
1.17	Photodynamic therapy and photodynamic antimicrobial chemotherapy.....	72
1.18	Aim and Objectives.....	75
Chapter 2:	Materials and Methods.....	76
2.1	Materials.....	77
2.2	Methods.....	77

2.2.1	Methods of cell culture	77
2.2.1.1	Splitting of cells.....	77
2.2.1.2	Cell line storage.....	77
2.2.2	Virology methods	77
2.2.2.1	Direct and indirect plaque assays and drug treatment.....	77
2.2.2.2	Selection of drug-resistant mutants	78
2.2.2.3	Direct effect of compound on the virus particle.....	79
2.2.2.4	Time of addition assay	79
2.2.2.5	Determination of compound-induced apoptosis by Nicoletti assay.....	79
2.2.2.6	Cell viability assays.....	80
2.2.2.7	Photodynamic inactivation effect of compounds and extracts.....	80
2.2.3	Molecular biology methods	81
2.2.3.1	Extraction of viral RNA using a QIAamp Viral RNA Mini Kit	81
2.2.3.2	Reverse transcription-PCR (RT-PCR)	81
2.2.3.3	Agarose gel electrophoresis.....	84
2.2.3.4	Gel extraction of DNA	84
2.2.3.5	Sequencing of DNA	84
2.2.3.6	Antioxidant activity assay	85
2.2.4	Methods of synthesis and structural modifications	86
2.2.4.1	Modification of hydroxyquinoline	86
2.2.4.2	Modification of fluoxetine.....	88
2.2.5	Redcurrant extracts	90
2.2.5.1	Extraction methods.....	90
2.2.5.2	Fractionation methods of redcurrant	90
2.2.5.3	Analytical analysis of the fractionated RC samples with HPLC.....	91
2.2.5.4	Analytical analysis of the fractionated RC samples with LC-MS/MS.....	91
Chapter 3: Antiviral Activity of Fluoxetine and Functionally Related Compounds.....		93
3.1	Introduction.....	94
3.2	Results.....	95
3.2.1	Inhibition of CAV9 infection by fluoxetine	95
3.2.2	The effects of imipramine and promethazine on CAV9.....	99
3.2.3	Inhibition of CAV9 infection by dibucaine	99
3.2.4	Drug sensitivity and analysis of the drug resistant mutants	106

3.2.4.1	Generation of CAV9 mutants resistant to fluoxetine	106
3.2.4.2	Cross resistance of fluoxetine with dibucaine	106
3.2.4.3	The sequence of the selected CAV9 mutants	106
3.2.5	Modification of fluoxetine and dibucaine to generate potential new drugs 111	
3.2.6	Antiviral activity of QHB and Flu-Buc	111
3.3	Discussion	115
3.3.1	Introduction.....	115
3.3.2	Fluoxetine as an antiviral drug	115
3.3.3	Antiviral activity of imipramine and promethazine.....	118
3.3.4	Dibucaine antiviral activity and restrictions of use	119
3.3.5	Drug resistant mutants (DRMs) against fluoxetine and dibucaine	122
3.3.6	Synthesis and antiviral activity of the modified drugs	125
Chapter 4: Drugs Affecting Lipid Metabolism and Lipid Droplets		128
4.1	Introduction.....	129
4.2	Results.....	129
4.2.1	Inhibition of CAV9 by A922500.....	129
4.2.2	Antiviral activity and toxicity of betulinic acid.....	135
4.2.3	Anti CAV9 activity of simvastatin	135
4.2.4	Antiviral activity of C75	140
4.2.5	Preliminary results of antiviral activity of aspirin and metformin	144
4.2.6	Drug Resistant Mutants of CAV9 against A922500	151
4.3	Discussion	155
4.3.1	Introduction.....	155
4.3.2	Antiviral activity of DGAT1 inhibitors; A922500 and betulinic acid.....	155
4.3.3	Drug resistant mutants of A922500.....	160
4.3.4	Antiviral activity of C75.....	160
4.3.5	Inactivity of the HMG-CoA reductase inhibitor, simvastatin	163
4.3.6	Cell specific type	164
4.3.7	Preliminary results on aspirin and metformin	164
4.3.7.1	Effects of aspirin on CAV9	164
4.3.7.2	Inhibitory effect of metformin on CAV9	166
Chapter 5: Natural Sources of Antiviral Drugs		169
5.1	Introduction.....	170

5.2	Results.....	171
5.2.1	Comparison of the effects of RC samples from different extraction methods on the CAV9 viral infection	171
5.2.2	Evaluation of the effects of RC crude extracts on CAV9 and HPeV1 viral infection	171
5.2.3	The concentration dependent inhibitory effect of the boiled RC extract on different strains of Coxsackie virus B3	172
5.2.4	Effect of RC extract on fluoxetine drug resistant mutants	172
5.2.5	Effect of the RC extract on the CAV9 virus particle.....	172
5.2.6	The effects of RC addition on replication during time-course of CAV9 pre-infection	172
5.2.7	Evaluation of the effects for the fractionated boiled RC on CAV9 viral infection/ plaque assay	181
5.2.8	Investigation of the effect of light on the activity of photosensitive constituents of RC extracts.....	184
5.2.9	The effect of different RC extracts on infection measured using MTT assays	184
5.2.10	Effect of light exposure and RC extracts on the viral infection and cell viability	185
5.2.11	The effect of microalgae extracts on CAV9 infectivity and cell viability in the absence and presence of light.	190
5.2.12	Quercetin antiviral activity in different cell lines	193
5.2.13	Evaluation of antioxidant activities of the crude RC extracts and related fractions in cell free media	197
5.2.14	LC-MS\MS analysis of RC fractions.....	202
5.2.15	Methods of LC-MS/MS analysis	202
5.2.16	Analysis of MS and MS/MS spectroscopy	209
5.3	Discussion	219
5.3.1	Redcurrant Extracts	219
5.3.1.1	Introduction	219
5.3.1.2	Antiviral activity of RC extracts	219
5.3.2	The effect of microalgae extracts on the viruses and cells viability.....	220
5.3.3	Photodynamic inactivation activity of RC and MA	222
5.3.4	Quercetin antiviral activity	223
5.3.5	Antioxidant activity of RC extracts and fractions	224
5.3.6	Analytical analysis of RC fractions	225

Chapter 6: General Discussion	229
6.1 Discussion and suggestions.....	230
6.2 Conclusion	237
References.....	239
Appendices	309

Table of Figures

Figure 1-1. The picornavirus capsid.	33
Figure 1-2. A and B, picornavirus genome and cleavage of polyprotein by viral proteases.	35
Figure 1-3. Replication cycle of EVs	36
Figure 1-4. The enterovirus pocket factor.	41
Figure 1-5. Picornavirus untranslated (non-coding) regions.	45
Figure 1-6. Diagram of the non-structural proteins of an enterovirus, showing some of the conserved features known to be important for function.	56
Figure 1-7. Photodynamic therapy states.	74
Figure 2-1 Schematic diagram of the PCR amplification component of the RT-PCR reaction.	83
Figure 3-1. Inhibition of CAV9 infection by fluoxetine.	96
Figure 3-2. Cytotoxic effect of different fluoxetine concentrations on A549 cells.	97
Figure 3-3. Flow cytometry analysis of the effect of fluoxetine on GMK cells and on CAV9 infection.	98
Figure 3-4. The effect of imipramine on CAV9 infection.	100
Figure 3-5. The effect of imipramine on CAV9 infection.	101
Figure 3-6. Cytotoxic effect of different imipramine concentrations on A549 cells.	102
Figure 3-7. The effect of promethazine on CAV9 infection.	103
Figure 3-8. Inhibition of CAV9 by dibucaine.	104
Figure 3-9. Cytotoxic effect of different dibucaine concentrations on A549 cells. ..	105
Figure 3-10. The effect of fluoxetine and dibucaine on two CAV9 fluoxetine-resistant mutants and the original CAV9 using a direct plaque assay.	108
Figure 3-11. Amino acid sequence alignment of 6 selected CAV9 fluoxetine-resistant mutants in comparison to the original virus by partial sequencing of the 2C protein.	109
Figure 3-12. The nucleotide sequence of the one selected CAV9 mutant (bottom, mutant 2) in comparison with the original virus (top) in the region of the I>V mutation.	110
Figure 3-13. Chemical structure of the original drug (fluoxetine) and fluoxetine conjugate fluoxetine-chlorambucil (Fl-Ch).	112
Figure 3-14. Chemical structure of the original drug (dibucaine) and a quinoline derivative with the same core structure but altered side chain (QHB).	112
Figure 3-15. Effects of increasing QHB concentrations on CAV9.	113
Figure 3-16. Effects of increasing Fl-Ch concentrations on CAV9.	114
Figure 3-17. Structural similarities between fluoxetine and some studied compounds.	121
Figure 3-18. ClustalW alignment of part of the amino acid sequences of the 2C proteins of CAV9 and CBV3, representing EVB, with a representative of species EVD (also susceptible to fluoxetine) and representatives of EVA and EVC (which are not susceptible to fluoxetine).	124

Figure 4-1. Role of DGATs in the biosynthesis of triacylglycerol in the glycerol phosphate pathway and inhibition of DGAT1 by A922500.	131
Figure 4-2. Antiviral activity of A922500 against CAV9 in GMK cells.	132
Figure 4-3. Antiviral activity of A922500 against CAV9 in A549 cells.	133
Figure 4-4. Cytotoxic effect of different A922500 concentrations on A549 cells.	134
Figure 4-5. Antiviral activity of betulinic acid against CAV9 by indirect plaque assay.	136
Figure 4-6. Cytotoxic effect of different betulinic acid concentrations on A549 cells.	137
Figure 4-7. Blocking of the mevalonate pathway in mammalian by statins.	138
Figure 4-8. Antiviral activity of simvastatin against CAV9 in GMK and A549 cells.	139
Figure 4-9. Role of fatty acid synthase in the early stage synthesis of triacylglycerol.	141
Figure 4-10. Antiviral activity of C75 against CAV9 in GMK.	142
Figure 4-11. Cytotoxic effect of different C75 concentrations on A549 cells.	143
Figure 4-12. Principle mechanism of NSAIDs action.	145
Figure 4-13. Antiviral activity of aspirin against CAV9 in A549 cells.	146
Figure 4-14. Cytotoxic effect of different aspirin concentrations on A549 cells.	147
Figure 4-15. Proposed mechanism of action of metformin on glucose production and lipid metabolism.	148
Figure 4-16. Antiviral activity of metformin against CAV9 in A549 cells.	149
Figure 4-17. Cytotoxic effect of different metformin concentrations on A549 cells.	150
Figure 4-18. Drug resistant mutants of CAV9 against A922500.	152
Figure 4-19. The effect of fluoxetine on the selected A922500 CAV9 mutants.	153
Figure 4-20 The effect of A922500 on the selected fluoxetine CAV9 mutants.	154
Figure 4-21. The role of DGAT enzymes in triacylglycerol and lipid droplet synthesis in the endoplasmic reticulum (ER).	159
Figure 4-22. Multi-step biosynthesis process of lipid droplets.	162
Figure 5-1. Inhibition of CAV9 infection by different crude RC extracts.	174
Figure 5-2. Inhibition of CAV9 infection by RC boiled extract.	175
Figure 5-3. Inhibition of HPeV1 infection by RC boiled extract.	176
Figure 5-4. Inhibition of 3 different CBV3 isolates by boiled RC extract.	177
Figure 5-5. The effect of RC on CAV9 fluoxetine-resistant mutants in GMK cells.	178
Figure 5-6. Analysis of the effect on infection of pre-treating CAV9 particles with boiled RC extract.	179
Figure 5-7. Comparison of the effects on infection of RC pre-treatment and addition of RC extract at different times after infection.	180
Figure 5-8. Effects of RC fractions on CAV9 infection.	182
Figure 5-9. Effects of higher or lower concentrations of RC fractions against CAV9.	183
Figure 5-10. Cytotoxic effect of different boiled RC concentrations on A549 cells.	186

Figure 5-11. The effect of RC extracts and sonicated fraction samples on GMK cells with/ without CAV9 in the dark.	187
Figure 5-12. The effect of RC extracts and sonicated fraction samples on GMK cells with/ without CAV9 after exposure to blue light (BL) for 20 minutes. RC crude extracts (conc. 4 mg/ml).	188
Figure 5-13. The effect of RC extracts and sonicated RC fraction samples on GMK cells with/ without CAV9 after exposure to red light (RL) for 20 minutes.	189
Figure 5-14. The effect of MA extracts on the viability of GMK cells and on CAV9 infectivity in the dark.	191
Figure 5-15. The effect of MA extracts on GMK cells with/ without CAV9 with exposure to A: Blue light (BL); B: Red light.	192
Figure 5-16. Effects of quercetin on CAV9 infection.	194
Figure 5-17. Comparison between CAV9 inhibition by quercetin in A549 and GMK cell lines.	195
Figure 5-18. Cytotoxic effect of different quercetin concentrations on A549 cells. ..	196
Figure 5-19. Antioxidant activity AO of boiled RC extract.	198
Figure 5-20. The myoglobin protective ratio (MPR) for AO activity of RC extract samples.	199
Figure 5-21. Kinetics and rate of reaction of antioxidant activity of boiled RC	200
Figure 5-22. Kinetics of AO activity for crude RC fractionated of boiled extract (RC-F1-F6) samples against time.	201
Figure 5-23. LC-MS elution of fraction F1.	204
Figure 5-24. LC-MS elution of Fraction F2.	205
Figure 5-25. LC-MS elution of Fraction F3.	206
Figure 5-26. The diode array UV spectra of RC F3 constituent recorded from the wavelength 200-800 nm.	208
Figure 5-27. Basic structures of anthocyanin and flavonoid.	211
Figure 5-28. Mass spectra of F1 fraction and the predicted structure of some predominant peaks.	211
Figure 5-29. Mass spectra of F2 fraction and the predicted structure of some predominant peaks.	212
Figure 5-30. Mass spectra of F2 fraction and the predicted structure of some predominant peaks.	213
Figure 5-31. MS/MS parent ions of m/z 287 spectra from F1 constituent at t_R of 13 min.	214
Figure 5-32. MS/MS Parent ions of m/z 827 spectra from F2 constituent at t_R of 22.2, 23.1, and 27.9 min.	215
Figure 5-33. MS/MS parent ions of m/z 303 spectra from F3 constituent at t_R of 9.3 min.	216
Figure 5-34. MS/MS parent ions of m/z 145 spectra from F3 constituent at t_R of 12.3 min.	217
Figure 5-35. Multiple reaction monitoring (MRM) parent and daughter ions of a) m/z 728 > 245; b) 728 > 455; c) 804 > 414; d) 827 > 610 spectra for F3 constituents.	218

List of Tables

Table 1. Selected Coxsackievirus members and related diseases.....	24
Table 2. Oligonucleotide primers used for the amplification and sequencing of part of the 2C protein-encoding region of CAV9.....	82

Abbreviations

Acronym/ Abbreviation	Term
AAA+ ATPase superfamily	ATPases Associated with cellular Activities
ACBD3	Acyl-coenzyme A binding domain containing 3 protein
AIDS	Acquired Immune Deficiency Syndrome
μl	Microliter
μM	Micro molar
$^1\text{O}_2$	Singlet Oxygen
3'-UTR	3'-untranslated region
5'-UTR	5'-untranslated region
A549	Lung Carcinoma cells
A922500	Selective DGAT1 inhibitor
AO	Antioxidant
ATGL	Adipose triglyceride lipase
BA	Betulinic acid
BL	Blue light
BOC	Tert-butyloxycarbonyl protecting group
CA	Catalase
CAV9	Coxsackievirus A9
CBV	Coxsackievirus B
CE	Collision energy
CL	Cloverleaf
CNS	Central Nervous System
COP-1	Coat protein complex
Cre	Cis-acting replication element
CVB	Coxsackievirus B
COX	Cyclooxygenase
DENV	Dengue Virus
DGAT1	Diacylglycerol acyltransferase 1
DRM	Drug resistant mutants
eIF4G	Eukaryotic Translation Initiation Factor 4 Gamma
eIFs	Eukaryotic initiation factors
EMCV	Encephalomyocarditis virus
ER	Endoplasmic Reticulum
ES+	Positive mode of electrospray
EV	Enterovirus
F1-F6	Fractions of boiled redcurrant
FA	Fatty acid
FASI	Fatty acid synthase inhibitor
FASN	Fatty Acid Synthase Enzyme
FMDV	Foot and mouth disease virus
GBF1	Golgi-specific brefeldin A-resistance guanine nucleotide exchange factor 1
GC	Gas chromatography
GHS	Glutathione
GMK	African Green Monkey Kidney Epithelial Cells
GPCR	G Protein-Coupled Receptor
GRP78	Glucose-Regulated Protein, 78-KD
HBB	2-(A-Hydroxybenzyl)-Benzimidazole

HCV	Hepatitis C virus
HIV	Human immunodeficiency virus
HMGCR	3-hydroxy-3-methylglutaryl (HMG) coenzyme A reductase
HPeV	Human Parechovirus
HPLC	High Performance Liquid Chromatography
HSL	Hormone-sensitive lipase
Hsp90	Heat Shock Protein 90
HT29	Human colorectal adenocarcinoma cells
I	Isoleucine
IC ₅₀	The half maximal inhibitory concentration
ICAM	Intercellular Adhesion Molecule
ICNV	The International Committee on Nomenclature of Virus
ICTV	International Committee on Taxonomy of Virus
IRES	Internal ribosome entry site
ITAFs	IRES-Specific Trans-Acting Factors
ITZ	Itraconazole
LDs	Lipid droplets
LFA-1	Leukocyte Function-Associated Antigen
La	Lupus antigen protein
m/z	Mass to charge ratio
MGL	Monoacylglycerol lipase
MHC	Major Histocompatibility Complex
MPR	Myoglobin protection ratio
MTT	3-[4,5-dimethylthiazole-2-yl]-2,5-diphenyltetrazolium bromide
Mu	Mutant
Nm	Nanometre
ORF	Open Reading Frame
OS	Oxidative Stress
OSBP	Oxysterol-Binding Protein
PABP	Poly(A) binding protein
PACT	Photodynamic Antimicrobial Chemotherapy
PCBP	Poly(C) binding proteins
PCR	Polymerase chain reaction
PDI	Photodynamic inactivation
PDT	Photodynamic Therapy
PFU	Plaques forming unit
PI4KB	Phosphatidylinositol 4-kinase beta
PI4KIIIb	Phosphatidylinositol-Phosphate-4-Kinase III Beta
PI4P	Phosphatidylinositol- 4 Phosphate
PK	Pseudoknots
PMOs	Phosphorodiamidate morpholino oligomers
PG	Prostaglandin
PGE2	Prostaglandin E ₂ (dinoprostone)
PQPS	Perylenequinonoid Pigments
PS	Photosensitizer
PTB	Polypyrimidine tract-binding protein
PV	Poliovirus
RC	Redcurrant

RC ₀	Replication complex
RC-Rt	Redcurrant extract at room temperature
RC-SS	Sonicated extract of redcurrant
RC-Bo1	Boiled extract of redcurrant
RC1-6	Fractions of sonicated redcurrant
RD	Rhabdomyosarcoma cells
RL	Red light
RNPs	Ribonucleoproteins
ROS	Reactive oxygen species
RT	Reverse transcriptase
Rt	Room temperature
SARS	Severe acute respiratory syndrome
SF3 helicases	Superfamily3 helicases
SL	Stem loop
SOD	Dismutase
SREBP	Sterol regulatory element-binding proteins
TAG	Triacylglycerol
TIC	Total ion currents
t _R	Retention time
UMP	Uridine monophosphate
UTR	Untranslated region
VP	Viral protein
VPg	Viral protein genome-linked
VPg-pUpU	Uridylylated state of Vpg

Appendices

Appendix 1 Materials used in this work and the sources	310
Appendix 2 Spectroscopies and masses of the fluoxetine-chlorambucil conjugate.	315

Chapter 1: Introduction

1.1 Introduction to viruses

1.1.1 Importance of viruses

Many virus families contain human pathogens and these cause mild diseases such as the common cold, cold sores and chickenpox (Vleck *et al.*, 2011), as well as fatal diseases like Ebola, severe acute respiratory syndrome (SARS), AIDS and pandemic influenza (Han *et al.*, 2003; Abdul-Quader & Collins, 2011; Mukherjee *et al.*, 2012; Narayanan *et al.*, 2014). It is calculated that 15% to 20% of all cancers may be related to viruses, including hepatitis B viruses, hepatitis C viruses (HCV) and papilloma viruses (McLaughlin-Drubin & Munger, 2008). Some chronic diseases have also been linked with viral infections (Tang & Holmes, 2017), and there is possible link with neurological diseases such as chronic fatigue syndrome, multiple sclerosis (Voumvourakis *et al.*, 2010) and psychiatric disease (Crow, 1978).

The increasing concentration of human populations into cities increases the opportunity for viruses to spread quickly and this has probably contributed to epidemics of emerging and re-emerging viruses. These can also be introduced rapidly to other countries due to increased travel. Human activity such as clearing of forests for farming may also displace animals, bats and insects and increase human exposure and this is the probable cause of some diseases such as Ebola and SARS. Therefore, there is steady increase in the number of known viruses around the world and an increase in outbreaks of infection. For example, between 2008 and 2012, enteroviruses (EVs) caused 7 million infections leading to 2457 deaths in China. Moreover, some viruses and RNA viruses in particular have high mutation rates due to errors during RNA replication which may result in more virulent viruses (Huang & Shih, 2015). For most virus infection there is no effective vaccine or drug. When drugs are available, resistance to these drugs occur early, especially if the drugs target specific virus proteins (de Chasse *et al.*, 2014).

1.1.2 History of virus classification

Virus taxonomy has been described as “a polarizing subject, based on the opinionated use of data” (Fauquet & Said, 2005). Evidence for the existence of viruses and their scientific study started to receive attention around the end of the 19th century (Van Der Want & Dijkstra, 2006; Arzt *et al.*, 2011). Virus classification has evolved with the continuous development of technologies used to study them. The background of virus classification is along the lines of the general classification of organisms, such as the Linnean and the

Adansonian systems. The Linnean system is a monothetic system proposed by Linnaeus, while the Adansonian classification is a polythetic system applied by Adanson (Wayne, 1967; Vasilyeva & Stephenson, 2008).

Virus classification was first attempted in 1927 (by Johnson, a plant virologist). Before 1940, virus classification depended on ecological and biological features, particularly the symptoms of infection, host and mode of transmission. For instance, all viruses that cause hepatitis (Hepatitis A, B, C, yellow fever and Rift Valley fever viruses) were classified as the hepatitis viruses, although these have been shown subsequently to belong to distinct virus families. In 1939, around 90 plant viruses were classified according to their host reaction and named by a binomial or trinomial system according to their host plants. Between 1940 and 1970, virus classification started to include virion properties depending on electron microscopy, centrifugation and biochemical studies that gave new information on virus shape, structure and size; biology (e.g. serology); and physicochemical properties (acid stability, sedimentation, density, the type of nucleic acid, the number and size of genome segments and proteins). Groups such as Herpes virus and Poxvirus were identified (Fauquet, 1994).

In 1966, the International Congress for Microbiology was held in Moscow and established the ICNV (the International Committee on Nomenclature of Virus) to generate a world-wide unique taxonomic and nomenclature system for all viruses. After 1970, virus genome structure (the sequence of the genome and the encoded proteins), as well as the replication cycle, started to be understood much more clearly. At this stage most virologists agreed to group all viruses at the family and genus levels, except plant virologists who still used groups for virus classification. Before 1990, the family level was the highest hierarchical classification. In 1977, ICNV was changed to ICTV (the International Committee on Taxonomy of Viruses) which is active today (Lefkowitz *et al.*, 2018). In 1991, a higher taxonomic level, the order, was introduced, starting with *Mononegavirales*. This order contained non-segmented ssRNA negative sense viruses, which comprised families *Filoviridae*, *Paramyxoviridae* and *Rhabdoviridae* (Afonso *et al.*, 2016). Despite its fundamental importance in virus classification, it was only in this year that the concept of virus species was uniformly applied (Van Regenmortel & Mahy, 2004). In 1993 the second order *Caudovirales* was added. Taxonomic levels higher than order, for instance, kingdom, class and subclass have not been used by ICTV yet. In 1993, the ICTV finally proposed a

united system for all virus types (animals, human and plants) then including 2 orders, 50 families, 9 subfamilies, 126 genera and 2644 virus species (Fauquet, 1994).

Classification of a virus within a genus or family is usually easier than assigning to a particular species. Usually a few morphology and chemical characteristics are enough to classify a virus into a family. For example, all members of the family *Picornaviridae* are non-enveloped with a small icosahedral particle and single-stranded positive-sense RNA of around 7000-9000 bases. However, these general features, cannot distinguish between viruses that potentially belong to different species or even genera as these will all share these basic properties. More discriminating properties are needed, which initially included genome sequence, physicochemical and antigenic properties, host range, tissue tropism, cytopathology, pathogenicity and mode of transmission (Van Regenmortel & Mahy, 2004; Buchen-Osmond, 2007).

The introduction of sequencing, and more recently metagenomics, have substantially increased the amount of virus information available for taxonomy. This includes genome expression, genome replication, genome organization, the presence or absence of characteristic motifs and evolutionary relationships. As well as better identifying species, using this information will expand taxonomy to a great extent and help to assign viruses to orders, and define higher rank taxa (Simmonds *et al.*, 2017).

1.1.3 The ICTV Nomenclature of virus taxa

According to ICTV taxonomic rules, the species and genus names end in *-virus*, the subfamily ends in *-virinae*, the family ends in *-viridae* and the order names end with *-virales*. The names of the specific virus order, family, subfamily, genus, and species should be printed in italics and the first letter is capitalized. The taxon name comes always before the taxonomic unit. Lower taxonomic levels such as serotypes, pathotypes and isolates have not been proposed by ICTV (Van Regenmortel & Mahy, 2004). As an example of up to down classification, coxsackievirus A9 (CAV9) belongs to *Picornavirales*, *Picornaviridae*, *Enterovirus*, *Enterovirus B*, CAV9 (type/serotype), and so on (isolate/strain).

Very recently, the introduction of new taxonomic ranks by the ICTV has considerably changed classification at the higher end. Realm is now the highest rank in the approved ICTV taxonomy, followed by subrealm, kingdom, subkingdom, phylum, subphylum, class, subclass, order, suborder, family, subfamily, genus, subgenus and species. Names of these

ranks end with the suffixes “-viria”, “-vira”, “-virae”, “-virites”, “-viricota”, “viricotina”, “-viricetes”, “-viricetidae”, “-virales”, “-virineae”, “-viridae”, “-virinae”, “-virus” and “-virus” (Gorbalenya *et al.*, 2017; Walker *et al.*, 2019). RNA viruses are assigned to the realm Riboviria, which is likely monophyletic and contains RNA viruses of both positive and negative strands, in addition to double stranded RNA viruses, as these all use a related RNA-directed RNA polymerase to replicate.

1.2 Picornaviridae

1.2.1 Picornaviridae classification

Picornaviridae family members infect humans and many animal hosts (e.g. foot and mouth disease virus [FMDV], which infects cows, sheep and pigs) and form one of the largest virus families with over 300 virus types, classified in 47 genera and 110 species, in addition to new 16 proposed genera and new 37 proposed species (Picornavirus Home Page, 2019).

1.2.2 Significance of picornaviruses

Although most picornavirus infections are asymptomatic, specific diseases are associated with particular groups of picornaviruses. Eight genera of the *Picornaviridae* family include pathogens infecting humans. They are *Enterovirus* (250 serotypes), *Parechovirus*, *Hepatovirus*, *Cardiovirus*, *Kobuvirus*, *Cosavirus*, *Salivirus*, *Rosavirus* (Zell *et al.*, 2018). *Enterovirus* (EV), the largest picornavirus genus, includes viruses that can cause a range of diseases such as mild respiratory and gastrointestinal infections and skin rashes (Chansaenroj *et al.*, 2017), or potentially fatal diseases involving the CNS (paralysis, encephalitis, meningitis) and heart (myocarditis) as well as pancreatitis and chronic inflammatory myopathy. Some cases of disease may be caused by persistent infections and these infections may also contribute to spread (Rhoades *et al.*, 2011). There is also great evidence of the relationship between coxsackievirus B (CBV) and diabetes (Alidjinou *et al.*, 2015). In addition, pre-existing clinical manifestation are sometimes aggravated by picornaviral infection. For instance, rhinovirus infection has been shown to exacerbate asthma and chronic obstructive pulmonary diseases (Hershenson, 2013). Though usually on the less severe side, the common cold, which is mainly caused by rhinovirus, leads to loss of working days and visits to doctors costing up to \$40 billion annually in the USA (van der Linden *et al.*, 2015).

1.2.3 Examples of clinically important picornaviruses

1.2.3.1 Poliovirus

Poliovirus (PV) is the best-known member of the enteroviruses and has been studied extensively. It is responsible for paralytic poliomyelitis. It is grouped into 3 distinct antigenic types, 1, 2, and 3, depending on neutralisation tests and this means that a second or third infection could occur caused by a different serotype (Mehndiratta *et al.*, 2014). Currently, there are 2 vaccine types against these 3 serotypes, the live attenuated oral poliovirus vaccine (OPV) and inactivated poliovirus vaccine (IPV) (Blake *et al.*, 2018). IPV use has replaced OPV use in many countries as part of the Global Poliovirus Eradication Initiative and because the live vaccine strains can revert to virulent forms.

The oldest evidence of PV dates back to 1580-1350 BCE and is a picture of an Egyptian man with a flaccid leg and holding a crutch (Nathanson & Kew, 2010). However, PV was only firstly isolated in 1909 and the sequence published in 1981 (Racaniello *et al.*, 1981; Baicus, 2012). The usual transmission mode of PV is the hand-to-hand-to-mouth route after excretion in feces and pharyngeal secretions. After ingesting the virus, it passes through the stomach and the principle replication site is the gastrointestinal tract. Viremia may result and, in this stage, the infection is often either asymptomatic or causing minor symptoms such as fever, headache and sore throat. However, in a low proportion of infections (less than 1%), the virus enters the CNS and replicates in motor neurons causing a clinically unique flaccid paralysis of legs and/or arms without a permanent sensory loss. More rarely, involuntary muscles responsible for breathing can be affected leading to respiratory arrest and death. Poliovirus is a strictly human pathogen and there is no known extra human reservoir to infect. (Melnick, 1996; Fine & Carneiro, 1999; Howard, 2005; Nathanson & Kew, 2010; Mehndiratta *et al.*, 2014). In 1988, the Global Polio Eradication Initiative was established by WHO in order to eradicate PV worldwide and this has decreased the global rate of the disease by more than 99% (from 350,000 cases per year to less than 2000 cases per year). However, there are 3 countries still endemic with PV type 1 and 3, Nigeria, Pakistan and Afghanistan (Thompson *et al.*, 2008, GPEI, 2020).

1.2.3.2 Coxsackievirus

Coxsackievirus (CV) is a relatively large and genetically diverse group within the *Enterovirus* genus. CVs affect different human age groups causing various clinical manifestation. The first CV was isolated in the New York State Department of Health in 1948-1949 (Afrose, 2017). In most cases the infection is symptomless, while sometimes it

gives a non-specific illness with fever and often upper respiratory tract symptoms, sore throat and occasionally a runny nose. Skin rash often appears at the end of the illness (Xiang *et al.*, 2012; Huang *et al.*, 2013; Afrose, 2017). During pregnancy, CV infection can cause early abortion, fetal myocarditis and delayed neurological development in new-born babies (Ornoy & Tenenbaum, 2006). Neonate and immunocompromised individuals are always at higher risk (Shin *et al.*, 2010; Weber *et al.*, 2016), and are prone to developing meningitis, encephalitis and myocarditis, as CNS and heart are main targets of infection. In adults, CV myocarditis is a leading cause of dilated cardiomyopathy which leads to 50% of heart transplants, in addition to demyelinating diseases including acute disseminated encephalomyelitis and acute transverse myelitis, delayed neuropathology including schizophrenia, encephalitis lethargica and amyotrophic lateral sclerosis (Kearney, 2001; Feuer *et al.*, 2009). CVs also replicate in bone marrow and affect hematopoietic progenitor cells (Althof & Whitton, 2013). The usual transmission routes include respiratory droplets, stool exposure, blister fluids, fomites and maternal secretion exposure during delivery.

Epidemiological studies in different areas throughout the world showed considerable prevalence of CV. For example, antibodies against certain CV strains were detected in 60-80% of French-Canadian population in Montreal. In China, one serotype of CV showed a prevalence as high as 50%, and in different areas of Greece, the seroprevalence of some CVs were between 6.7 and 21.6%. (Khelifa *et al.*, 1999; Sin *et al.*, 2015). Coxsackievirus is divided into 2 subgroups A (CAV) and B (CBV) depending historically on histopathology and clinical signs detected in new-born mice. There are 23 serotypes of subgroup A and 6 serotypes of subgroup B (Kuan, 1997; Harvala *et al.*, 2002). In terms of tropism which may reflect clinical findings, CAV infects mainly striated muscles (skeletal and heart muscles) and CBV replicates in addition to the striated muscles, in the CNS, pancreas, liver and brown fat. As a result, CAV can cause flaccid paralysis. Some CAV serotypes are also frequent causes of hand-foot-and-mouth disease (HFMD) and herpangina in different human age groups. CBV causes spastic paralysis and has been associated with autoimmune and chronic diseases including diabetes mellitus, chronic myocarditis and chronic inflammatory myopathy. Severe hepatitis often with a high mortality rate is commonly seen in neonates. However, it is much less common in adults (Talsma *et al.*, 1984; Hyypiä *et al.*, 1993; Hyypiä *et al.*, 1997; Harvala *et al.*, 2002). Diseases reportedly caused by some CV serotypes are listed in Table 1.1

Table 1. Selected Coxsackievirus members and related diseases.

CV group	Related disease(s)	References
CAV4	HFMD.	(Li <i>et al.</i> , 2015).
CAV5	HFMD.	(Andreoni & Colton, 2017).
CAV6	HFMD and onychomadesis.	(Zeng <i>et al.</i> , 2015; Puenpa <i>et al.</i> , 2016).
CAV9	HFMD and aseptic meningitis.	(Harvala <i>et al.</i> , 2002; Moreau <i>et al.</i> , 2011).
CAV10	HFMD and onychomadesis.	(Mirand <i>et al.</i> , 2012).
CAV16	HFMD and onychomadesis.	(Shin <i>et al.</i> , 2014; Gan & Zhang, 2017).
CAV21	Respiratory tract infection.	(Xiang <i>et al.</i> , 2012).
CAV24	Acute haemorrhagic conjunctivitis.	(Oh <i>et al.</i> , 2003; Medina <i>et al.</i> , 2016).
CBV1	HFMD and onychomadesis.	(Cabrerizo <i>et al.</i> , 2010).
CBV3	Chronic inflammation and immunology and diabetes mellitus.	(Drescher <i>et al.</i> , 2004; Feuer <i>et al.</i> , 2009).
CBV4	Meningoencephalitis and diabetes mellitus.	(Dotta <i>et al.</i> , 2007).
CBV5	Schizophrenia and onychomadesis.	(Suvisaari <i>et al.</i> , 2003; Andreoni & Colton, 2017).
CBV2	Myocarditis.	(Mehta <i>et al.</i> , 2018).

1.2.3.3 Enterovirus 71

Enterovirus 71 (EV71, or EVA71) is a serotype showing great genetic diversity and is classified into the human EVA species of the *Enterovirus* genus (Fernandez-Garcia *et al.*, 2018; Mandary & Poh, 2018). EV71 infection is a potentially life-threatening and communicable disease and is one of the most common causes of the worldwide hand-foot-and-mouth disease (HFMD) and herpangina. These are also caused by other viruses, such as CAV16, however EV71 is often associated with more severe symptoms and higher incidence of severe complications (Lee, 2016). EV71 infection exhibits a wide spectrum of symptoms. It could be asymptomatic or show symptoms ranging from skin eruption and flu-like symptoms to visceral manifestation. EV71 can also be a highly neurotropic virus

affecting most commonly the brainstem and sometimes causing with polio-like myelitis, aseptic meningitis and death (McMinn, 2002; Linsuwanon *et al.*, 2014; Chang *et al.*, 2018).

EV71 was firstly detected and then isolated from a child with encephalitis in California in USA in 1969 (Schmidt *et al.*, 1974). However, retrospective studies in the Netherland and evolutionary analysis indicated EV71 emergence as early as 1941 (Tee *et al.*, 2010). Although EV71 epidemics have been reported since 1970s in different regions including America, Europe and Australia, it is particularly prevalent in the Asia-Pacific region with a high incidence rate during summer months and mortality rate of 0.5% to 19% (Cardosa *et al.*, 2003; Linsuwanon *et al.*, 2014; Lin *et al.*, 2018a). EV71 has shown a rapid evolutionary change and has diverged into different genetic lineages with differences in pathogenicity and morbidity between countries (Chang *et al.*, 2016). Most EV71 infections occur in 5-year-old children or younger with more cases of viremia and sepsis reported in the under 2-year-olds and higher rates in boys than girls (Chang *et al.*, 2016, 2018; Lin *et al.*, 2018b).

Because of the significant mortality and morbidity rates, especially in younger children, there have been remarkable efforts to develop effective vaccines for EV71 and inactivated vaccines were approved in China in 2015 and give a protection rate of up to 90% against EV71-related HFMD and up to 80% against other diseases related to EV71 (Liang *et al.*, 2014; Chang *et al.*, 2018; Lin *et al.*, 2018a).

1.2.3.4 Enterovirus 70

Enterovirus 70 (EV70 or EVD70), a member of the EVD species, is a causative of acute haemorrhagic conjunctivitis (AHC) and was the first identified AHC virus. It has also been associated with neurologic poliomyelitis-like illness, although in a lower proportion of cases than poliovirus. It was identified in 1971 by two independent groups in Japan and India. Subsequently, EV70 was detected in different parts of India during 1975, 1981, 1986 and 1991 (Wadia *et al.*, 1983; Maitreyi *et al.*, 1999). In addition, during the early 1980s there was a large pandemic spread of EV70 in different parts of the world, including the USA (Mirkovic *et al.*, 1973; Takeda *et al.*, 1994). EV70 infection usually starts by direct entry into the eye, rather than an initial enteric infection leading to viremia and spreading to other organs (Langford *et al.*, 1986; Kim & Racaniello, 2007). Paralysis occurs in around 0.01% of symptomatic EV70 infections (Wright *et al.*, 1992), and it is usually transient but more permanent flaccid paralysis of the lower limbs and cranial nerve paralysis can occur.

However, the understanding of EV70 pathogenesis is sketchy as it has not been studied thoroughly and there is no suitable animal model (Kim & Racaniello, 2007).

1.2.3.5 Enterovirus 68

Enterovirus 68 (EV68 or EVD68) is another member of the EVD species within the *Enterovirus* genus. It shows some biological characteristics more usually associated with rhinoviruses, including acid sensitivity. Indeed, it was realised that EV68 and rhinovirus 87 are actually the same virus (Blomqvist *et al.*, 2002). EV68 (and EV69) infects both upper (the principle entry route) and lower respiratory tract via virus-containing respiratory secretions (Esposito *et al.*, 2015). Infection does not require prior enteric infection as EV68 is acid labile so cannot survive passing through the stomach (Oberste *et al.*, 2004). As well as respiratory infections, rare CNS neuro-complications have been reported and several recent reports have highlighted acute flaccid myelitis cases (Oermann *et al.*, 2015; Pfeiffer *et al.*, 2015; Lau *et al.*, 2016a). Although most cases of respiratory EV68 infections are asymptomatic or mild (similar to influenza-like illness), a few cases are severe enough to require intensive care (Oermann *et al.*, 2015).

The first report of EV68 was published in 1967, 5 years after virus recovery from 4 children with bronchitis and pneumonia in California. Subsequently, sporadic respiratory cases were reported in the Philippines, Japan, Netherlands and USA in 2008-2010. Thereafter, increasing outbreaks started to appear in other places such as the UK, France, Italy, China, Thailand, New Zealand and Africa and the majority of cases in all areas were from children (Esposito *et al.*, 2015; Oermann *et al.*, 2015; Lau *et al.*, 2016a). However, the largest and the most widespread outbreak of EV68 was reported in USA in 2014 with higher morbidity and mortality rates. It has been suggested that recombination has been the reason for the increase in prevalence and virulence of EV68 in recent years. For instance, 26 cases were detected in USA between 1970 and 2005 and up to 1000 cases since 2014 with 14 fatal cases (Khetsuriani *et al.*, 2006; Midgley *et al.*, 2014; Oermann *et al.*, 2015). Phylogenetic analysis of VP1, 2C and 3D showed 4 clades of EV68, A1, A2, B1 and B3 (Lau *et al.*, 2016a), while other authors describe 3 distinct genetic groups, clade A to C (Tokarz *et al.*, 2012).

1.2.3.6 Rhinoviruses

Rhinoviruses (RV) include about 160 serotypes divided into 3 species within the *Enterovirus* genus, RV-A, RV-B and RV-C (Lee *et al.*, 2012; Palmenberg & Gern, 2015;

Fawkner-Corbett *et al.*, 2016). RV infections occur throughout the world and these viruses have been extensively studied (Arakawa *et al.*, 2012; Lu *et al.*, 2014; L’Huillier *et al.*, 2015; Launes *et al.*, 2015; Tsatsral *et al.*, 2015; Wildenbeest *et al.*, 2016; Leotte *et al.*, 2017). In humans, RV infection is the most common cause of common colds and acute respiratory infections (responsible for one half to two thirds of cases), particularly in childhood, but also in adulthood, which are the most frequent cause of lost work days in the USA. RV infections are generally confined to the upper respiratory tract, but recent investigations have strongly implicated RV in complications such as bronchitis and pneumonia, as well as the making worse symptoms of chronic respiratory diseases like asthma, chronic obstructive pulmonary disease and cystic fibrosis (Kennedy *et al.*, 2012; Cox *et al.*, 2013; Cathcart *et al.*, 2015; Annamalay *et al.*, 2016; Klaiber, 2018). RV, particularly RV-C, are also frequently reported viruses in cases that have to be admitted to paediatric intensive care units, the rate being equal to or even exceeding that of respiratory syncytial virus (RSV). RV may also be more significant in allergic sensitizations and recurrent wheezing than RSV (Sun *et al.*, 2016a; Cox *et al.*, 2018). RV infection predisposes to secondary bacterial infection, including *Haemophilus influenzae* and *Streptococcus pneumoniae*, that sometimes lead to otitis media and sinusitis (Jacobs *et al.*, 2013). Unlike other EVs, RVs are acid and temperature labile (the optimum temperature growth is 33 °C and they are inactivated at pH 3.0) (Jacobs *et al.*, 2013; Tapparel *et al.*, 2013). Humans (and chimpanzees) are the only known reservoir for RV and nasal secretion is the usual way of viral spread (nose to hand to hand to nose) rather than respiratory droplets and aerosols (Blaas & Fuchs, 2016).

1.2.3.7 Parechoviruses

Human parechovirus (HPeV) belongs to the *Parechovirus A* species of the *Parechovirus* genus and contains 19 genotypes (Picornavirus Home Page, 2019). When the first two HPeVs were isolated in 1956 they were classified as echovirus 22 and 23 in the *Enterovirus* genus due to shared cell-culture features and infection symptoms with enteroviruses (Nix *et al.*, 2008; Faria *et al.*, 2009). Later analysis showed that HPeVs are genetically distinct from enteroviruses and other genera (Stanway *et al.*, 1994; Stanway and Hyypiä, 1999) and they are now classified in a separate genus, *Parechovirus* (Zell *et al.*, 2017).

The prevalence of HPeVs has been underestimated until recently and they seem to be at least as prevalent as EVs according to several recent data. HPeVs are estimated as the second most important cause of viral sepsis-like illness and meningitis in infants (van der

Linden *et al.*, 2015). In areas where HPeV infections have been studied most thoroughly (Europe, USA, Japan and Australia), genotypes HPeV1 to HPeV6 are isolated most frequently, with HPeV1 usually being the most common (de Crom *et al.*, 2016; Britton *et al.*, 2018a; Olijve *et al.*, 2018). In fact, based on the presence of antibodies against HPeV1 which indicate an infection at some point in life, a very high proportion of people in some countries have been infected with HPeV1 (Westerhuis *et al.*, 2013). Infections by HPeV1 commonly take place during the first years of life (Wildenbeest, 2014; de Crom *et al.*, 2016). It usually causes relatively mild symptoms, including fever, rash and otitis media (Benschop *et al.*, 2006; Tauriainen *et al.*, 2008).

HPeV1, and also HPeV4, have been associated with some more serious conditions such as sepsis-like illness, meningitis, paralysis and myocarditis (de Crom *et al.*, 2016; Kolehmainen *et al.*, 2014; Kolehmainen *et al.*, 2017). However, it is HPeV3 which is most frequently associated with serious disease, particularly in neonates and young infants (Harvala *et al.*, 2009; Britton *et al.*, 2018a; Olijve *et al.*, 2018; Aizawa *et al.*, 2017; Nelson *et al.*, 2017). HPeV3 is associated with severe sepsis-like disease and is the HPeV most likely to be recovered from the CNS in cases of meningitis and encephalitis, as well as being reported as the cause of serious myalgia. Most severe HPeV3 infections occur in children under 3 months old and can be fatal. It is also possible that some children who recover from an HPeV3 infection subsequently show developmental difficulties (Britton *et al.*, 2018b).

1.2.3.8 Hepatitis A virus

Hepatitis A virus (HAV) is classified in the *Hepatovirus A* species of the *Hepatovirus* genus and all isolates belong to a single serotype (Nainan *et al.*, 2014). Other viruses which infect the liver belong to different families, for instance, hepatitis B virus is a small DNA virus from the *Hepadnaviridae* family, and hepatitis C virus is an RNA virus from the genus *Hepacivirus* of *Flaviridae* (Liang, 2009; Bukh, 2016; Smith *et al.*, 2017). Human, chimpanzees and some small non-human primates are natural hosts for HAV, and liver is the primary replication site. The infection by itself causes little hepatocellular injury although it is usually accompanied by elevated ALT (Kwo *et al.*, 2017; Malakouti *et al.*, 2017).

HAV is transmitted by the fecal-oral route, mainly by ingestion of contaminated food or water. Transmission is facilitated by this route as HAV has stability towards freezing, moderate heating and low pH (Sattar *et al.*, 2000). Acute infection is accompanied initially by hepatic necro-inflammation which cures spontaneously in $\geq 99\%$ of cases. There are

many infrequent complications including rash, pancreatitis, myocarditis, arthritis, aplastic anaemia and fulminant hepatitis (0.015-0.5%). In addition, there are some reported prolonged symptoms such as fatigue, weight loss, fat intolerance, bilirubinaemia, cholestasis and emotional instability (Glikson *et al.*, 1992; Lemon *et al.*, 2018). In terms of severity of clinical outcomes, there is an increased incidence of infection and its complications with an increase of age. For example, only 10% of under “6 years of age” children with HAV develop jaundice compared to 70% of older children and adults. In addition, co-infection of HAV with other viruses like HBV, HCV, HEV, HIV, and dengue virus leads to increase rate of hepatic failure (Lemon *et al.*, 2018).

According to WHO estimates acute HAV hepatitis cases increased from 117 million to 126 million between 1990 and 2005, with an increase in HAV-related deaths from 30,283 to 35,245 (WHO, 2012). HAV is a preventable disease. Good personal hygiene is an effective way to protect against the disease. In addition, the availability of a vaccine has reduced infection rates. For example, in Israel after high levels of vaccination coverage (one dose 90%, two doses 85%) HAV incidence dropped from 33-70/100,000 between 1992-1998 to 2.5/100,000 cases in 2002 (Dagan *et al.*, 2005).

1.2.3.9 Foot-and-Mouth Disease Virus

Foot-and-mouth disease virus (FMDV), from the genus *Aphthovirus*, causes foot-and-mouth disease (FMD) in cloven-hoofed farm animals including cattle, sheep, goats, and pigs, as well as wild animals such as antelope, bison and deer. Infection gives vesicles spread around the mouth, feet and mammary glands, which is not fatal but causes loss of productivity and is therefore economically important (Verma *et al.*, 2012; Pal, 2018; Paton *et al.*, 2018). Chronic infection drops milk production by 80% and impairs growth and increases the mortality rate of young livestock (Knight-Jones & Rushton, 2013; Truong *et al.*, 2018). Losses are concentrated in dairies and intensive pig farms, which are the main protein sources particularly in poor countries (James & Rushton, 2002).

Beside a great loss in livestock and its products, FMD infection control is expensive, and is needed not only in endemic countries but also their neighbours and even FMD-free countries. These costs include outbreak control, culling, vaccination, import control, early detection, restrictions on the livestock sector and research. For instance, worldwide vaccinations against FMDV cost 1-7 billion dollars annually and up to 21 billion dollars in some years (Sutmoller *et al.*, 2003; Forman *et al.*, 2009). In the UK, the 2001 outbreak cost

respectively with £4-5 billion in lost tourism alone, while the 2001 outbreak in Uruguay cost \$700 million (Knight-Jones & Rushton, 2013).

There are 7 known serotypes of FMDV, O, A, C, Asia 1, SAT-1, SAT-2 and SAT-3 with different distribution patterns through the affected areas. For instance, there are 6 serotypes of FMDV (O, A, C, SAT-1, SAT-2, SAT-3) in Africa, 4 serotypes in Asia (O, A, C, Asia-1) and 3 in South America (O, A, C). In addition, a high mutation rate and quasi-species dynamic has led to several subtypes (OIE, 2009; Ludi *et al.*, 2013, 2014; Eldaghayes *et al.*, 2017; Paton *et al.*, 2018). FMD spreads mainly in Africa and Asia and there have been a periodic outbreak of types SAT-1 and SAT-2 from Africa in the Middle East (Rweyemamu *et al.*, 2008; Ludi *et al.*, 2013, 2014). Several outbreaks of FMD in some FMD-free countries including the UK in 2007 and Korea and Japan in 2010 have occurred (Verma *et al.*, 2012).

The virus transmits by respiratory aerosols, secretions (milk and semen), shedding from burst blisters, ingestion and abrasion. Virus-contaminated equipment and vehicles can also spread infections. Pigs transmit a high level of air-borne virus compared with cattle or sheep but are less sensitive to infection by this route. The virus can survive from days to months in the environment and in animal products including meat and can be spread by wind across long distances as occurred in 1981 when virus from a pig farm on the coast in North France infected animals on the Isle of Wight (Donaldson & Alexandersen, 2002; Cottam *et al.*, 2008; Paton *et al.*, 2018). FMDV is also transmissible to humans causing conjunctivitis, skin vesicles and mild influenza-like symptoms. Because symptoms in human are usually very mild and self-limiting, they are often unnoticed (Hyslop St., 1973).

1.2.3.10 Aichi virus

The *Kobuvirus* genus consists of 3 species *Aichi virus A* (AiV-A), *Aichi virus B* (AiV-B) and *Aichi virus C* (AiV-C). The prototype strain, Aichi virus (strain A846/8) was first detected in humans in the Aichi prefecture, Japan in 1989 (Reuter *et al.*, 2011; Cathcart *et al.*, 2015). *Aichi virus A* comprises of 4 types, Aichi virus 1 (AiV-1, which includes the prototype Aichi virus), canine kobuvirus 1, feline kobuvirus 1 and murine kobuvirus 1. Aichi virus 1 is distributed worldwide and causes a low incidence of gastroenteritis in humans. The usual infection route is fecal-oral transmission and good hygiene and avoiding raw food is important to prevent the disease (Kitajima & Gerba, 2015). The prevalence of Aichi virus seemed to rise with age. For instance, 30% of young adults are seropositive to

the virus and 80% are positive by middle age. Globally, AiV-1 infection has been responsible for several outbreaks of acute gastroenteritis in Asia (Japan, China, Vietnam, Thailand and Bangladesh) and its prevalence has been reported in European countries including Germany, France, Sweden, Finland and Hungary, as well as Brazil and Tunisia. Reports of other Aichi virus A members have also been published such as canine kobuvirus in domestic dogs and murine kobuvirus in wild rodents (Khamrin *et al.*, 2014; Kitajima & Gerba, 2015; Lu *et al.*, 2018).

AiV-B was firstly found in Japan and then isolated from stool sample of cattle in Brazil, Italy, Belgium, Korea (where the virus is particularly prevalent) and Thailand. The prevalence varied between 1 and 34.5% using RT-PCR. Samples from domestic sheep in Hungary and black goat in Korea were also seropositive to the AiV-B (Khamrin *et al.*, 2014b; Kitajima & Gerba, 2015).

AiV-C infection is common in pigs and the virus has been detected in countries throughout the world with reported prevalence rates of 3.9-100%. Infection can be bloodborne and can also occur through suckling and from contaminated food (Reuter *et al.*, 2011, 2013).

1.2.3.11 Other picornaviruses

Cosavirus (HCoSV) contains five species from *Cosavirus A* to *F*, excluding the candidate species “*Cosavirus C*”, which is not yet officially recognised. The first cosaviruses were found in Pakistan and Afghanistan in stool samples of healthy and non-polio acute flaccid paralysis (NPAFP) patients. Other cosaviruses were identified in several countries from samples of different origin, such as diarrhoea, stools of NPAFP patients, sewage, river water and pig stools (Khamrin & Maneekarn, 2014a; Okitsu *et al.*, 2016).

The *Cardiovirus* genus consists of 3 species, *Cardiovirus A* (formerly called *Encephalomyocarditis virus*), *Cardiovirus B* (formerly called *Theilovirus*) and *Cardiovirus C* (ICTV, 2019; Drexler *et al.*, 2008). *Cardiovirus B* contains Saffold virus (SAFV), a virus which has recently been found to be highly prevalent in the human population, as well as Vilyuisk human encephalomyelitis virus. The role of SAFV in human disease is not yet understood, but it is found in respiratory and gastrointestinal samples (Zoll *et al.*, 2009; Drexler *et al.*, 2011; Himeda & Ohara, 2012; Tan *et al.*, 2017). SAFV has been identified in stool samples from children having gastroenteritis in in the USA, Brazil, Germany, Denmark, Thailand, China, South Asian and Malaysia, and in the respiratory specimens from children with influenza-like disease in China, Japan and Canada. More recently,

SAFV has been detected in the blood, the CSF, and myocardium of a child who experienced a sudden death (Zhang *et al.*, 2015).

Viruses of the genus *Salivirus* with a single species, *Salivirus A*, were originally identified in 2009 in the stool of children with gastroenteritis in the USA and Australia and called klasseviruses, and in children with NPAFP in Nigeria (called salivirus). Later, several molecular and seroepidemiology studies associated salivirus with acute gastroenteritis and paediatric diarrhoea and it has been subsequently reported worldwide (Yu *et al.*, 2015; Itta *et al.*, 2016).

1.2.4 Picornavirus particle and replication

The picornavirus particle consists of a protein capsid containing the genome, which is a single strand of positive-stranded RNA varying in length between 6700–8800 nucleotides between members of different genera (Zell *et al.*, 2017). Picornavirus capsids contain 60 copies of each capsid protein (Figure 1.1). In EVs, as in the majority of picornaviruses, there are 4 capsid proteins VP1, VP2, VP3 and VP4. VP4 and VP2 are released from a precursor VP0 and some picornaviruses, such as parechoviruses, have only 3 capsid proteins, VP0, VP1 and VP3, because VP0 is not cleaved. VP2 (or VP0), VP3 and VP1 are similar in size and are structurally related as they share a common 8-stranded β -barrel fold. These pack together into a triangular protomer and 5 protomers assemble into a pentamer with VP1 closest to the 5-fold axis and VP2 (or VP0) and VP3 alternating further away from the 5-fold axis and arranged around the 3-fold axis. The capsid is made of 12 pentamers.

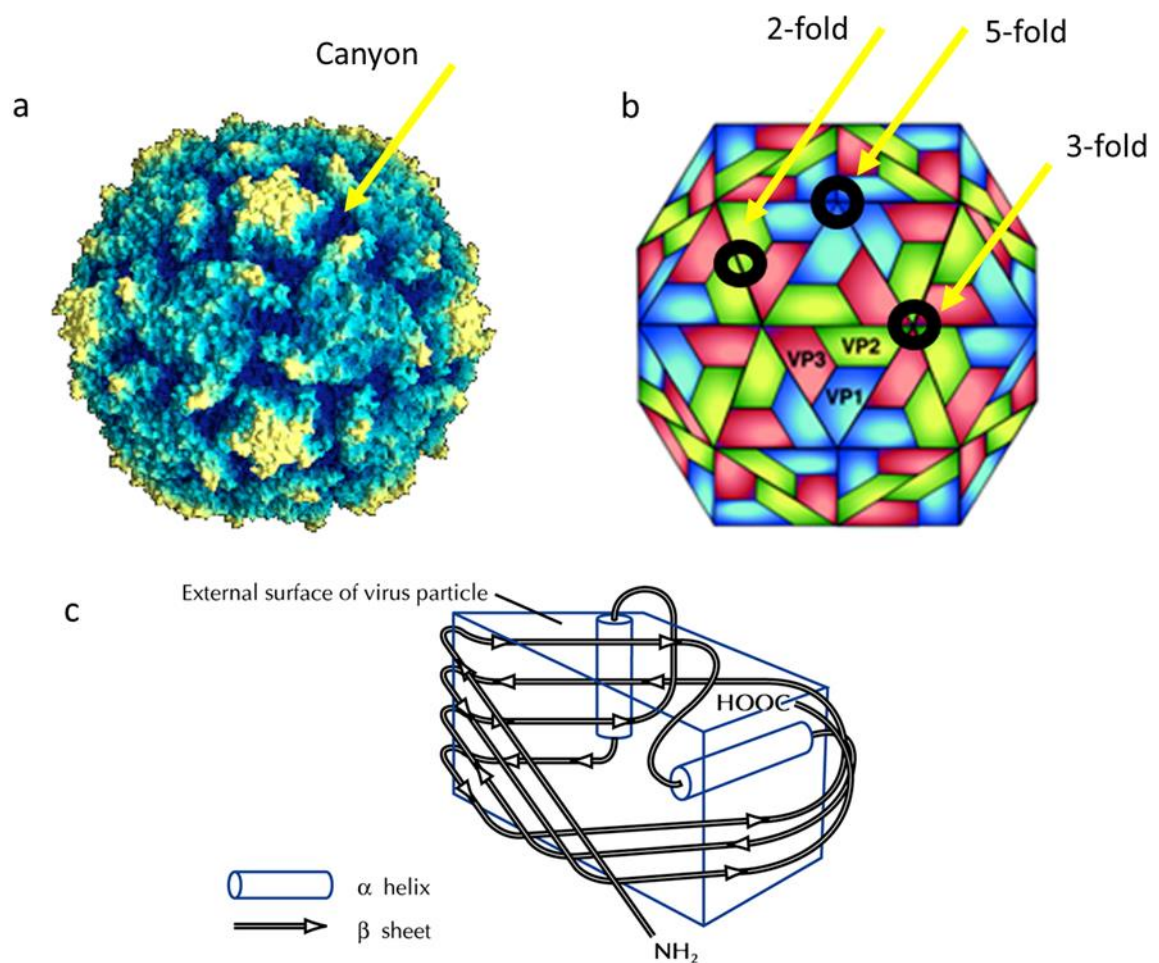


Figure 1-1. The picornavirus capsid.

a. The X-ray crystal structure of a typical EV, poliovirus. The image is colour-coded to show the highest parts of the structure in yellow and the deepest in dark blue. The deep region surrounding the 5-fold axis is the canyon which is used for receptor attachment in many picornaviruses. b. Schematic of the icosahedral arrangement of the 60 copies of the capsid proteins VP1, VP2 and VP3. VP4 is an internal protein so not visible. The axes of symmetry of the icosahedron (5-fold, 3-fold and 2-fold) are also shown. c. The 8-stranded beta barrel structure seen in VP1, VP2 and VP3. Images from Zell *et al.*, 2017 and Cann, 2001.

The genome encodes one open reading frame (ORF) and this is preceded by a long 5`- untranslated region (5`UTR) and followed by a 3`UTR and a poly-(A) tail. The 5`UTR contains an internal ribosome entry site (IRES) required for translation of the RNA. A small viral protein, VPg, is covalently linked to the 5`end of the viral genome (Norder *et al.*, 2011; Kempf *et al.*, 2013). (Figure 1.2). A single polyprotein is encoded, and this is processed by virus proteases to give precursors and the final proteins, 1A-1D, 2A-2C and 3A-3D.

Picornaviruses differ between genera in the details of virus replication and *Enterovirus* (EV) replication will be described as these are the best studied picornaviruses (Figure 1-3). EV infection starts with binding to a specific receptor on the cell surface. Sometimes more than one receptor is needed and there may be an initial binding to a less specific molecule such as heparan sulfate (Figure 1.3). The virus then enters the cell by endocytosis. Several mechanisms have been seen e.g. clathrin-mediated endocytosis. This triggers uncoating of the virus RNA and its release into the cytoplasm. VPg is separated away from the viral RNA, which is then translated to give a polyprotein. Proteins released from the polyprotein include structural (capsid) proteins that will form the new virus particles, as well as those involved in RNA replication and altering the host cell, for instance by shutting-off of cellular cap-dependent translation and stimulation of viral IRES-mediated translation. Replication of the genomic RNA occurs inside the cytoplasm, within newly-made double-membrane vesicles derived mainly from the ER, and the new RNAs are either used for translation or packaged into preassembled procapsids. The assembled particles undergo a final maturation steps and are released by cell lysis.

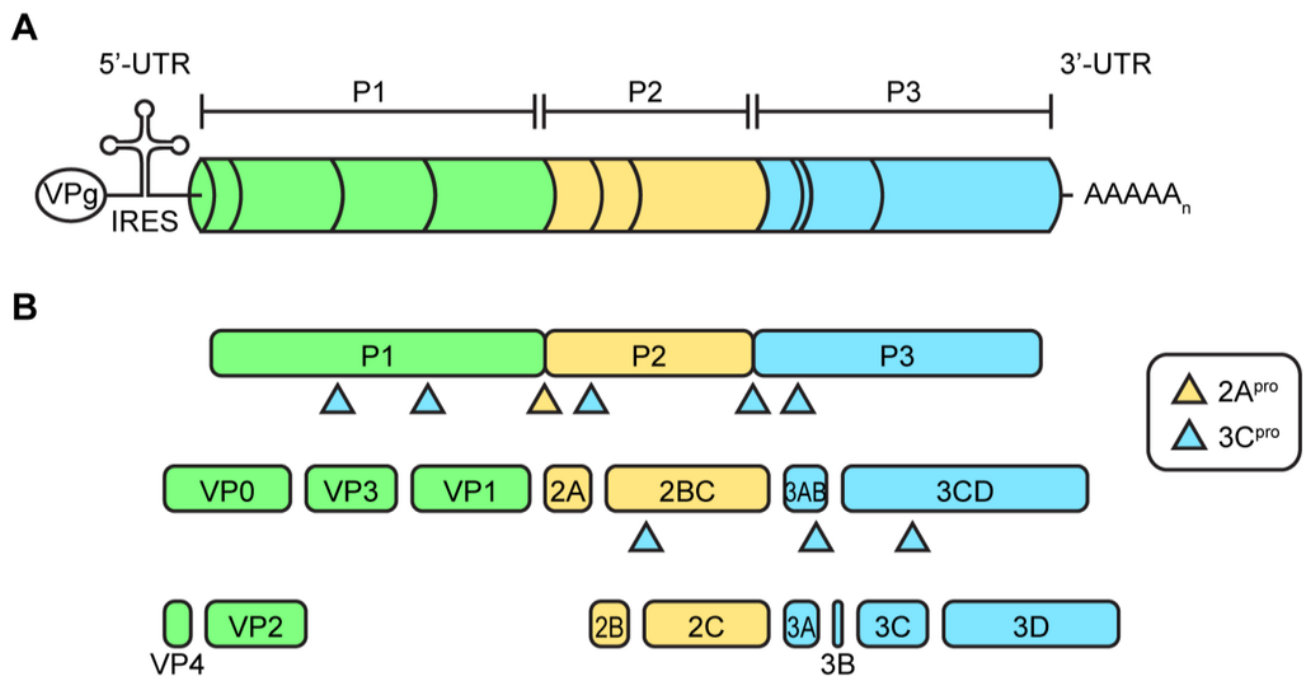


Figure 1-2. A and B, picornavirus genome and cleavage of polyprotein by viral proteases.

(A) The 5'UTR contains the IRES (internal ribosome entry site) which is needed for translation. The genome encodes a single polyprotein (cylinder) which is cleaved into the precursors P1 (green), P2 (yellow) and P3 (blue) and then into the final proteins (boundaries marked on the cylinder). (B) Viral proteases namely 2A^{pro} and 3C^{pro} (and its precursors) cleave the single polyprotein into some stable precursors (e.g. 2BC and 3CD) and the final viral proteins. VP0 cleavage to VP4 and VP2 occurs by an apparently autocatalytic process. (Image from van der Linden *et al.*, 2015).

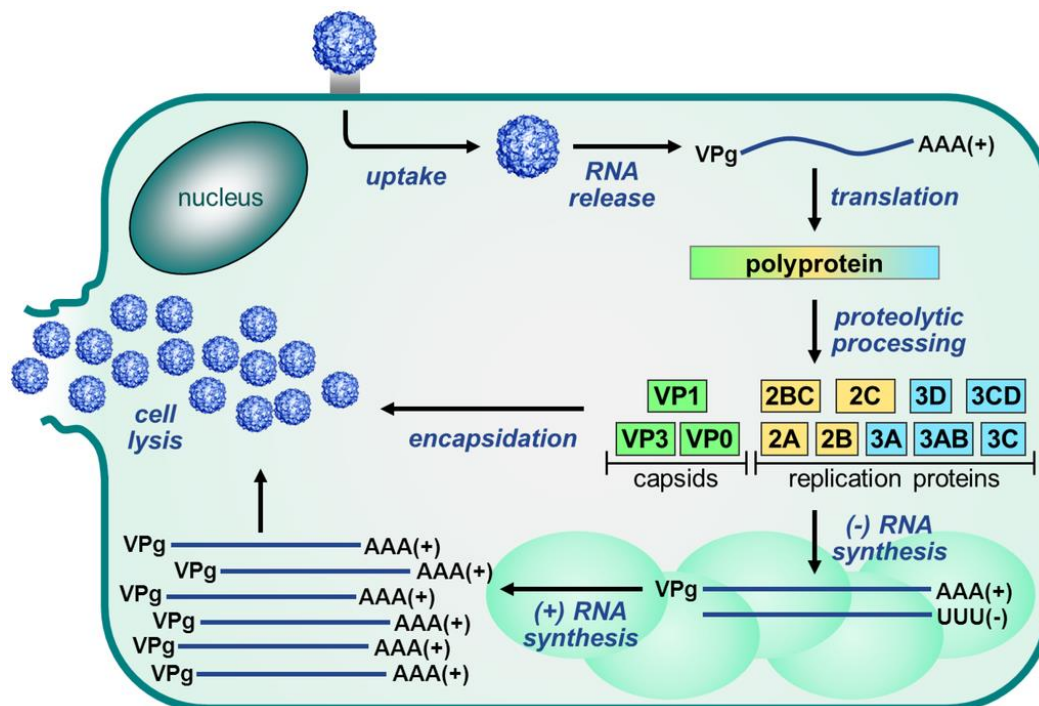


Figure 1-3. Replication cycle of EVs

First, the bind to a receptor and is internalized into the cell, The virus is usually taken into the cell in a vesicle (not shown). Then the viral RNA is released from the virion and translated into a single polyprotein. After that, viral proteases split this polyprotein into capsid proteins non-structural proteins, which copy the genome RNA in a two-stage process, where negative sense molecules are produced and then copied to give further positive sense ones. Almost all these events occur in the replication complex that is created by virus induced membrane rearrangement. The new positive-stranded RNA molecules are then either translated, used for further RNA replication or packaged to form infectious viruses which become released by cell lysis. (Image from van der Linden *et al.*, 2015).

1.3 The importance of receptors in picornavirus infection

1.3.1 Receptors in infection and disease

Cells employ multiple barriers against virus infection. Some of these are physical such as the plasma membrane, which protects individual cells, or epithelia which protect the whole body or specific tissues. Others are restriction factors, usually triggered by interferon (Drummond *et al.*, 2017; Ingle *et al.*, 2018). Viruses use general common tactics to overcome these barriers. In the case of the plasma membrane, the virus interacts with a cell surface molecule, its receptor to allow entry into the cell. Sometimes multiple receptors, which are usually proteins, carbohydrates or glycolipids are involved (Domingo *et al.*, 2012; Kato & Ishiwa, 2015). Cellular receptors are exploited as these can allow the virus to be efficiently delivered to specific locations in the cell by endocytosis, as well as possibly activating distinct signalling pathways that facilitate entry, induce conformational changes or enhance infection (Grove & Marsh, 2011). The presence or absence of specific receptors on a given cell type contributes to virus cell tropism, as only cells with the appropriate receptor can be infected. Variations in the sequence and structure of a receptor between different organisms may also limit host range or determine the nature of disease caused (Domingo *et al.*, 2012). For instance, normally mice are not infected by poliovirus. However, they become liable to poliovirus infection when they are manipulated to express the human poliovirus receptor (PVR) and show similar neurological diseases to those seen in humans (Ren & Racaniello, 1992; Khan *et al.*, 2014). However, viral productivity and cell permissiveness is not defined only by receptor recognition but also by other host components. For example, substitution of amino acids in non-structural viral proteins which interact with intracellular factors can also modify cell tropism or host range (Harris & Racaniello, 2005; Pan *et al.*, 2011). In addition, tissue susceptibility and tropism are not always determined by involvement of receptors and in many cases the tissue distribution of a receptor is wider than the tropism would suggest. For example, PVR is distributed in many tissues including neurons, small intestine, heart, liver, spleen, pancreas, kidney and lung. However, heart, liver, kidney and lung have not been identified as efficient sites for PV replication (Crotty *et al.*, 2002; Racaniello, 2006; Nomoto, 2007).

1.3.2 The main receptor types of picornaviruses

Like other viruses, different picornavirus species, or even serotypes within a species, recognise distinctly different receptors. Many of these are proteins and have an intracellular domain, a transmembrane domain that anchors the protein into the cell membrane, and a usually larger extracellular domain, part of which is recognised by the virus to allow attachment followed by internalisation.

The coxsackie and adenovirus receptor (CAR) is a receptor coxsackie B viruses (CBV). This molecule is part of a tight junction complex between cells involved in an early embryonic cardiac development and is expressed on human islets, which may explain the possible link between these viruses and heart disease and type 1 diabetes (Dorner, 2005; Hodik *et al.*, 2016). Intercellular adhesion molecule 1 (ICAM1), involved in cell adhesion and the immune response, is a receptor for the major group human rhinovirus (HRVs) (Winther *et al.*, 2002; Shukla *et al.*, 2017), as well as some CBV and CAV types. Both these molecules, as well as PVR (CD155, nectin-like molecule-5) belong to the Ig-like superfamily of receptors which have an extracellular domain made of varying numbers of 70–110 amino acid Ig-like domains (Schneider-Schaulies, 2000; Tu *et al.*, 2009).

Decay accelerating factor (DAF or CD55) functions to decrease cell lysis caused by the complement system and it is a receptor for several echoviruses, some CBVs and EV71 (Bergelson *et al.*, 1994). In at least some of these viruses DAF is only a primary receptor and internalisation/uncoating requires a second, often Ig-like, receptor.

Integrins are dimeric molecules made up of one α and one β chain. There are several different α and β chains and these combine to give 24 different integrins (Campbell & Humphries, 2011). Several of these recognise the Arg-Gly-Asp (RGD) tripeptide and a few picornaviruses, including FMDV, some parechoviruses, CAV9 and echovirus 9 contain this motif in the capsid protein VP1 and bind to an RGD-recognising integrin (e.g. $\alpha v \beta 6$, $\alpha v \beta 3$, $\alpha v \beta 1$, $\alpha v \beta 8$) during entry (Shakeel *et al.*, 2013; Merilahti *et al.*, 2016; Kotecha *et al.*, 2017). Echovirus 1 binds to integrin $\alpha 1 \beta 2$ in a non-RGD-dependent manner (Smyth & Martin, 2002; Xing *et al.*, 2004) Like DAF, at least for some picornaviruses, binding to integrins is not sufficient for infectious entry and other cell molecules are required. In addition, compared with HPeV1, which is absolutely integrin dependent, CAV9 can infect cells even after RGD deletion (Boonyakiat *et al.*, 2001).

Low density lipoprotein receptor (LDLR), LDLR-related protein, and very LDL receptor (VLDLR) have been recognized as receptors for minor group HRV. LDLR binds at the

virus 5-fold axis and does not induce structural alteration to the virus, but as HRVs are acid-labile their particles are destabilised in the acidic environment of endosomes leading to uncoating (Reithmayer *et al.*, 2002; Blaas, 2016). The scavenger receptor B2 (SCARB2) and P-selectin glycoprotein ligand-1 (PSGL-1) have been identified as receptors for EV71 and other members of the species EVA (Yamayoshi *et al.*, 2014). Heparan sulphate is found to support FMDV and echovirus adherence to cellular membranes (Schneider-Schaulies, 2000).

1.3.3 The role of canyon in some viral infection

In the major HRV receptor group (but not minor group), coxsackie A and B viruses and poliovirus (PV) the receptor binding sites are amino acids within a deep and narrow depression which runs around 5-fold axis to form a moat-like canyon (Newcombe *et al.*, 2003; Shingler *et al.*, 2015). The amino acids making up the binding site are highly conserved within the groups and cannot be contacted by neutralizing antibodies as these are too large to penetrate the canyon (Shingler *et al.*, 2015; Dong *et al.*, 2017).

In the viruses containing a canyon, receptors also function in the triggering of the conformational changes required for subsequent virus entry/uncoating (Rossmann *et al.*, 2002). In non-canyon viruses like FMDV, or viruses where the canyon is not the site of binding like minor receptor group HRVs, other triggering factors like endosomal acidification are crucial for virus entry (Smyth & Martin, 2002). In CAV9, which is acid stable, it is expected that interaction with a canyon-binding molecule is needed to destabilise the particle after RGD/integrin interaction, which does not take place in the canyon. GRP78 and/or MHC1 have been found to be involved in CAV9 entry/uncoating and could function in this way (Triantafilou *et al.*, 2002).

1.3.4 Virus movement and entry across the host cell membrane

The first interaction between a virus and a molecule/molecules on the cell surface can often be non-specific and just allow an initial, often weak, attachment. This is often mediated by charged proteins such as heparan sulphate, gangliosides and sialic acid (Mothes *et al.*, 2010; Boulant *et al.*, 2015).

Following attachment, and depending on the mobility of the receptor, some viruses remain where they are attached before endocytosis in a passive or signal induced manner, while others migrate around the surface until recognised by a specific receptor that mediates virus

uptake (Yamauchi & Helenius, 2013). Some viruses apparently use one type of receptor molecule, such as CD155 for PV and LDLR for minor receptor group HRVs. Some others can infect cells, sometimes different types of cells, using one of two or more efficient receptors such as PSGL-1 or SCARB2 for EV71. Others, such as CAV9 probably use two or more molecules with different roles. Different viruses use distinct strategies as some receptors allow multivalent binding which increases avidity, leads to irreversible binding, stimulates signalling and mediates membrane curvature to facilitate endocytosis. On the other hand, multivalent attachment can reduce mobility and interactions with further molecules needed for entry as well as engaging a preformed endocytic structure (Smith & Helenius, 2004; Burckhardt & Greber, 2009; Yamauchi & Helenius, 2013).

Enteroviruses have a lipid “pocket factor” contained within a hydrophobic pocket, made up of amino acids in VP1 and located under the canyon (Smyth & Martin, 2002). The pocket factor stabilises the capsid and its removal by receptor attachment is essential for uncoating (Figure 1.4). Binding of cellular receptor(s) also destabilizes the N-terminus region of VP1 and VP4 and causes them to be externalised from inside the capsid, so that the myristoyl group at the N-terminus of VP4 can help the hydrophobic N terminus of VP1 to attach to the cell membrane. Six to 10 copies of myristoylated protein, together with the associated VP1 make a channel with 5 amphipathic helices. An irreversible expansion of the particle then causes the RNA genome to exit through the hole made near the 2-fold axis (Wade *et al.*, 2013).

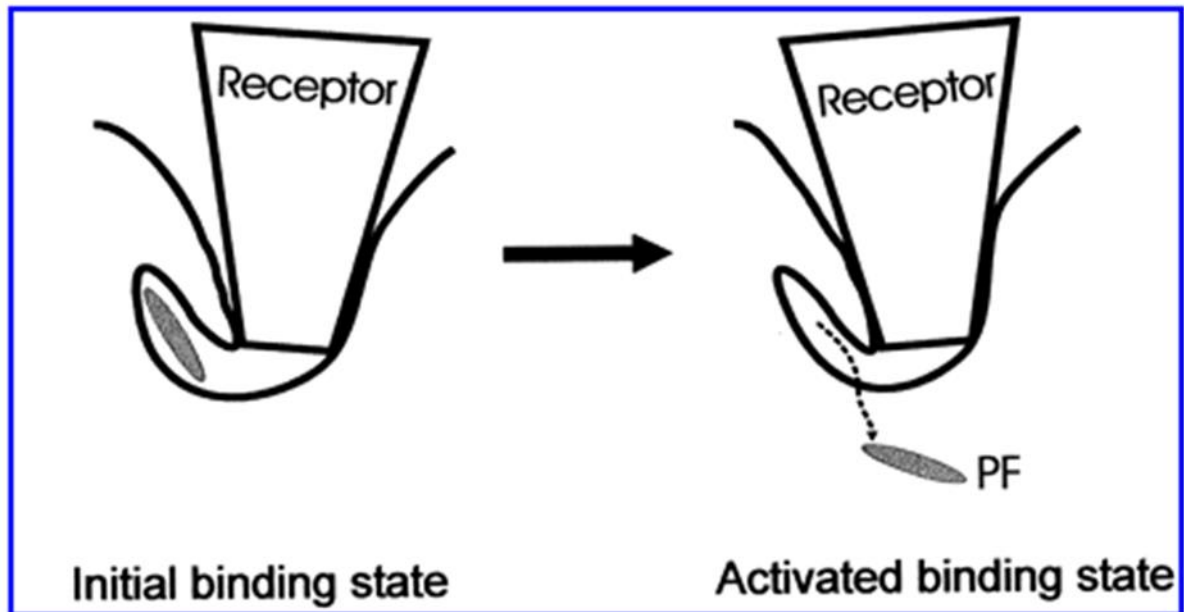


Figure 1-4. The enterovirus pocket factor.

The pocket factor (PF) is a small lipid-like molecule that fits into a hydrophobic pocket underneath the canyon. The initial binding of the receptor into the canyon leads to the loss of the PF, and the space now vacant allows a deeper interaction of the receptor with the canyon (activated binding state) which is needed for uncoating. Drugs such as pleconaril can replace the PF and bind irreversibly into the pocket. Receptor binding does not remove the drug and so uncoating cannot take place and infection of the cell is prevented.

1.3.5 Endocytosis, the principle pathway of entry

Most picornaviruses use a specific cellular endocytic vesicle, which either already exists or is made after virus-induced signalling, to pass through the cell membrane and be internalized into an endosome, before releasing their genetic material into the cytoplasm. Viruses which depend on low pH for uncoating are absolutely endosome-dependent, while those which uncoat at neutral pH may release their RNA directly through the plasma membrane or use an endocytic mechanism (Jha *et al.*, 2011). Using an endocytosis pathway enables the virus to penetrate the cell membrane, avoid the immune system and move through the cytoplasm to the desired location (Marsh & Helenius, 2006). Vesicles include several dynamic types such as recycling, early and late endosomes and lysosomes. Some of these endosomes can return the virus to the cell surface and so cell infection would not occur, while others expose it to harsh environment of very low pH, proteases or nucleases. To avoid that, many viruses uncoat and penetrate the endosome membrane at the mild acidic pH (around pH6) found in the early endosome. Others can time their penetration precisely with the changing environment inside the endosome (Grove & Marsh, 2011; Huotari & Helenius, 2011).

Several endocytosis pathways are used by viruses. The best identified one is clathrin-mediated endocytosis. A ligand (or virus particle) binds to the receptor which is located in a pit with a clathrin coat. The curvature of the pit changes to form a sphere surrounding the receptor and this sphere is sealed and detached from the cell membrane by dynamin. The clathrin-coated vesicle is then uncoated and fuses with an endosome (Vidricaire & Tremblay, 2007; Kim *et al.*, 2017). Caveolae are another type of coated pits found on the cell surface. They occur in regions of the cell surface, called lipid rafts, which are enriched for specific lipids and caveolae are coated with caveolin proteins. Receptors and ligands are internalised in caveolae in a similar dynamin-dependent process to clathrin-mediated endocytosis and the caveolae fuse with endosomes. There are also several clathrin/caveolin-independent mechanisms, such as micropinocytosis and routes dependent on flotillin and Arf6 but these all tend to also lead to fusion with endosomes (Mercer *et al.*, 2010). In general, the route of virus entry is usually determined by the receptor type. For example, integrin αv -dependent picornaviruses usually use clathrin-mediated endocytosis, while integrin $\alpha 2\beta 1$ -dependent EV uses caveolin-mediated endocytosis. Nevertheless, in a few cases viruses which bind to similar receptors may have different entry routes (Merilahti *et al.*, 2012).

1.4 Virus replication within the host cell

Synthesis of viral protein from the released RNA is the next step in replication. Approximately, 2 hours after infection, the virus genome is uncoated and translated (van Kuppeveld *et al.*, 1995). This uses a cap-independent IRES element in the 5'UTR of the genome to recruit both standard initiation factors and IRES-specific trans-acting factors (ITAFs), to allow ribosome binding and translation initiation (Pilipenko *et al.*, 2000; Tan *et al.*, 2014). The viral genome is translated to give viral proteins, initially synthesized as a large polypeptide that is cleaved into individual structural, and non-structural proteins. In enteroviruses cleavage is done by the virus-encoded proteases 2A^{pro} and 3C^{pro} (Garmaroudi *et al.*, 2015). The proteins include the virus polymerase 3D^{pol} which adds U residues to VPg to give the uridylylated state of VPg (VPg-pUpU), which is the primer for the synthesis of new RNA. 3D^{pol} uses the positive sense viral RNA as a template to synthesize the negative strand, which then acts as the template to synthesize new positive strands (Yang *et al.*, 2002; Sun *et al.*, 2012; Kempf & Barton, 2016). RNA synthesis occurs on intracellular, tubule-vesicular membranes, the replication complex (RCo), which are only present in virus-infected cells and which originate from different organelles such as the endoplasmic reticulum or Golgi (Strating *et al.*, 2015). These modified membranes provide the platform needed to assemble host and virus components needed for RNA replication. RCo also hide viral RNA and proteins from the innate immune system, so host defence mechanisms can be avoided (Martín-Acebes *et al.*, 2013). In addition, as RCo formation diverts components of the cellular protein secretion system, such as endoplasmic reticulum, it plays an important role in viral pathology and also prevents MHC-mediated presentation of virus peptides which again limits the host response to infection (Tan *et al.*, 2014; Murat & Tellam, 2015). The newly-synthesized positive-strand RNA genomes and structural proteins are assembled to make the complete virus particle. The uncleaved precursor of VP4 and VP2, VP0, together with VP1 and VP3 come together to form a protomer initially. After that, five protomers aggregate together to bring about a pentamer. The virus particle is then formed by accumulation of twelve pentamers that surround the RNA genome. There is then a maturation step when VP0 is cleaved to give VP4 and VP2 (Stanway, 2013).

The final step of the life cycle is the release of the mature viruses so they can infect other cells, which occurs by cell lysis (Garmaroudi *et al.*, 2015; Kirkegaard, 2017). However, non-lytic spread of PV in the central nervous system (the spinal cords of Bonnet monkeys) has been observed (Ponnuraj *et al.*, 1998). According to more recent investigations, PV

particles, as well as other enteroviruses, can be released non-lytically from cells within phosphatidylserine-lipid-enriched autophagosome-like vesicles which are more infectious than single viral particles (Garmaroudi *et al.*, 2015; Bird and Kirkegaard, 2015; Kirkegaard, 2017).

1.5 Functions and interactions of untranslated regions

1.5.1 5'-untranslated region (5'-UTR)

Conserved structures and sequences within the 5' and 3' ends of the picornaviral RNA play important roles in viral replication (Figure 1.5). The 5'-untranslated region (5'-UTR) is involved in the initiation of translation and RNA replication, and also contains determinants of virulence of viruses including PV and EV71 (Kloc *et al.*, 2018).

The picornavirus genome functions like a cellular mRNA, but unlike cellular mRNA the 5' end is not capped. The 5' UTR is exceptionally long compared to cellular mRNAs but variable in length (between 415 nts for passerivirus and 1451 nts for cardiovirus) (Duke *et al.*, 1992; Woo *et al.*, 2010).

The 5'UTR has extensive secondary structure, with several stem-loops, some forming complex domains. Taking enteroviruses as an example, the 5'-UTR consists mainly of 2 distinct elements, the cloverleaf (CL) and the internal ribosome entry site (IRES). Other structures seen in some 5'-UTRs include pseudoknots (PK), poly (C) and poly-pyrimidine tracts (Liu *et al.*, 2009). Some antiviral classes have been identified to target the 5' UTR, including phosphonodiamidite morpholino oligomers (PMOs) used in single-stranded DNA-like antisense approaches to inhibit gene expression (Chen *et al.*, 2008a).

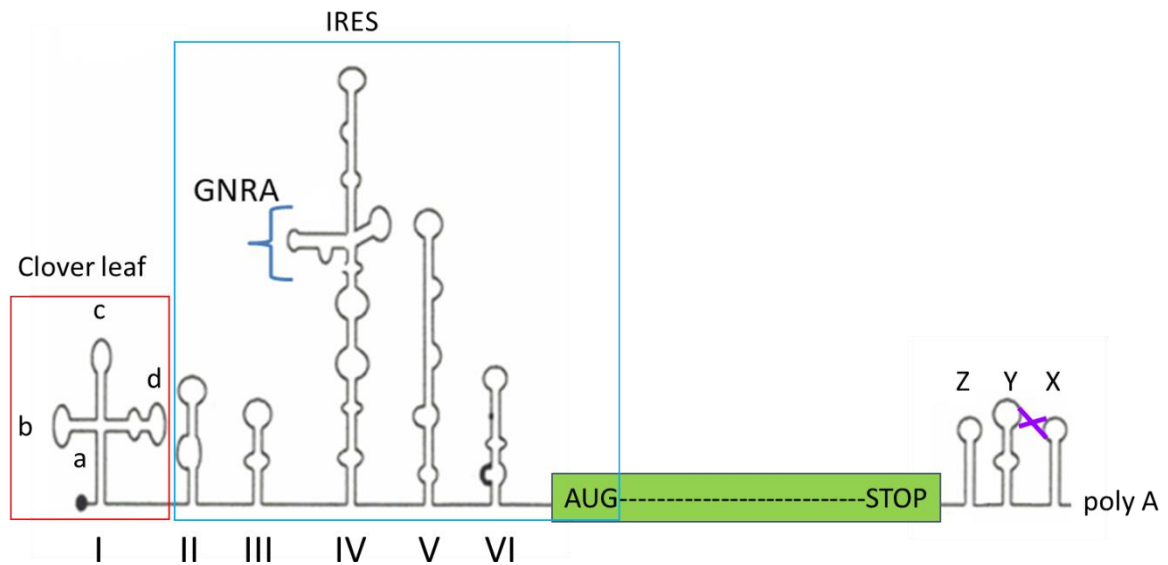


Figure 1-5. Picornavirus untranslated (non-coding) regions.

The structure of the 5' and 3'-UTRs differ between picornaviruses and the EV structures are given as an example. VPg (black oval) is linked to the 5' end of the genome. There is a 5'-end clover leaf structure (I) made up of a stem (a) and three stem-loops, b, c and d. The loops of b and d bind cell and virus proteins. Much of the rest of the 5' UTR consists of the IRES, internal ribosome entry site, needed for translation of the virus RNA. This involves structures II-VI which contain binding sites for proteins needed for translation and a critical GNRA motif. Structure VI contains a polypyrimidine region (heavy line and an AUG motif (black dot), which is the site of ribosome binding. The ribosome then scans along the genome and protein synthesis is initiated at the AUG at the start of the open-reading frame. The open reading frame is shown as a green box. The EV 3'-UTR folds into either two (e.g. EVC, Y, X) or three (e.g. EVB, Z, Y, X) stem-loops. The loops of X and Y are complementary in sequence and form a tertiary "kissing" interaction (purple lines). This is needed for RNA replication (Lin *et al.*, 2009; Mirmomeni *et al.*, 1997).

1.5.1.1 The cloverleaf structure

The cloverleaf (CL) structure is at the 5′ terminus of the enterovirus RNA. Many other picornaviruses have a single stem-loop at this position but have been less well-studied and the function of this structure is largely unknown. The CL is highly conserved in enteroviruses and involved in different parts of genome replication (Sharma *et al.*, 2009). In PV, the CL functions to enhance VPg uridylation and the initiation of negative-strand synthesis (Lyons *et al.*, 2001). The CL gets its name because it has the same shape as a cloverleaf, with a stem (domain a) topped by three stem-loops (b, c and d) (Rieder *et al.*, 2003). Binding of the cell protein PCBP2 (poly C binding protein) to stem-loop b enhances binding of the virus protein 3CD to stem-loop d which inhibits translation initiation (Lloyd, 2015). The loop in domain b is the most stable one and a C-rich sequence has been found to be essential for PCBP binding (Toyoda *et al.*, 2007). Cleavage of 3CD releases the active 3Dpol allowing RNA replication (Headey *et al.*, 2007). This mechanism prevents ribosomes from attaching to the RNA, so they do not interfere with RNA replication, as well as allowing RNA replication to start.

1.5.1.2 The internal ribosome entry site

The internal ribosome entry site (IRES) is an RNA sequence element that occupies much of the enterovirus 5′ UTR extending from stem loop II to stem loop VI, about 450 nts (Martinez-Salas & Fernandez-Miragall, 2018). Using a cap-independent mechanism and recruiting necessary host translation machinery including canonical (initiation factors [eIFs]) and non-canonical (ITAFs) factors the IRES directs host ribosomes to initiate an internal initiation of translation of the viral genome (Pickering *et al.*, 2003; Walsh *et al.*, 2013). This mechanism is different from the cap-dependent mechanism used to translate most cell mRNAs and so can still occur when the virus shuts off host cell protein synthesis, e.g. by cleaving some proteins needed for cap-dependent translation.

The IRES contains domains that bind specifically to eIFs or directly to ribosomes, as well as to ITAFs such as La and PTB and these domains are required for IRES function. For example, it was found that in PV stem-loop V binds to eIF4B and eIF4G, as well as PTB and this binding is weaker in the attenuated vaccine strains, which contain a critical mutation in this stem-loop (Ochs *et al.*, 2003). IRES mediated functions are modulated by many stimulatory and inhibitory factors, for instance the 3′-UTR and poly (A) tail sequences strongly stimulate IRES activity while some ITAFs are found to inhibit IRES

function after they are cleaved like La autoantigen and PTB (Back *et al.*, 2002; Dobrikova *et al.*, 2006). In addition, some IRES sub-domains can make long range RNA-RNA interactions. For instance, an interaction between part of domain III and the cre may block IRES activity and stimulate switching from translation (protein synthesis) to RNA replication (Romero-López *et al.*, 2012).

1.5.2 The role of the 3'-untranslated region in virus replication

There is still little information of the precise role of 3'-UTR in virus translation and/or replication. However, the extensive sequence and structural conservation between related viruses of this relatively short length region (e.g. around 40-120 nt in EV) (Duque & Palmenberg, 2001) indicate its importance. The 3'-UTR is thought to have signals to initiate negative strand RNA synthesis and to play a role in regulating polymerase activity (Iwakawa *et al.*, 2007; Lodeiro *et al.*, 2009; Gebhard *et al.*, 2011). Interestingly, the poly (A) of picornavirus is genetically encoded. However, there is a special mechanism which regulates its length and part of the 3'-UTR (oriR) has a key position in this mechanism.

The predicted secondary structures of all EV (except rhinovirus) 3'-UTRs show 2 stem-loop structures, the loops of which interact in a tertiary “kissing” interaction. Members of EVA and EVB also show a third stem-loop (Mirmomeni *et al.*, 1997). The kissing interaction has been called oriR and implicated in RNA replication as well as regulating the length of the poly A tail (van Ooij *et al.*, 2006a).

1.5.2.1 The importance of poly (A) tail in viral replication

Poly (A) is a stretch of adenine nucleotides found at the 3' end of cell mRNAs, following polyadenylation by poly A polymerase which recognises a polyadenylation sequence near to the end of the immature mRNA. In picornaviruses, poly (A) is instead genetically encoded by complementary transcription in the minus strand from poly (U) (Steil *et al.*, 2010; Kempf *et al.*, 2013). The poly (A) tail has important functions in viability, RNA stability, genome translation and viral replication (Barr & Fearn, 2010; Steil *et al.*, 2010). Reporter mRNA translation mediated by the picornaviral IRES is greatly stimulated by poly (A) (Bergamini *et al.*, 2000; Michel *et al.*, 2001). In addition, the PABP-poly (A) complex may enhance the interaction between eIF4G and IRES which is very important for translation initiation (Svitkin *et al.*, 2001). The template for negative strand synthesis most likely adopts a circular conformation, where the 5' and 3' ends are close together due

to an interaction between PABP (poly A binding protein) and PCBP2. PABP binds to the 3' poly A tail, while PCBP2 binds to the CL near to the 5' end of the genome (Andino *et al.*, 1993; Parsley *et al.*, 1997; Herold *et al.*, 2001; Svitkin *et al.*, 2007). Poly (A) is variable in length between different picornaviruses and for normal functions there is a minimum length (Silvestri *et al.*, 2006). In case of PV, it has average length between 50 and 90 nucleotides with a minimum length for virus viability of 12 nucleotides, shown by the non-ability to recover viruses from complete cDNA copies of the virus genome with poly A lengths of to less than 12 nucleotides (Yogo & Wimmer, 1972; Kempf *et al.*, 2013).

1.5.3 Cis-acting replication element (cre)

The cre is a stem-loop structure found at different locations within the genome of different picornaviruses, but most often within the coding region. In EVs except rhinoviruses, the cre locates within the 2C-encoding region, while in RV-A, RV-B and RV-C it is located in the regions encoding 2A, VP1 and VP2 respectively (Goodfellow *et al.*, 2000; van Ooij *et al.*, 2006b). However, it can be found the 5'UTR in FMDV (Mason *et al.*, 2002). The diversity of genomic location does not affect its function significantly. Based on biochemical, computational and nuclear magnetic resonance spectroscopy analysis, cres have a similar hairpin shape with a terminal loop (usually 14 nt in EVs), although the size is variable in different picornaviral species (Cordey *et al.*, 2008). The main function of the cre is to template the uridylylation of VPg to VPgpU/VPgpUpU by 3Dpol (Rieder *et al.*, 2003; Goodfellow *et al.*, 2003). A single A (adenosine) residue in the cre loop acts as the template. Poly (A) is also a potential template for 3Dpol-catalysed VPg uridylylation besides the cre, with the exception of FMDV, in which poly (A) is not used as a template (Herold *et al.*, 2001; Paul & Wimmer, 2016). Interestingly, the cre-mediated VPgpUpU seems only to prime positive-strand RNA initiation (Murray & Barton, 2003). The presence of the cre structure in the positive-strand RNA may enable the replication complex to distinguish the viral and host mRNA poly (A) tails to avoid competition with virus RNA replication (Barton *et al.*, 2001).

1.6 Protein roles during viral infection

Picornavirus proteins have critical contributions to make during the virus life cycle. They are either structural (also called capsid proteins) that form the virus particle, protect the genome, mediate cellular entry and allow release of the genome into the cell cytoplasm of the host cell, or non-structural, which act only intracellularly (e.g. facilitate viral

translation, polyprotein processing and RNA replication) (Ross *et al.*, 2017), and are never packaged in the virion (Ogawa *et al.*, 2009).

1.6.1 Capsid proteins (Structural proteins)

The picornavirus virion become complete and infectious only after the capsid is assembled around the genome (Lucas & Knipe, 2010).

Capsid proteins may also interact with non-structural proteins, such as VP3 which interacts with 2C and plays a role in assembly of the particle, or with cell proteins, for example VP2 of CBV3, binds to proapoptotic protein Siva, leading to apoptosis, viral spread, and tissue damage (Lin *et al.*, 2009).

1.6.2 Non-structural proteins

The non-structural proteins (2A, 2B, 2C, 3A, 3B, 3C^{pro}, 3D^{pol} and in some picornaviruses L protein) are involved in translation and replication, as well as interfering with defence mechanisms and generating the RCo needed for RNA replication. Figure 1-6 shows the sizes and conserved structures in picornavirus non-structural proteins.

1.6.2.1 2A protein

2A gets its name from its position in the viral polyprotein, but it is important to understand that this protein can be a completely different type of protein, with different function, size etc, between picornaviruses in different genera (Hughes & Stanway, 2000). This is in contrast to other viral proteins (except L) that are homologous in all picornaviruses. For instance, 2A^{pro} of EVs (Figure 1-6) acts as a trypsin-like protease. However, in aphthoviruses and many other picornaviruses, 2A is very short, around 18 amino acids, and is involved in an unusual function at the 2A-2B junction, where during translation no peptide bond is formed between the third and fourth amino acids of an NPGP motif at the 2A/2B boundary. Translation then continues, so that the polyprotein is made in two pieces (Donnelly *et al.*, 2001). Several picornaviruses, including parechoviruses, have a 2A with H box and NC motifs, but the function of these has not been identified. (Hughes & Stanway, 2000). A number of picornaviruses have multiple copies of 2A (Picornavirus Home Page, 2019).

During EV translation, 2A^{pro} cleaves at its own N-terminus, separating capsid proteins in the P1 region from non-capsid proteins in the P2-3 region (Teterina *et al.*, 2010). In addition, EV 2A^{pro} functions also include dealing with shutoff of cellular processes by cleaving of a number of cellular proteins. 2A^{pro} cleaves the initiation factor eIF4GI and/or PABP to

prevent cap-dependent translation and selectively facilitate viral RNAs translation. In addition, 2A^{pro} cleaves several other cell proteins involved in cap-dependent translation, transcription, splicing and nucleocytoplasmic shuttling (Castello *et al.*, 2011). For example, under experimental condition, transient increase of 2A^{pro} expression results in increase of nuclear permeability and translocation of its proteins in to the cytoplasm (Belov *et al.*, 2004). A recent study showed that this protease inhibits stress granule formation, so blocking their antiviral effect, and stimulate atypical stress granule formation which enhances viral translation (Yang *et al.*, 2018).

1.6.2.2 Leader protein

Leader protein (L protein) is encoded before the capsid-encoding region in some, but not all, picornaviruses and has different structures and functions among L protein-encoding genera. In aphthoviruses, L^{pro} is a papain-like protease responsible for releasing itself from the P1 region of the polyprotein and also cleavage of eIF4G (Liu *et al.*, 2015), a process which is done by 2A^{pro} in EVs, and this contributes to shut down of cellular cap-dependent translation (Watters & Palmenberg, 2011; Su *et al.*, 2018).

In cardioviruses such as EMCV and Theiler's murine encephalomyelitis virus (TMEV), L protein has no enzymatic activity. Instead, it stimulates kinases to hyper phosphorylate nuclear pore protein FG-repeat domains and so interferes with nucleocytoplasmic trafficking (Porter & Palmenberg, 2009; Ciomperlik *et al.*, 2016). Treatment of cells with staurosporine, a protein kinase inhibitor, reverses the inhibitory effect of L protein on nuclear import/export process. In addition, EMCV's L protein binds directly to RAN-GTPase giving an additional way to disrupt nucleocytoplasmic trafficking (Porter *et al.*, 2006; Porter & Palmenberg, 2009; Flather & Semler, 2015).

The Aichi virus L protein has a distinct sequence from that of aphthovirus and cardiovirus and different functions including morphogenesis and viral replication. For instance, mutation of this protein caused a significant decrease of mature virus but not the empty capsid although its importance for RNA encapsidation has been already identified. In addition, deletion of its C-terminal region resulted in a severe reduction in virus yield (Sasaki *et al.*, 2003; Jiang *et al.*, 2014).

1.6.2.3 2BC and 2B proteins

2BC protein is a relatively stable precursor which in some picornaviruses induces accumulation of vesicles, derived from the secretory pathway, that will form replication

complexes (RCo) (Bienz *et al.*, 1987). In addition, 2BC, but not either 2B or 2C separately, has the ability to induce autolysosome accumulation in cells infected with PV and EV71 (Taylor & Kirkegaard, 2007; Klein & Jackson, 2011; Lai *et al.*, 2017).

2B protein is a small hydrophobic membrane protein (Figure 1-6) which is usually localized closer to ER and Golgi complex membranes in infected cells. In EVs, 2B is functional as a part of 2BC and as a mature protein (Bienz *et al.*, 1987; Schlegel *et al.*, 1996; de Jong *et al.*, 2008). In some picornaviruses, including EVs, 2B acts as a viroporin and permeabilizes membranes, probably by forming homomultimers to build up pores through these membranes, and this increases the levels of cytosolic Ca^{+2} and decrease ER-Golgi complex Ca^{+2} concentration. 2B also disrupts Golgi-protein trafficking and localises to ER surfaces in EVs. Mutations that disrupt coxsackievirus 2B viroporin activity change 2B localization and prevent its effect on host secretory pathways, as well as inhibiting viral replication (de Jong *et al.*, 2004).

However, in other picornaviruses that are not closely related to EV, such as HAV, FMDV and ECMV, 2B shows a different localization pattern and has very little effect on Ca^{+2} homeostasis (Van Kuppeveld *et al.*, 1997a, 1997b; Jecht *et al.*, 1998; de Jong *et al.*, 2008).

In Aichi virus (AiV), 2B seems to act with other proteins like 2BC, 2C, 3A and 3AB to bind acyl-coenzyme A binding domain containing 3 protein (ACBD3), which binds and forms a complex with PI4KB to synthesize PI4P for RNA replication (Ishikawa-Sasaki *et al.*, 2014a). 2B also interacts with oxysterol binding protein (OSBP) which is then recruited to AiV-induced RCos. OSBP was also found to interact with 2BC but little with 2C, 3A, 3AB and ACBD3 (Aldabe *et al.*, 1996; Ishikawa-Sasaki *et al.*, 2018).

1.6.2.4 2C protein

Although 2C viral protein is essential for picornavirus replication, highly conserved, multifunctional, the location of mutations that give resistance to many potential anti-picornavirus drugs and has been extensively studied, it is still little understood (Norder *et al.*, 2011). The explanation of its structure (Figure 1-6), functions and interactions often depends on assumptions from 2C sequence motifs, and it is predicted to have an RNA binding motif, an N-terminal membrane-binding motif (an amphipathic helix) and an ATPase domain seen in RNA SF3 helicases of the AAA+ ATPase superfamily (Pfister *et al.*, 2000). RNA helicase activity has recently been demonstrated for the EV71 2C (Xia *et al.*, 2015). The recently described EV71 2C structure should be very useful as a basis for

understanding this protein more clearly (Guan *et al.*, 2017). 2C is likely to form a hexameric ring structure held together by interactions between a C-terminal amphipathic helix and a hydrophobic pocket in an adjacent 2C molecule. The structure also emphasizes the importance of a cysteine-rich region in zinc binding (Guan *et al.*, 2017).

In general, 2C and its precursor 2BC protein localise to the EV RCo and are probably needed for their formation (Teterina *et al.*, 1997; Norder *et al.*, 2011). Viral proteins 2B, 2C, 2BC and 3A are hydrophobic, interact with membranes and modify these membranes. 2B or 2BC proteins interact with Golgi and cause its disassembly and also alter the permeability of the plasma membrane which causes cell lysis (Norder *et al.*, 2011). Producing RCo from components of the protein secretion system prevents presentation of virus peptides on the surface of the infected cell, so 2C/2BC, and in some viruses 3A, help to hide virus infection from the immune system. Another event of the virus lifecycle in which 2C protein has been shown to be essential is encapsidation of RNA to give the virus particle. An interaction between 2C and VP3 is essential for this process (Liu *et al.*, 2010).

1.6.2.5 3AB and 3A

3AB is a small basic protein that is involved in several functions in replication. For example, the hydrophobic 3A domain of 3AB binds cellular membranes and interacts with their vesicles anchoring induced RCo to vesicles. The 3B domain interacts strongly with 3D^{pol} stimulating its elongation activity (Lama *et al.*, 1994; Plotch & Palant, 1995; Xiang *et al.*, 1998a; Cameron *et al.*, 2010). 3AB itself is a nonspecific RNA binding protein. However, in PV after interacting with 3CD, 3AB has the tendency to specifically bind the 5'-clover leaf and 3'-UTR, stimulating 3CD proteolytic activity, and probably also anchoring 3D^{pol} protein to the replication complex and strongly stimulating its polymerization activity. In addition, 3AB is an identified substrate for 3D itself during VPg uridylylation (Plotch & Palant, 1995; Xiang *et al.*, 1995; Richards *et al.*, 2006). 3AB was also found to have a helix destabilization activity in PV, indicating a nucleic acid chaperon action which can destabilise secondary structures to make replication of complementary RNA more efficient (DeStefano & Titilope, 2006). In vitro, 3AB has the ability to multimerize through both the N-terminal region and the hydrophobic domain of 3A to form higher oligomers in solution (Xiang *et al.*, 1998b; Strauss *et al.*, 2003). This may be related to possible viroporin action through forming multimeric ion channels in membranes.

When proteolytically cleaved, 3AB gives 3A and 3B. In addition to functioning as a domain within 3AB, 3A (Figure 1-6) has some individual functions. Some mutations in 3A have been found to affect positive strand RNA synthesis, but not negative strand. In some picornaviruses, 3A inhabits ER-Golgi traffic of membrane and secretory proteins and facilitates translocation of some ADP-ribosylation factors into the membrane (Doedens *et al.*, 1997; Belov *et al.*, 2005). Recently, it was found that the experimental expression of 3A protein in CBV3 and PV recruits phosphoinositol-4 kinase (PI4K) III β to membranes and this enzyme is known to be important for viral replication by increasing PI4P levels at replication complexes. Recently, oxysterol-binding protein (OSBP) was found to be important for regulating lipid homeostasis between the ER and the Golgi complex. It traffics cholesterol and PI4P between these membranes and stabilises ER-Golgi membrane contact sites. It is also involved in recruiting cholesterol to RCos, due to accumulation again stimulated by 3A (Strating *et al.*, 2015; van der Linden *et al.*, 2015). In vitro, 3A is also found to bind GBF1 protein and prevent its binding to COP-1 which is needed to generate vesicles needed for the protein secretion system. This recruits these vesicles for RCo formation as well as inhibiting proteins secretion (Belov *et al.*, 2007).

1.6.2.6 Viral genome-linked protein (VPg)

The first step of viral RNA synthesis is the production of uridylylated VPg (3B) made by the 3D polymerase (3D^{pol}) to give VPgpU and VPg-pUpU. The uridylylated VPg (Figure 1-6) primes both positive- and negative-strand RNA transcriptional synthesis (Lin *et al.*, 2009). VPg is therefore attached covalently to the 5' end of both negative and positive (genome) sense RNA (through a phosphodiester bond) because it was the primer. Unlike some other positive sense RNA viruses, VPg is not necessary for translation and is actually removed by a cellular enzyme after entry into the cell and before translation. It may be that whether VPg is removed from or kept by the newly made positive sense RNA controls whether these are used for transcription or packaging into new virus particles (Lin *et al.*, 2009).

1.6.2.7 3C^{pro}

3C^{pro} a chymotrypsin-like member of the trypsin proteases in all picornaviruses. Unlike most members of this protease family, 3C^{pro} (Figure 1-6) has an active site cysteine rather than a serine. Two other amino acids, a glutamic or aspartic acid and a histidine are located close to the cysteine in the folded protein and form a catalytic triad (Birtley *et al.*, 2005). 3C^{pro} and its precursor 3CD^{pro} do several inhibitory duties by cleaving cell proteins, as well

as their primary function of performing most cleavages in the viral polyprotein. These events results in shutting off transcription, impairing host RNA processing and polyadenylation by cleavage of the cellular CstF-64 protein (Weng *et al.*, 2009), inhibition of protein synthesis, blocking nucleocytoplasmic shuttling and which eventually induce cell death (Sun *et al.*, 2016b), by triggering apoptosis mediated by the caspase pathway (Li *et al.*, 2002). When the virus shuts off host cell protein synthesis by inactivating cap-dependent translation, its own translation can continue as this is initiated by a different mechanism which is IRES-mediated initiation (Martinez-Salas & Fernandez-Miragall, 2018).

1.6.2.8 3D^{pol}

3D polymerase (3D^{pol}) is an RNA-dependent RNA polymerase (RdRP) which is found exclusively in RNA viruses and is one of template-directed nucleic acid polymerase superfamily characterised by “a cupped right-hand structure” including fingers, palms and thumb domains (Peersen, 2017). The crystal structure of 3D^{pol} has been described for several EVs (Figure 1-6) including CBV3, PV, EV71, FMDV and some HRVs (Ferrer-Orta *et al.*, 2004; Wu *et al.*, 2010; Gong *et al.*, 2013). 3D^{pol} has a central catalytic role in the viral lifecycle including both priming and elongation activities as it forms, together with VPg, 3C^{pro}, and probably the 3CD precursor, the VPg uridylylation complex that organizes the uridylylation of VPg *in vivo* at the cre element (Ferrer-Orta *et al.*, 2004, 2015; Pathak *et al.*, 2007; Paul & Wimmer, 2016). The first initiation step in this process is to uridylylate the very conserved (position 3 in all picornavirus VPgs) tyrosine of VPg by 3D^{pol} which catalyzes covalent addition of 2 UMP molecules to its hydroxyl group using an A in loop of the cre element as a template (in some other viruses like caliciviruses the nucleo-adding step is template-independent) (Paul *et al.*, 2003; Paul & Wimmer, 2016). Then 3D^{pol} uses the uridylylated form (VPg-pUpU) as a primer to start replication of negative and positive RNA strands (Paul *et al.*, 2003; Steil & Barton, 2009). The fingers, palm and thumb domains within 3D^{pol} contain conserved residues that were found to stabilize VPg in the binding cavity and mutation of 3D^{pol}-conserved residue that interact with VPg resulted in an extreme defect in the uridylylation of VPg (Richards *et al.*, 2006). In addition to primer formation, 3D^{pol} also copies the viral RNA genome to make new copies. 3D^{pro} is less accurate than cellular replication polymerases as it lacks proof-reading and (wrong sequence) excision activities, and this means that high mutation frequencies are observed during the picornavirus replication, as is the case for other RNA viruses. This correlates

with the high rate of addition of nucleotides in RNA viruses, i.e. the faster polymerases are lower in accuracy (Campagnola *et al.*, 2015). The mutation rate allows a prompt adaptation to different conditions within host cells and tissues, as well as rapid resistance to drugs.

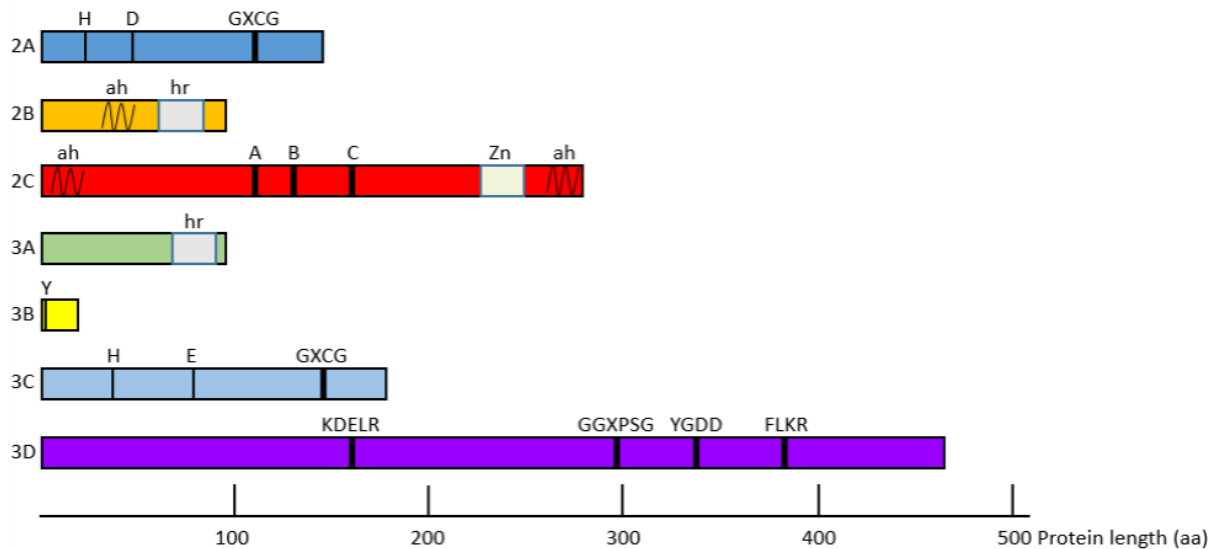


Figure 1-6. Diagram of the non-structural proteins of an enterovirus, showing some of the conserved features known to be important for function.

In enteroviruses 2A is a chymotrypsin-like protease with a catalytic triad made up of conserved histidine (H), aspartic acid (D) and a cysteine (C) within the sequence GXCG, where X is any amino acid. 3C, the protease which performs most cleavages of the virus polyprotein, is a similar type of protein with a catalytic triad containing a glutamic acid (E) instead of aspartic acid. 2B and 3A are small proteins which interact with membranes using hydrophobic regions (hr) and also an amphipathic helix (ah) in the case of 2B. 2C is a helicase with three domains (A, B and C) which are found in ATPase enzymes. It also has a cysteine-rich sequence which binds zinc ions (Zn). An N-terminal ah binds to membranes, while a C-terminal ah is involved in protein-protein interactions that bring 6 2C molecules together to give a hexamer. 3B is VPg. All picornavirus VPgs have a tyrosine (Y) at position 3 and the –OH of the tyrosine is used by 3D to uridylylate VPg to form the primer for RNA replication, VPgpUpU. 3D is the virus polymerase and contains several motifs seen in all picornavirus 3Ds (KDEL, GGXPSG, YGDD, FLKR). The sequence GDD is found in polymerases of all types.

1.7 Lipids as important host factors mediating infection

Lipids are involved in replication of both enveloped and non-enveloped viruses (van der Schaar *et al.*, 2016; Guo *et al.*, 2017). They are involved in early events including endocytosis, as well as the formation of the viral replication complexes (RCo) by manipulation of organelles, including mitochondria, peroxisomes, endosomes, Golgi and the ER, as well as assembly of some viruses (Ogawa *et al.*, 2009).

Some viruses require cholesterol-enriched microdomains (lipid rafts) in the cell membrane for entry (Strating *et al.*, 2015). Lipid rafts use cholesterol to accumulate proteins which can be used as receptors for viruses (Simons & Ehehalt, 2002). Following entry and translation, picornavirus non-structural proteins stimulate formation of protrusions within the host membranes in which lipids are integral to giving the curvature of the membranes to form RCo (Reid *et al.*, 2015). In addition, it is also found that picornaviruses use different unexpected mechanisms to increase the pool of cholesterol available for RCo formation. For example, CBV3 and PV have been demonstrated to use clathrin-mediated endocytosis to transfer cholesterol from extra cellular compartment (Ilnytska *et al.*, 2013). The 3A-mediated accumulation of OSBP and PI4KIII β to RCo described above also increases the available cholesterol pool and PI4KIII β knock down caused a serious decrease in EV RNA synthesis.

During infection by many viruses an important enzyme needed for fatty acid production, fatty acid synthase, is recruited to the viral RCo by specific interaction with virus proteins and its level has been found to increase in some virus infected tissues (Heaton *et al.*, 2010a). Similarly, inhibition of enzymes known to catalyse cholesterol synthesis reduces viral RNA synthesis. One example is HMG-CoA reductase which has been found to be relocalized to viral RCo in West Nile Virus (Mackenzie *et al.*, 2007).

Added to that, the rearrangement of lipid metabolism during infection can lead to the increased synthesis of ATP to provide the required energy for replication (Corsetto *et al.*, 2017; Duncan *et al.*, 2017). Apart from damaging cells by relocalization or activity changes to host proteins, changed lipid composition may also lead to host complications. For instance, elevated liver lipid content during viral infection, may result in liver diseases (Zhang *et al.*, 2012), and also causes down-regulation of the interferon-stimulated antiviral signalling response to infection (Martín-Acebes *et al.*, 2013).

Finally, in the later stage of infection, cholesterol and lipid raft microdomains have an essential role in the assembly of a variety of viruses. For instance, HCV assembly occurs on the surface of lipid droplets (Martín-Acebes *et al.*, 2013).

1.8 Lipid droplets

Lipid droplets (LDs), also called lipid bodies, oil bodies or adiposomes are dynamic and mobile cellular components whose structure and size (usually 0.4–100 μm) differ considerably in different cells and in response to different situations (Thiam *et al.*, 2013). They are vitally involved in various physiological activities and human pathologies. Recently, LDs were also detected in nuclei where they were found to regulate aspects of nuclear homeostasis (Sołtysik *et al.*, 2019).

LDs consist of a hydrophobic core of neutral lipids (NLs), usually triacylglycerols (TAGs) and/or cholesterol esters (CEs), inside a phospholipid monolayer which is usually decorated by some specific proteins (Vanni, 2017). However, the relative amount of the NLs and the types of LD surface proteins vary according to cell type. For instance, adipocyte LDs are composed mainly of TAGs and macrophage foam cells LDs are primarily CEs. LDs of yeast are a mixture of both lipids possibly arranged in layers (Buhman *et al.*, 2001; Czabany *et al.*, 2008). In addition, some other lipids can also be found within LDs such as retinyl esters in the hepatic stellate and the retina cells (Blaner *et al.*, 2009; Orban *et al.*, 2011), and wax ester and ether lipids form 10-20% of some mammalian neutral lipids (Yamamoto *et al.*, 2010). Ribosome-like structures can be seen inside some LDs using electron microscopy (Fujimoto & Parton, 2011). The dynamic nature of LDs can be seen in that there can be a threefold increase in LD diameter within hours and a tenfold increase in the surface area (Walther & Farese, 2012).

Isolating the hydrophobic neutral lipid from the hydrophilic cytoplasmic medium, phospholipids covering the monolayer surface layer are polar and amphipathic. In mammals these are mostly phosphatidylcholine (PC) which accounts for 60% of phospholipid mainly as lyso-PC and is important for LD emulsification and coating to avoid adhesion, followed by phosphatidylethanolamine (PE) as lyso-PE and phosphatidylinositol (PI) and small amounts of phosphatidylserine, phosphatidic acid and sphingolipids. The surface layer also contains some other polar lipids like sterols. (Bartz *et al.*, 2007).

LDs associate with a specific and characteristic set of proteins, both transiently and permanently, LD-associated proteins including membrane trafficking proteins, signalling proteins, intracellular organelles-associated proteins and chaperone proteins (Onal *et al.*, 2017). The Parkinson's disease-related protein, α -synuclein and chromatin-associated histones (in *Drosophila* embryo) are transiently recruited to LDs (Colebc *et al.*, 2002; Cermelli *et al.*, 2006). Some proteins stimulate LD fusion such as FSP27, a fat-specific protein that enhances triglyceride storage, or a cell death-inducing DFF45-like effector C which are also transiently recruited to LDs (Nishino *et al.*, 2008). There are proteins that have amphipathic properties like viperin (HCV endogenous inhibitor) which can distinguish the phospholipid monolayer surface of the LD from that of other cellular membranes (Hinson & Cresswell, 2009). PAT (which refers to **p**erilipin, **a**dipocyte differentiation-related protein, and **T**IP47, a tail-interacting protein of 47 kDa, two of the members) is the main known family of LD-related proteins. Perilipin3/Tip47 is localized to the ER along with DAG (diacylglycerol) and organizes DAG functions, along with other LD proteins for LD formation (Bulankina *et al.*, 2009; Skinner *et al.*, 2009). A small GTPase, Rab18, integrates with LDs using lipid-like modifications of certain amino acids to anchor it and this facilitates ER-LD interaction (Ozeki *et al.*, 2005). It is known that the unique composition of the LD phospholipid membrane affects the biogenesis, size, expansion and degradation of LDs (Ferré *et al.*, 2009; Zanghellini *et al.*, 2010; Singh & Cuervo, 2012) and is regulated by LD proteins. For instance, long chain FA CoA ligase (which is also important for lipid metabolism), squalene epoxidase and lanosterol synthase are important for lipid biosynthesis and patatin-like phospholipase domain containing protein 2 (CGI-58) for lipid degradation (Hodges & Wu, 2009).

LDs have multiple interactions with other intracellular organelles particularly the ER, but also including mitochondria, endosomes and peroxisomes. In mammals, ER membrane partially covers the LD forming an egg-cup shape (Robenek *et al.*, 2006). Rab18, perilipin2/ADRP and caveolin are possibly involved in LD-ER interactions as may be OSBP and related proteins, as these are ER resident and involved in lipid trafficking (Hynynen *et al.*, 2009). LDs can recruit proteins such as HMG-CoA reductase when the ER is degraded, suggesting there is a close LD-ER connection (Olzmann & Kopito, 2011).

Synthesis of LDs is thought to occur within the ER even though LDs and ER have different membrane structures (Tauchi-Sato *et al.*, 2002). When LDs become large enough, they are released from the ER, but the mechanism is not clear. The simplest model is that they bud

from the ER with an outer bilayer membrane. Excision of LDs as a bicelle has also been reported (Walther & Farese, 2009; Pol *et al.*, 2014).

LDs seem to associate with other organelles, in addition to ER. In skeletal muscle, during exercise and training activities, LDs number and mitochondrial contacts increase. Along with peroxisomes, this interaction may allow a pathway for lipids stored in LDs to be degraded by lipases to fatty acids which can then be oxidised in mitochondria (Binns *et al.*, 2006; Tarnopolsky *et al.*, 2006). Endosomes have been also found to coil round the LDs, transporting them to lysosomes through macrophageal autophagy. Rab5 may have a role in the early LDs-endosomes interaction as it was found in purified LDs (Liu *et al.*, 2007; Ouimet *et al.*, 2011).

LDs are largest in adipocyte cells, which specialise in lipid storage. In white adipocytes, there is one very large LD in the cytoplasm, mainly made up of triglycerides as an energy store, cholesterol esters and fat-soluble vitamins. Leptin, the primary adipocyte-associated hormone is the principle regulator of the long-term energy stability. Mammalian adipocyte brown cells degrade lipids within mitochondria to produce heat. LDs are also abundant in these cells but are much smaller than the single LD of white adipocytes. The liver is the second main reservoir of LDs after adipose tissue, but LDs are also present extensively in skeletal muscle, intestine, lactating mammary glands, adrenal cortex and macrophages (Walther & Farese, 2012; Nishimoto & Tamori, 2017).

There are two main ways for LDs break down, lipolysis and autophagy. Lipolysis is usually triggered by changing energy levels in the cell and involves three main lipolytic enzymes, ATGL, HSL and MGL which eventually liberate energy from the disintegrated TAGs. Autophagy is activated by cellular starvation, pathogenic infection and ER stress and takes unwanted cellular structures to degradation centres (Zhang *et al.*, 2017).

Apart from lipid and cholesterol storage, metabolism and breakdown, LDs have other important roles in the cell. These include membrane trafficking and providing building blocks for new membranes as well as, more unexpectedly, cell signalling, autophagy, immunity and clearance of inclusion bodies (Farese & Walther, 2009; Moldavski *et al.*, 2015; Molenaar *et al.*, 2017). Some hydrophobic drugs and fat-soluble vitamins are also recruited to LDs core (Thiam *et al.*, 2013). In addition, LDs also harbour and protect some specific unfolded and hydrophobic proteins which otherwise causes adverse effects by interactions with intracellular compounds such as histones and α -synuclein and they also

store certain amphipathic proteins. These can be exploited by viruses during assembly and are targeted by other pathogens such as bacteria, fungus and parasite (Cermelli *et al.*, 2006; Bozza *et al.*, 2017; Vallochi *et al.*, 2018). In some flaviviruses, including HCV and Dengue Virus, LDs are known to function as a place for the processing of viral protein and RNA production, (Samsa *et al.*, 2009; Lindenbach, 2013; Martins *et al.*, 2018). Hydrolysis of cholesterol esters derived from LDs was shown to be important in human rhinovirus A16 replication (Ilnytska *et al.*, 2013). LDs have also been identified as a store of fatty acids for specific phosphatidylcholine and phospholipid synthesis for building PV RCos (Viktorova *et al.*, 2018).

Although LDs are normally important in cellular homeostasis and cellular functions, they are a significant source of cellular dysfunction and metabolic diseases where excessive lipid aggregation within LDs exceeds the capacity of cells to buffer or detoxify. Abnormal LD accumulation within the liver gives hepatic steatosis which may end with chronic fibrosis, cirrhosis, hepatic resection or transplantation (Tevar *et al.*, 2010). Other complications that directly related to excessive LDs accumulation are obesity, diabetes mellites and heart diseases including atherosclerosis (Onal *et al.*, 2017). LDs are also upregulated in most cancer cells, possibly due to an increase in the rate of FA synthesis for rapidly proliferating membranes or a decrease in FA oxidation (Tirinato *et al.*, 2017). LD deficiency that results in lipodystrophy is a rare genetic mutation encoding for generalized lipodystrophy that results from mutation of caveolin (coxsackie A1), seipin (BCSL2) and an acylglycerol-phosphate acyltransferase (AGPAT2), or for partial lipodystrophy by mutations including peroxisome proliferator-activated receptor- γ (PPARG), lamin A/C (LMNA), protein kinase B (AKT2) and endo-protease Face-1 (ZMPSTE24). Some of these are associated with white adipose tissue insufficiency and others cause leptin deficiency leading to kind of diseases like massive hepatic steatosis, abnormal lipid deposition in non-adipose tissue and insulin resistance (Wideman *et al.*, 2009; Walther & Farese, 2012).

1.9 Antiviral agents with their therapeutic targets

Although all virus families have a generally similar life cycle including attachment, uncoating, genome replication, assembly, maturation and release, they differ considerably in the detailed mechanisms and requirements of each stage of the life cycle. This partially explains the challenge to find wide spectrum antiviral drugs. However, for some specific

viruses a range of drugs have developed. HIV-1 is the clearest example of a virus where a number of drugs are available, that each target one of the steps of replication listed above.

HIV-1 is an enveloped, single-stranded RNA virus, that uses reverse transcriptase (RT) to copy the RNA genome to DNA, which is then integrated into the chromosomal DNA of the infected cell. CD4 is the primary HIV-1 receptor and there is a requirement for a second co-receptor molecule, CCR5 or CXCR4, for entry (Martínez-A. *et al.*, 2002; Wei *et al.*, 2019). The drug Maraviroc binds to CCR5 and prevents the HIV-1 gp120 protein from binding, thus blocking infection. Due to the evolution of HIV-1 to use of CXCR4 in later stages of infection, this drug is useful only in patients at an early stage of infection.

Following binding of gp120 to CCR5/CXCR4, a fusion domain on the virus protein gp41 causes fusion of the virus envelope with the cell membrane which is needed for entry. The peptide drug enfuvirtide binds to gp41 and prevents this fusion. The experimental peptide drug VIR-576 is based on a molecule found in human blood, VIRIP, which is a naturally-occurring anti-HIV-1 peptide. VIR-576 also inhibits fusion (Raja *et al.*, 2003; Falkenhagen & Joshi, 2018).

Drugs which inhibit reverse transcription of viral RNA into cDNA by viral RT were the first class of anti-HIV-1 molecules to be developed. They include substrate-binding site molecules, called nucleoside RT inhibitors (NRTI, e.g. lamivudine, tenofovir and zidovudine), which are incorporated into the DNA chain being made and prevent it being extended. Non-nucleoside RT inhibitors (NNRTI, e.g. delavirdine, efavirenz, nevirapine and travertine) are allosteric, non-substrate-binding site molecules, which bind to RT and prevent its enzyme activity (Pau & George, 2014). Drugs which inhibit HIV-1 integrases prevent integration of viral cDNA into the cellular genome. Both integrase binding inhibitors (INBI) and integrase strand-transfer inhibitors (INSTI) have been developed, but only INSTI such as raltegravir, elvitegravir and dolutegravir have been used for the treatment of patients successfully (Thierry *et al.*, 2017).

HIV-1 RNA is translated to give a polyprotein which is cleaved by the viral protease. The development of drugs which inhibit this protease was very important in advances in HIV-1 therapy. Drug resistance is a major problem in HIV-1 therapy, but having drugs with different targets e.g. NRTI, NNRTI, protease, meant that combination therapy (or highly active anti-retrovirus therapy [HAART]), using two or three drugs, could be used and this reduces the risk of drug resistance. Protease inhibitors include nelfinavir, ritonavir,

saquinavir and amprenavir and these are peptide-like molecules which irreversibly bind to the protease active site work (Borrajó *et al.*, 2017).

Influenza virus is another virus where several antiviral drugs have been developed. The most useful (e.g. oseltamivir and peramivir) decrease viral maturation and infectivity by inhibiting viral surface neuraminidase to prevent viral release. Amantadine and rimantadine block the influenza M2 protein, which is needed to allow pH-dependent breakdown of the virus particle and release of the virus genomic content during release from an endosome in the entry process. However, they inhibit only influenza A, and do not affect influenza B which has another substitute protein named NB that is not affected by these drugs (Stiver, 2003).

Drugs against herpesviruses (double-stranded, DNA genomes) include nucleoside and nucleotide analogue compounds (acyclovir, famciclovir, ganciclovir, penciclovir, valacyclovir and cidofovir) which selectively inhibit viral thymidine kinase (TK) (Piret & Boivin, 2011; Said & Abdelwahab, 2013). Hepatitis B virus (double-stranded DNA virus which uses RT during replication) can be inhibited by different synthetic thymidine nucleoside analogues such as telbivudine, tenofovir and entecavir which block RT activity and have showed better antiviral activity than both lamivudine and adefovir, which also inhibit HIV-1 RT (Clercq *et al.*, 2010). These examples explain the complexity of and diversity of antiviral agents and their targets.

Most of the antivirals developed so far against picornaviruses target the virus capsid itself, to prevent early stages of infection, or the proteases to prevent polyprotein processing and later steps in replication. However, despite several drug strategies that look promising in clinical trials, there are no anti-picornavirus drugs in use (Norder *et al.*, 2011). For instance, pleconaril (capsid binder) and rupintrivir (a protease inhibitor), were in clinical trials but pleconaril was not accepted by the FDA due to side-effects and rupintrivir was stopped because it proved to be ineffective in a clinical context. However, pleconaril is again being assessed for treating high-risk patients with chronic respiratory diseases (Wildenbeest *et al.*, 2012).

As picornaviruses need many cell structures and machinery e.g. Golgi apparatus, endoplasmic reticulum and stress granules, as well as several cell proteins such as PI4KIII and OSBP for their successful replication, these structures and proteins could be used as potential targets for antiviral drugs. In addition, several natural products and herbal

medicines seem to be able to inhibit picornaviral infections. Furthermore, incorporating nanotechnology, photodynamic and sonodynamic approaches may even improve drug effects toward viruses, and/or decrease their side effects.

The first step of picornavirus infection is entry. Kappa carrageenan, a sulphated polysaccharide from seaweed, has shown potential antiviral activity by targeting viral attachment and entry. Lactoferrin also exhibited antiviral effects *in vitro* and *in vivo* through interfering with viral attachment to the cell surface (Wakabayashi *et al.*, 2014). Uncoating blockers, also called pocket binders, which include pleconaril, have been extensively studied in many picornaviruses. The reason behind the efficacy of the pocket binder is the ability to fit into a hydrophobic pocket underneath the canyon, the site of receptor binding, causing capsid structure stabilization which means that uncoating of the RNA cannot occur (refer to figure?). However, and despite this promising and highly-specific mechanism some EVs readily generate drug resistant mutants. Another problem is that they do not inhibit all EVs (van der Linden *et al.*, 2015). In addition to pleconaril, another group of capsid binders, pyridazinyl oxime ethers, chemically derived from pirodavir, such as BTA39 and BTA188, inhibited EV71 infection to a significant degree (Tan *et al.*, 2014).

Amantadine, a tricyclic amine developed to treat influenza A infections, interferes with EV IRES-mediated translation (Wakabayashi *et al.*, 2014). Translation inhibition was also observed with a flavonoid, kaempferol, due to its ability to inhibit ITAF e (complex or make it plural? Because it not just one) binding to the IRES (Wakabayashi *et al.*, 2014). Regarding viral polyprotein processing, as already discussed, rupintrivir, which is a peptidomimetic protease inhibitor, has been tested for the treatment of rhinovirus infections. It has also shown to be effective against other picornaviruses as well as members of other virus families such as coronaviruses and caliciviruses (Rocha-Pereira *et al.*, 2014).

Many drugs against other viruses target the virus polymerase and so inhibition of the picornavirus polymerase 3D^{pol} could be a successful antiviral approach. Two types of polymerase inhibitors are being explored. Some nucleoside analogues lack the 3'OH needed for the addition of the next nucleotide during RNA replication and so incorporation by 3D^{pol} causes chain termination. Others are incorporated into the RNA and result in mutations. (van der Linden *et al.*, 2015). One example of the second type is ribavirin, a synthetic purine analogue, which leads to a high level of mutations which is lethal. Another class of polymerase inhibitor includes non-nucleoside inhibitors. Amiloride inhibits EV replication

possibly by increasing the error rate of 3D^{pol}, although this may be due to its effect on intracellular Mg²⁺ concentration as it blocks ion channels, and inhibition of VPg uridylylation may be more important (Ogram *et al.*, 2014). In addition, several antiviral compounds have been shown to target 2C including guanidine hydrochloride and fluoxetine, but their mechanisms of action are not clear yet (van der Linden *et al.*, 2015). Currently, Hsp90 inhibitors have been tested and shown to have antiviral activity toward some picornaviruses including poliovirus, coxsackieviruses and rhinovirus (Geller *et al.*, 2012), as well as a wide spectrum of enveloped and non-enveloped, RNA and DNA viruses. A potentially important finding is that these compounds do not seem to lead to drug resistant viruses. This was found for poliovirus which did not show any resistance after extensive repeated passaging of the virus in cells containing Hsp90 inhibitors. This is important as poliovirus becomes resistant to all other antivirals studied, regardless of their mechanisms (against viral or host factors) (Geller *et al.*, 2012).

1.10 G-protein-coupled receptors Inhibitors

G-protein coupled receptors (GPCRs) are part of the seven-transmembrane receptor superfamily that can modulate gene expression by transmitting signals from outside the cell to intracellular pathways. They form a very large superfamily with hundreds of members, and it is estimated that 35% of approved drugs target GPCRs. Several GPCRs are encoded by some larger DNA viruses such as herpesviruses and poxviruses (Beisser & Verzijl, 2005). It has been reported that some viruses enter the cell using a specific GPCR complex, the best-known one being HIV which uses one of two GPCRs chemokine receptors CCR5 or CXCR4. The HIV drug maraviroc blocks the CCR5 pathway and other inhibitors of these receptors may be useful as antiviral compounds (Wilén *et al.*, 2012). Some *in vivo* studies showed that GPCRs are very important for viral replication as well as virus-induced cellular pathogenesis (Paulsen *et al.*, 2005). GPCR antagonists have been reported to inhibit both Ebola virus and Marburg virus either by interfering with viral entry, such as trimipramine maleate and promethazine hydrochloride, and/or antagonising the replication of infectious viruses as with benztropine mesylate (Cheng *et al.*, 2015). It has been also found that fluoxetine (a distinct class of GPCR antagonist), is an effective inhibitor of EVs replication by blocking an early step of CBV3 replication (Zuo *et al.*, 2012).

1.11 Lipids, lipid droplets and lipoproteins targeting agents

Lipids play a critical role in many parts of virus life cycle and several strategies have been tried to exploit lipids as antiviral targets. To begin with, interference with the biosynthesis of cholesterol by inhibiting 3-hydroxy-3-methyl-glutaryl-CoA reductase (3-HMG-CoA reductase) is one approach and statins have some antiviral activity (Chang & Jo, 2011; Peng *et al.*, 2011). Apart from suppression of the 3-HMG-CoA reductase pathway, statins also inhibit the binding of leukocyte function-associated antigen-1 (LFA-1) to the intercellular adhesion molecule (ICAM-1) which affects the immune system and can enhance the response against several viruses (Weitz-Schmidt *et al.*, 2001).

Another potential antiviral approach with wide activity spectrum is the use of C75, (4-methylene-2-octyl-5-oxotetra-hydrofuran-3-carboxylic acid). It targets lipid droplets (LD) by acting on FASN and inhibiting one of the prominent pathways of fatty acid biosynthesis (Tan *et al.*, 2015). It has been reported to suppress the replication of CBV3 and PV (Martín-Acebes *et al.*, 2015). Similar results had been previously obtained for many enveloped viruses (Munger *et al.*, 2008; Yang *et al.*, 2008; Heaton *et al.*, 2010b; Targett-Adams *et al.*, 2010; Martín-Acebes *et al.*, 2011).

Itraconazole (ITZ), which was developed as an antifungal drug and has also been found to have anticancer properties, has recently been found to be active against EVs and cardioviruses, as well as HCV (Strating *et al.*, 2015). The host protein OSBP was identified as the target of ITZ antiviral effect. ITZ binds OSBP and blocks cholesterol and PI4P-transport activities of OSBP. This leads to a decrease in cholesterol levels on RCos in infected cells (Strating *et al.*, 2015).

For viruses to replicate successfully, they have to use phospholipid in multiple steps. PI4P a specific phospholipid component has been found to be important for replication of most EVs (Albulescu *et al.*, 2015; Berryman *et al.*, 2016). PI4P is produced by the enzymes PI4KIII α and β and these lipid kinases have become more attractive targets for drug design. A drug which targets 3A (Chen *et al.*, 2008b), enviroxime, which is a benzimidazole derivative, and two related molecules T-00127-HEV1 and GW5074, act by inhibiting lipid kinase activity (Martín-Acebes *et al.*, 2015). Finally, being part of lipid rafts and involved in different steps of viral replication, cycle sphingolipids are expected to be potential targets for antivirals for many viruses (Martín-Acebes *et al.*, 2016). They also modulate the host cell immune system, which could be another important feature as antiviral agents (Olivera & Rivera, 2005).

1.12 Some aspects of using antiviral compounds

It is important to mention that drug resistant viruses commonly emerge with drugs that target viral proteins. This is due to the fact that the virus polymerase does not have proof-reading activity and makes many errors during replication. Random errors in proteins targeted by drugs can lead to drug resistance and these mutants will be rapidly selected. In contrast, the target site for drugs against cell proteins is unlikely to change (Van Der Schaar *et al.*, 2012). Blocking important cell metabolism pathways may cause more side effects than blocking viral proteins. However, most drugs apart from antibiotics work on important cellular functions without major side effects, so targeting host components may not cause problems. For example, inhibiting cellular protein cyclophilin A, which is needed for HCV replication, and which makes up 0.1%–0.4% of the total cellular protein, gives few side effects (van der Linden *et al.*, 2015). Many of the drugs mentioned, including statins and ITZ, in addition of drugs from different classes such as amantadine and ribavirin have been used clinically for several years for other conditions and are considered safe so their use as antivirals should not cause problems (Tan *et al.*, 2014).

EVs and HPeVs are usually considered to be the most important picornaviruses from the point of view of human health. Therefore, it would be useful to have a drug(s) which inhibit both. This is feasible as they belong to the same virus family and so share many structural and mechanistic similarities. However, there are many differences between them as they are genetically distinct and belong to different picornavirus supergroups and this may result in difference effects of drugs (Picornavirus Home Page, 2019). Known differences include: VP0 cleavage or not, N-terminal myristoylation of VP0 (VP4) or not, presence/absence of a canyon and hydrophobic pocket, IRES type, 2A protein type. Pleconaril, a capsid binder which showed a good response towards EVs, has no effects against HPeVs as these viruses have no hydrophobic pocket for pleconaril binding (Kalynych *et al.*, 2016). Other successful capsid binders of EVs may be inactive against HPeVs and vice versa. The fact that VP0 is not cleaved to VP2 and VP4 in HPeVs, despite this being an essential step in EV assembly and maturation, may mean that the viruses have completely different assembly pathways, and this may mean that any assembly inhibitors would not have broad specificity (Stanway *et al.*, 1994; Alho *et al.*, 2003).

The well-known EV 3C^{pro} inhibitor, rupintrivir has no activity regarding HPeV 3C^{pro} but it is not clear why not as the HPeV 3C^{pro} structure is not known. HPeV and EV 2As are completely different types of protein so EV drugs which target 2A will not work against

HPeVs (Hughes and Stanway, 2000). Compounds like guanidine HCl and HBB (2-(α -hydroxybenzyl)-benzimidazole) inhibit all tested EV 2Cs but are ineffective against HPeV. Other 2C protein inhibitors may also be inactive on HPeVs. The activity of fluoxetine and TBZE-029 was proposed to require the presence of a certain amino acid motif (AGSINA) in the EV 2C. This is absent in HPeV 2C and these drugs do not seem to be effective inhibitors for HPeVs (van der Linden *et al.*, 2015).

In summary, it may be possible but difficult to identify or design compounds active against EVs and HPeVs.

1.13 Naturally occurring antiviral agents

Natural products including herbal medicines are an indispensable source for novel antiviral approaches. Many effective drugs for non-infectious diseases were introduced from nature, such as aspirin, digitoxin, morphine, ephedrine, atropine and reserpine, and most chemicals developed as drugs (respectively 60% and 75% in the field of cancer and infectious diseases) between 1981 and 2002 were also derived from natural products. General speaking, natural medicines are relatively cheap, easily obtained and have a good long-term safety profile (Kurokawa *et al.*, 2010).

Some herbs and natural products are active against lots of picornaviruses. For instance, extracts of the herb *Ocimum basilicum* inhibit replication of both EV71 and CBV1 effectively and extracted molecules such as linalool, apigenin, and ursolic acid are effective. A previously tested inhibitor of CBV1, raoulic acid, again blocks EV71 infection. In addition, epigallocatechin gallate from green tea inhibits EVs by modulating the cellular redox environment (Lin *et al.*, 2014).

Regarding viruses other than *Picornaviridae*, *Houttuynia cordata* extracts have been found to inhibit coronaviruses by targeting both 3CL protease and RNA-dependent RNA polymerase activity. Moreover, Xiao Chai Hu Tang, a Chinese herb has antioxidant, antiproliferative and immunomodulating properties. It promotes synthesis of antibodies and interferon in chronic hepatitis patients and inhibits reverse transcriptase in HIV and murine leukemia virus (Zheng *et al.*, 2013). *Pelargonium sidoides* roots extracts inhibit influenza A by blocking entry (Lin *et al.*, 2014). According to Zandi *et al.*, the flavone baicalein was a potent inhibitor all stages of the Dengue virus replication cycle including

adsorption and intracellular replication (Zandi *et al.*, 2012). Investigation of different plants could identify large numbers of useful drugs.

1.14 Berries

Berries are small, fleshy fruit with no stones, and many are known to be rich in bioactive compounds (BAC). They are produced by many plant families including *Rosaceae* (strawberry, raspberry, blackberry), and *Ericaceae* (blueberry, cranberry) and species such as *Ribes nigrum* (blackcurrant), *Ribes rubrum* (redcurrant) but also contain species with only low to medium BAC content such as elderberries (*Sambucus* spp.), bilberries (*Vaccinium myrtillus*), gooseberries (*Ribes uva-crispa*), cape gooseberries (*Physalis peruviana*), honeyberries (*Lonicera caerulea*), chokecherries (*Prunus virginiana*), marionberries (*Rubus* spp.), saskatoon berries (*Amelanchier alnifolia*), arctic brambles (*Rubus arcticus*), cloudberrries (*Rubus chamaemorus*), crowberries (*Empetrum nigrum*), lingonberries (*Vaccinium vitis-idaea*), loganberries (*Rubus loganobaccus*), Rowan berries (*Sorbus* spp.), and sea buckthorn (*Hippophae rhamnoides*) (Beattie *et al.*, 2005; Suvetha & Shankar, 2014; Skrovankova *et al.*, 2015).

Broadly, berries contain some sugars such as glucose and fructose and small amounts of fat. They are also rich in fibre such as cellulose, hemicellulose and pectin; organic acids including citric, tartaric, malic, oxalic, ellagic and fumaric acid; vitamins like ascorbic acid and folic acid; trace amounts of minerals and more importantly in terms of antimicrobial and anticancer activities, the bioactive phytochemicals including phenolics which is in turn involve flavonols such as quercetin, kaempferol, myricetin, flavonoids, such as anthocyanins and flavanols such as catechins and epicatechin. These may be partly the basis of antioxidant properties and other reported health benefits of berries, including effects on oxidative stress, blood pressure, platelet aggregation, detoxification enzymes, the immune system inflammatory processes and cancer (Cosmulescu *et al.*, 2015; Skrovankova *et al.*, 2015; Paunović *et al.*, 2017).

In addition, berries are considered to be a potential source of antiviral and antibacterial pathogens of different classes. Cranberries which contain high levels of polyphenols have been demonstrated to prevent some bacterial infections such as *Helicobacter pylori*, and infection by viruses from different families including reoviruses, rotaviruses, and 7 (Ikuta *et al.*, 2013). Anti-influenza effect has been also seen with flavonoids from elderberry fruit extracts (Tiralongo *et al.*, 2016). Blackcurrant extracts inhibit herpes simplex virus type I, influenza virus type A and B and respiratory syncytial virus. Anthocyanins from

blackcurrant block both influenza virus adsorption and release from infected cells (Weiss *et al.*, 2005, Ikuta *et al.*, 2013).

1.15 Microalgae

The recently growing importance of microalgae comes from many features they have. Firstly, they can accommodate stressful growing conditions including cold, heat, salinity, drought, anaerobiosis, osmotic pressure, UV exposure and photo-oxidation. This makes them easy to grow and also increase the range of biological products as the microalgae adapt to different conditions. Microalgae resemble higher plants in efficient photosynthesis and simple nutritional requirements and at the same time, they are generally similar to microorganisms regarding the fast rates of growth and production of many primary and secondary metabolites (Guedes *et al.*, 2011). They are flexible metabolically and a variety of metabolites can be easily obtained by just changing their nutritional state e.g. removing a nitrogen source (Amaro *et al.*, 2011).

Microalgae include at least 30,000 species and so there is a very great potential for the identification of novel drugs (Guiry, 2012). They produce many types of compounds like polysaccharides, vitamins, fatty acids, chlorophyll, acetogenins, xanthophylls, halogenated compounds and amino acids. The products are widely used commercially e.g. in food stuffs, cosmetics and for pharmaceuticals. For instance, 9% of all compounds isolated from marine organisms are from algae (Ahmadi *et al.*, 2015). Microalgae also contain many different antibacterial, antifungal, antiplasmodial and antiprotozoal materials (Amaro *et al.*, 2011). Algae contain several compounds with reported antiviral activities, and they are rich in polysaccharides. Carrageenans, sulfated polysaccharides, are produced by red algae and inhibit many viruses at the entry stage, including papilloma viruses that can lead to cervical cancer and genital warts. Another type of polysaccharide, alginates are found in the cell wall of brown algae and have been shown to inhibit hepatitis B virus and HIV. Fucans are high molecular weight sulphated polysaccharides with several reported biological activities. They are diverse in structure among species raising the possibility that they may include several potential drugs (Ahmadi *et al.*, 2015). Recent research has also found many further applications of microalgae metabolites as diagnostic tool, including fluorescent agents which can be used additionally for photodynamic therapy (Schuermans *et al.*, 2015).

1.16 Oxidative stress and its relationship to viral replication

Oxidative stress (OS) occurs when the production of reactive oxygen species (ROS) exceeds the capacity of antioxidant (AO) defences (Costantini *et al.*, 2010). Normally, ROS are involved in useful physiological functions including mitochondrial electron transport and signal transmission (Sena & Chandel, 2012). However, in some conditions such as infection, stress and other pathological conditions, the level of ROS overwhelms AO capacity and causes oxidative changes, leading to dysfunction of proteins, lipids, carbohydrates and nucleic acids (Bargagli *et al.*, 2009). The altered proteins are more susceptible to photolytic activity and loss of function. Membrane phospholipids are oxidised by ROS resulting in lipid peroxidation. Oxidative DNA deletion and gene mutation caused by OS often cause cell death, but cancerous changes could also occur, while OS in the immune system cells can reduce protective immunity and response to vaccination (Valle *et al.*, 2013). OS may be induced by virus infection and could enhance viral replication. On the other hand, an increase of ROS enhances the activity of some cellular transcription factors activity and increases cytokine secretion and inflammatory response (Narayanan *et al.*, 2014). Long term elevation of ROS caused by viral infection can increase AO consumption and lead to serious damage of major cell components, as seen in Newcastle Disease Virus infection in chicken (Venkata *et al.*, 2013). In addition, it was found that acute HCV infection was associated with a significant increase in ROS levels and a decrease in AO levels. In contrast, the chronic phase in infected cells was associated with a low ROS production and elevated GSH level that could serve viral persistence. It was also found that pro-oxidant treatment of the chronically infected cells caused an increase in the titre of HCV-RNA (Anticoli *et al.*, 2019).

AOs are one of most important defence mechanisms against OS. AOs can be classified as enzymatic such as superoxide dismutase (SOD), catalase (CA), peroxidase and other enzymes, and non-enzymatic (Sharma *et al.*, 2012; Power *et al.*, 2013). The most important non-enzymic AOs are scavengers, including hundreds of agents such as carotenoids, flavonoids, tocopherols, ascorbic acid, amino acids, phospholipids, and sterols which are mostly derived from food, with some sources like berries being rich in AOs (Choe & Min, 2009). Mammalian cells can synthesize some types of AOs such as glutathione (GSH) and nicotinamide adenine dinucleotide phosphate (Eriksson *et al.*, 2015; Moreira *et al.*, 2015). Vitamin E, the major mitochondrial AO, and polyphenols protect against lipid peroxidation by scavenging free radicals (Saeidnia & Abdollahi, 2014).

Different AOs can inhibit viral replication and different mechanisms have been identified. Vitamin C inhibits HIV-1 RT and suppresses replication. GSH blocks influenza virus infection by inhibition of apoptosis which then decreases the influenza release (Cai *et al.*, 2003). N-acetyl-L-cysteine that is often used to treat acetaminophen overdose-induced OS, increases intracellular GSH, which is depleted by HIV-1 infection, and can reduce AIDS symptoms in animal models, while 2,3-dimercapto-1-propanol blocks HIV-1 replication by inhibiting viral trans-activating protein. AOs have also been investigated as possible anti-EV therapeutics. Both N-acetylcysteine (Ho *et al.*, 2008), and gallic acid (Choi *et al.*, 2010), are reported to inhibit EV71 infection.

1.17 Photodynamic therapy and photodynamic antimicrobial chemotherapy

Photodynamic therapy (PDT) refers to using harmless visible light in combination with photosensitizers (PS). These are chemical dyes, usually administered either parenterally or externally, and after reaching the target tissues are triggered using visible or infrared light (Reddy *et al.*, 2009). When the PS is a photo-antimicrobial the process is termed photodynamic antimicrobial chemotherapy (PACT). As soon as light is absorbed by a PS, it undergoes transition to an excited state at which it can react with molecular oxygen to produce either reactive oxygen species (type 1 reaction) or singlet oxygen ($^1\text{O}_2$) (Figure 1.7). PDT is both useful and highly selective. This is due to the fact that cells growing rapidly specifically up take PS and the effect of the whole process is confined to the area of applied light. PACT is applicable for antimicrobial use as microbes are highly proliferative cells (Denis & Hamblin, 2011). For PACT treatment to be both effective and safe, many factors need to be considered such as light sources, photosensitizer properties, dose of photosensitizer, barriers to reaching the target site and patient acceptability (Cassidy *et al.*, 2009).

In terms of safety profiles, human cells such as keratinocytes and fibroblasts can tolerate PACT doses that are fatal to microbes. This is probably because of big differences in structures and sizes of cells. Human cells are much larger than other microorganisms (they are between 25-50 times larger than bacteria cells) and therefore can survive in more damaging environments. Photodynamic antimicrobial chemotherapy has many applications including infected wounds, nail infection, intranasal complications like

maxillary sinusitis, oral candidiasis, periodontal disease, cystic fibrosis and lung infection (Cassidy *et al.*, 2009), in addition to warts and psoriasis (Monge-fuentes *et al.*, 2015).

Increasingly, PDT is applied for a variety of tumour and cancer types of different stages. For instance, porfimer sodium (Photofrin) has been licensed for treating non-small cell lung cancer and obstructing oesophageal cancer in the UK (Cassidy *et al.*, 2009). In addition, PACT was studied extensively for many pathogens including *Staphylococcus aureus* and *Pseudomonas aeruginosa*. It has been found that multidrug-resistant members are equally susceptible to PACT as normal strains. In recent years several types of PS have been tried for various types of viruses (Xu *et al.*, 2019). Both enveloped and non- enveloped viruses have demonstrated susceptibility in vitro (Cassidy *et al.*, 2009). However, enveloped viruses have shown better sensitivity than non-enveloped viruses to photodynamic destruction (Costa *et al.*, 2012).

The natural photosensitizers, psoralens (furanocoumarins) have been used for a long time to treat different skin disorders in Asia. Recently, psoralen photomedicine was shown to be significantly active for lymphoma. Psoralen therapy has also been investigated for blood treatment against both intracellular and non-associated viruses. Perylenequinonoid pigments were shown to be possible antiviral candidates, due to their high lipophilicity and negative charge along with large pseudoplanar area. It is thought that hypericin has photo-destruction activity toward HIV-1 by cross linking viral capsid proteins, and also has an inhibitory action on protein kinase C, an important target for antiviral drugs. In addition, there is possibility PACT could be used for deep and disseminated viral infection by exploiting optical fibre technology (Wainwright, 1998).

There are many drawbacks of antibiotic drugs such as limited spectrum of antimicrobial effects, emerging resistant strains, failure to reach areas with limited blood flow, systemic adverse effects and lack of patient compliance. PACT may be able to overcome some of these drawbacks, since this technique is less invasive, causes least damage to normal cells, has broad spectrum of action and minimal side effects and is cost-effective (Khandge *et al.*, 2013).

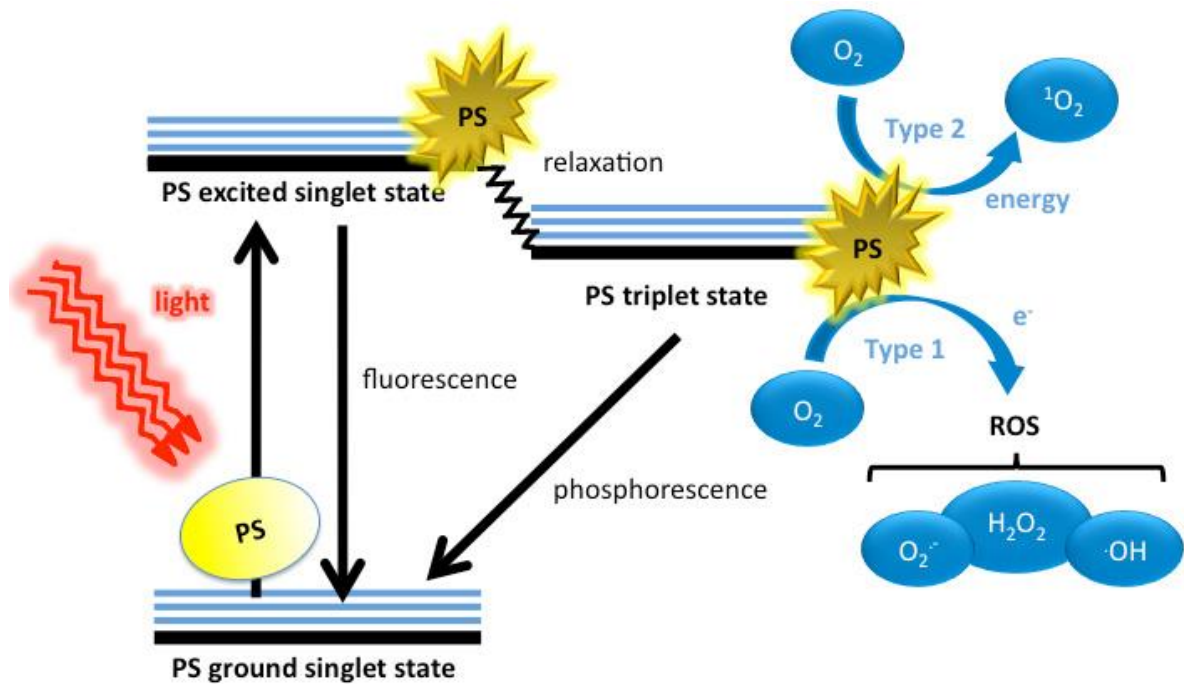


Figure 1-7. Photodynamic therapy states.

In the first step light absorption stimulate the photosensitizer (PS) to move up an excited singlet state, then it may lose its energy and return back ground singlet state or relax to triplet state, at which, it is either falling down ground state or combing molecular oxygen to produce reactive oxygen species (ROS) by entering type 1 reaction or singlet oxygen (¹O₂) which occur via type 2 reaction (Denis and Hamblin, 2011).

1.18 Aim and Objectives

At present there are no drugs against picornaviruses in clinical use. The large number of medically important viruses in this family, particularly in the *Enterovirus* genus (nearly 300 distinct types), means that vaccine development is not feasible in most cases and so effective drugs are required. The aim of the project is to identify compounds which can potentially be used to combat these important viruses. The works will focus mainly on enteroviruses, but some comparisons will be made with parechoviruses, as these are genetically very different human pathogens. In this way, broadly active anti-picornavirus approaches may be discovered. There are two objectives:

1. To use compounds present in biological materials as a “library” of potential anti-virus agents, which can be identified, studied and chemically modified for optimisation.

To explore existing drugs which may be repurposed for use as anti-picornavirus agents. Work published on the anti-enterovirus effect of fluoxetine will be extended to investigate the limitations of this compound and if these can be overcome by chemical modification. Previous work in the laboratory showed that enterovirus, and particularly parechovirus, 2C protein interacts with lipid droplets. A second approach to repurposing existing drugs is to investigate if drugs which inhibit lipid droplet formation are effective against enterovirus and parechovirus replication.

Chapter 2: Materials and Methods

2.1 Materials

The viruses, cells, reagents, chemicals and biological material use are listed in Appendix 1.

2.2 Methods

2.2.1 Methods of cell culture

2.2.1.1 Splitting of cells

Cells were observed using a microscope to ensure they were confluent and healthy. The old medium was discarded, and cells washed twice with 1X PBS. Then 600 µl of 0.25 % trypsin-EDTA or accutase solution was added and the flask was placed on a rocking platform until the cells were detached when checked under the microscope. DMEM medium (20 ml containing 10% FBS, 1% MEM non-essential amino acid and 1% Penicillin-Streptomycin) in the case of GMK cells and A549 cells, or McCoy's 5A medium (20 ml containing 10% FBS and 1% Penicillin-Streptomycin) in the case of HT29 cells was added to the flask and the cell suspension was divided into 4 new 25 cm². These were incubated in a 5% CO₂ incubator at 37 °C. Cells were passaged every 5 days.

2.2.1.2 Cell line storage

Old medium of a confluent cell line was discarded, and the cells were washed twice with 1X PBS. Trypsin-EDTA (600 µl of a 0.25 % solution) or 600 µl of accutase solution was added and the flask was placed on a rocking platform until the cells were detached. FBS (1 ml) was added and mixed. A 1 ml aliquot of the mixture was placed in a cryo tube and 111 µl of DMSO was added. The tube was placed in an insulated container, to ensure slow freezing, for three days at -80 °C, then stored at -80 °C.

To recover the cells, the tube was thawed, and the cell suspension was transferred to a flask containing 4 ml of new medium and 1 ml FBS and incubated in a 5 % CO₂ incubator at 37 °C. The medium was changed next day and the cells observed until they became confluent. The cells were then propagated as described in section 2.2.1.1.

2.2.2 Virology methods

2.2.2.1 Direct and indirect plaque assays and drug treatment

To evaluate the antiviral effect of drugs and extracts, plaque assays (Bird & Britton, 1979; Cornelis *et al.*, 1982; Hung *et al.*, 2010; Baer & Kehn-Hall, 2014) were performed, mostly

in 6 well plates. For the direct plaque assay approach a flask of confluent cells was used and detached as described in section 2.2.1.1. The detached cells were re-suspended in 12 ml medium and 2 ml was added to each well of the 6-well plate. The cells were incubated at 37 °C in a humidified incubator with 5 % CO₂ for 3 days until they were confluent. The old growth medium was aspirated away, and 0.5 ml of new medium was added. Then compounds, either the drugs or the natural extracts, were applied at different concentrations in growth medium. Two wells had no drug added to give a cell control and a virus control. The plate was placed on a rocking platform for 30 min. Diluted virus (370 PFU in 15 µl) was added to all wells except the cell control and the plate was held on the rocking platform for 45 minutes. CMC medium (2 ml), made up of a 2:1 mixture of growth medium: 2 % CMC, was added to each of the 6 well-plate. The plate was incubated at 37 °C for 3 days. The growth medium was discarded, and the cells were washed with PBS then stained with crystal violet to stain cells and make plaques, areas where cells have been killed and detached from the plate, more visible. These plaques were then counted.

The same initial steps described for the direct plaque assay were applied for indirect plaque assay approach, including the preparation of confluent cells, drug treatments and virus infection. Subsequently, 2 ml of media (instead of growth medium: CMC) were added and the plate was incubated for 48 h instead of 3 days, then frozen and thawed 3 times without discarding the growth media. The amount of virus present in the samples was then measured using a plaque assay. Confluent cells were prepared and 370 PFU in 15 µl of each sample was allocated in plate wells and the plate incubated for 45 minutes on the rocking table and added by 2 ml CMC and incubated at 37 °C for 3 days and stained. Dilutions of the sample were made and 15 µl of each dilution was applied to a well of a 6 well plate containing a confluent cell monolayer, overlaid with 0.5 ml of growth medium. The plate was incubated for 45 minutes on the rocking table and then 2 ml of growth medium: CMC was added. The plate was incubated at 37 °C for 3 days and stained. The plaques were counted and the virus concentration was calculated, taking into account the dilution factor and volume of the sample.

2.2.2.2 Selection of drug-resistant mutants

To evaluate the potential usefulness of a drug, and to gain information on the possible virus protein targeted by the drug, a multi-step experiment was conducted to obtain drug-resistant mutants (Boucher *et al.*, 1993; Brown *et al.*, 2003). In the first step, 50 µl of a 10x virus

dilution was added to confluent cells that were previously treated with the lowest inhibitory concentration of drug under investigation. This was incubated at 37 °C and checked daily using a microscope to see cytopathic effect which usually appears after 3 days of incubation. The infected cells were then frozen and thawed 3 times before they were collected in a small tube and labelled as first passage. Each passage was carried out by taking a sample volume from the previous passage, diluting it by 10 times and repeating the same procedure with 50 µl of the sample, with increased drug concentration each time. Plaque assay at a drug concentration found to inhibit the original virus was applied to some of the passages during the process, and compared with the original virus, to assess whether the passaged virus showed drug resistance.

2.2.2.3 Direct effect of compound on the virus particle

In this assay, an effective concentration of the active compound was mixed directly in a tube with a virus being tested. An active compound or extract was mixed with growth medium in a microcentrifuge tube to give a 990 µl solution of drug at an effective concentration. 10 µl of neat virus were added to make 1000 µl of media with virus and drug. The mixture was incubated for different times then plaque assay was performed.

2.2.2.4 Time of addition assay

A time-of-addition assay was performed to study the mechanism of drugs and inhibitors (Daelemans *et al.*, 2011; Aoki-Utsubo *et al.*, 2018). A six well plate with each well containing a cell monolayer and 1 ml of growth medium was used. The drug or inhibitor was added to one well (zero time point). After 30 min 100 PFU of virus was added to all the wells and the plate were placed on a rocking platform for 45 min. The drugs or inhibitors were added at 1, 3, 5 and 8 hours post- infection. The plate was incubated, (36 hours for CAV9 and 42 hours for HPeV1) in a 5 % CO₂ 37 °C incubator. The plate was frozen-then-thawed three times and a plaque assay was applied on the liquid from each well.

2.2.2.5 Determination of compound-induced apoptosis by Nicoletti assay

The Nicoletti method is an assay for cell apoptosis detection and quantification. The principal purpose of this assay in the current work is to confirm safety and antiviral activity of investigated compounds. Cells were treated with or without the investigated compounds using certain concentrations to measure the intrinsic toxicity of the compounds. Others were incubated with the virus only. In addition, there were cells which were pre-treated

with a range of concentrations of each compound for 30 min and then infected with 5 μ l of neat virus. The plate was incubated for 45 min on a rocking table and each well was covered by 2 ml of growth medium. After incubation for 12 h at 37 °C, media was discarded, and cells were washed with PBS and trypsinized. The detached cells were collected separately in tubes and centrifuged at 2000 rpm for 2 min. The cells were washed twice with PBS (250 μ l) and centrifuged again to be fixed with 4% formaldehyde for 10 min at 4 °C in the dark and then washed with PBS and centrifuged twice. Finally, 0.5 ml of Nicoletti buffer was added to each sample and kept cool briefly until analysis using a BD Accuri cytometer[®] (C6). The results were processed using Flowing Software version 2.5.1.

2.2.2.6 Cell viability assays

Cell viability assays were conducted according to the colorimetric MTT method (Mosmann, 1983; Vistica *et al.*, 1991; Bahuguna *et al.*, 2017). GMK cells were grown (until 80 % confluent) in 96-well plates. Some cells were incubated with the compounds or extracts, and some with the viruses. Other cells were treated with the compounds or extracts plus virus. The incubation period was 3 days at 37 °C. MTT (3-(4,5-dimethylthiazol-2-yl)-2,5-diphenyl tetrazolium bromide) was dissolved in media at 1 mg/ml and filtered using a 0.22 μ m sterile filter (Millipore). Media in each well were discarded and 100 μ l of MTT in medium were applied for 2 h at 37 °C and then carefully aspirated. The resulting blue crystals were mixed thoroughly with 100 μ l DMSO to dissolve and the absorbance at λ 550 was recorded on a plate reader (infinite M200PRO, TECAN[®]). The absorbance value given by the treated sample as a percentage of that of the cells only sample were calculated as a measure of cell viability.

2.2.2.7 Photodynamic inactivation effect of compounds and extracts

Blue light (BL) and red light (RL) LED sources (Phantom, Shenzhen CIDLY Optoelectronic Technology, China), equipped with a fan to eliminate any heat and emit a uniform field of low-power, LED (25 pieces x 3 Watt) were used in experiments with microalgae and RC extracts in order to stimulate active phototensitive compounds within the extracts. Using 96-well plates, several wells containing confluent cells in duplicates were designated as controls incubated with/without the photosensitive compounds, other wells were cells incubated with the viruses only, or with viruses and photosensitisers. The plates were exposed to BL or RL alone to assess the effect of the light on the cells. The

plates were exposed to the light for 20 min. In order to assess the effect of light exposure on the cells, on the viral infection of the cells, and on the treatment efficacy of the photosensitisers, certain plates with the same arrangement were kept in the dark without light exposure and wrapped with aluminium foil. Plates were incubated for 3 days at 37 °C then cell viability was assessed using the MTT assay.

2.2.3 Molecular biology methods

2.2.3.1 Extraction of viral RNA using a QIAamp Viral RNA Mini Kit

Virus RNA was isolated from infected cells which had been freeze-thawed 3 times, using a QIAamp viral RNA mini kit (Monleau *et al.*, 2009; Cornelissen *et al.*, 2017; Zhang *et al.*, 2018). The virus-containing sample (140 µl) was added to a 1.5 ml microcentrifuge tube containing 560 µl of AVL buffer and 5.6 µl of RNA-AVE carrier. The tube was vortexed for 15 seconds, incubated at room temperature for 10 min and briefly centrifuged. Next, 560 µl of ethanol (100%) was added, vortexed for 15 seconds and centrifuged briefly. Then, 560 µl of the solution was added to the QIAamp Mini column and centrifuged at 8000 rpm for 1 minute. The column was placed into a clean 2 ml collection tube and once again 560 µl of the solution was added and the column was recentrifuged. The column then was washed with AW1 buffer (500 µl) and centrifuged at 8000 rpm for 1 minute. A second wash was done with AW2 buffer (500 µl) followed by centrifugation for 3 minutes at 14,000 rpm after discarding the flow-through and changing of the collecting tube. The column was placed in a clean 1.5 ml microcentrifuge tube and 50 µl of AVE buffer was added and centrifuged for 1 min at 8000 rpm to elute the RNA. The purified RNA was stored at -80 °C.

2.2.3.2 Reverse transcription-PCR (RT-PCR)

Purified virus RNA was reverse transcribed, and the cDNA amplified using a SuperScript™ III One-Step RT-PCR System with Platinum™ Taq DNA Polymerase (Invitrogen). To construct a 50 µl RT-PCR reaction, 25 µl of reaction mix, 1 µl of forward and reverse primers (Table 2.1), 1 µl RT/Taq, 5 µl of RNA and 17 µl DNase free water were mixed and placed in a PCR machine (GeneAmp PCR System 2400, PERKIN ELMER®). The machine was programmed (Figure 2.1) to give an initial RT step of 30 min at 50 °C. The thermocycling pattern of the PCR reactions consisted of an initial denaturation step at 94 °C for 2 minutes, followed by 35 cycles of denaturation at 94 °C for

30 seconds, annealing at 48 °C for one minute and extension 68 °C for 90 seconds. The PCR was completed by a final extension step of 68 °C for 5 minutes.

Table 2. Oligonucleotide primers used for the amplification and sequencing of part of the 2C protein-encoding region of CAV9.

Oligo name	Sequence (5'-3')
CAV92C5d	AGCCCTCATCGGTTGCACCTCGT
CAV92C3r	GAGTAGATCAGCGATGACAGGTGGT
CAV92Cmf	TGCTCCTACATGGGAGTCCAGGT
CAV92cmr	TCCATCAGGGTTCTGGCATAGGTC

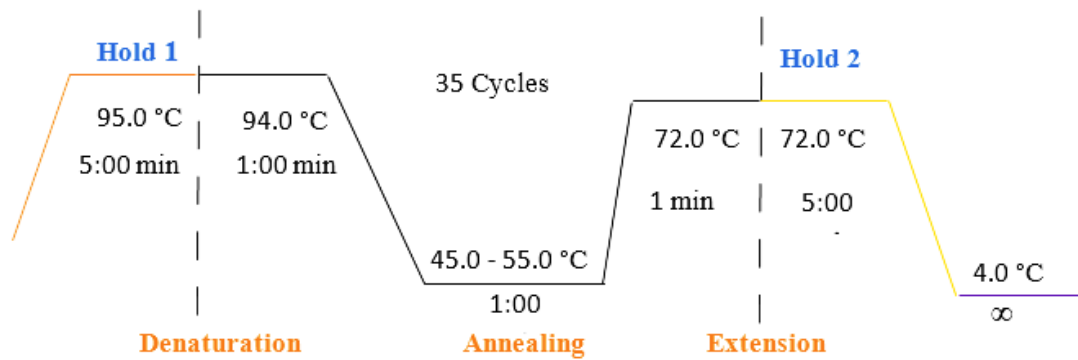


Figure 2-1 Schematic diagram of the PCR amplification component of the RT-PCR reaction.

Following a 50 °C incubation for 30 min to allow reverse transcription, the first denaturation step at 95 °C for 5 minutes is to activate the polymerase enzyme which is followed by 35 cycles of denaturation (94 °C for one minute), annealing (45 °C – 55 °C, 1 min) and extension (72 °C for 1 min). The final extension step takes 5 minutes (72 °C) to complete any incomplete DNA chains.

2.2.3.3 Agarose gel electrophoresis

Agarose powder (0.5 g) was added to 50 ml of 1X Tris-EDTA buffer and heated in a microwave until it was completely dissolved. After cooling down to around 50 °C, Safe View (5 µl) was added and the agarose solution was poured into the gel tray. The gel tray had a comb to form slots. When the gel had set, it was placed in the electrophoresis tank, and enough Tris-EDTA buffer was poured into the tank to cover the gel. The comb was removed. 5 µl of the DNA sample for analysis or 50 µl for purification was mixed with 1 µl or 8 µl respectively of 6x gel loading buffer and each sample was loaded onto the gel. The gel was run for 18 minutes at 118V (using CROSSPOWER 1000, ATTA and FHU6 mini submarine gel, serial number 30025588) and the DNA was viewed using a blue light LED transilluminator (SYNGENE®). Subsequently, a clean scalpel was used to isolate and purify fragments of interest from the gels for DNA sequencing.

2.2.3.4 Gel extraction of DNA

Purification of DNA from agarose gel bands was performed using a QIAquick gel extraction kit (Abraham *et al.*, 2017; Shi *et al.*, 2018). Using a 1.5 ml microcentrifuge tube, each slice of agarose gel containing the DNA of interested component was soaked in 300 µl of QG buffer and incubated at 50 °C until it was completely dissolved. The dissolution was facilitated by vortexing every 2-3 minutes. Isopropanol (100 µl) was added to the tube, mixed and the solution was uploaded to the QIAquick column and centrifuged at 13000 rpm for one min. The flow-through was discarded and the column set back into the same tube. To wash, 750 µl of PE buffer was added and re-centrifuged and the flow-through was discarded. The QIAquick column was placed into a clean 1.5 ml microcentrifuge tube and 50 µl of EB buffer was added. The column was left for up to 4 minutes at room temperature and centrifuged at 13000 rpm for one min to elute the DNA. The tube was labelled and stored at -80 °C.

2.2.3.5 Sequencing of DNA

For DNA sequencing, 2 1.5 ml microcentrifuge tubes were prepared, one of them contained 10 µl of the resultant purified DNA and the other tube contained 3.3 µl of the sequencing primer and 96.7 µl of purified water. The products were sequenced by Source BioScience LifeSciences Company. All results were analysed using the ExPASy-Translate tool (web.expasy.org/translate/), Reverse complement (Reverse-complement.com) and Multiple Sequence Alignment-CLUSTALW (www.genome.jp/tools-bin/clustalw).

2.2.3.6 Antioxidant activity assay

The antioxidant activity in this assay utilizes the spectroscopic absorbance spectra of myoglobin after its reaction with hydrogen peroxide. This reaction oxidises the ferric ions (Fe III) of the myoglobin to ferryl ions (Fe IV) resulting in spectral changes. The highest intensity absorbance of the myoglobin with Fe III ions is usually at the wavelength of 409 nm. Whereas, the highest absorbance of the oxidised myoglobin with Fe IV will be shifted to the wavelength 425 nm. Antioxidant compounds have the capacities of reversing the above process. The rate of the reaction can be monitored kinetically, and the rate depends on the antioxidant power of the compounds (Terashima *et al.*, 2007, 2010, 2012, 2013; An *et al.*, 2014; Morikawa *et al.*, 2015). Firstly, the spectrophotometer (8453 UV-spectrophotometer) was setup at a wavelength of 350-750 nm for spectra trace of myoglobin only (Mb). The kinetics of oxidised myoglobin (ferry-myoglobin) with antioxidant (RC) reaction was followed at two wavelengths 409 nm (highest intensity of the normal myoglobin (ferric-myoglobin) and 420 nm the oxidised myoglobin (the ferryl-myoglobin). The kinetics steps started with filling a cuvette with 3 ml PBS as blank for background correction. Then, cuvettes prepared for the reactions with (according to the number of samples to be tested) were prepared with 3 ml PBS and 30 μ l of PBS was taken from each one. Working solution of myoglobin (Mb) was prepared by adding of (13.5 μ M) Mb working solution was added to the PBS at pH 7.2 and the absorbance was recorded at wavelength of 409 nm. To create a state of oxidative stress, 10 μ l of hydrogen peroxide (H₂O₂, 140 μ M) was added at room temperature. The reaction was terminated after 10 min by adding 2 μ l of catalase enzyme and the absorbance spectra was recorded again after 2 min. The samples that contain AO activity were added and the kinetics of oxidised myoglobin (ferryl-Mb) was followed after addition of antioxidants (RC) at two wavelengths 409 nm and 425. The absorbance of Mb before and after AOs (RC) was recorded at 409. The percentage of myoglobin protection ratio (%MPR) was calculated according to the following calculation:

$$\text{Myo Protective Ratio (MPR) \%} = 1 - \left[\frac{(\text{Abs}^\circ) - (\text{Abs}^{\text{ROS with antiox}})}{(\text{Abs}^\circ) - (\text{Abs}^{\text{ROS No antiox}})} \right] \times 100$$

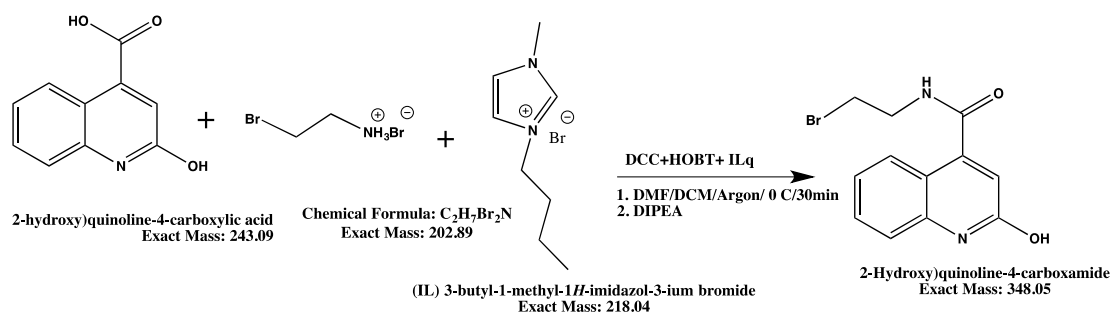
Where (Abs[°]) is absorbance of at myoglobin only at (λ_{409}) and Abs^{ROS} is the absorbance with hydrogen peroxide with/without AO samples.

2.2.4 Methods of synthesis and structural modifications

Modification methods were aimed to improve the antiviral activity of some compounds that were inactive against virus resistant mutants in spite of their activity on parent viruses.

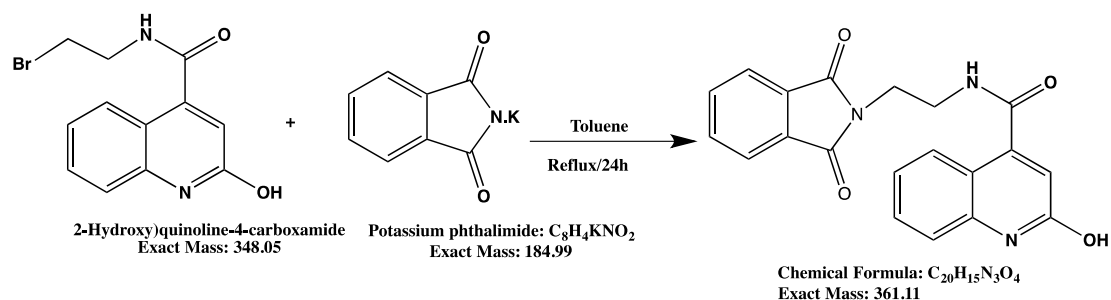
2.2.4.1 Modification of hydroxyquinoline

1- Linker formation



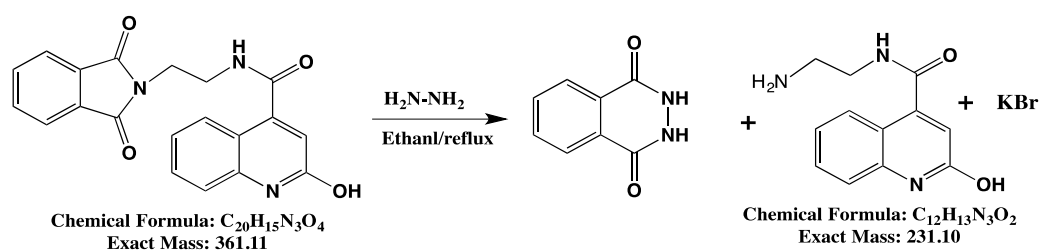
(E)-N-(2-bromoethyl)-2-hydroxy quinoline-4-carboxamide 2-Hydroxy quinoline-4-carboxylic acid (QHC) (1 g, 4.2 mmol) dissolved in DMF (10 ml) with Bromo ethyl amino hydrobromide (1.1 g, 1.2 eq, 4.9 mmol), DCC (0.93 g, 1.1 eq), HOBT (0.61 g, 1.1 eq), and Bmim (0.99 g, 1.1 eq.) were mixed and stirred at 0 °C for 1h. DIPEA was added (1.0 ml, 1.1 eq). The mixture was stirred for 3 h at 0 °C then 18 h at room temperature. The precipitate was filtered off and the solvent was evaporated in vacuum. The residue was dissolved in DCM and washed with water (100 ml) five times. The solvent was evaporated, and the residue was purified by flash chromatography using ethyl acetate/methanol to obtain yellow paste of 987 mg.

2- Conversion of halide group to amino group/Hydroxy quinolone ethyl carboxamide



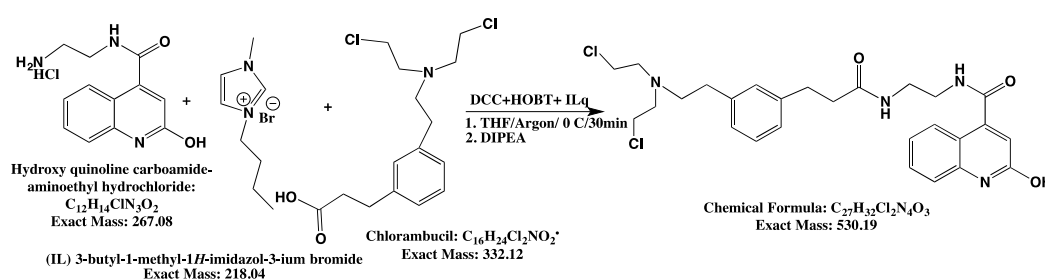
(2-Hydroxy)quinolone-4-carboxamide (1.4 g, 4 mmol) was dissolved in toluene, potassium phthalimide (0.75 g, 4 mmol) was added and the mixture was refluxed for 24 hours. The solvent was evaporated under reduced pressure. The residue was dissolved in DCM and washed with dilute HCl (0.5 M) and water. The solvent then evaporated to yield solid material.

3- Synthesis of N-(2-aminoethyl)-2-hydroxyquinoline-4-carboxamide chlorambucil conjugate



Compound N-(2-(1,3-dioxoisindolin-2-yl)ethyl)-2-hydroxyquinoline-4-carboxamide dissolved in ethanol and hydrazine was added and the mixture was refluxed for one hour. The solvent was evaporated, and the mixture was dissolved in DCM and washed with HCl (1M) the phthalimide.

4- Formation of N-(2-aminoethyl)-2-hydroxyquinoline-4-carboxamide-chlorambucil conjugate



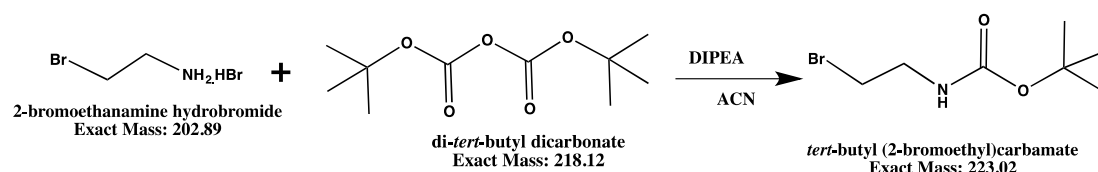
N-(2-aminoethyl)-2-hydroxyquinoline-4-carboxamide (1 g, 3.75 mmol) dissolved in THF (10 ml) with chlorambucil (1.37 g, 1.1 eq.), DCC (0.93 g, 1.1 eq), HOBT (0.56 g, 1.1 eq), and Bmim (09 g, 1.1 eq)), all at once, and the mixture was stirred at 0 °C for 1h. DIPEA (0.81 ml, 1.1 eq.) was added. The mixture was stirred for 3 h at 0 °C then 18 h at room temperature. The precipitate was filtered off and the solvent was evaporated in vacuum.

The residue was dissolved in DCM and washed with water (100 ml) five times. The solvent was evaporated, and the residue was purified by flash chromatography using ethyl acetate/methanol to obtain the compound. The fractions were evaporated and dissolved in acetone. The m/z of quinoline chlorambucil conjugated molecule was confirmed by GC technique to be m/z 530 D.

2.2.4.2 Modification of fluoxetine

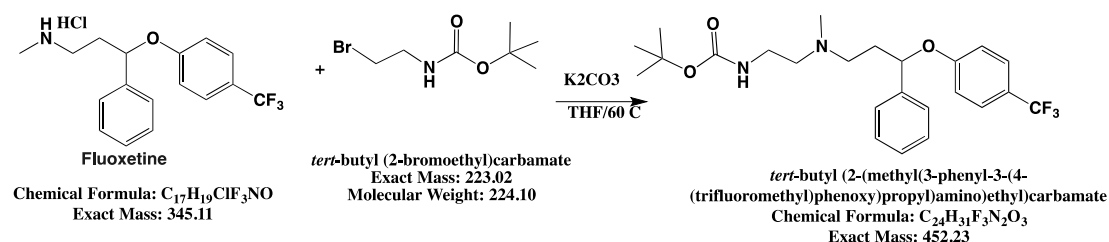
a- Synthesis of Linker amino-BOC protection: *tert*-Butyl (2-bromoethyl) carbamate

In order to reduce the steric hindrance between two conjugated bulky moieties small spacer was prepared to link between them.



The compound (2-bromoethanamine hydrobromide, 5 g, 0.025 mol) dissolved in acetonitrile (50 ml) and di-*tert*-butyl dicarbonate (8.09g, 0.037 mol, 1.5 eq) was added with stirring at 0 °C on an ice-bath. DIPEA (5.3 ml, 0.041 mol, 1.2 eq) was added drop-wise over 30 min. The mixture was stirred for 2 h on an ice-bath, then 18 h at room temperature. The solvents were evaporated under reduced pressure and the residue was dissolved in DCM (50 ml) then washed three times with water. The solvent then was evaporated in vacuum.

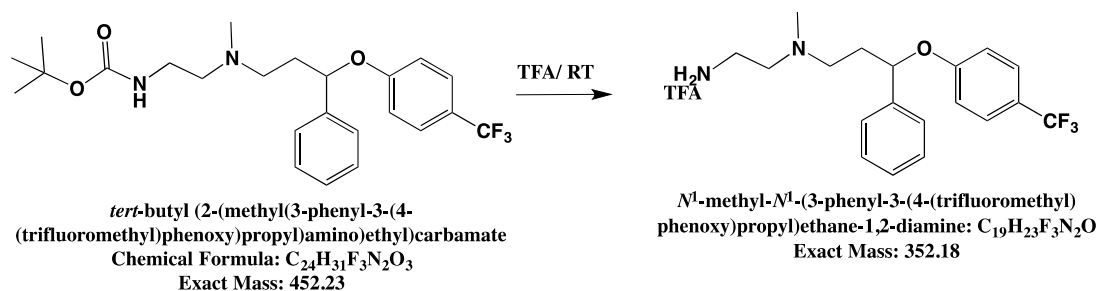
b- Formation of fluoxetine N-BOC Ethyl linker



Fluoxetine (0.2 g, 0.57 mmol) dissolved in acetonitrile (50 ml) under argon. Anhydrous potassium carbonate (2 g) and N-BOC ethyl bromide were added to the above solution. The mixture was refluxed for 18h. The solvent was then evaporated, and the residue was

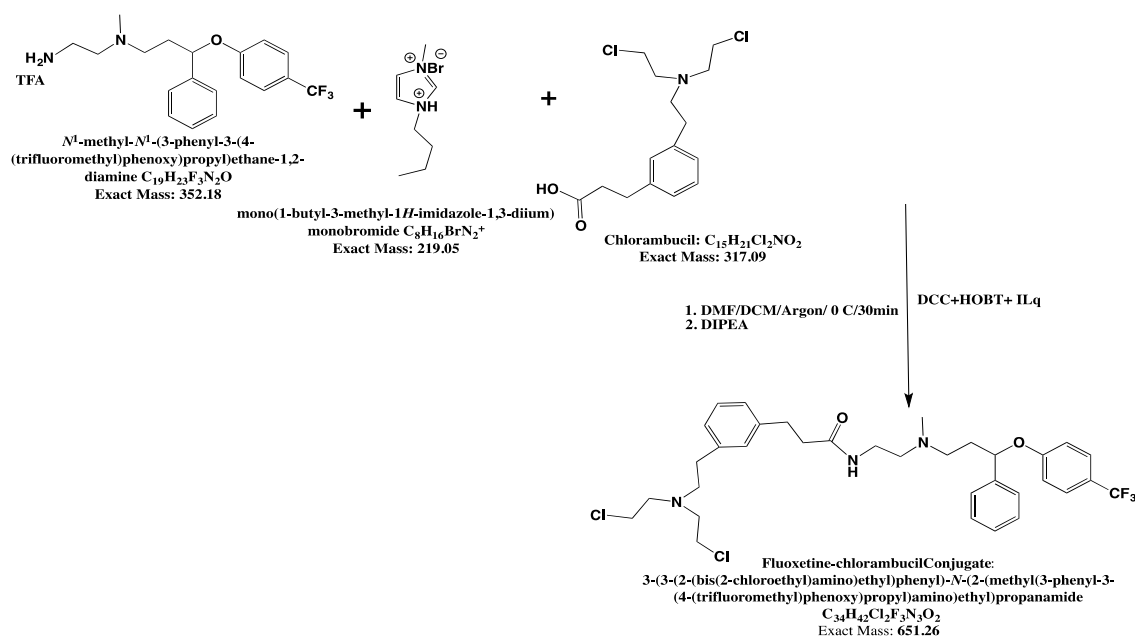
dissolved in 50 ml of DCM and washed several times with water. The organic layer was evaporated to yield the impure linker, which had the appearance of a yellow paste.

c- Fluoxetine-linker amino group deprotection/BOC Cleavage



Fluoxetine-N-BOC ethyl (0.2 g) dissolved in 20 ml of trifluoroacetic acid (TFA). The solution was stirred at room temperature for 1 h. The excess of TFA was evaporated under reduced pressure to yield a yellow paste.

d- Formation of fluoxetine-chlorambucil conjugate



N-(2-aminoethyl)-fluoxetine (0.15 g, 0.43 mmol) dissolved in THF (10 ml) with chlorambucil (0.14 g, 1.1 eq.), DCC (0.13g, 1.1 eq), HOBT (0.16 g, 1.1 eq), and Bmim (0.15 g, 1.1 eq)) were combined and the mixture was stirred at 0 °C for 1 h. DIPEA (0.11 ml, 1.1 eq) was added. The mixture was stirred for 3 h at 0 °C then 18 h at room temperature. The precipitate was filtered off and the solvent was evaporated in vacuum. The residue was dissolved in DCM and washed with water (50 ml) five times. The solvent was evaporated,

and the residue was purified by flash chromatography using ethyl acetate/methanol to obtain a yellow residue. The residue was purified by flash chromatography using DCM and methanol as the mobile phase with a gradient over 1 h. The fraction at 12 min gave the correct product and this was confirmed to have the correct mass of 651 dalton using analytical gas chromatography-mass spectroscopy.

2.2.5 Redcurrant extracts

2.2.5.1 Extraction methods

Initially, crude RC extracts were made using four different methods:

1- Refluxing: Red currants (RC, 500 g) were placed with 500 ml of ultrapure water in a glass round bottom flask connected to a condenser. The mixture was refluxed for 1 h then the residue was filtered off through several Whatman® filter papers. The filtrate was freeze-dried and yielded 7 g of red, solid gum.

2- Room temperature direct filtration: The RC (500 g) were soaked in water for 2 h at room temperature then blended slightly with an electric blender (monilex blender). The mixture was filtered through Whatman® filter papers and the filtrate was frozen dried to yield 4 g of red gum.

3- Sonication: RC was blended with an equivalent amount of water and placed in a sonicator (by applying agitated energy to the sample) at room temperature for 30 min and solid materials was filtered off. The water was evaporated by freeze-drying to yield 5 g as a red gum.

4- Solid-liquid phase extraction: The residue that was filtered off after reflux and sonication (about 300 g of each) were placed separately in the thimble of a Soxhlet apparatus for solid-liquid phase extraction. Reflux was continued for 3 h using the organic solvents, dichloromethane (300 ml) and methanol (200 ml). The organic solvents were evaporated under vacuum to yield 2 g of yellowish oily paste of each one.

The antiviral activity of each of these extracts was examined. Refluxed RC extract showed much more antiviral activity and was not toxic on cells. Therefore, all subsequent extraction processes were done by reflexing.

2.2.5.2 Fractionation methods of redcurrant

The crude RC extract was fractionated to try to purify the active molecules. The fractionation was carried out using automated flash chromatography (*puriFlash*® 430, Interchim, France) on a reversed phase C18 column (*puriFlash*®, Interchim, France, 30 µ,

40 bar). The crude extract was fractionated and monitored at two wavelengths (230 and 270 nm, the highest absorbance peaks of the extract) with a gradient mobile phase of 0.1 % trifluoroacetic acid in aqueous acetonitrile and flow rate of 40 ml/min. The chromatography was initially run with water 100 % and acetonitrile was then introduced and increased gradually. The cartridge was finally flushed with 100% acetonitrile. Fractions within peaks and between peaks were all collected separately. The organic solvents of each fraction were evaporated at reduced pressure at 30 °C using a rotary evaporator (BUCHI®, vacuum pump V-710 and water bath B-480) and the water was evaporated with freeze drier (MINI LYOTRAP®, LTE Scientific). The fractions were kept at -20 °C for further analysis and biological testing on viruses.

2.2.5.3 Analytical analysis of the fractionated RC samples with HPLC

High performance liquid chromatography (Agilent, 1100 series, UK) was used to analyse fractions in terms of number of bands contained in each fraction and to optimise the eluent system for the further fractionation procedures. The HPLC was run with a reversed phase C18 cartridge (Waters, 100x 2.1 mm). The fractions were monitored at 4 wavelengths (230 and 270, 400 and 520 nm) with both isocratic and gradient mobile phase of 0.1 % trifluoroacetic acid in aqueous acetonitrile and flow rate of 0.25 ml/min. After eluent system optimisation, the run was initiated with 95 % acetonitrile in the aqueous mobile phase and the percentage of water was increased by 20% until 100% and ended with 95% of acetonitrile in aqueous solution.

2.2.5.4 Analytical analysis of the fractionated RC samples with LC-MS/MS

A- Reversed-phase high-performance liquid chromatography

A Micromass Quattro microTM (Waters®) Mass Spectrometer coupled with a Waters ACQUITY Ultra Performance LCTM (Manchester, UK) was used for LC-MS/MS analytical procedures. A reversed-phase Waters column (150 mmx2.1mm i.d. and particle size 4 µm) and mobile phase of A: trifluoroacetic acid (TFA)-water, 0.1% and B: TFA-acetonitrile, 0.1% were used after optimization for better resolution. Three standards were used, quercetin, quercetin 3-glucoside, and keracynin hydrochloride. 5 µl volumes of standards solutions (50 µg/l) and RC samples were injected. The chromatograms with complete spectral data were monitored and recorded in the range 200-800 nm. The applied

elution condition for each cycle was: 95 % of ACN in water for the first 5 minutes and then a gradient concentration of ACN, 95% to 70%, for another 5 minutes. After that, the gradient concentration of ACN was decreased from 70% to 50 % for 10 minutes and further from 50% to 10 % for 10 minutes. The isocratic concentration of 10 % was continued for 5 minutes and the elution processes were ended by using a 95 % ACN concentration for 5 minutes to prepare the system for the next elution cycle.

B- Mass spectrometry

Spectral mass analysis was obtained on a Micromass (waters/ UK) Quattromicro triple quadrupole mass spectrometer coupled at the exit of the diode array detector and equipped with a Z-spray ESI source. A flow of 250 $\mu\text{l}/\text{min}$ from the DAD eluent was directed to the ESI interface using a flow-splitter. The source block temperature was held at 120 °C and the desolvation gas (nitrogen gas) temperature was 350 °C. The flow rate of 650 l/h, and cone gas of 82 l/h was used. The capillary potential of 3.2 kV was used. MS spectra recorded between m/z range 100-1500, in the positive mode at different cone voltages (CV) (15, 30 and 45 V, and 60V). Parent and daughter ions spectra were also recorded using argon as collision gas at 1.5×10^{-3} mbar and different collision energies (CE) in the range 5-40 eV.

Chapter 3: Antiviral Activity of Fluoxetine and Functionally Related Compounds

3.1 Introduction

In addition to development of anti-picornavirus drugs based on inhibition of specific virus targets such as 3C^{pro} or 3D^{pol}, screens of libraries of drugs developed, approved and widely-used for treatment of other conditions have identified potentially useful compounds (van der Linden *et al.*, 2015; Bauer *et al.*, 2017). The information already available on these compounds could shorten the time needed to progress to clinical trials and approval for their repurposing as anti-picornavirus drugs, making this an attractive approach (Bauer *et al.*, 2017).

Investigation of the potential usefulness of a group of drugs or compounds that could be repurposed in this way is challenging in many ways. For instance, identifying the basis of their antiviral activity and finding if it is related to the mechanism of action exploited to achieve its original purpose. Secondly, are there common features among this drug group that is expected to give them similar antiviral activity? Potential side-effects and how quickly the virus can develop resistance against the drugs could finally prevent their repurposing.

The aim of the work included in this chapter is to investigate the antiviral activities of several drugs that have been used for a long time in other medical areas. These drugs include fluoxetine, a selective serotonin re-uptake inhibitor, and several related drugs namely imipramine, a tricyclic antidepressant, promethazine, a neuroleptic and antihistamine agent, and dibucaine, a topical anaesthetic. Although all these mentioned drugs are from different chemical families, they all share some similar properties. For instance, all 4 are considered to be GPCR inhibitors. Dibucaine, imipramine and promethazine were found to be effective against Ebola and Marburg viruses *in vitro* (Cheng *et al.*, 2015), while both fluoxetine and dibucaine have been found to inhibit some enteroviruses by binding to the 2C protein (Ulferts *et al.*, 2016). The work also includes the selection and analysis of drug resistant mutants (DRMs) that could help in determining the mechanism of the antiviral activity of active compounds and how rapidly the virus develops these mutants. There will also be an attempt to structurally modify some active drugs to make them more effective and reduce the possibility of generating DRM viruses.

3.2 Results

3.2.1 Inhibition of CAV9 infection by fluoxetine

Antiviral activity of fluoxetine was previously confirmed against CBV types 1, 2 and 3 (Zuo *et al.*, 2012). In addition, it is found that fluoxetine inhibits members of other EVB species members including echovirus 1 (E-1), E-9 and E-11, as well as EVD members EV70 and EV68. However, no antiviral activity was detected against EVA, EVC, RVA or RVB species (Ulferts *et al.*, 2013). So, there are key differences in the response to fluoxetine between enteroviruses. CAV9 is closely related to CBV3 and also belongs to EVB, so it is likely also to be inhibited by fluoxetine. To investigate this, a plaque reduction assay in the presence of different concentrations of fluoxetine (Figure 3.1) was firstly performed. The results showed a dose dependent effect and complete inhibition of virus growth at 0.05 mM concentration. The effect of the drug alone on the cell monolayer seemed insignificant, as there was no clear difference in the staining of the treated cells in comparison to untreated, control cells (data not shown). This was confirmed using an MTT cell viability assay (Figure 3.2). This showed some toxicity at lower fluoxetine concentrations, but a continuous increase in cell viability above 0.01 mM, reaching 100 % at the concentration seen to be 100 % effective for CAV9 inhibition (0.05 mM) and exceeding 100 % (i.e. some stimulation of growth) at 0.1 mM. To further confirm the effects of fluoxetine (0.05 mM), a flow cytometry approach was used which identifies healthy and damaged/apoptotic cells using propidium iodide. Figure 3.3 clearly shows that fluoxetine was very active toward CAV9 infection and lacked cell toxicity. The proportion of apoptotic cells in the presence (Figure 3.3B) of fluoxetine is at the background level seen in the cell-only sample (Figure 3.3A). Virus infection (Figure 3.3C) greatly increases the proportion of apoptotic cells, but this is reduced in the presence of fluoxetine (Figure 3.3D). The results suggest that fluoxetine could be a useful, non-toxic drug for CAV9 infections.

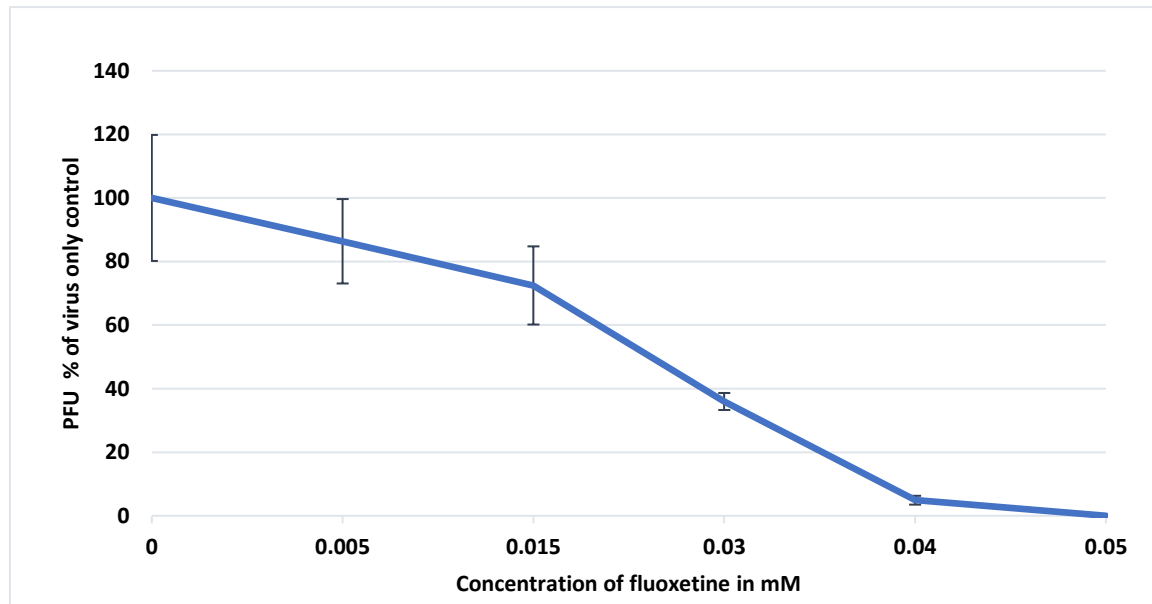


Figure 3-1. Inhibition of CAV9 infection by fluoxetine.

GMK monolayers in a 6 well plate were pre-treated with different concentrations of fluoxetine in 0.5 ml of culture medium for 30 minutes. 370 PFU (in 15 μ l medium) of CAV9 were added and the cells were incubated on a rocking platform for 45 minutes at room temperature. 2 ml of a 2:1 mixture of culture medium and 2% CMC were added, and the plate were incubated for 3 days in a humidified CO₂ incubator at 37 °C. The medium was discarded, and cells were washed and stained with crystal violet solution. The number of plaques were counted and expressed as a % of the number seen in the mock-treated (no drug) control. Error bars show standard error from 3 independent experiments.

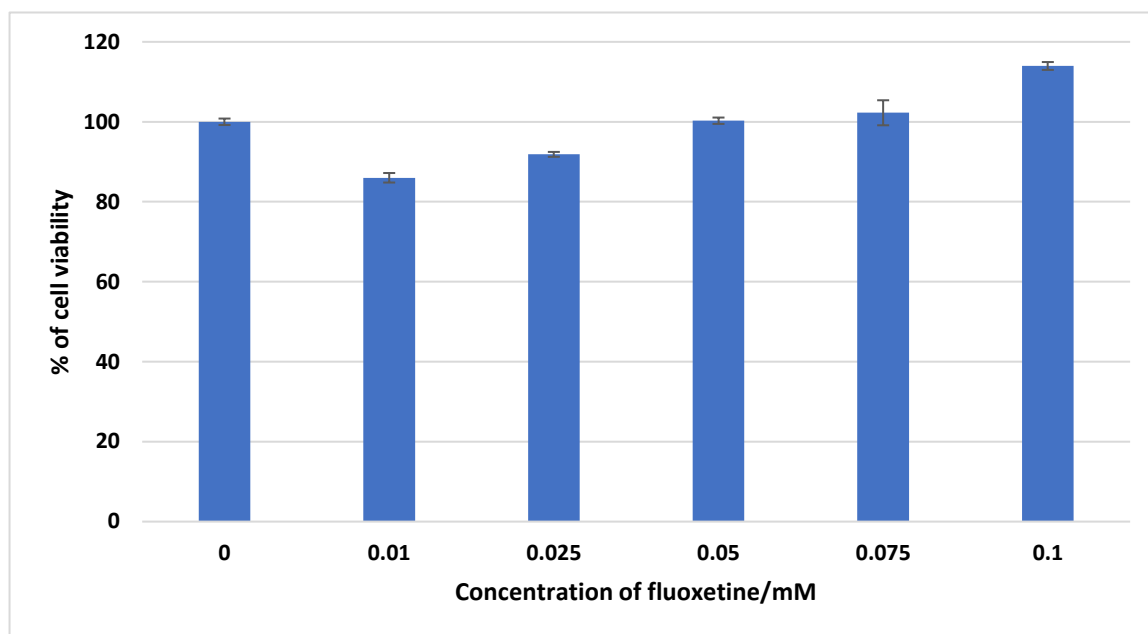


Figure 3-2. Cytotoxic effect of different fluoxetine concentrations on A549 cells.

A549 monolayers were pre-treated with different concentrations of fluoxetine in 0.5 ml of culture medium for 30 minutes and the cells were incubated on a rocking platform for 30 minutes at room temperature. 1 ml of a 2:1 mixture of culture medium and 2% CMC were added, and the plate were incubated for 2 days in a humidified CO₂ incubator at 37 °C. The medium was discarded, and cells were washed and 1 mg/ml of MTT in media were applied for 2 h, the resulting blue crystals were dissolved in DMSO and absorbance at λ_{550} was recorded. The cell viabilities were calculated as percentages of the control of cells alone.

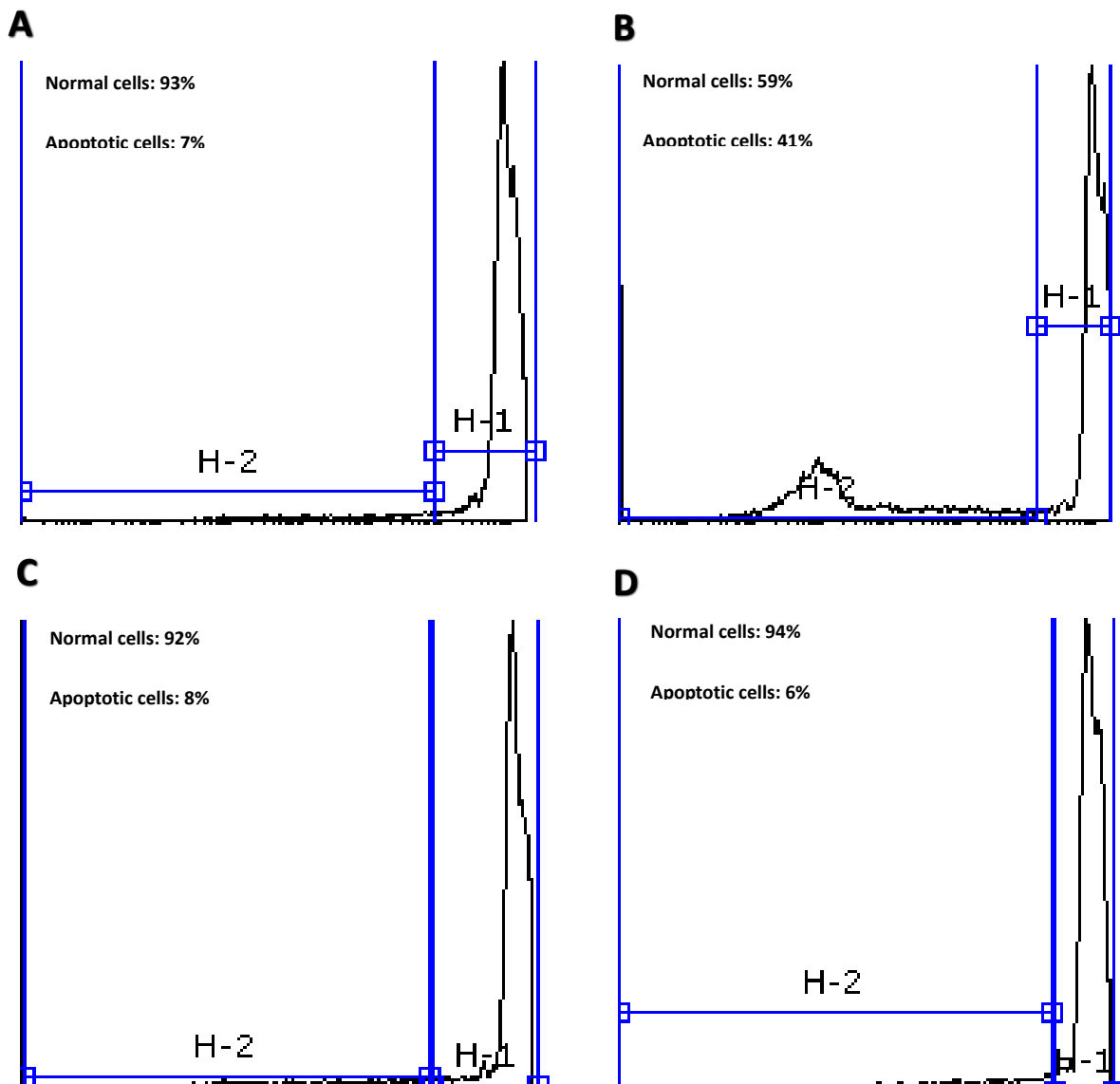


Figure 3-3. Flow cytometry analysis of the effect of fluoxetine on GMK cells and on CAV9 infection.

Cells in wells of a 24 well plate were treated with fluoxetine (50 μ M [0.05 mM]) in cell medium or only cell medium, and either undiluted CAV9 (100,000 PFU) or just medium for 12 hours. Then cells were washed, trypsinized with propidium iodide (PI). They were then analysed by flow cytometry. Gating was used to define an apoptotic or damaged cell population (H-2) and a normal cell population (H-1). Y-axis: cells count. X-axis: fluorescence intensity. A: Control (cells only), B: Cells with virus, C: Cells with fluoxetine, D: Cells with fluoxetine and virus.

3.2.2 The effects of imipramine and promethazine on CAV9

Imipramine and promethazine along with fluoxetine are GPCR inhibitors and it has recently been found that several GPCR inhibitors blocked infection by some viruses including Ebola virus (Cheng *et al.*, 2015). This means that these could be useful agents against CAV9 and other EVs. Beside fluoxetine, two of these GPCR inhibitors namely, imipramine (Dempsey *et al.*, 2005) and promethazine (El-Shehabi *et al.*, 2012) were used to investigate if they have an effect on CAV9 infection. Plaque reduction experiments were performed for imipramine and promethazine at concentrations ranged from 0.03 mM up to 0.09 mM (Figures 3.4 to 3.7). It can be seen that imipramine did not block infection, at these concentrations, in fact the infection seemed to be enhanced by pre-treatment with these drugs (Figure 3.4). Visual appearance of the monolayers did not reveal toxicity of imipramine. When the concentration of imipramine was increased to 0.2 mM, surprisingly inhibition of CAV9 infection (around 85%) was seen (Figure 3.5). A cell viability assay for imipramine (Figure 3.6) revealed that it was not toxic even at the higher concentration of 0.2 mM, in which the viability was up to 90% of the control. Promethazine also did not inhibit, and again stimulated, CAV9 infection at 0.03 mM up to 0.09 mM (Figure 3.7). There was no inhibition at a concentration of 0.2 mM (data not shown).

3.2.3 Inhibition of CAV9 infection by dibucaine

Like fluoxetine, dibucaine was found to inhibit several enteroviruses, including CBV3, EV68 and to a lesser extent EV71 (Zuo *et al.*, 2012). To see the effect on CAV9, a direct plaque assay was applied (Figure 3.8) and dibucaine caused a decrease in infectivity above 0.01 mM, and complete inhibition of virus growth at 0.04 mM. It had no serious effect on the cell monolayer judged visually. However, a viability assay (Figure 3.9) showed dose dependent toxicity started as low as 0.01 mM and caused cell viability to be reduced to less than 60% at the 0.04 mM concentration.

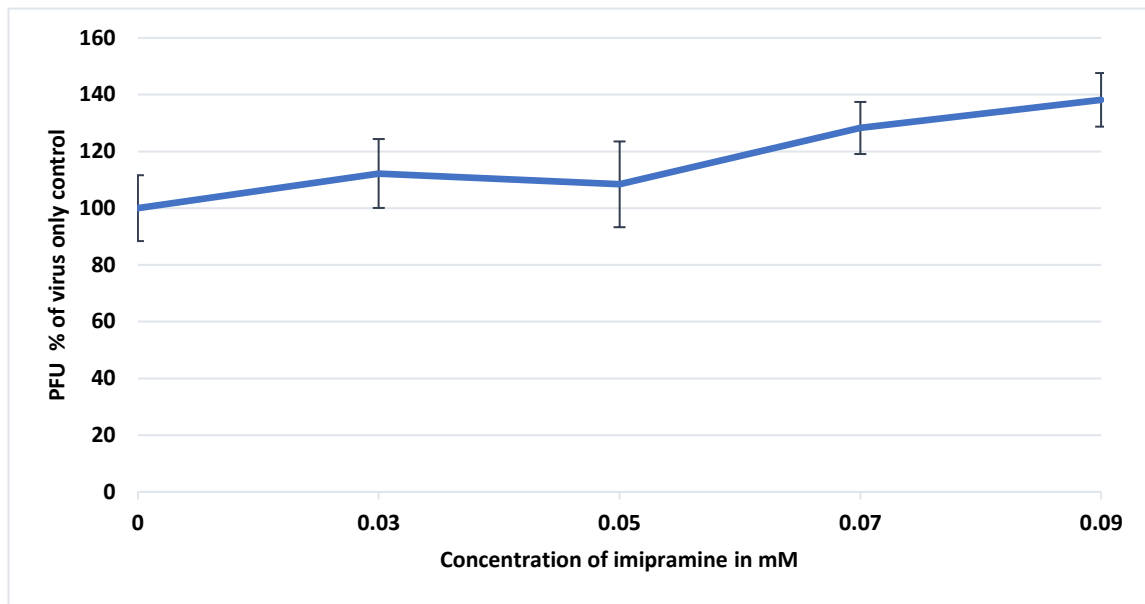


Figure 3-4. The effect of imipramine on CAV9 infection.

GMK monolayers in a 6 well plate were pre-treated with different concentrations of imipramine in 0.5 ml of culture medium for 30 minutes. 370 PFU (in 15 μ l medium) of CAV9 were added and the cells were incubated on a rocking platform for 45 minutes at room temperature. 2 ml of a 2:1 mixture of culture medium and 2% CMC were added, and the plate was incubated for 3 days in a humidified CO₂ incubator at 37 °C. The medium was discarded, and cells were washed and stained with crystal violet solution. The number of plaques were counted and expressed as a % of the number seen in the mock-treated (no drug) control. Error bars show standard error from 3 independent experiments.

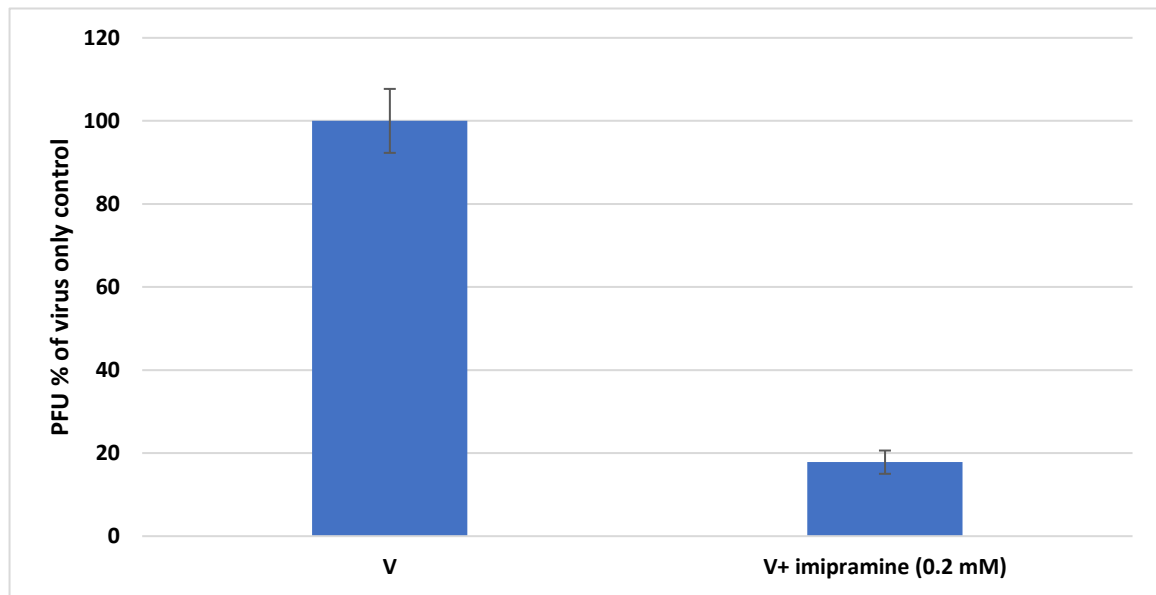


Figure 3-5. The effect of imipramine on CAV9 infection.

A549 monolayers were pre-treated with imipramine at a concentration of 0.2 mM in 0.5 ml of culture medium for 30 minutes or 0.5 ml of culture medium. 370 PFU (in 15 μ l medium) of CAV9 were added and the cells were incubated on a rocking platform for 45 minutes at room temperature. 2 ml of a 2:1 mixture of culture medium and 2% CMC were added, and the plate were incubated for 3 days in a humidified CO₂ incubator at 37 °C. The medium was discarded, and cells were washed and stained with crystal violet solution. The number of plaques were counted and expressed as a % of the number seen in the mock-treated control. Error bars show standard error from 3 independent experiments. V, virus.

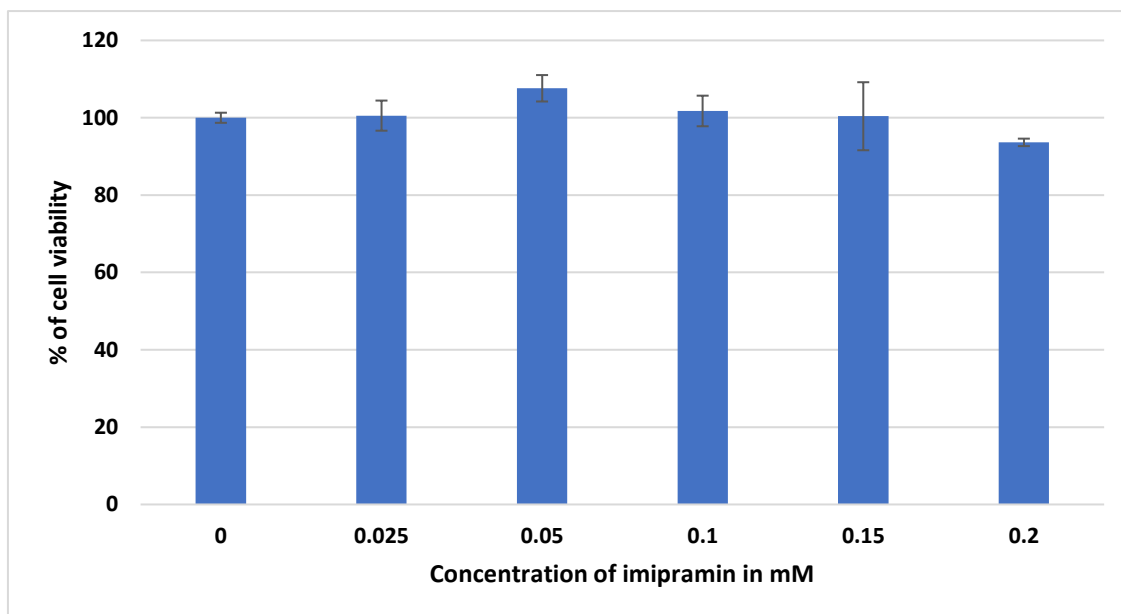


Figure 3-6. Cytotoxic effect of different imipramine concentrations on A549 cells.

A549 monolayers were pre-treated with different concentrations of imipramine in 0.5 ml of culture medium for 30 minutes and the cells were incubated on a rocking platform for 30 minutes at room temperature. 1 ml of a 2:1 mixture of culture medium and 2% CMC were added, and the plate was incubated for 2 days in a humidified CO₂ incubator at 37 °C. The medium was discarded, and cells were washed and 1 mg/ml of MTT in media were applied for 2 h, the resulting blue crystals were dissolved in DMSO and absorbance at λ_{550} was recorded. The cell's viabilities were calculated as percentages of the control of cells alone.

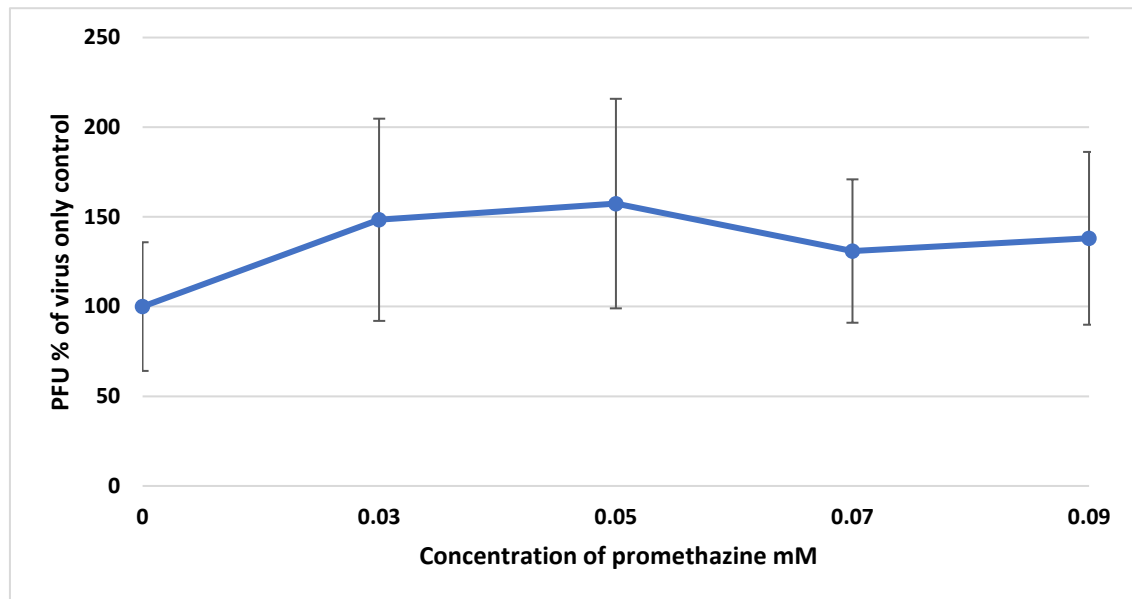


Figure 3-7. The effect of promethazine on CAV9 infection.

GMK monolayers in a 6 well plate were pre-treated with different concentrations of promethazine in 0.5 ml of culture medium for 30 minutes. 370 PFU (in 15 μ l medium) of CAV9 were added and the cells were incubated on a rocking platform for 45 minutes at room temperature. 2 ml of a 2:1 mixture of culture medium and 2% CMC were added, and the plate was incubated for 3 days in a humidified CO₂ incubator at 37 °C. The medium was discarded, and cells were washed and stained with crystal violet solution. The number of plaques were counted and expressed as a % of the number seen in the mock-treated (no drug) control. Error bars show standard error from 3 independent experiments.

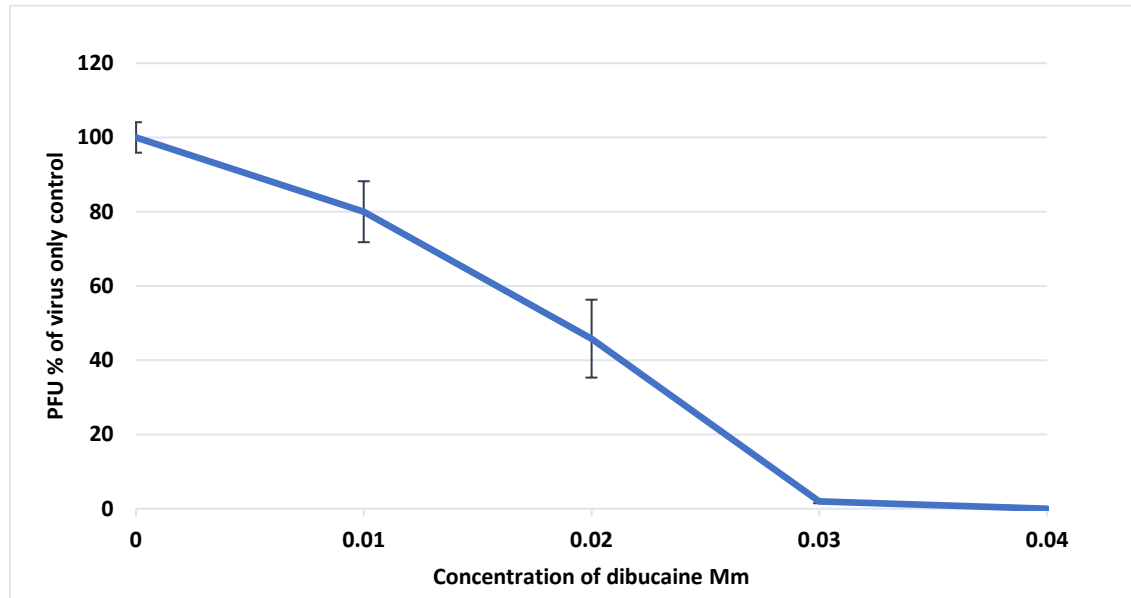


Figure 3-8. Inhibition of CAV9 by dibucaine.

GMK monolayers in a 6 well plate were pre-treated with different concentrations of dibucaine in 0.5 ml of culture medium for 30 minutes. 370 PFU (in 15 μ l medium) of CAV9 were added and the cells were incubated on a rocking platform for 45 minutes at room temperature. 2 ml of a 2:1 mixture of culture medium and 2% CMC were added, and the plate were incubated for 3 days in a humidified CO₂ incubator at 37 °C. The medium was discarded, and cells were washed and stained with crystal violet solution. The number of plaques were counted and expressed as a % of the number seen in the mock-treated (no drug) control. Error bars show standard error from 3 independent experiments.

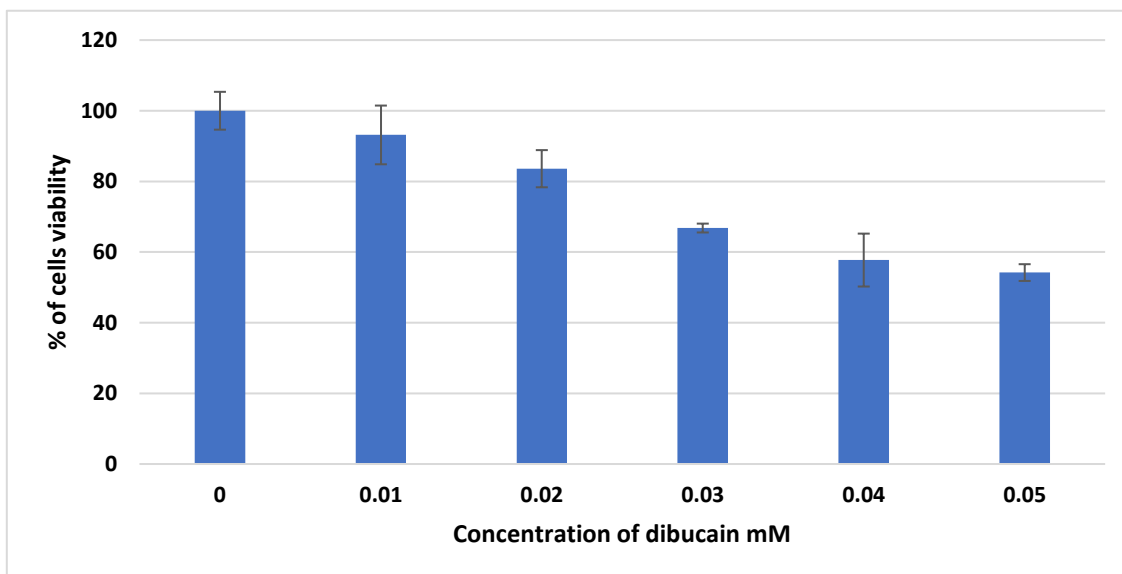


Figure 3-9. Cytotoxic effect of different dibucaine concentrations on A549 cells.

A549 monolayers were pre-treated with different concentrations of dibucaine in 0.5 ml of culture medium for 30 minutes and the cells were incubated on a rocking platform for 30 minutes at room temperature. 1 ml of a 2:1 mixture of culture medium and 2% CMC were added, and the plate were incubated for 2 days in a humidified CO₂ incubator at 37 °C. The medium was discarded, and cells were washed and 1 mg/ml of MTT in media were applied for 2 h, the resulting blue crystals were dissolved in DMSO and absorbance at λ_{550} was recorded. The cell viabilities were calculated as percentages of the control of cells alone.

3.2.4 Drug sensitivity and analysis of the drug resistant mutants

3.2.4.1 Generation of CAV9 mutants resistant to fluoxetine

Although fluoxetine anti-CAV9 activity and cell tolerability were clearly confirmed in this study, drug resistance is a large problem in the use of antiviral drugs. CBV3 mutations in the viral 2C protein were previously reported to give resistance to the drug TBZE-029 (de Palma *et al.*, 2006). A CBV3 mutant carrying these mutations, A224V, I227V and A229V was also found to be resistant to fluoxetine (Ulferts *et al.*, 2013). To investigate if similar or different mutations give resistance of CAV9 to fluoxetine, the virus was propagated in the presence of increasing concentration of fluoxetine. The emergence of resistant mutants occurred after 9 passages, when the virus was propagated at a fluoxetine concentration of 0.04 mM. Resistant viruses were picked and propagated. Plaque assays of the original and mutant viruses showed a clear difference in the presence and absence of 0.05 mM fluoxetine (Figure 3.10). It can be seen that the original virus was almost completely inhibited by fluoxetine as only a few tiny plaques were seen compared to the sample without fluoxetine. In contrast, the drug resistant mutants showed almost equal numbers of plaques in the presence and absence of fluoxetine, although the ones in the presence of fluoxetine were smaller than those in its absence, suggesting that resistance was not complete.

3.2.4.2 Cross resistance of fluoxetine with dibucaine

The presence of cross resistance between compounds means in many cases that they have similar mechanism of antiviral activity. In order to predict if other investigated compounds used in study have similar antiviral activity as fluoxetine, some of the selected mutants from CAV9 against fluoxetine were tested with dibucaine (Figure 3.10). Using a direct plaque assay, it can be seen that the original virus was completely inhibited by dibucaine as no plaques were seen compared to the sample without dibucaine (Figure 3.10), while the drug resistant mutants showed some but otherwise fewer of plaques in the presence of dibucaine, indicating partial resistance.

3.2.4.3 The sequence of the selected CAV9 mutants

Sequencing of part of the 2C-encoding region of CAV9 of six selected mutants showed mutation of the same amino acid isoleucine which was converted to valine at position 227 (I227V) (Figure 3.11). This mutation seemed to come from a complete conversion of an ATA codon to GTA codon as shown in Figure 3.12. In addition, there was another mutation

seen in mutant 4 (Figure 3.11), conversion of glycine present in the original virus into serine (G258S) in mutant 4. This mutant seemed to show a little more resistance than the others to fluoxetine. However, the G258S mutation does not seem to have a major role in the mechanism of virus resistance.

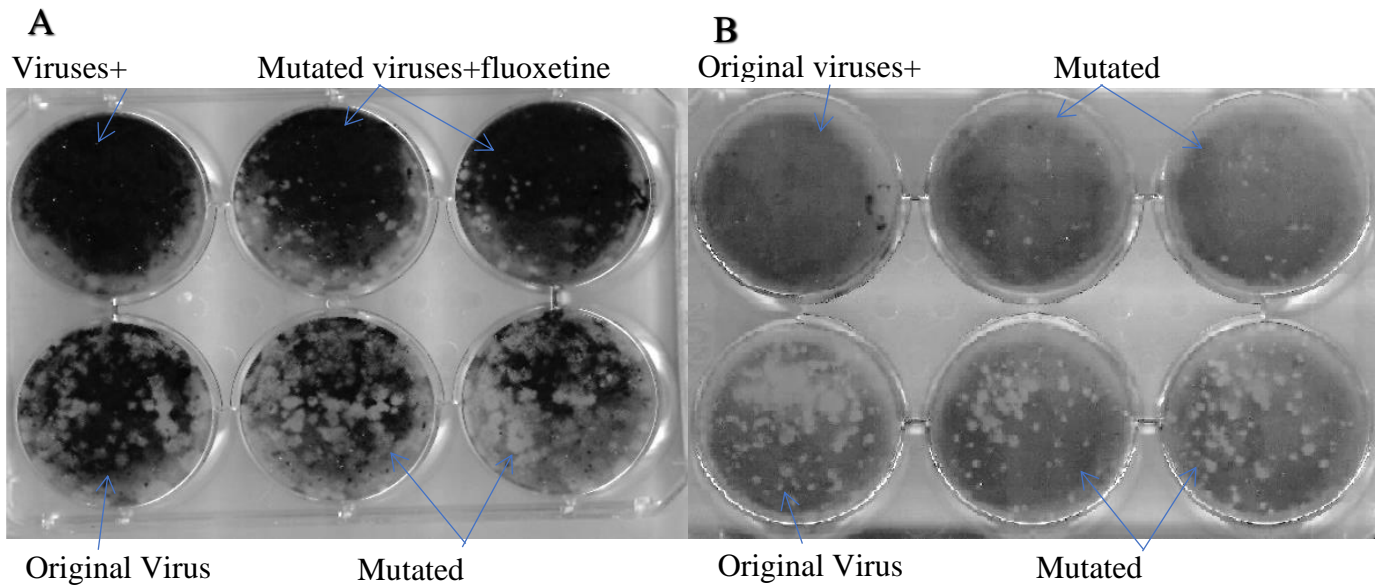


Figure 3-10. The effect of fluoxetine and dibucaine on two CAV9 fluoxetine-resistant mutants and the original CAV9 using a direct plaque assay.

Cells were pre-treated with (A) fluoxetine 0.05 mM and (B) dibucaine 0.04 mM before adding the viruses, then direct plaque assay was applied. The mutated viruses are resistant to fluoxetine, and to less extent to dibucaine.

```

CAV9      LASTNAGS I NAPTVSDSRALARRFHFD MNIEVISMY SQNGKINMPMSVKTCD EEECCPVNF
Mutant1   LASTNAGS V NAPTVSDSRALARRFHFD MNIEVISMY SQNGKINMPMSVKTCD EEECCPVNF
Mutant2   LASTNAGS V NAPTVSDSRALARRFHFD MNIEVISMY SQNGKINMPMSVKTCD EEECCPVNF
Mutant3   LASTNAGS V NAPTVSDSRALARRFHFD MNIEVISMY SQNGKINMPMSVKTCD EEECCPVNF
Mutant4   LASTNAGS V NAPTVSDSRALARRFHFD MNIEVISMY SQNSKINMPMSVKTCD EEECCPVNF
Mutant5   LASTNAGS V NAPTVSDSRALARRFHFD MNIEVISMY SQNGKINMPMSVKTCD EEECCPVNF
Mutant6   LASTNAGS V NAPTVSDSRALARRFHFD MNIEVISMY SQNGKINMPMSVKTCD EEECCPVNF

*****:*****.*****

```

Figure 3-11. Amino acid sequence alignment of 6 selected CAV9 fluoxetine-resistant mutants in comparison to the original virus by partial sequencing of the 2C protein.

All the mutants showed the same mutation (I>V), while Mutant 4 shows an additional mutation of G>S. The I>V mutation is at position 227 in CAV9 2C. CAV9 is the original virus and Mutants1-6 are the selected mutant viruses.

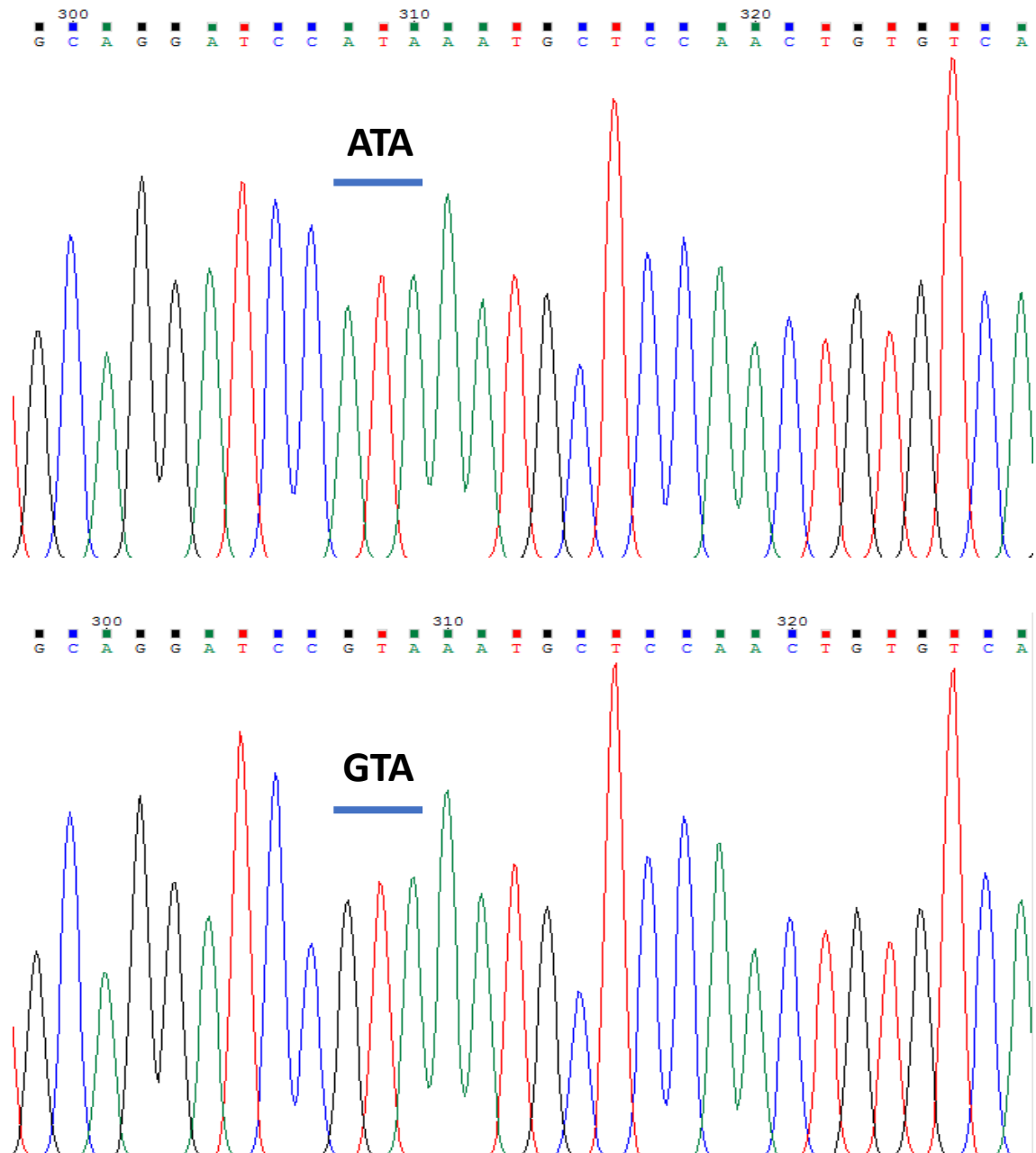


Figure 3-12. The nucleotide sequence of the one selected CAV9 mutant (bottom, mutant 2) in comparison with the original virus (top) in the region of the I>V mutation.

The program Chromas was used to show the raw output from the sequence analysis. The Chromas trace shows that there has been complete conversion of the ATA codon (encoding isoleucine [I]) to GTA (encoding valine [V]).

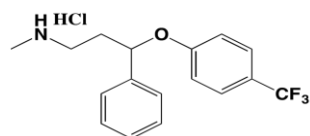
3.2.5 Modification of fluoxetine and dibucaine to generate potential new drugs

Although fluoxetine and dibucaine were active against CAV9, such activity was largely absent with the resistant mutants. Therefore, as a first attempt to improve the antiviral activity, and possibly overcome the problem of the selection of resistant mutants, modifications were made. Fluoxetine was conjugated to the nitrogen mustard drug chlorambucil (Figure 3.13). Coupling was through an amide bond and achieved through a multi-step process described in section 2.2.4.2. The final fluoxetine-chlorambucil conjugate (Fl-Ch) is 3-(3-(2-(bis(2-chloroethyl)amino)ethyl) phenyl)-3-(4-(trifluoromethyl) phenoxy) propyl)amino) ethyl)propenamide.

To start to explore how dibucaine could be modified to generate novel anti-virus compounds, 2-hydroxyquinolin 2-4-carboxylic acid (the core structure of dibucaine) (Figure 3.14) was linked to a butene group, an unsaturated hydrocarbon to give the compound (E)-2-(but-2-en-1-yloxy) quinoline-4-carboxylic acid (QHB).

3.2.6 Antiviral activity of QHB and Flu-Buc

Both QHB and Fl-Ch activities were measured by direct plaque assay. In the case of QHB (Figure 3.15), there was no inhibition of the virus. In fact, there seemed to be some stimulation of virus growth as plaque numbers increased steadily with increasing drug higher concentration, up to 60% at 1 mM. The inhibition effect of the fluoxetine-based Fl-Ch compound (Figure 3.16) was more promising and inhibition was complete at 0.3 mM, but this is 10 times the concentration of fluoxetine needed to achieve similar inhibition (Figure 3.1).

Fluoxetine**Fluoxetine-chlorambucil conjugate: (Fl-Ch)**

3-(3-(2-(bis(2-chloroethyl)amino)ethyl)phenyl)-N-(2-(methyl(3-phenyl-3-(4-(trifluoromethyl)phenoxy)propyl)amino)ethyl)propanamide

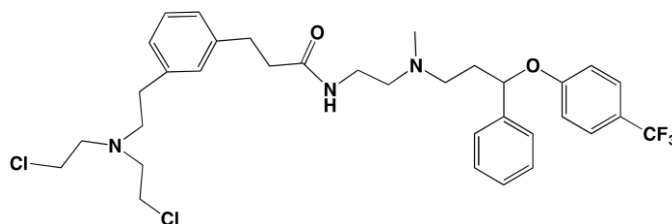
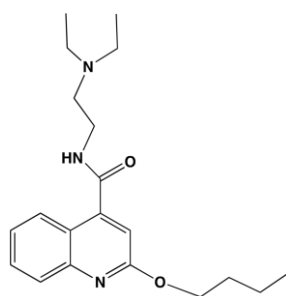


Figure 3-13. Chemical structure of the original drug (fluoxetine) and fluoxetine conjugate fluoxetine-chlorambucil (Fl-Ch).

Dibucaine

2-butoxy-N-(2-(diethylamino)ethyl)quinoline-4-carboxamide

**QHB**

(E)-2-(but-2-en-1-yloxy)quinoline-4-carboxylic acid

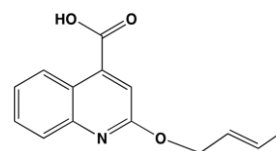


Figure 3-14. Chemical structure of the original drug (dibucaine) and a quinoline derivative with the same core structure but altered side chain (QHB).

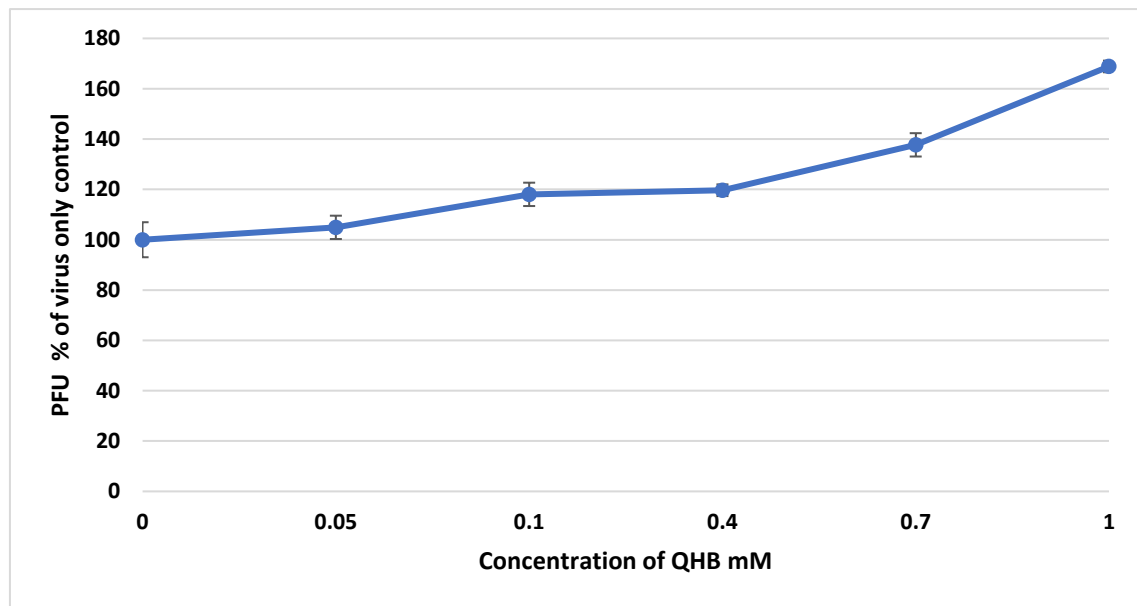


Figure 3-15. Effects of increasing QHB concentrations on CAV9.

GMK monolayers in a 6 well plate were pre-treated with different concentrations of QHB in 0.5 ml of culture medium for 30 minutes. 370 PFU (in 15 μ l medium) of CAV9 were added and the cells were incubated on a rocking platform for 45 minutes at room temperature. 2 ml of a 2:1 mixture of culture medium and 2% CMC were added, and the plate was incubated for 3 days in a humidified CO₂ incubator at 37 °C. The medium was discarded, and cells were washed and stained with crystal violet solution. The number of plaques were counted and expressed as a % of the number seen in the mock-treated control. Error bars show standard error from 3 independent experiments.

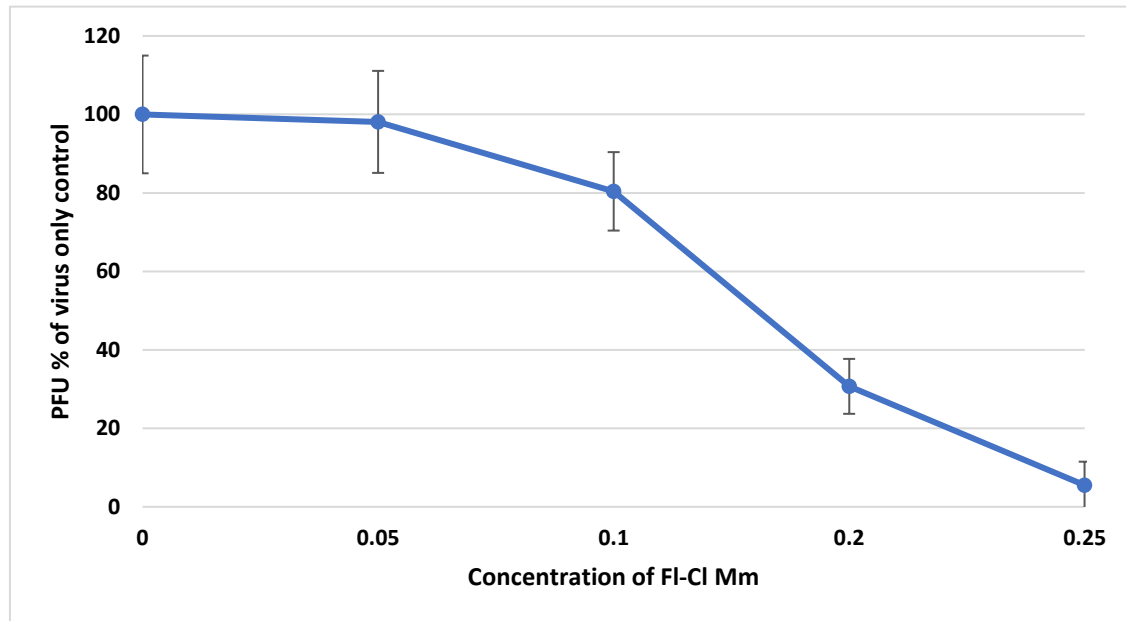


Figure 3-16. Effects of increasing FI-Ch concentrations on CAV9.

GMK monolayers in a 6 well plate were pre-treated with different concentrations of FI-Ch in 0.5 ml of culture medium for 30 minutes. 370 PFU (in 15 μ l medium) of CAV9 were added and the cells were incubated on a rocking platform for 45 minutes at room temperature. 2 ml of a 2:1 mixture of culture medium and 2% CMC were added, and the plate were incubated for 3 days in a humidified CO₂ incubator at 37 °C. The medium was discarded, and cells were washed and stained with crystal violet solution. The number of plaques were counted and expressed as a % of the number seen in the mock-treated control. Error bars show standard error from 3 independent experiments.

3.3 Discussion

3.3.1 Introduction

In general, repurposing of already used drugs as antiviral approaches potentially reduces by several years the timescale needed to discover general mechanism of action, formulations, side effects, interactions, bioavailability, metabolism and excretion properties of the investigated compounds. Fluoxetine (Prozac) is the first selective serotonin reuptake inhibitor known and has been in medical use since 1986. Fluoxetine is FDA approved [and on WHO list of essential medicines (WHO, 2015)] for the treatment of wide range of neurological disorders from depression to schizophrenia. The principle mechanism of its action is to selectively inhibit serotonin (5-HT) uptake by the membrane transporter and is an antagonist at 5HT_{2C} receptors. Uptake studies of fluoxetine in vivo indicated a 57% decrease in 5-HT uptake with little or no effect on noradrenaline and dopamine transport (Perez-Caballero *et al.*, 2014).

Dibucaine (cinchocaine) is a quinolone derivative used as a topical anaesthetic for relief of haemorrhoid-associated pain. It acts by inhibition of voltage-activated sodium channels and it is also an inhibitor of plasma cholinesterase (Neitlich, 1966; Elamin, 2003; Torrens & Castellano, 2006; White *et al.*, 2012).

3.3.2 Fluoxetine as an antiviral drug

Screening a library of small molecules for antiviral activity towards CBV3 (grown in Hela-Rw cells) identified fluoxetine (and its metabolite norfluoxetine) (Zuo *et al.*, 2012). Fluoxetine showed peak inhibition at a concentration of 6.25 μ M. Addition of fluoxetine to virus stock had no effect on infectious titre, so there is no direct interaction with the capsid, instead an early post-entry step of CBV3 infection seemed to be targeted (Zuo *et al.*, 2012).

As CAV9 was found to have high degree of structural similarity and amino acid sequences identity with CBV3 (Chang *et al.*, 1989), it was interesting to find if CAV9 is also inhibited. Our results show that CAV9 infection was completely inhibited at a 0.05 mM concentration of fluoxetine (Figure 3.1) and there was no toxic effect of the drug on cells in all concentrations used (Figures 3.2 and 3.3). In preliminary experiments (data not shown), we found no direct effect of fluoxetine on the CAV9 particle and that an early step in infection is inhibited, as seen for CBV3 (Zuo *et al.*, 2012).

Working independently, a second research group screened a library of bio-active molecules and also identified fluoxetine as an inhibitor of CBV3, as well as the other CBVs and also echoviruses tested (Ulferts *et al.*, 2013). As CAV9 is a member of the same EV species (EVB) as all these viruses, it is not surprising that it is also inhibited by fluoxetine. However, our work is useful direct evidence that CAV9 infection could potentially be treated with fluoxetine, as CAV9 is one of the most frequently isolated EV types from clinical cases. In addition to EVB, fluoxetine inhibited EVD species members, but not the other EV species important from the point of view of human health, EVA (including EV71, one of the most important EVs clinically), EVC and RV-A/RV-B, major causes of the common cold. RV-C was not tested, presumably because members of this species are difficult to propagate. So, fluoxetine use would require accurate identification of the infecting virus and it would only be effective against a sub-set of EVs, unless broader-acting derivatives could be developed. Using a range of techniques, including analysis of in vitro translation and using luciferase or GFP-expressing viral replicons to study RNA replication, it was found that the basis of fluoxetine antiviral activity was inhibition of RNA replication (Ulferts *et al.*, 2013). Use of CBV3 mutants, discussed more thoroughly later, indicated that the CBV3 2C protein is key to fluoxetine activity, as mutations giving drug resistance map to this protein (Ulferts *et al.*, 2016). These researchers also demonstrated a direct binding of dibucaine, which we confirmed to be functionally related to fluoxetine as CAV9 mutants resistant to fluoxetine were also resistant to dibucaine (Figure 3.10), to purified 2C protein from CBV3.

In this work, the investigation of fluoxetine activity depended mainly on plaque assay which allows viral determination of the actual number of infectious viral particles within fluoxetine treated and untreated samples. Direct plaque assay also allows a rough estimation of the degree of compound toxicity. The more toxic the compound, the fainter the purple colour appears in comparison with the control. It is also easy to work out and it is cost efficient. However, it takes a significant time, 3 days for direct plaque assay and an even longer for indirect plaque assay. The MTT assay was used to give a more accurate estimation of toxicity. In the case of fluoxetine, toxicity and antiviral activity were also confirmed independently by using a flow cytometric technique (Figure 3.3), which was reliable in terms of giving quantitative results and a quick analysis time (Wlodkowic *et al.*, 2009). However, the experimental procedure is time-consuming, and this technique was not used to study the other drugs.

Fluoxetine antiviral activity has been reported to extend beyond picornaviruses, as was also found to inhibit HCV (Young *et al.*, 2014). This did not seem to be due to binding a virus protein, but to targeting several host factors. It prevents HCV- driven accumulation of lipids and synthesis of reactive oxygen species by regulating the c-Jun amino-terminal kinase (JNK) and peroxisome proliferator-activated receptor (PPAR β/γ) pathways and also inhibited HCV replication through the JNK signals, transcription activator (STAT)-1 pathways, which enhanced antiviral responses. Likewise, the post-entry stage of dengue virus was found to be inhibited by fluoxetine, most probably by interaction with the endo-lysosomal pathway and autophagy induction (Medigeshi *et al.*, 2016). The anti-inflammatory activity of fluoxetine has been well documented and may also contribute to antiviral effects (Sacre *et al.*, 2010). HCV and dengue virus are both positive sense RNA viruses, as are picornaviruses, and are expected to share some features, such as replication complex formation. It may therefore be that fluoxetine-induced changes to cellular pathways which inhibit HCV and dengue virus replication, could also contribute to the anti-EV effect, in addition to direct interaction with 2C.

Fluoxetine has a long half-life of 2 days after a single dose and 4 days following multiple doses. Within the liver, cytochrome a P450 (CYP2D6) enzyme demethylates fluoxetine to an active metabolite, norfluoxetine which has a very long half-life of up to 7 days and it was also found to have antiviral activity against CBV3, and thus, it may increase the duration of action of fluoxetine antiviral activity if it is used clinically (Kam & Chang, 1997). .

There are several psycho-dependent and independent side effects of fluoxetine. Being almost serotonin selective, fluoxetine has much lower side effect than antidepressants from other groups, but as there are at least 7 classes of serotonin receptors some side-effects are inevitable, and these include weight gain, sexual dysfunction and sleep disturbances. If fluoxetine were to be used clinically to treat EV infections and if 2C binding is the basis of its inhibitory effect, then presumably modifications to the drug could remove the GPCR blocking activity and so the effect on the CNS and side effects. However, recently, in a multi-centre cohort study of US patients, treated with fluoxetine for EV68-associated acute flaccid myelitis, it was found that fluoxetine was well tolerated by patients, but unfortunately did not improve the neurological outcome of the infection (Messacar *et al.*, 2018). This study is the only reported use of fluoxetine as an anti-EV drug, apart from a

case study on an immunocompromised child with chronic enterovirus encephalitis, who was treated successfully (Gofshtevn *et al.*, 2016).

Fluoxetine can also cause side effects by interacting with other drug groups. For instance, it suppresses cytochrome P450 2D6 (debrisoquine hydroxylase) which hydroxylates debrisoquine and sparteine and thus interacts with drugs that are metabolised by this isoenzyme including the tricyclic antidepressants (TCAs) and lipophilic β -blockers. Fluoxetine also interferes with the use of diazepam, amitriptyline, omeprazole, warfarin, tolbutamide, phenytoin and some nonsteroidal anti-inflammatory agents through inhibition of the P450 2C enzyme group. P450 3A4 enzyme substrates such as benzodiazepines, calcium blockers, cyclosporin, erythromycin, lignocaine, steroids and carbamazepine are also best avoided in fluoxetine-treated patient (Kam & Chang, 1997). Again, modification of the drug could overcome these contraindications while retaining antiviral activity.

3.3.3 Antiviral activity of imipramine and promethazine

It has been found that imipramine blockage of the spingomyelinase decreases the production of ceramide and synthesis of ceramide-rich membrane domains leading to complete inhibition of infection by rhinoviruses, RV2, RV14, and RV16. These membrane domains contain receptors that are required for RV entry, ICAM-1 for RV14 and RV16 and the LDLR for RV2 (Grassmé *et al.*, 2005). Niemann-Pick C1 (NPC1) is a cholesterol transporter important for several viral families. As a potent NPC1 antagonists, imipramine efficiently blocks many viral groups including Ebola virus, Marburg virus, Hepatitis C virus, Chikungunya virus, Zika virus, West Nile virus, Dengue virus and Baculovirus (Haque *et al.*, 2015; Cheng *et al.*, 2015; Li *et al.*, 2018).

Along with related drugs, promethazine inhibits Middle East respiratory syndrome (MERS) coronavirus infection via blocking of clathrin-mediated endocytosis (Liu *et al.*, 2015). It also has an effect on HIV-1, herpes simplex virus, bovine herpes virus and Newcastle disease virus. (Poste & Reeve, 1972; Cheng *et al.*, 2016).

These reports of inhibition of different virus infections by imipramine and promethazine could mean that they would be useful agents against CAV9 and other EVs. However, these two GPCR inhibitors, imipramine (Dempsey *et al.*, 2005) and promethazine (El-Shehabi *et al.*, 2012) showed no activity towards CAV9 (Figure 3.4 and 3.7) at concentrations up to 0.09 mM. At a higher concentration of 0.2 mM imipramine showed significant inhibition

of CAV9 but also cell toxicity (Figures 3.5 and 3.6). GPCRs are the largest protein superfamily in mammalian genomes and include -more than 800 proteins (Katritch *et al.*, 2013). Therefore, being a GPCR does not mean that a protein has the same effects, and different GPCRs subgroups mediate different physiological and pharmacological functions. In addition, there are many drugs known to be GPCR inhibitors and are inactive against CBV3. For instance, During the Zuo *et al.* screening project, up to 1200 GPCR inhibitors were assessed for antiviral activity and only 7 compounds showed some antiviral activity (Zuo *et al.*, 2012).

3.3.4 Dibucaine antiviral activity and restrictions of use

Dibucaine was previously identified to act on the same viruses as fluoxetine, with a more potent effect and some suggestion of an effect also on species EVA viruses (Ulferts *et al.*, 2016). In the current study, both dibucaine (Figure 3.8) and fluoxetine (Figure 3.1) were found to inhibit CAV9 in a dose dependent manner and caused complete inhibition of virus growth at concentrations of 0.04 mM and 0.05 mM. However, a viability assay (Figure 3.9) revealed considerable toxicity at these concentrations. This might mean that some apparent antiviral activity of dibucaine might be because of cell toxicity, which makes less cells available for virus to replicate.

The antiviral activity of dibucaine against EVB and EVD was confirmed to be through binding to and inhibiting the 2C protein (Ulferts *et al.*, 2016), and not by the principal cellular effect of Na-channel blocking action (Torrens & Castellano, 2006; White *et al.*, 2012). There is some structural similarity (Figure 3.17) between dibucaine, fluoxetine, and also TBZE-029, which is another compound found to act on the 2C protein of CBV3 (de Palma *et al.*, 2008). Dibucaine is similar to fluoxetine in terms of having a considerable inhibitory activity against some EV groups and also viruses from other families, including HCV, Ebola virus, Marburg virus and Lassa virus but the mechanism of action is unknown in these cases (Madrid *et al.*, 2013; Ekins *et al.*, 2014; Bösl *et al.*, 2019). In another study, dibucaine was hypothesized to affect the morphogenesis of Semliki Forest virus (an alphavirus), after the stage of reaching plasma membrane (Richardson & Vance, 1978). Dibucaine also inhibits envelope/cell fusion during entry of several enveloped viruses, including those reported to be inhibited by promethazine listed (Poste & Reeve, 1972). The anti-inflammatory properties of dibucaine has been also investigated at a relatively high concentration and it may contribute to its antiviral activity (Cassuto *et al.*, 2006).

The systemic adverse effects of dibucaine are considered to be serious including cardiac arrhythmia, CNS effects and methemoglobinemia (Welch, 2000). Therefore, dibucaine is now rarely used systemically and for spinal anaesthesia and confined to topical uses of haemorrhoids and other rectal and skin irritations (Yacoubian, 2017). If antiviral activity of dibucaine is proved, it will be a new agent for a topical but not for systemic treatment of virus infection unless structural modification of dibucaine will otherwise improve its systemic adverse effects.

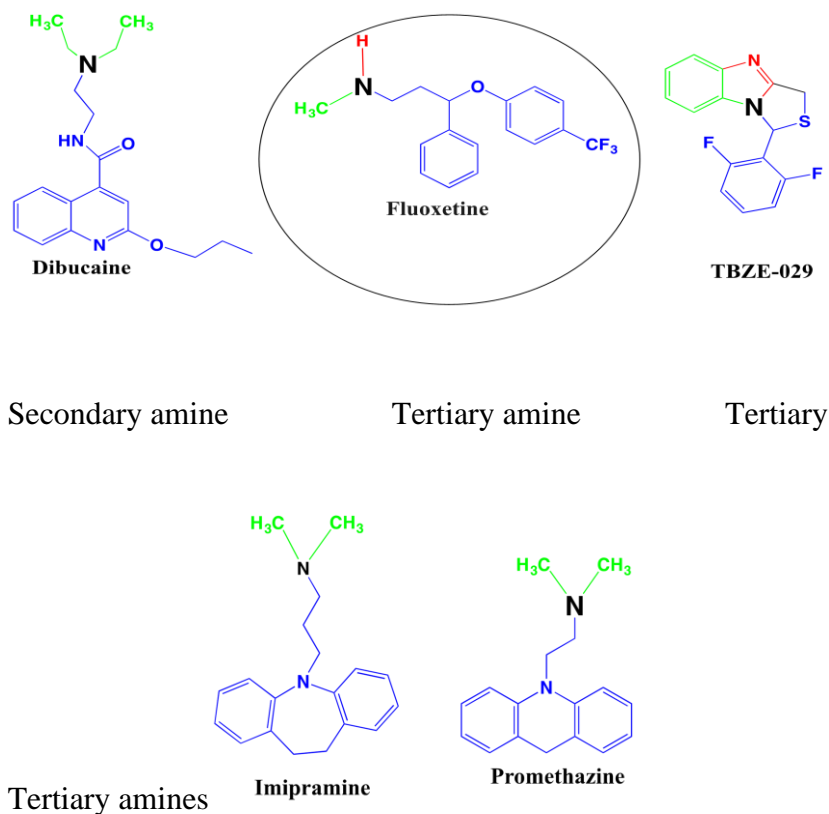


Figure 3-17. Structural similarities between fluoxetine and some studied compounds.

Fluoxetine features aromatic and aliphatic groups beside secondary amine and three fluoride atoms while dibucaine contains aromatic and aliphatic groups beside the tertiary amine. Also, TBZE-29 shared some common points with the structure of fluoxetine that TBZE-29 contains aromatic, aliphatic groups, and tertiary amine but fluoride atoms are the main common feature with fluoxetine. Imipramine and promethazine both contain a tertiary amine and fused polycyclic aromatic and heterocyclic aliphatic rings together with aliphatic groups.

3.3.5 Drug resistant mutants (DRMs) against fluoxetine and dibucaine

To increase understanding of the mechanism of fluoxetine inhibition of CAV9, DRMs were produced (section 3.5.1). Previously, CBV3 DRMs were selected against a novel anti-EV drug TBEZ-029 (de Palma *et al.*, 2008). All the DRMs produced had 3 mutations in common, clustered in the 2C protein, A224V, I227V, A229V. These were analysed individually and in combinations by making specific virus mutants, to find their contribution to the DRM phenotype. A complicated pattern was observed. Alone A229V gave a drug-dependent mutant that could not replicate in the absence of TBEZ-029, but a virus with I227V and A229V was drug resistant not drug dependent. Alone neither A224V nor I227V gave a resistant virus, but with both mutations in the same virus drug resistance was observed. A mutant with all 3 mutations was used in studies on fluoxetine and dibucaine and was resistant to both these drugs (Ulferts *et al.*, 2016), suggesting a common mechanism of inhibition, involving 2C, with TBEZ-029. A direct binding of dibucaine to purified CBV3 was then observed and presumed to be the inhibitory mechanism (Ulferts *et al.*, 2016). The EV71 2C crystal structure has been determined (Guan *et al.*, 2017) and the similarity in sequence with CBV3 allowed a model of the CBV3 2C to be derived (Bauer *et al.*, 2019). This revealed a pocket in the region of the 2C mutants into which fluoxetine was predicted to fit. This modelling now allows a more detailed understanding of the interaction of fluoxetine and other drugs and their modification to retain and optimise binding, while removing unwanted interactions with other proteins.

There is no report of an attempt to generate DRMs against fluoxetine itself and so our work offers valuable insights. After propagation, selection and purification, the sequence (Figure 3.11) of the mutated viruses showed that all the mutants had the same mutation (I>V) at position 227 in 2C. This mutation found in CAV9 is the same as one of the 3 mutations, 2C-A224V, I227V, A229V found in TBEZ-029 resistant CBV3 and also known to give CBV3 resistance to fluoxetine and dibucaine (Ulferts *et al.*, 2013). The region where the mutations are found is highly conserved between CAV9 and CBV3 (both EVB species), and also with the EVD virus known to be susceptible to fluoxetine, but not EVA or EVC viruses, which are not susceptible to fluoxetine (Figure 3-18). Results from sequencing of one CAV9 dibucaine DRM showed an identical mutation to that in the fluoxetine DRM (I>V) at the same position of 227 in 2C. The results need to be extended by analysing additional independent mutants. One explanation for getting only one mutation, rather than the 3 seen in all CBV3 DRMs is that I227 could be the only amino acid that is responsible

for the fluoxetine-2C binding in CAV9 and the other two amino acids (A224 and A229) are not important, alternatively they are key to the function of CAV9 2C and alteration of these amino acids would be lethal.

```

CAV9  DPDHFDGYKQQA VVIMDDL CQNP DGKDV SLFCQ MVSSVDFV PPM AALEEK GILFTSPFVL
CBV3  DPDHFDGYKQQA VVIMDDL CQNP DGKDV SLFCQ MVSSVDFV PPM AALEEK GILFTSPFVL
EVD   DPKYFDGYKQQ TTVLMD DLMQN PDGN DIAMFC QMVSTVDFI PPMAS LEEKGTLYTSPFLI
EVC   APSHFDGYKQQ GYD-MDDL NQNPDG MDMKL FCQMVSTV E FIPPMAS LEEKGILFTSDYVL
EVA   DPDQFDGYKQQ VVTVMDDL CQNP DGKDM SLFCQ MVSTVDFI PPMAS LEEKGVSFTSKFVI
* ***** * * * * * * * * * * * * * * * * * * * * * * * * * * * * * * * * * * *
CAV9  ASTNAGSINA PTVSDSRALARRFH FDMNIEVISMYSQN-GKINMP-----MSVKT-CDEE
CBV3  ASTNAGSINA PTVSDSRALARRFH FDMNIEVISMYSQN-GKINMP-----MSVKT-CDDE
EVD   ATTNAGSIHA PTVSDSKALARRFK FDMIEESMESYKDG-VRLDMFKAVELCNPEK-CRPT
EVC   ASTNSHSIAPPTVAHSDALTRRF AFDVEVYTMSEHSVK-GKLN M-----ATATQLCKDC
EVA   ASTNASNIIVPTVSDSDAIRRRFY MDCDIEVTDSYKTDLGRLDAG-----RAAKLCSEN
* * * * * * * * * * * * * * * * * * * * * * * * * * * * * * * * * * *

```

Figure 3-18. ClustalW alignment of part of the amino acid sequences of the 2C proteins of CAV9 and CBV3, representing EVB, with a representative of species EVD (also susceptible to fluoxetine) and representatives of EVA and EVC (which are not susceptible to fluoxetine).

The region believed to be involved in fluoxetine binding is shown in yellow. The position of the CAV9 mutation associated with resistance to fluoxetine and dibucaine is shown in red. The position of the 3 mutations seen in CBV3 resistant to TBEZ-029 and giving resistance to fluoxetine are shown in blue. The EVD representative has only one difference (in grey) from CAV9 and CBV3 in this region, while there is little sequence identity with EVA and EVC. * indicates that the amino acid at this position is conserved in all viruses.

Another thing to mention is that CAV9 resistant mutants were isolated at a fluoxetine concentration of 0.05 mM. If the propagation was continued further at concentrations above 0.05 mM, additional mutations might be required to overcome the effect of the drug. It is noticeable that fluoxetine was still having a marked effect on CAV9 at this concentration, as plaques were smaller than in the absence of fluoxetine. Finally, the CBV3 mutants were generated against TBEZ-029, not fluoxetine, and it may be that all three mutations are needed for resistance against this molecule (de Palma *et al.*, 2008). Subsequent work with fluoxetine was apparently done only using the mutant with all 3 mutations, which was resistant to fluoxetine, but this does not prove that all 3 mutations are needed for CBV3 resistance to fluoxetine.

The fluoxetine resistant mutants in this work were treated with dibucaine and found to be partially resistant to it. This means that fluoxetine and dibucaine may target the same virus component. In addition to dibucaine, it has been reported that 2 other compounds, pirlindole and zuclopenthixol were effective against some CBVs but they lost their activity against TBEZ-029 DRM (Ulferts *et al.*, 2016). It seems that many drugs target this region of 2C, but there may be subtle differences between how they bind into the observed pocket which could determine the mechanism of DRM selection. This is important clinically as a drug such as fluoxetine, which can be overcome by a single mutation, at least by CAV9, will be more susceptible to DRM selection than one where multiple mutation is required for DRM selection.

The resistance mutation (I>V) at position 227 in 2C in our work and 3 mutations in the previous work (2C-A224V, I227V, A229V) are located C terminal to ATPase motif C, and this short stretch is conserved in viruses that are sensitive to fluoxetine, but there is no clear data on whether these compounds affect 2C ATPase activity (Ulferts *et al.*, 2016).

3.3.6 Synthesis and antiviral activity of the modified drugs

A fluoxetine chlorambucil conjugate was devised to exploit the 2C binding activity of fluoxetine and exploit the ability of chlorambucil to damage nucleic acid. 2C has an RNA binding activity (Xia *et al.*, 2015) so binding of the conjugate to 2C should bring virus RNA into close proximity. Synthesis of the fluoxetine chlorambucil conjugate was carried out by a multi-step procedure (Chapter Two, 2.2.4). A spacer with a suitable functional group, bromoethyl amine (with BOC protection group) was used to couple fluoxetine in order to reduce steric hindrance around the reaction sites between fluoxetine and

chlorambucil moieties. The nucleophilic reaction of the secondary amine took place replacing the bromide. The amino group of the spacer was protected first with BOC protection group in order to link it to the secondary amine of fluoxetine at end of the spacer. BOC was then cleaved with neat TFA to give free amino group at the other end ready for conjugation. The final step of the conjugation was coupling of the amino group of the spacer that linked to fluoxetine with the chlorambucil carboxyl group to form an amide bond. Using the standard coupling reagents DCC, HOBt, and LQ under argon at low temperature, the reaction yielded the conjugated compound fluoxetine-chlorambucil (Fl-Ch) in a reasonable yield. The novel compound was purified with flash chromatography and its molecular mass of m/z 651 Daltons was confirmed with GC spectroscopy (Appendix 2)

Quinoline is expected to be the active part of dibucaine structure and preparation of a quinoline derivative (QHB) was an attempt to exploit its main core (quinoline unit) in derivatization. The aim was to have an insight into the quinoline unit in the biological activity of dibucaine. Therefore, a quinolone-based molecule (QHB) with an unsaturated hydrocarbon linker (butenyl group) was prepared by coupling the hydroxy group of the quinoline with bromobutene. QHB was expecting to be more hydrophobic than the quinoline itself, providing more interaction with cellular lipid compartments including lipid droplets that are very important for virus replication and seem to interact with CAV9 and parechovirus 2C protein. However, QHB (Figure 3.15) did not inhibit the virus. Instead, the viral growth seemed to be stimulated at higher concentrations.

Viral inhibition by Fl-Ch only at high concentration (Figure 3.16) raises the probability that the chlorambucil has impaired the ability of fluoxetine to bind to 2C, possibly by masking some components needed for the interaction.

Two other quinoline conjugates were also prepared in an attempt to search for a new antiviral candidate based on the main unit of dibucaine (quinoline moiety), but time prevented these being tested fully.

The fluoxetine and dibucaine derivatives were designed without taking into account the CAV9 2C structure, which has not been determined. However, the EV71 2C structure (Guan *et al.*, 2017) could be used to model a structure for CAV9 2C, using a similar approach to Bauer *et al.*, 2019. This should allow detailed molecular simulations which

could lead to the rational design of effective drugs, lacking toxicity and with reduced ability to select DRMs, and these could be highly useful to combat infections by CAV9 and related viruses.

Chapter 4: Drugs Affecting Lipid Metabolism and Lipid Droplets

4.1 Introduction

For successful intra-host infectious cycle, viruses including positive stranded RNA viruses, have multiple interactions with various lipids and lipid based intracellular structures (Wells & Coyne, 2019). These interactions are potentially attractive targets for antiviral agents (Fernández-Oliva *et al.*, 2018). It was previously found in our laboratory that CAV9 and HPeV1 infection changes lipid droplets (LDs) number and/or size and that EGFP-2C fusions co-localise with lipid droplets and cause them to aggregate into large clusters (Khrid, unpublished). This manipulation of LDs during infection could suggest that these structures are involved in picornavirus replication. This opens up the possibility that drugs which target LDs could be useful for anti-picornavirus therapy and may have an effect on many different picornaviruses, as CAV9 and HPeV1 belong to genetically diverse picornavirus genera but both have some effect on LDs. Several drugs which target LDs have been developed, to combat obesity, excessive blood lipid levels etc., and a number of other widely used drugs also have an effect on lipid droplets (Daneschvar *et al.*, 2016). These could potentially be repurposed for anti-picornavirus therapy. Therefore, the effects of various drugs reported to affect LDs/lipid metabolism were analysed. These include A922500 and betulonic acid which are diacylglycerol acyltransferase 1 (DGAT1) inhibitors, simvastatin which is a 3-hydroxy-3-methylglutaryl (HMG) coenzyme A reductase (HMG-CoA reductase) inhibitor, C75 a fatty acid synthase (FASN) inhibitor. Preliminary experiments were also performed on aspirin, a nonsteroidal anti-inflammatory drug (NSAID) and metformin a biguanide blood glucose lowering agent, both of which have been reported to affect LDs.

4.2 Results

4.2.1 Inhibition of CAV9 by A922500

Although the role of DGAT1 (Figure 4.1) in some viral infections, like HCV (Crawford & Desselberger, 2017), has been confirmed, it has not been investigated in picornaviruses yet. Initially we tested the selective DGAT1 inhibitor A922500 (Han *et al.*, 2003). This successfully decreased CAV9 growth in GMK cells (Figure 4.2) in a dose dependent manner and caused a significant decrease in viral PFU at 0.075 mM and a complete inhibition of virus beyond 0.125 mM in a direct plaque assay.

The A922500 effect was compared in two cell lines, GMK and A549 cells. Figure 4.3 shows the higher antiviral activity started from lower concentrations (0.05 mM) to reach near zero percent at 0.075 mM in A549 compared to GMK cells in which complete inhibition did not occur until 0.125 mM. However, significant and higher toxicity than expected from the intensity of cell staining by crystal violet was revealed by an MTT viability assay (Figure 4.4). The reduction in cell viability (of less than 80%) started with lower applied concentration of 0.05 mM and became 70% at 0.075 mM (the concentration that caused a complete inhibition of virus-related PFU% in A549 cells). The decrease in viability percent was clearly evident at 0.125 and 0.15 mM causing serious loss of cell viability, of 60% and 80%, respectively.

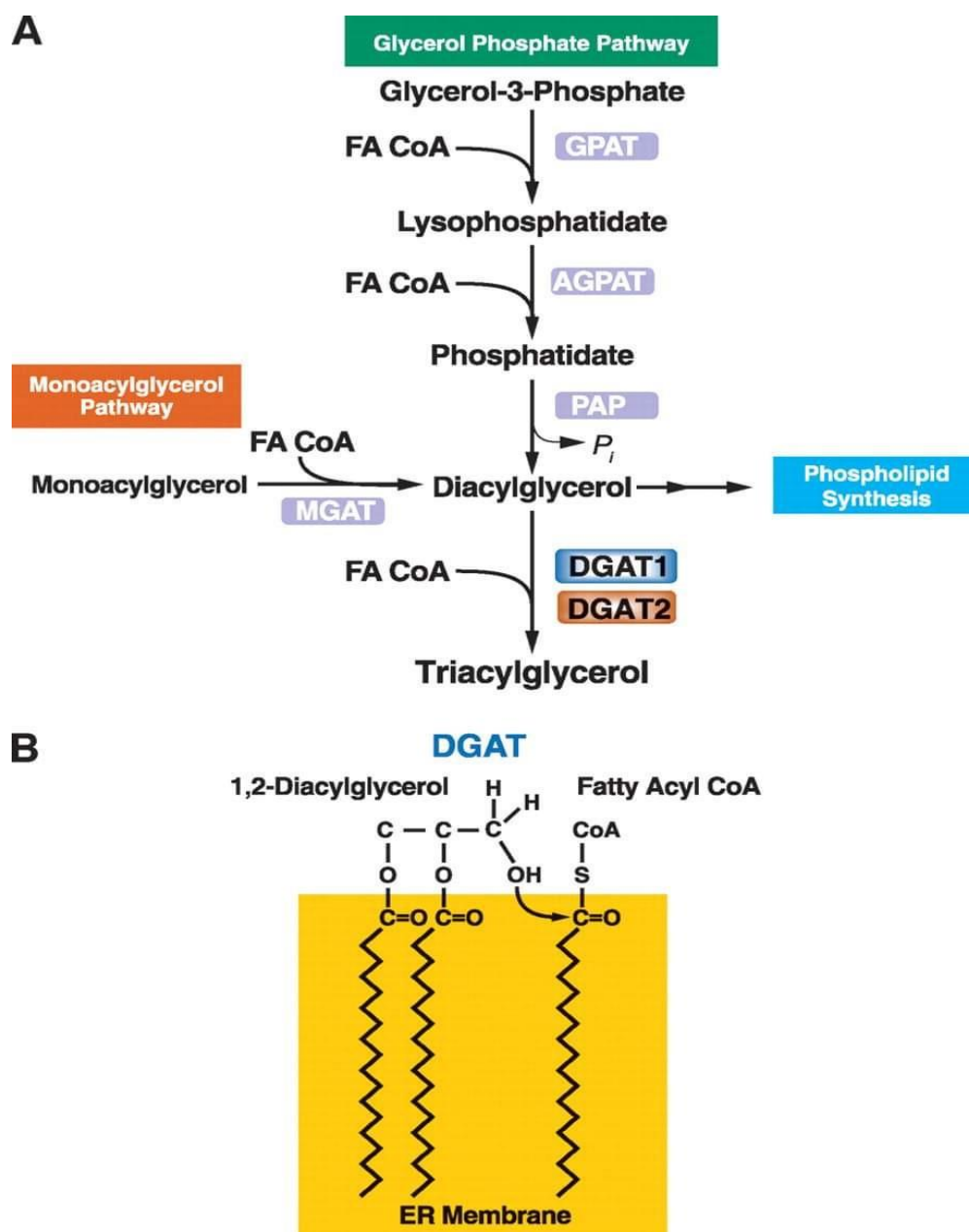


Figure 4-1. Role of DGATs in the biosynthesis of triacylglycerol in the glycerol phosphate pathway and inhibition of DGAT1 by A922500.

DGAT1 and DGAT2 enzymes (A) catalyse the final multi-steps of triacylglycerol synthesis by (B) linking fatty CoA to the hydroxy group of diacylglycerol at the surface of the ER. GPAT, glycerol-phosphate acyltransferase; AGPAT, acylglycerol-phosphate acyltransferase; PAP, phosphatidic acid phosphohydrolase; MGAT, monoacylglycerol acyltransferase. A922500 inhibits DGAT2. Figure modified from (Yen *et al.*, 2008).

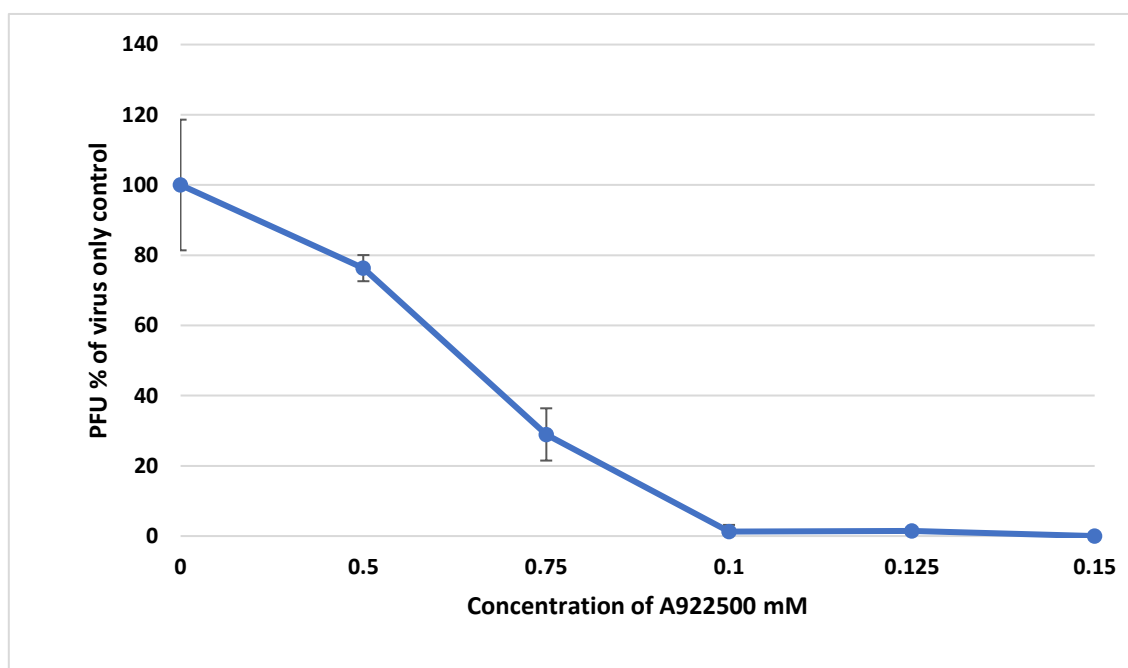


Figure 4-2. Antiviral activity of A922500 against CAV9 in GMK cells.

GMK monolayers in a 6 well plate were pre-treated with different concentrations of A922500 in 0.5 ml of culture medium for 30 minutes. 370 PFU (in 15 μ l medium) of CAV9 were added and the cells were incubated on a rocking platform for 45 minutes at room temperature. 2 ml of a 2:1 mixture of culture medium and 2% CMC were added, and the plate was incubated for 3 days in a humidified CO₂ incubator at 37 °C. The medium was discarded, and cells were washed and stained with crystal violet solution. The number of plaques were counted and expressed as a % of the number seen in the mock-treated control. Error bars show standard error from 3 independent experiments.

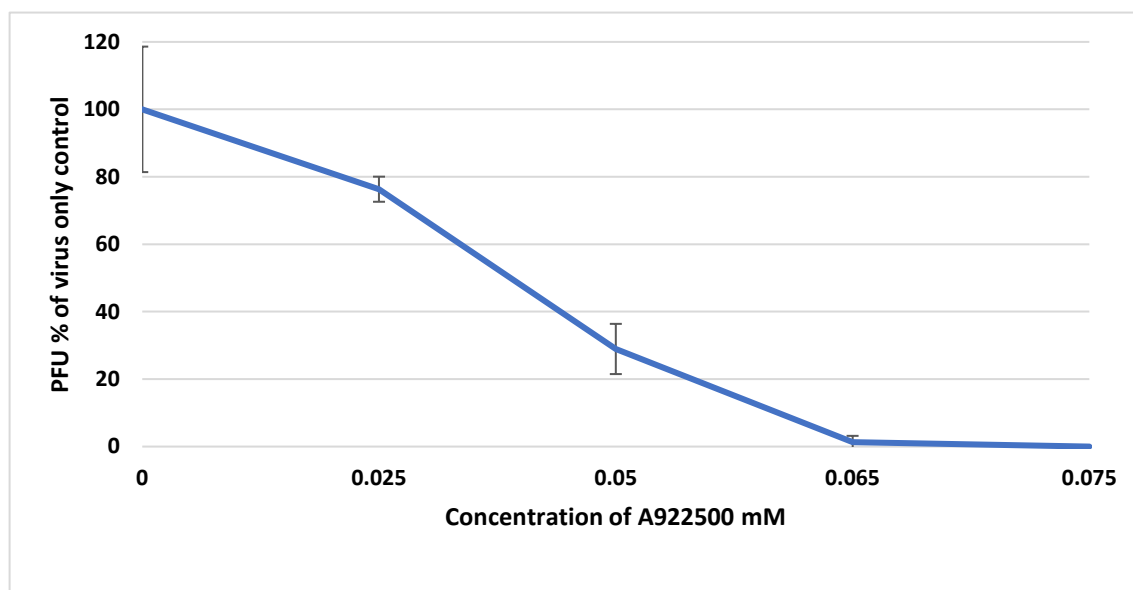


Figure 4-3. Antiviral activity of A922500 against CAV9 in A549 cells.

A549 monolayers in a 6 well plate were pre-treated with different concentrations of A922500 in 0.5 ml of culture medium for 30 minutes. 340 PFU (in 20 μ l medium) of CAV9 were added and the cells were incubated on a rocking platform for 45 minutes at room temperature. 2 ml of a 2:1 mixture of culture medium and 2% CMC were added, and the plate was incubated for 3 days in a humidified CO₂ incubator at 37 °C. The medium was discarded, and cells were washed and stained with crystal violet solution. The number of plaques were counted and expressed as a % of the number seen in the mock-treated control. Error bars show standard error from 3 independent experiments.

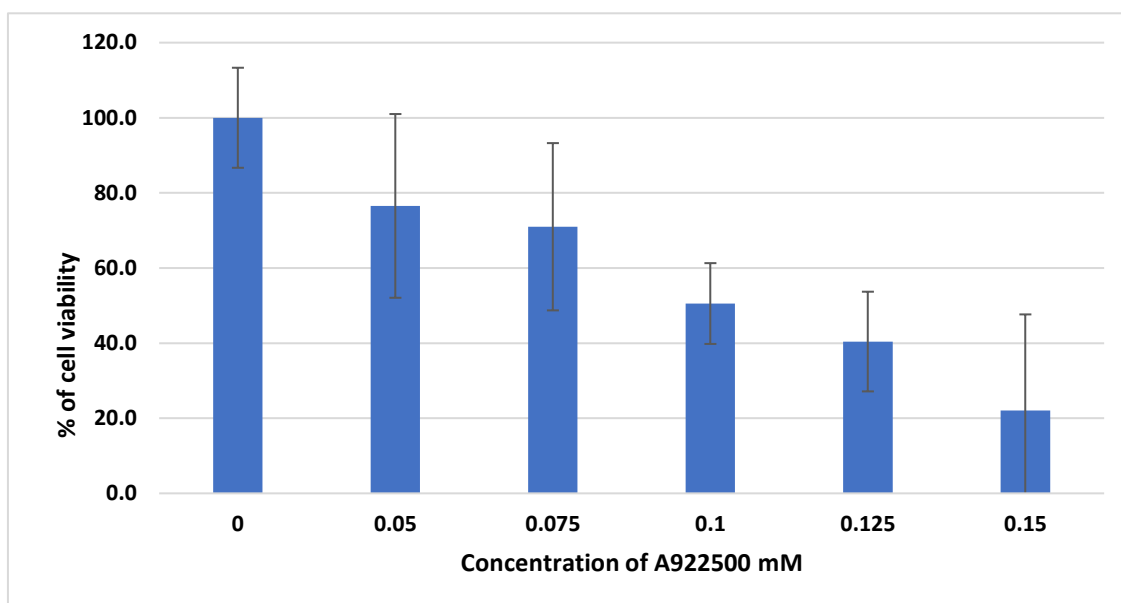


Figure 4-4. Cytotoxic effect of different A922500 concentrations on A549 cells.

A549 monolayers were pre-treated with different concentrations of A922500 in 0.5 ml of culture medium for 30 minutes and the cells were incubated on a rocking platform for 30 minutes at room temperature. 1 ml of a 2:1 mixture of culture medium and 2% CMC were added, and the plate was incubated for 2 days in a humidified CO₂ incubator at 37 °C. The medium was discarded, and cells were washed and 1 mg/ml of MTT in media were applied for 2 h, the resulting blue crystals were dissolved in DMSO and absorbance at λ_{550} was recorded. The cell's viabilities were calculated as percentages of the control of cells alone.

4.2.2 Antiviral activity and toxicity of betulinic acid

Betulinic acid (BA) inhibits DGAT1 and the sterol regulatory element-binding proteins (SREBP) (Quan *et al.*, 2013), and has been shown to have potential against HIV infection (Cichewicz & Kouzi, 2004), although it is not clear if this is mediated through its effect on LDs.

When a direct plaque assay was applied, BA visibly showed a strong toxic effect on cells, with large patches of detached cells. An indirect plaque assay was therefore used, which involves a shorter incubation of the cells (2 days, instead of 3 for direct plaque assay). By applying an indirect plaque assay (Figure 4.5), BA showed considerable but not complete antiviral activity, with continuous decrease in viral PFU, up to almost 80% inhibition at 0.15 mM. A viability assay (Figure 4.6), under the same conditions as the first part of the indirect plaque assay, showed less than 15% loss of viable cells at concentrations of 0.05 mM or less and lower than 30% loss at 0.1 mM. This suggests that BA does have inhibitory activity against CAV9.

4.2.3 Anti CAV9 activity of simvastatin

Simvastatin (Figure 4.7) is a statin and an inhibitor of 3-hydroxy-3-methylglutaryl (HMG) coenzyme A reductase (HMG-CoA reductase). It is one of the widely prescribed anti-hypercholesterolemic agents (Schachter, 2005). The antiviral activity of simvastatin and some other statins against HIV, HBV and HCV has been confirmed (Varma *et al.*, 2011; Mehrbod *et al.*, 2014; Del Campo *et al.*, 2018). In our first experiments, simvastatin had no activity against CAV9 when tested to up to 0.04 mM. The concentration was therefore increased, and the drug was tested in both A549 and GMK cells (Figure 4.8). However, no antiviral activity was seen for up to 0.1 mM of simvastatin using GMK. In A549 cells, there was actually a dose dependent increase in viral infection after 0.06 mM, achieving a level of nearly 200% with a simvastatin concentration of 0.1 mM. Simvastatin therefore did not have an inhibitory effect on CAV9 replication.

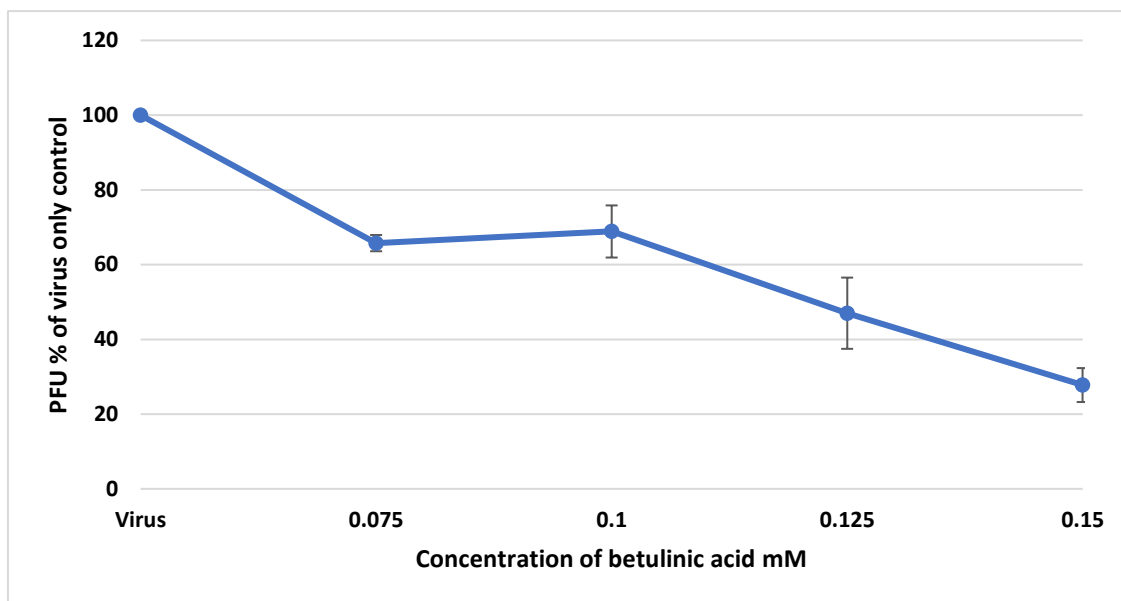


Figure 4-5. Antiviral activity of betulinic acid against CAV9 by indirect plaque assay.

GMK monolayers in a 6 well plate were pre-treated with different concentrations of betulinic acid in 0.5 ml of culture medium for 30 minutes. 370 PFU (in 15 μ l medium) of CAV9 were added and the cells were incubated on a rocking platform for 45 minutes at room temperature. 2 ml of culture medium were added, and the plate was incubated for 48 hours in a humidified CO₂ incubator at 37 °C. then the plate was frozen and thawed 3 times without discarding the growth media. The amount of virus present in the samples was then measured using a normal direct plaque assay using 15 μ l medium of 10² dilution of each sample.

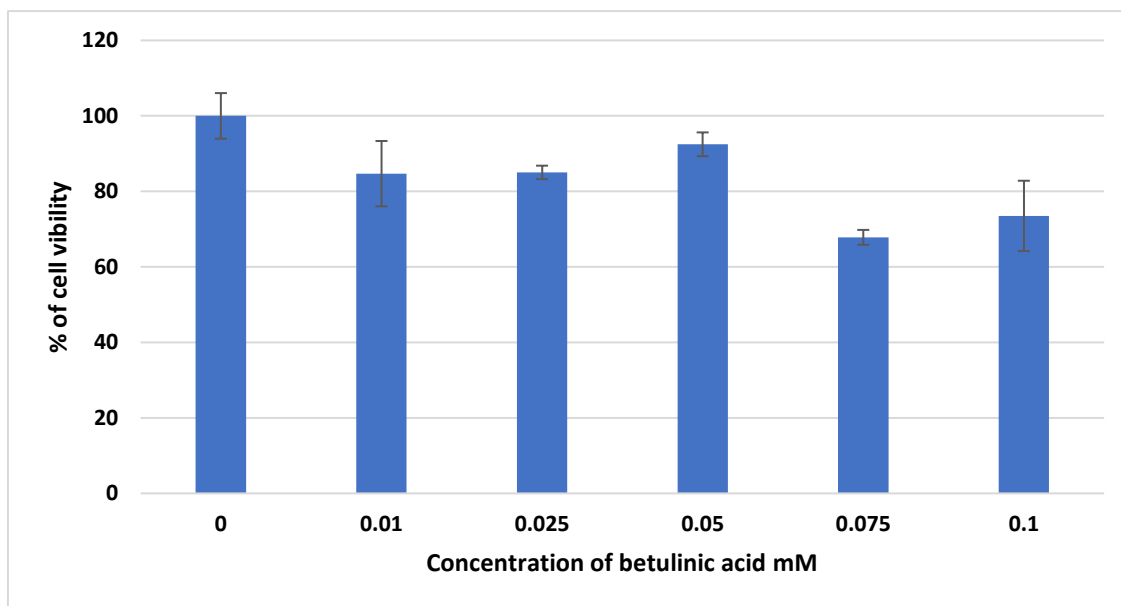


Figure 4-6. Cytotoxic effect of different betulinic acid concentrations on A549 cells.

A549 monolayers were pre-treated with different concentrations of betulinic acid in 0.5 ml of culture medium for 30 minutes and the cells were incubated on a rocking platform for 30 minutes at room temperature. 1 ml of a 2:1 mixture of culture medium and 2% CMC were added, and the plate was incubated for 2 days in a humidified CO₂ incubator at 37 °C. The medium was discarded, and cells were washed and 1 mg/ml of MTT in media were applied for 2 h, the resulting blue crystals were dissolved in DMSO and absorbance at λ_{550} was recorded. The cell's viabilities were calculated as percentages of the control of cells alone.

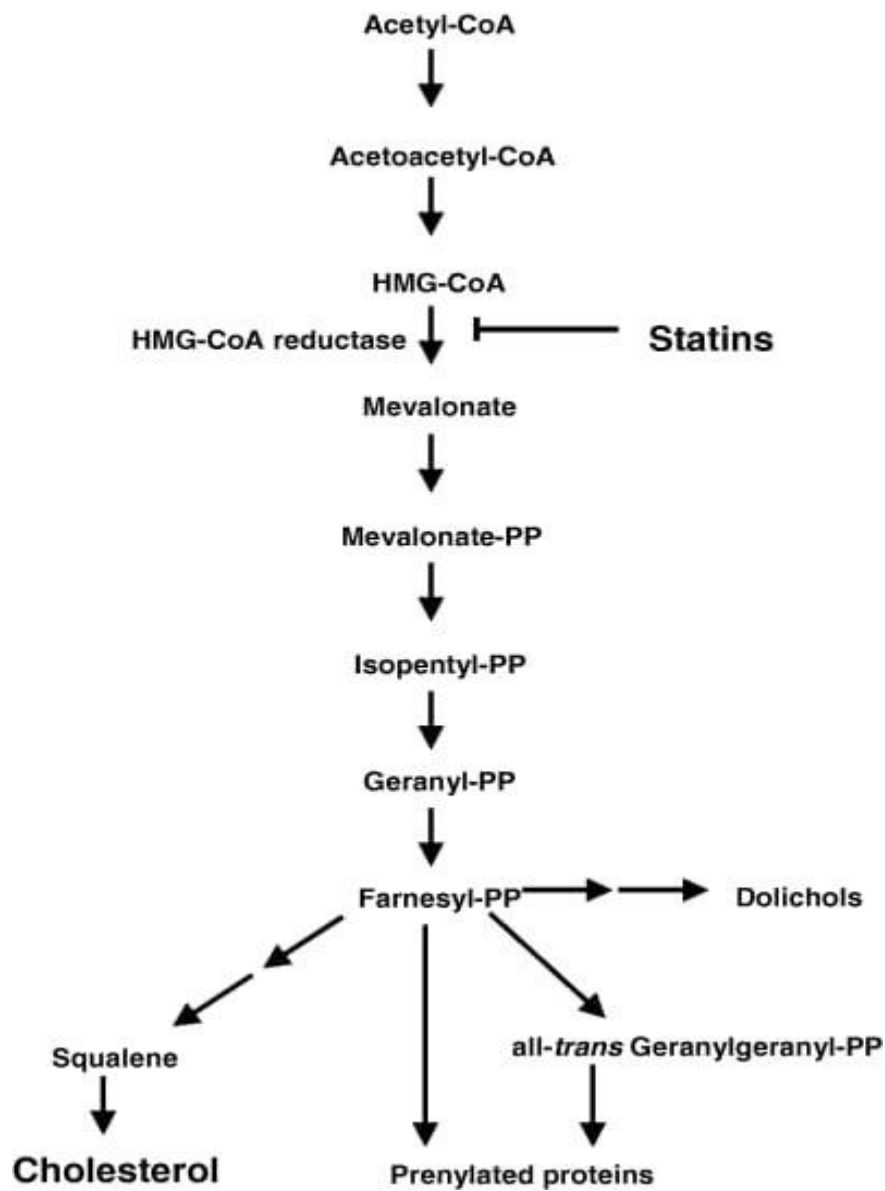


Figure 4-7. Blocking of the mevalonate pathway in mammalian by statins.

Statins inhibit HMG-CoA reductase which converts HMG-CoA to mevalonate blocking early stages of cholesterol biosynthesis. PP, pyrophosphate. Image from (Schachter, 2005).

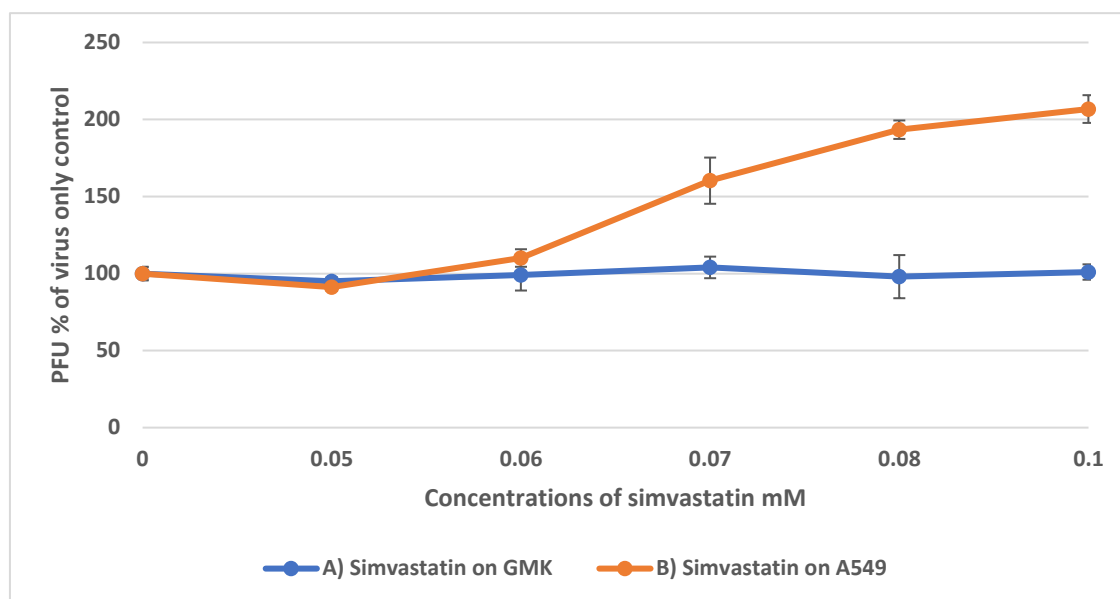


Figure 4-8. Antiviral activity of simvastatin against CAV9 in GMK and A549 cells.

GMK (A) and A549 (B) monolayers in a 6 well plate were pre-treated with different concentrations of simvastatin in 0.5 ml of culture medium for 30 minutes. 370 PFU and 340 PFU of CAV9 were added to GMK and A549 treated cells respectively and the cells were incubated on a rocking platform for 45 minutes at room temperature. 2 ml of a 2:1 mixture of culture medium and 2% CMC were added, and the plate was incubated for 3 days in a humidified CO₂ incubator at 37 °C. The medium was discarded, and cells were washed and stained with crystal violet solution. The number of plaques were counted and expressed as a % of the number seen in the mock-treated control. Error bars show standard error from 3 independent experiments.

4.2.4 Antiviral activity of C75

C75 is fatty acid synthase (FAS) inhibitor (Figure 4.9) which has been investigated for several viruses including CBVs, rotavirus, West Nile virus and Epstein-Barr virus (Perera *et al.*, 2012; Papageorgiou *et al.*, 2015; Boldescu *et al.*, 2017; Fernández-Oliva *et al.*, 2019). C75 (Figure 4.10) showed only a slight dose dependent PFU inhibition after 0.05 mM using a direct plaque assay in GMK cells and caused up to a maximum of 20% inhibition at a higher concentration of 0.2 mM. However, cellular toxicity was revealed by the cell viability MTT assay (Figure 4-11), decreasing viability significantly by up to 60 % at 0.2 mM, and this may be the reason for the apparent reduction in the virus growth seen.

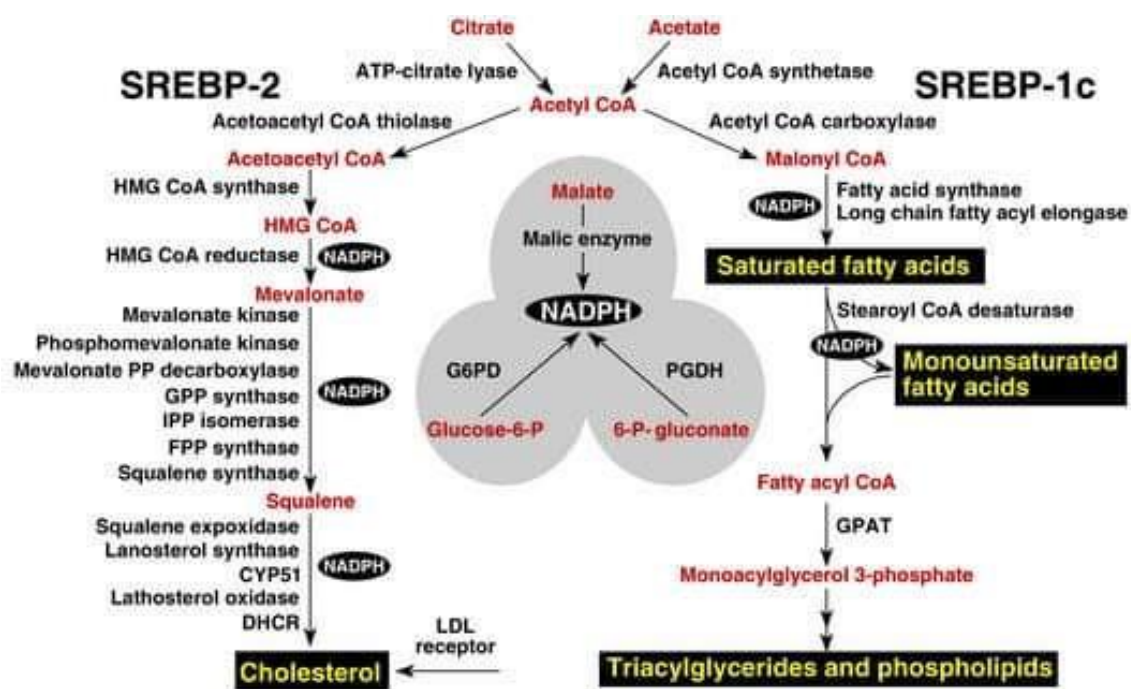


Figure 4-9. Role of fatty acid synthase in the early stage synthesis of triacylglycerol.

Fatty acid synthase catalyses the early stage synthesis of triacylglycerol by stimulating production of saturated fatty acids from malonyl CoA which then converted to unsaturated fatty acids to be transformed to monoacylglycerol which then becomes di and eventually triacylglycerol through SREBP-1c pathway. DHCR, 7-dehydrocholesterol reductase; FPP, farnesyl diphosphate; GPP, geranylgeranyl pyrophosphate synthase; CYP51, lanosterol 14 α -demethylase; G6PD, glucose-6-phosphate dehydrogenase; PGDH, 6-phosphogluconate dehydrogenase; GPAT, glycerol-3-phosphate acyltransferase. Adapted from (Horton *et al.*, 2002).

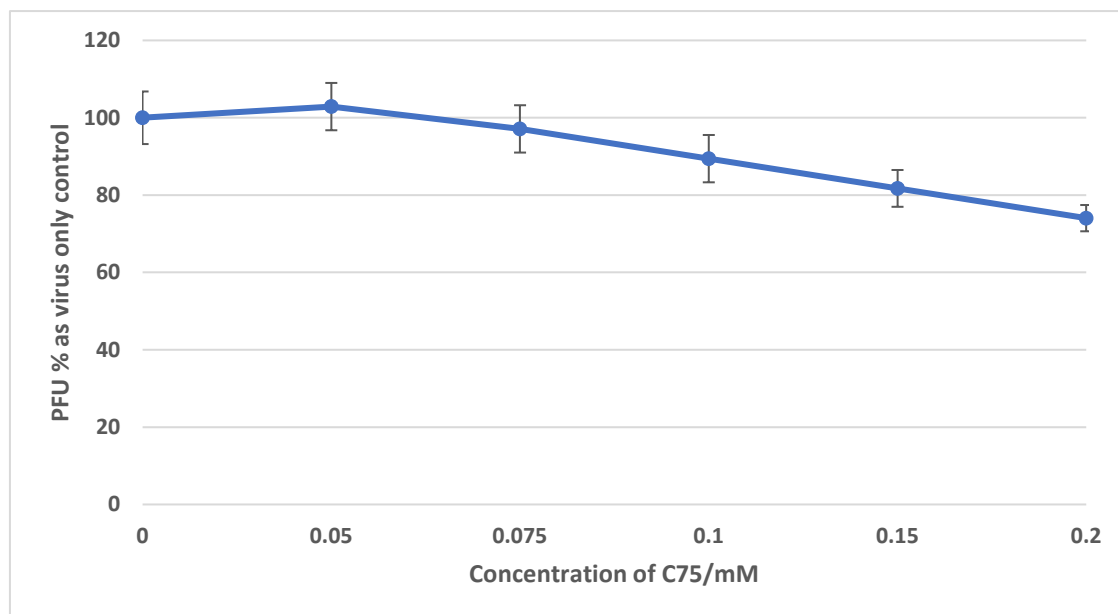


Figure 4-10. Antiviral activity of C75 against CAV9 in GMK.

GMK monolayers in a 6 well plate were pre-treated with different concentrations of C75 in 0.5 ml of culture medium for 30 minutes. 370 PFU of CAV9 were added to GMK treated cells and the cells were incubated on a rocking platform for 45 minutes at room temperature. 2 ml of a 2:1 mixture of culture medium and 2% CMC were added, and the plate was incubated for 3 days in a humidified CO₂ incubator at 37 °C. The medium was discarded, and cells were washed and stained with crystal violet solution. The number of plaques were counted and expressed as a % of the number seen in the mock-treated control. Error bars show standard error from 3 independent experiments.

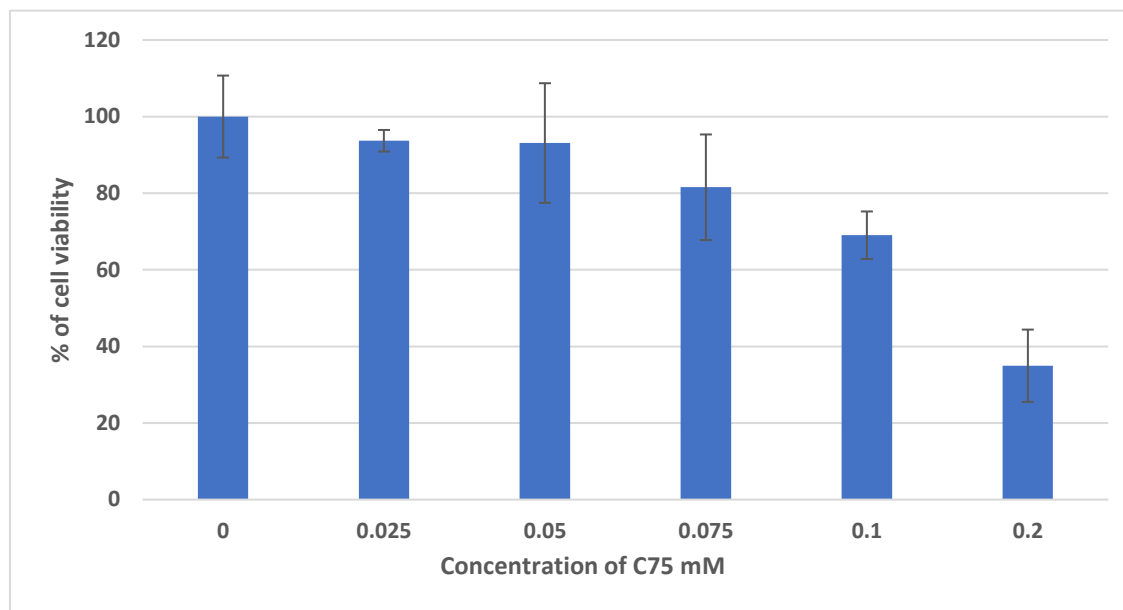


Figure 4-11. Cytotoxic effect of different C75 concentrations on A549 cells.

A549 monolayers were pre-treated with different concentrations of C75 in 0.5 ml of culture medium for 30 minutes and the cells were incubated on a rocking platform for 30 minutes at room temperature. 1 ml of a 2:1 mixture of culture medium and 2% CMC were added, and the plate was incubated for 2 days in a humidified CO₂ incubator at 37 °C. The medium was discarded, and cells were washed and 1 mg/ml of MTT in media were applied for 2 h, the resulting blue crystals were dissolved in DMSO and absorbance at λ_{550} was recorded. The cell's viabilities were calculated as percentages of the control of cells alone.

4.2.5 Preliminary results of antiviral activity of aspirin and metformin

Aspirin and metformin (**Figure 4-12**) are two of the most commonly used drugs. They have been used for long time with strong evidence of their tolerability. As they were investigated in the end of time of the current work, the results shown are preliminary and require confirmation particularly that of aspirin which was tested with CAV9 only once.

Aspirin is a nonsteroidal anti-inflammatory drug (NSAID). The mechanism of action of aspirin (Figure 4.12) on LDs is yet unclear. However, the preliminary data of aspirin by one direct plaque assay on A549 cells (Figure 4.13) showed a significant and dose dependent viral PFU inhibition by up to 50%, 60%, 80% and 90% at concentrations of 4mM, 6mM, 8mM and 10 mM, respectively with no serious toxicity on the same cells type when viability assay was set up (Figure 4.14) in which cell viability percent was around 90% at aspirin concentration of 10 mM and 12 mM.

Duplicate direct plaque assays of metformin (Figure 4.16) demonstrated a significant inhibition of viral PFU by approximately 50% at 5mM and 100% for up to 7 mM. The viability of cells (Figure 4.17) was reduced slightly by nearly 15% at 7mM and 9 mM.

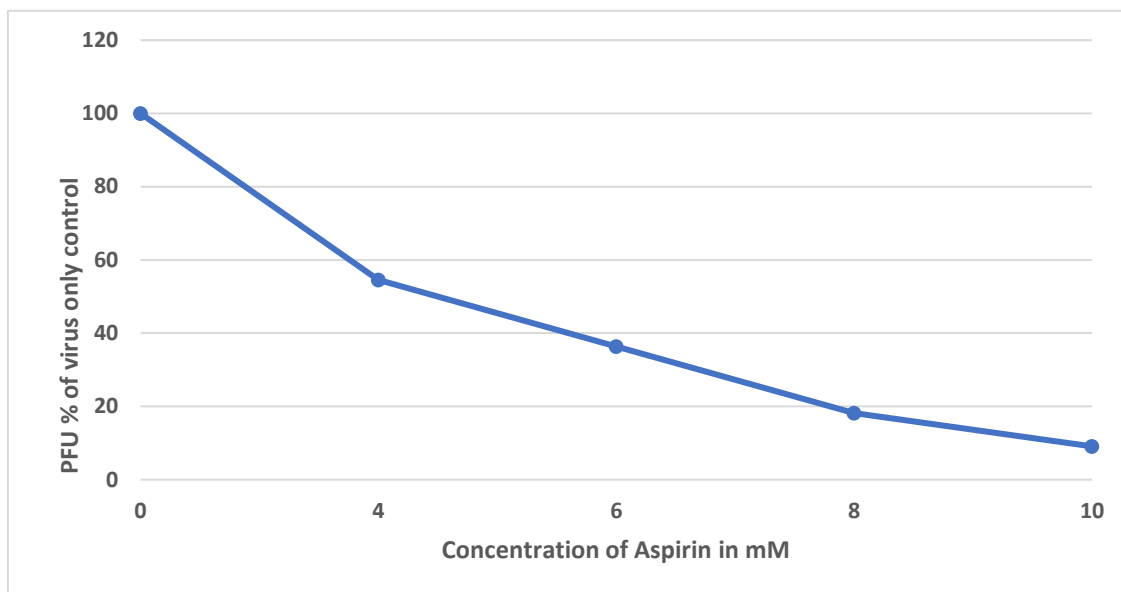


Figure 4-13. Antiviral activity of aspirin against CAV9 in A549 cells.

A549 monolayers in a 6 well plate were pre-treated for one time with different concentrations of aspirin in 0.5 ml of culture medium for 30 minutes. 340 PFU (in 20 μ l medium) of CAV9 were added and the cells were incubated on a rocking platform for 45 minutes at room temperature. 2 ml of a 2:1 mixture of culture medium and 2% CMC were added, and the plate was incubated for 3 days in a humidified CO₂ incubator at 37 °C. The medium was discarded, and cells were washed and stained with crystal violet solution. The number of plaques were counted and expressed as a % of the number seen in the mock-treated control.

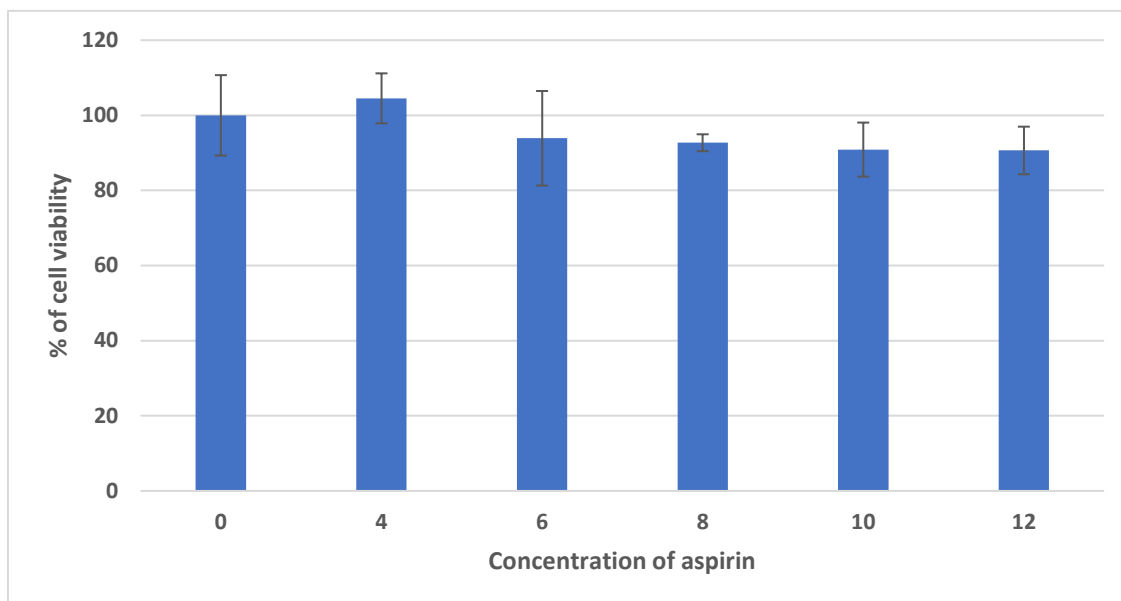


Figure 4-14. Cytotoxic effect of different aspirin concentrations on A549 cells.

A549 monolayers were pre-treated with different concentrations of aspirin in 0.5 ml of culture medium for 30 minutes and the cells were incubated on a rocking platform for 30 minutes at room temperature. 1 ml of a 2:1 mixture of culture medium and 2% CMC were added, and the plate was incubated for 2 days in a humidified CO₂ incubator at 37 °C. The medium was discarded, and cells were washed and 1 mg/ml of MTT in media were applied for 2 h, the resulting blue crystals were dissolved in DMSO and absorbance at λ_{550} was recorded. The cell viabilities were calculated as percentages of the control of cells alone.

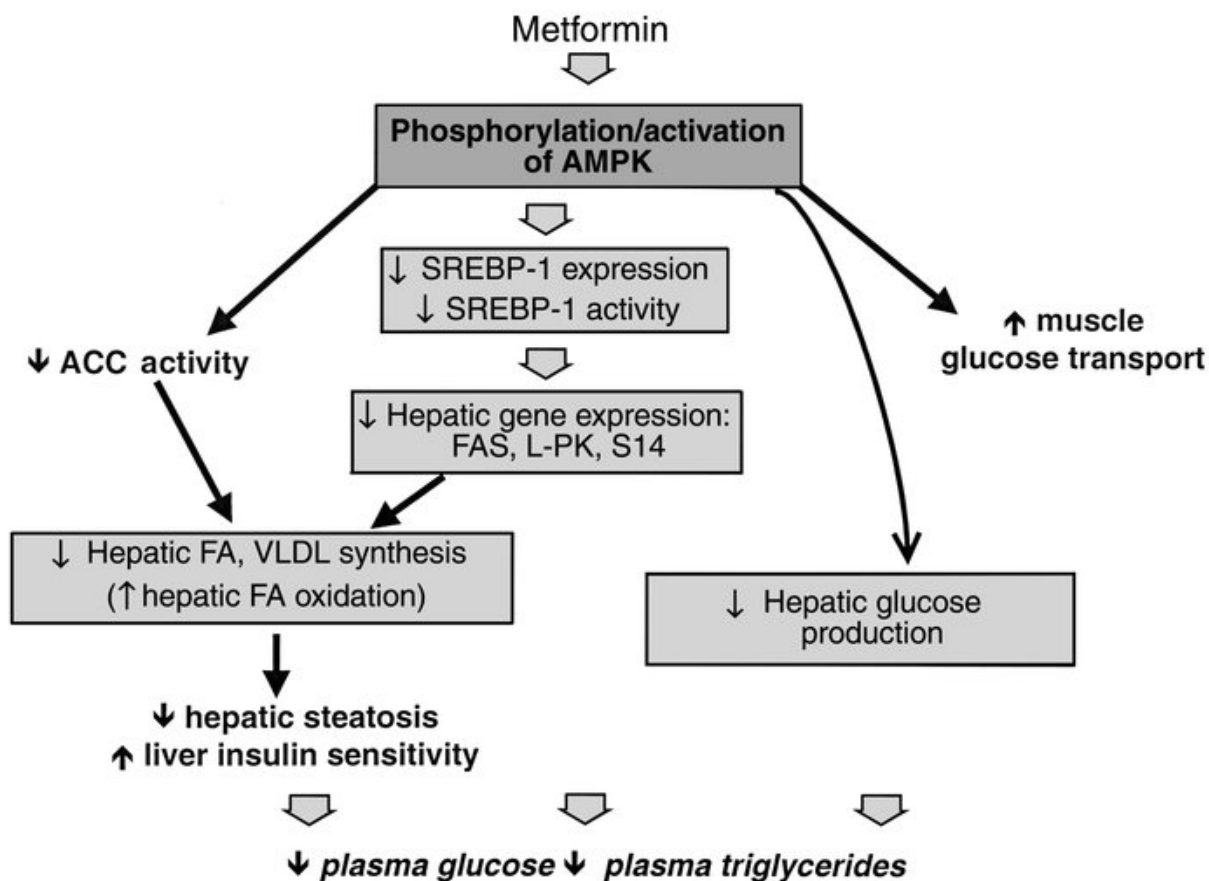


Figure 4-15. Proposed mechanism of action of metformin on glucose production and lipid metabolism.

Metformin stimulates phosphorylation of AMPK which causes directly and by decreasing ACC activity inhibition of hepatic production of fatty acids and very low-density lipoprotein and increase hepatic fatty acid oxidation. Metformin also principally regulate glucose metabolism by decreasing hepatic glucose production and increasing muscle glucose transport. AMPK: AMP-activated protein kinase; SREBP-1: sterol regulatory element-binding protein 1; ACC: acetyl-CoA carboxylase; FA, fatty acid; FAS: fatty acid synthase; L-PK: L-type pyruvate kinase; S14: Spot-14 (Zhou *et al.*, 2001).

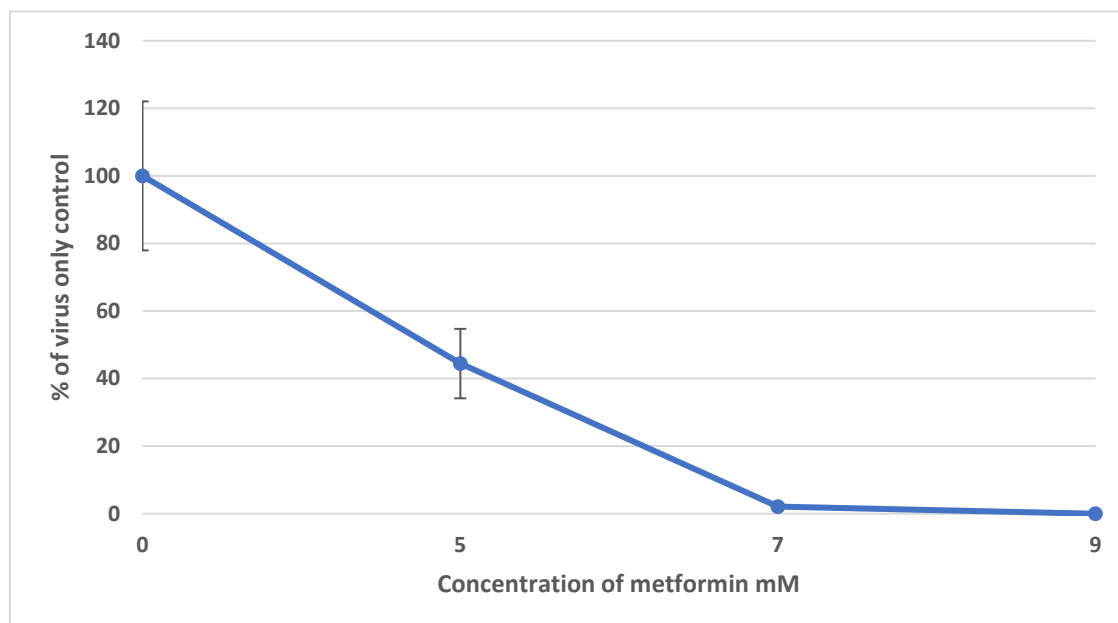


Figure 4-16. Antiviral activity of metformin against CAV9 in A549 cells.

A549 monolayers in a 6 well plate were pre-treated with 3 concentrations of metformin in 0.5 ml of culture medium for 30 minutes. 340 PFU (in 20 μ l medium) of CAV9 were added and the cells were incubated on a rocking platform for 45 minutes at room temperature. 2 ml of a 2:1 mixture of culture medium and 2% CMC were added, and the plate was incubated for 3 days in a humidified CO₂ incubator at 37 °C. The medium was discarded, and cells were washed and stained with crystal violet solution. The number of plaques were counted and expressed as a % of the number seen in the mock-treated control. Error bars show the error from duplicate experiments.

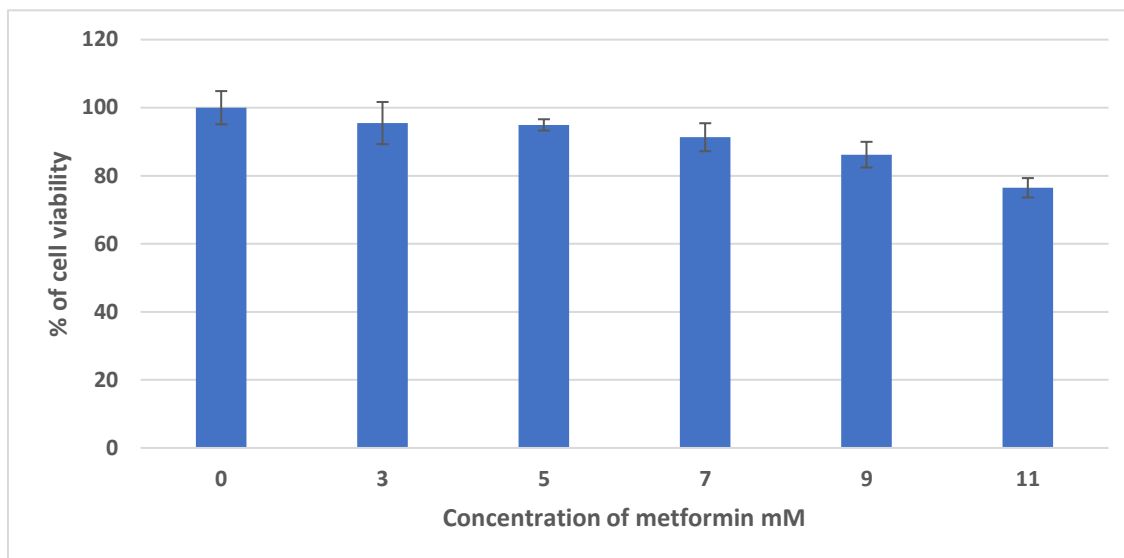


Figure 4-17. Cytotoxic effect of different metformin concentrations on A549 cells.

A549 monolayers were pre-treated with different concentrations of metformin in 0.5 ml of culture medium for 30 minutes and the cells were incubated on a rocking platform for 30 minutes at room temperature. 1 ml of a 2:1 mixture of culture medium and 2% CMC were added, and the plate was incubated for 2 days in a humidified CO₂ incubator at 37 °C. The medium was discarded, and cells were washed and 1 mg/ml of MTT in media were applied for 2 h, the resulting blue crystals were dissolved in DMSO and absorbance at λ_{550} was recorded. The cell's viabilities were calculated as percentages of the control of cells alone.

4.2.6 Drug Resistant Mutants of CAV9 against A922500

The antiviral activity of A922500 (Figure 4.2 and 4.3) was confirmed in the current work in 2 cell lines, GMK cells and A549 cells, although toxicity was evident with the cell viability assay. In general, the results suggest that A922500 could be a potential agent for enterovirus infections. However, drug resistance is a large problem in the use of antiviral drugs. To investigate if mutations give resistance of CAV9 to A922500, the virus was propagated in the presence of increasing concentration of A922500. The emergence of resistant mutants occurred after 7 passages, when the virus was propagated at an A922500 concentration of up to 0.1 mM using GMK cells. Mutated viruses were also seen at A922500 concentrations of 0.15 mM. Plaque assays of the original and mutant viruses showed a clear difference in the presence and absence of 0.125 mM A922500 (Figure 4.18). The figure shows that the original virus was completely inhibited by A922500 as no plaques were seen compared to the sample without A922500, while the drug resistant mutants showed several plaques in the presence and absence of A922500 although the plaques were smaller and fewer in number when the drug was added, suggesting that the selected virus was not fully resistant.

To try to identify the basis of drug resistance, which may give information on how inhibition of LD formation affects CAV9 replication, we have started to sequence a drug resistant mutant. Time has only allowed so far the analysis of the region sequenced in the identification of fluoxetine/dibucaine resistant mutants i.e. a 225 amino acid part of the polyprotein including the C-terminal 188 amino acids of 2C and 27 amino acids from the N-terminus of 3A. This region contains no differences from the original CAV9.

To study whether the resistant mutants of A922500 confer resistance to fluoxetine, the mutants were added to GMK cells pre-treated with 0.05 mM fluoxetine (its details are mentioned in chapter three). The results (Figure 4.19) did not show any cross resistant between A922500 and fluoxetine. Fluoxetine DRMs were also treated with A922500 (Figure 4.20) and no viral growth were seen, and this confirms that there is no cross resistance between 2 drugs, and they seem to act by different mechanism of action. This is consistent with the absence of mutations associated with fluoxetine resistance in the A922500 mutant.

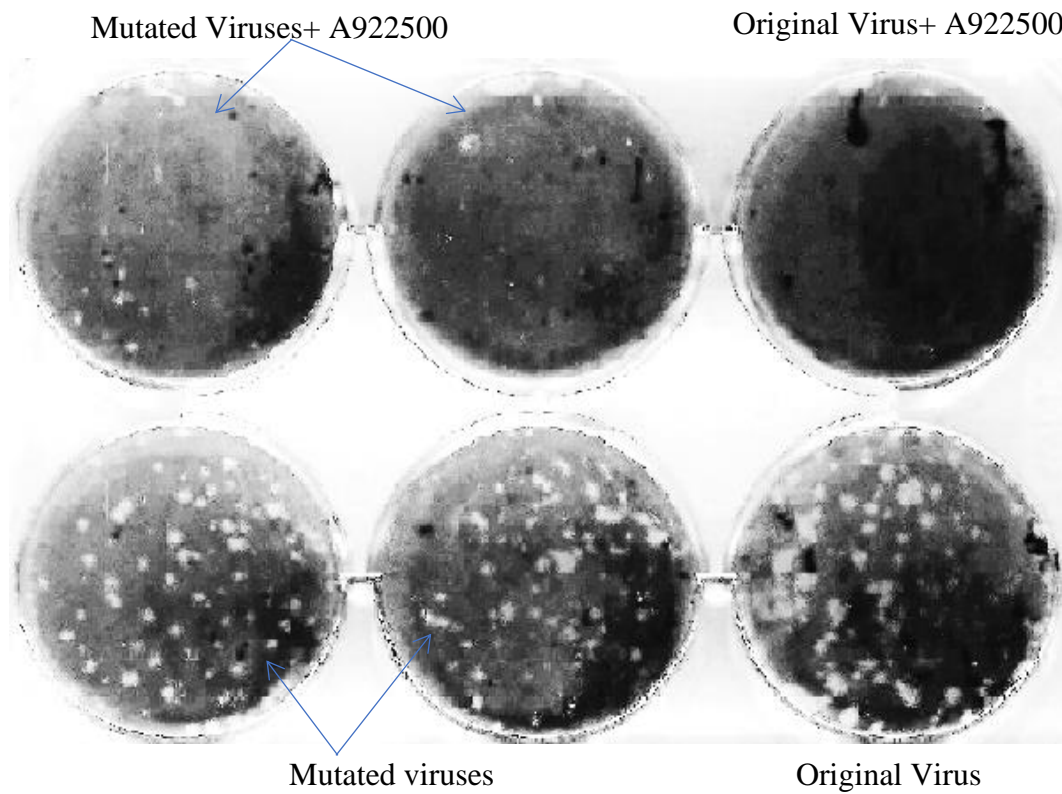


Figure 4-18. Drug resistant mutants of CAV9 against A922500.

Some cells were treated with 125 μM of A922500. Equal volumes and dilutions of the original virus and 2 different mutated viruses were added to A922500 compound treated cells and to cells without the compound. Direct plaque assay then was applied.

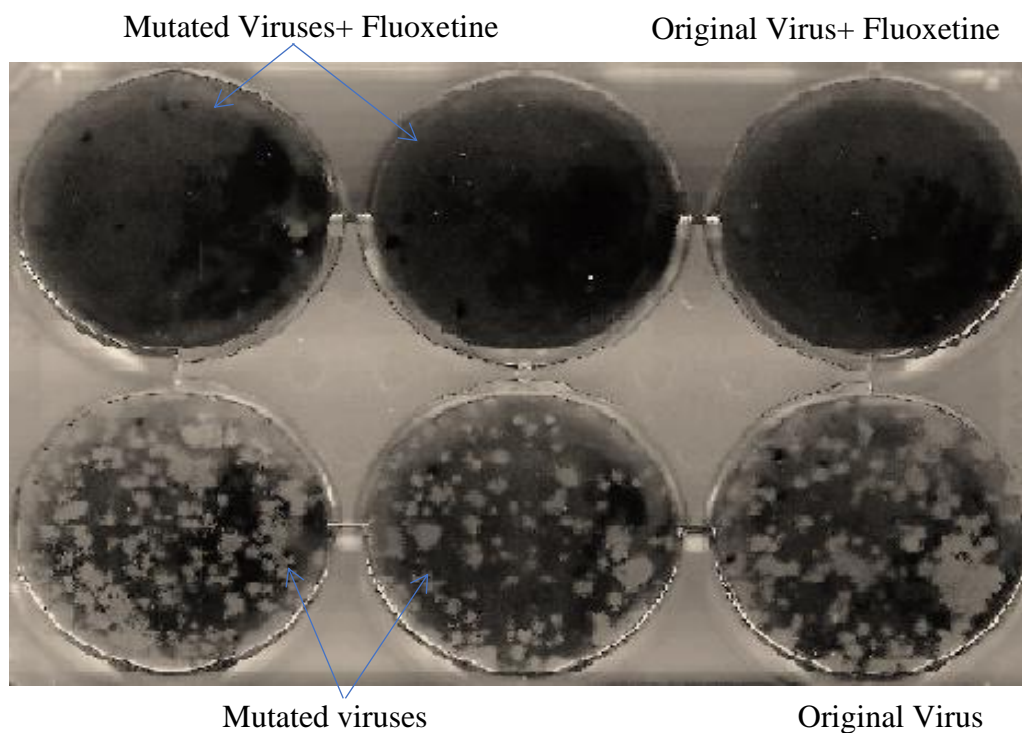


Figure 4-19. The effect of fluoxetine on the selected A922500 CAV9 mutants.

Some cells were treated with 125 μ M of A922500. Equal volumes and dilutions of the original virus and 2 different mutated viruses were added to A922500 compound treated cells and to cells without the compound. Direct plaque assay then was applied.

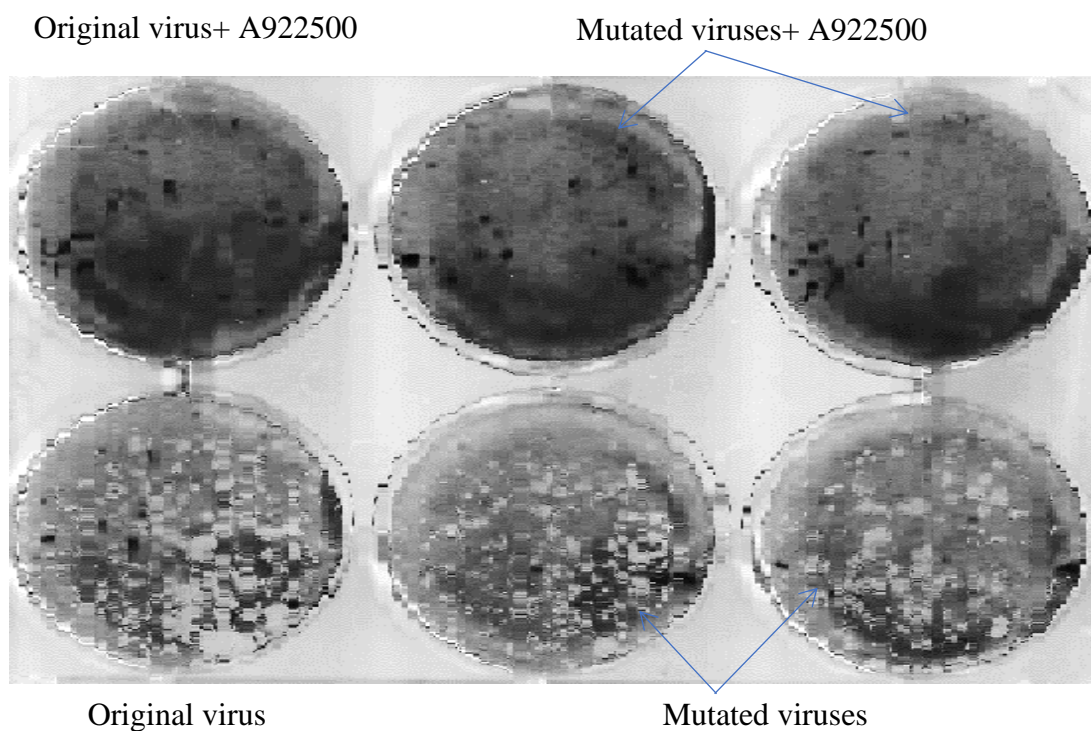


Figure 4-20 The effect of A922500 on the selected fluoxetine CAV9 mutants.

Some cells were treated with 125 μ M of A922500. Equal volumes and dilutions of the original virus and 2 different mutated viruses of fluoxetine were added to A922500 compound treated cells and to cells without the compound. Direct plaque assay then was applied.

4.3 Discussion

4.3.1 Introduction

Lipid droplets (LDs) are dynamic organelles which take part in many cellular processes including lipid homeostasis, signal transduction and membrane trafficking. Alteration of LD formation, size and composition can have significant effects on the biology of the cell and the development of metabolic and infectious diseases (Crawford & Desselberger, 2017).

4.3.2 Antiviral activity of DGAT1 inhibitors; A922500 and betulinic acid

Diacylglycerol acyltransferase 1 (DGAT1) catalyses the final step in the biosynthesis of triglycerides (TG) (Figure 4.21) and it is essential for LD formation (Yen *et al.*, 2008). DGAT1 has been reported as an important factor for the replication of several viruses such as hepatitis C (HCV). It was found that DGAT1 interacts with the HCV nucleocapsid core and is required for the trafficking of core to LD, where assembly occurs (Yen *et al.*, 2008). Both betulinic acid (BA) (Crawford and Desselberger, 2017) and A922500, which is commercially available and more specific than BA (Han *et al.*, 2015), are DGAT1 inhibitors. A922500 has been widely used in different biological fields to study lipid processing through its ability to inhibit the last step of TG esterification (i.e. from DAG to TAG) (Han *et al.*, 2015). In the current study, A922500 was investigated as an example of a DGAT1 inhibitor to block picornavirus replication. Our studies (Figures 4.2 and 4.3) showed dose dependent suppression of CAV9 replication to entirely inhibit growth at concentrations beyond 0.065 mM and 0.125 M on A549 and GMK cells, respectively. However, it showed significant toxicity by viability assay (using A549 cells) at higher concentrations of 0.125 and 0.15 mM (Figure 4.4). The optimal activity-toxicity relationship of A922500 should be considered to be 0.065 mM (Figure 4.3), because this was the concentration when A922500 caused complete inhibition of virus growth on A549 cells with low effect in the viability-toxicity assay was carried out on A549 cells (Figure 4.4).

The antiviral activity of A922500 has not been previously explored for a picornavirus but has been observed in other RNA virus families. A922500 was found to decrease HCV levels (*Flaviviridae* family) by more than 50% intracellularly and a little less extracellularly determined from cell lysates or supernatants of infected cells, respectively (Boson *et al.*,

2017). Rotavirus (*Reoviridae*) yields were also reduced in cells treated with A922500 or betulinic acid, or with the ACAT (Acyl-CoA:cholesterol acyltransferase) inhibitors CI-976 or PHB (Crawford & Desselberger, 2017). In another study, replication of SA11 rotavirus were significantly reduced with A922500 and betulinic acid, as well as the FASN inhibitors cerulenin and C75 (Kim *et al.*, 2012).

DGAT1 and DGAT2 have the same enzymic action and are both integral ER proteins. They take part in the final step in TG biosynthesis by introducing an acyl group to diacylglycerol to form triacylglycerol. DGAT1 and DGAT2 are different in many important aspects. Firstly, DGAT1, and DGAT2 have no sequence homology and belong to distinct gene families. DGAT1 belongs to the DGAT1 gene family which includes also ACAT1 and CAT2 genes that encode acyl-CoA: cholesterol acyl transferase enzyme (Turchetto-Zolet *et al.*, 2011). DGAT2 gene belongs to DGAT2 gene family which contains also MOGAT1, MOGAT2, MOGAT3, and wax alcohol acyltransferases. Both genes are expressed widely in adipose tissue, liver (the primary place of DGAT2) and intestine (which hosts most of DGAT1). Within the cell and in the ER, DGAT2 has been found to be in close proximity to SCDI (stearoyl-coenzyme A desaturase 1), FATP1 (fatty acid transport protein 1) and MOGAT2 while DGAT1 is not (Jin *et al.*, 2014).

The two DGATs might also have diverse roles regarding lipid metabolism. DGAT1 mutant mice in one experiment were healthy and unaffected by dietary -induced obesity and more sensitive to insulin or leptin activity. However, it was found to be a rare cause of human congenital diarrhoea. DGAT2 deficient mice showed very low TAG level which lead to death (Tschapalda *et al.*, 2016).

As DGAT1 and DGAT2 have the same enzymic activity, it is important here to mention that there is a significant functional difference between mutational absence of the gene (in DGAT1- mutant mice) and pharmacological inhibition of DGAT1. When it is pharmacologically inhibited, DGAT1 is still present, though inactive, and acts as a dominant negative mutant preventing DGAT2 from fully replacing it (Liu *et al.*, 2013). The same may be true of inhibiting DGAT2, but it would be interesting to investigate later whether DGAT2 inhibitors have a similar or different antiviral activity from DGAT1. Moreover, although the selective DGAT1 inhibitor A922500 was significantly effective against CAV9, introduction of DGAT2 inhibitors might synergistically increase the antiviral effect. For instance, A922500 was found to inhibit HCV infection by preventing

assembly and virus release from cell, without having a significant effect on the earlier steps of viral replication. However, only 25% of intracellular triglycerides were inhibited at 20 μM of A922500 and at the same concentration there was actually a 45% increase in LD number with no change in LD size or neutral lipid content. An inhibitor (10j), which acts on DGAT1 and DGAT2, caused both TG and LD suppression and also inhibition of early HCV replication, as well as assembly and release, probably because an interaction of the HCV non-structural protein NS5A and the LD protein TIP47 is needed for virus replication (Kim *et al.*, 2018).

A922500 is a potent orally active compound. It inhibits DGAT1 enzyme of both human (with IC_{50} 7 nM) and mouse (with IC_{50} 24 nM). Chronic use of A922500 causes a significant reduction of plasma and hepatic triglycerides without affecting DGAT2, ACAT1 or ACAT2 (Zhao *et al.*, 2008).

Inhibition of DGAT1 results in an increased amount of unesterified FAs and acyl-CoAs which could cause serious adverse effects on cells, including signalling dysfunction and death because of lipotoxicity. However, there is an evidence of increase of DGAT1 inhibition-induced beta oxidation which is an important pathway of FAs breakdown (Villanueva *et al.*, 2009). A922500 may also cause a significant weight reduction in a short time without affecting food intake (Zhao *et al.*, 2008). Despite some adverse effects after longer term use, it is feasible that A922500 could be safe for the relatively short term of an antiviral treatment.

Betulinic acid (BA) is a pentacyclic triterpene and a DGAT1 inhibitor, extracted from different plant species. BA antitumor and especially antimelanoma activity have been investigated and it has also shown analgesic, anti-inflammatory, antibacterial and antimalarial activity (Yogeeswari & Sriram, 2005). The inhibitory activity of betulinic acid and derivatives against HIV-1 and HIV2 replication *in vitro* has been reported (Marken & Munro, 2000; Kato & Ishiwa, 2015; Chinsembu, 2019). BA was also found to inhibit influenza A virus, rotavirus, HSV and more importantly in the context of the present work, echovirus 6 (Pohjala *et al.*, 2009; Phillips *et al.*, 2018), indicating its wide range of antiviral activity including against picornaviruses. Both BA and betulonic acid and its derivatives showed better antiviral activity toward Semliki Forest virus (which is another positive-stranded RNA virus) compared with the parent compound betulin from which they were derived (Pohjala *et al.*, 2009).

In the present work we showed that BA has some antiviral activity on CAV9 by indirect plaque assay. However, this was not complete even when cell toxicity became substantial (Figures 4.5 and 4.6). The toxic effect found could be due to an apoptotic effect that BA exerts on some, but not all, cell lines (Patočka, 2003; Yogeeswari & Sriram, 2005).

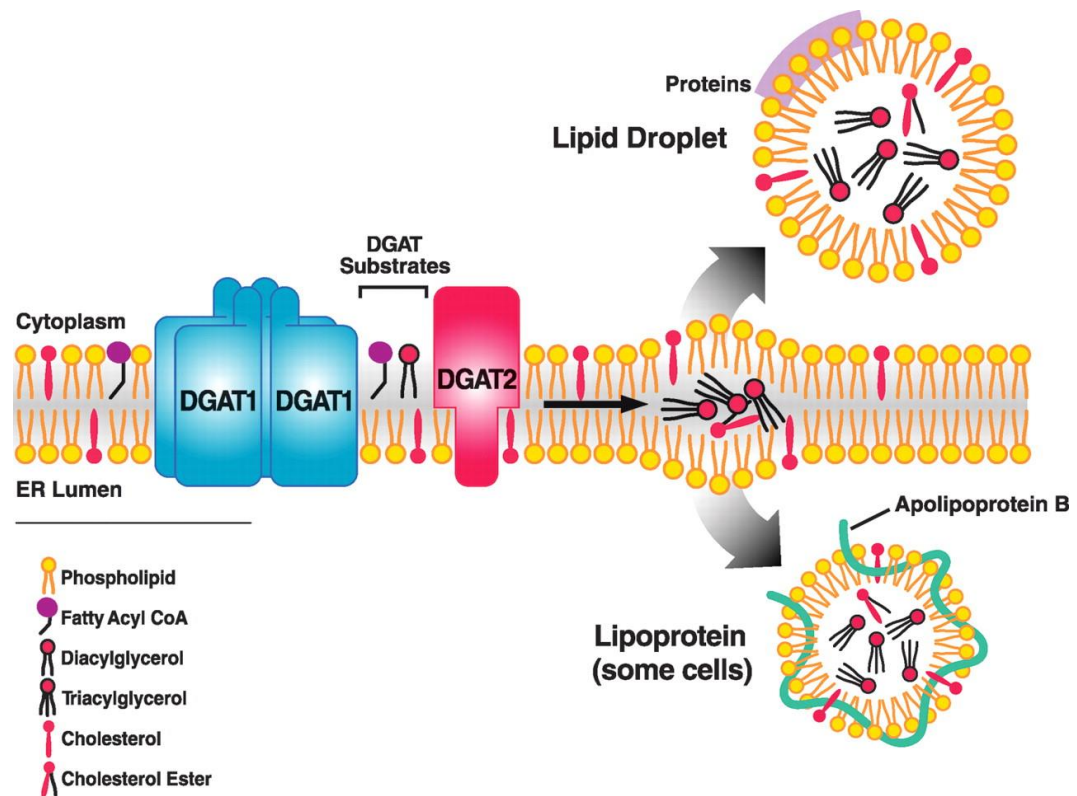


Figure 4-21. The role of DGAT enzymes in triacylglycerol and lipid droplet synthesis in the endoplasmic reticulum (ER).

DGAT1 forms triacylglycerol which gives rise to lipid droplets, derived from ER, or specific lipoproteins in some cells (Yen *et al.*, 2008).

4.3.3 Drug resistant mutants of A922500

The resistance of viruses to drugs usually involves mutations that mediate modification of the target of the drug. As it was found in our lab that the 2C protein of CAV9 and also HPeV1 co-localise with lipid droplets, it was interesting to investigate if drug resistant mutants are produced against these drugs and if mutations localise to 2C. CAV9 virus was propagated in the presence of increasing concentration of A922500. We found some evidence for the presence of resistant mutants after 7 passages. The mutants then were treated with effective dose of fluoxetine and fluoxetine DRM were also treated with A922500 (Figures 4.18-4.20) to see if there is any cross resistance among them. The presence of cross resistance would strongly indicate the probability of having same target (same mechanism of antiviral activity). However, no virus grew the presence of these compounds. This means that A922500 might act in a different way from fluoxetine/dibucaine. The sequencing of the region of the A922500 2C protein which contains the fluoxetine mutation confirms this result, as no mutation was observed in the A922500 DRM. There was also no mutation in the rest of the C-terminal part of 2C or part of 3A. The mutation(s) could be in another part of 2C or 3A, but also in another viral structural or non-structural protein and this needs to be investigated by complete genome sequencing.

4.3.4 Antiviral activity of C75

Fatty acid synthase (FASN) is a primary lipogenic enzyme of the long chain fatty acids biosynthesis (Figure 4-22). The synthetic drug C75 is used to inhibit FAS. C75 inhibits both enoyl reductase domains and partially inhibits thioesterase and beta-ketoacyl synthase domains of FASN. Inhibition of these domains cause malonyl-CoA accumulation and mediate non-specific inhibition of viral replication (Rendina & Cheng, 2005; Chen *et al.*, 2014).

Triglyceride-related biosynthetic intermediates have also been found to be down-regulated by C75 and these include mono- and di-acyl glycerol, in addition to phospholipids and sphingolipids. All these elements are used to produce LDs, the synthesis of which has been found to be inhibited by C75. C75 has been found through its effect on LDs to inhibit Dengue virus (Perera *et al.*, 2012) as well as viruses from other diverse families, including rotavirus, West Nile virus, Epstein-Barr virus (EBV), Usutu virus Feline herpesvirus , Yellow fever virus (YFV) and Kaposi's sarcoma-associated herpesvirus (KSHV) (Perera *et*

al., 2012; Boldescu *et al.*, 2017; Fernández-Oliva *et al.*, 2019). In the case of CBVs which are genetically very close to CAV9, C75 was found to decrease some harmful effects of CBV3 on the host cells. However, significant inhibition of the virus was only obtained when C75 was used in combination with 25-HC, an SREBP-1c (sterol regulatory element-binding protein 1c) inhibitor (Papageorgiou *et al.*, 2015). Consistent with this mentioned study, in the current study (Figure 4.10), C75 showed some but not significant antiviral activity even at higher concentration of 0.2 mM, which was accompanied by considerable toxicity on the cells. However, it likely to exhibit significant antiviral activity at lower concentration if it is combined with antipicornaviral compounds from other classes as it was found in the Papageorgiou et al study mentioned above.

It is worth here mentioning that the description of C75 as a FASN inhibitor is not absolute. For example, although C75 was found to down-regulate several fatty acids such as stearic acid palmitic acid, it was also found to up-regulate others such as oleic acid (Perera *et al.*, 2012) and therefore, it is important to investigate the effects of these specific fatty acids on picornavirus infection.

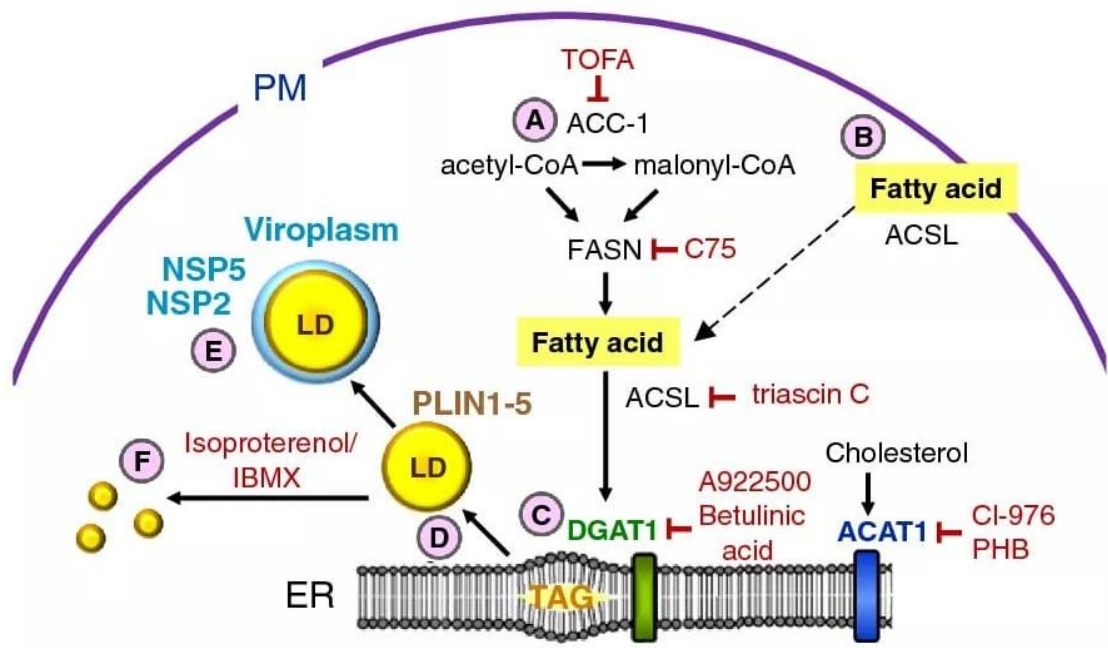


Figure 4-22. Multi-step biosynthesis process of lipid droplets.

C75 blocks fatty acid synthase (FASN) which catalyses the conversion of acetyl-CoA and malonyl-CoA to fatty acids and acting earlier than A922500 and betulinic which act on the final steps of triacylglycerol synthesis (Crawford & Desselberger, 2017).

4.3.5 Inactivity of the HMG-CoA reductase inhibitor, simvastatin

Simvastatin belongs to the statin family which is considered to be a competitive inhibitor of HMG-CoA reductase (hydroxyl methylglutaryl-coenzyme A reductase), a rate limiting enzyme in cholesterol biosynthesis (Schachter, 2005). Mechanism of statin action also include blockage of downstream mediators, isoprenoids including farnesyl pyrophosphate (FPP) and geranylgeranylpyrophosphate (GGPP) which are important for modification of some membrane proteins and for replication of some viruses (Blanco-Colio *et al.*, 2003; Sun & Whittaker, 2003).

Statins have been found in vitro to inhibit a variety of viruses including poliovirus, HCV, HIV, influenza virus, dengue virus, cytomegalovirus and RSV (Gower & Graham, 2001; del Real *et al.*, 2004; Potena *et al.*, 2004; Liu *et al.*, 2006; Martínez-Gutierrez *et al.*, 2011). Cholesterol-enriched lipid domains have been shown to be related to enterovirus replication and cholesterol inhibition with statins is associated with decreased viral replication (Ilnytska *et al.*, 2013).

Simvastatin could thus have antiviral activity. However, both animal and human studies have remained inconclusive about the effectiveness of statins for different virus infections. Lovastatin was proposed by a study as an antiviral agent to control RSV replication and the results were confirmed by a work involved simvastatin which showed significant protection on LPS-induced lung vascular inflammation (Jacobson *et al.*, 2005). Atorvastatin was also tested on 6 mice and there were reduced mortality rates and lung virus titers. Some protection against influenza-related symptoms and pneumonia, and alleviation of some coxsackievirus-related diseases has been reported in patients treated long-term with statins (Gamble *et al.*, 1996). However, several studies have concluded there is no benefit of simvastatin treatment for influenza or acute respiratory infections (Mehrbod *et al.*, 2014; Debing *et al.*, 2015).

Simvastatin in the current work (Figure 4.8) had no antiviral activity in GMK cells and it even stimulated virus growth in A549 cells. Simvastatin is used to decrease cholesterol biosynthesis. However, it also modestly increases fatty acid (FA) synthesis. This is because as an inhibitor of HMG-CoA reductase, it can block cholesterol synthesis, and this in turn increase SREBP production, and thus stimulates FA synthesis (Tang *et al.*, 2011). This in turn may stimulate triglyceride synthesis which provides materials needed for LD synthesis, which could be the basis of the enhancement of CAV9 replication seen.

Statins in general are well tolerated with few adverse effects and have been used for long time, in spite of very recently reported side effects including HMG-CoA reductase pathway-associated mitochondrial toxicity and calcium signalling and also muscle symptoms (Ward *et al.*, 2019). Therefore, simvastatin would have been a good, repurposed antiviral candidate had it shown significant antiviral activity.

4.3.6 Cell specific type

In terms of cell specific effects, the effects of cell type on the requirements of virus replication and effective drug concentration has observed previously. It has been reported that lovastatin inhibited dengue virus assembly to a greater extent in HMEC than in Vero cells (Martínez-Gutierrez *et al.*, 2011). Both A922500 and simvastatin (Figures 4.2, 4.3, and 4.8) showed significantly different effects when the cell line was changed. This could be due to differences in the levels of cell structures, proteins or other components needed for CAV9 replication. Cell type-specific effects may strengthen or weaken the case for the use of a particular drug, depending on the relevance of a cell type in virus infection. This needs to be investigated further using different cell lines, primary cells rather than the permanent cell lines used in this study (which may be very different from normal cells), or in animals, before the use of a drug is judged feasible or not.

4.3.7 Preliminary results on aspirin and metformin

4.3.7.1 Effects of aspirin on CAV9

Aspirin is a trade name of acetylsalicylic acid and it is a prototype of non-steroidal anti-inflammatory drugs (NSAIDs). Like other nonselective NSAIDs aspirin through its acetyl group irreversibly inactivates cyclooxygenase 1 and 2 (COX-1 and -2), although inhibition of COX-2 is much slower than COX-1. COX-2 is a rate-limiting enzyme in eicosanoids formation steps producing prostaglandin (PG) and other downstream eicosanoid products from arachidonic acid (AA) (Brock *et al.*, 1999; Mekaj *et al.*, 2015). Aspirin also decreases oxidative phosphorylation in mitochondria and stimulates NO radicals that decrease inflammation in addition to modulation of transcription and signalling of NF- κ B which in turn stimulates expression of inflammation-related genes such as interleukin-1 interleukin-6 and adhesion molecules in cells and in viruses (Somasundaram *et al.*, 2000; Paul-Clark *et al.*, 2004; McCarty & Block, 2006). In platelets, aspirin inhibits thromboxane A₂ formation and decreases platelet aggregation. Other main uses of aspirin along with other

NSAIDs include mild to moderate pains, fever and various inflammatory reactions (Mekaj *et al.*, 2015). NSAIDs are also suggested to have antiproliferative and anticarcinogenic properties reported from epidemiological, experimental and clinical findings (but recently has been reported that NSAIDs prevent but might trigger cancer formation) (Pannunzio & Coluccia, 2018; Wong, 2019).

Lipid droplets have been found to host COX-2 and PGs. A significant correlation in cancerous colonic cells were observed between LDs and levels of PGE₂ which was found to be synthesized in LDs. COX-2 and PGs have been also observed within LDs in some blood cells such as neutrophils, eosinophils and mast cells and in adenocarcinoma cells as well. Treatment of cells with aspirin has been reported to significantly block LDs and PGE₂ and these effects were similar to that of C75 on these parameters. However, in COX2-free cells, biosynthesis of LDs was found to be normal and significantly inhibited when aspirin was applied. Therefore, the inhibitory effects of aspirin on LDs need to be investigated and could be independent or only partially dependent on COX-2, rather than absolutely dependent (Weinstein, 1980; Triggiani *et al.*, 1995; Accioly *et al.*, 2008; Hartigh *et al.*, 2010).

Primary data on aspirin from a single experiment using a direct plaque assay (Figure 4.13) and a cell viability assay (Figure 4.14) showed that aspirin significantly inhibited virus replication and did not inhibit cell viability significantly, giving encouraging data for future work.

An effect of aspirin on CAV9 replication is not unexpected. Although results regarding aspirin are sometimes contradictory for some viruses, in general they often suggest considerable antiviral activity. In one study, it had no significant antiviral activity on influenza A virus and only a weak effect on rhinoviruses (Crump *et al.*, 2015). CBV3 (closely related to CAV9) was found to increase in titre and interferon response was decreased in infected mice treated with aspirin and also there was an increase in pathological changes and deaths (Rezkalla *et al.*, 1986; Zavagno *et al.*, 1987). In contrast, the effectiveness of aspirin along other NSAIDs against influenza and also EMCV, Sindbis virus and Newcastle disease virus were reported and a high concentration of aspirin also inhibited varicella-zoster virus (Inglot, 1969; Primache *et al.*, 1998). In a study conducted at the time of the current work, aspirin in a concentration of 1 mM was reported to cause about 71% and 72% inhibition in influenza H1N1 and CAV9 respectively, but no clear

activity towards HSV-1 or adenovirus C subtype 5. Aspirin also showed a variable but significant inhibition on several HRV serotypes: HRV-1A and HRV-2 were inhibited by 48% and 66% respectively while HRV-14 and HRV-39 were inhibited by up to 95% (Glatthaar-Saalmüller *et al.*, 2017). Aspirin and indomethacin also found to inhibit cytomegalovirus (CMV) and its induced ROS. Aspirin effects are reported to be due to COX-2 inhibition activity, antioxidant and direct ROS scavenging properties, infection-related NF-κB inhibition and reduction of H₂O₂ capacity to transactivate ROS mediators (Speir *et al.*, 1998). These results, including our own preliminary data, indicate that aspirin might have a wide spectrum of activity as it inhibits viruses from different RNA families including *Picornaviridae*, but it also has specific antiviral activity as it was not active against some tested DNA viruses such as HSV-1 and adenovirus. The antiviral activities of aspirin usually appear at a millimolar rather than micromolar concentration range which might be argued to be high (and toxic) to see antiviral effect in human bodies. Although effective aspirin concentrations did not show significant toxic effects on cells in the current work, there are always differences between controlled tissue culture conditions and conditions *in vivo*. In this regard, it was found that lower effective concentrations were required for virus inhibition in infected mice than their equivalent for cell culture when aspirin was administered with drinking water (Mazur *et al.*, 2007).

Viral infection including that of picornavirus is often accompanied by fever headache and minor pains. If the antiviral activity of aspirin is confirmed and then clinically applied, aspirin would have dual effect as antiviral and as analgesic, antipyretic and anti-inflammatory. However, antiviral effect is expected to need higher concentration than usually used for pain relief. Aspirin like other NSAIDs is widely used and well-tolerated. It has also showed a very little tendency to cause viral resistance. One of the most common side effects of aspirin is gastric ulcer and the predisposition to peptic ulcer which usually occurs in patients with gastrointestinal problems and it is minimised when the drug is administered with, or after, meals despite some evidence that taking NSAIDs with or after food might result in less pain relief and shorter lasting pain relief, and this reduced effect may also be true of its antiviral activity (Moore *et al.*, 2015).

4.3.7.2 Inhibitory effect of metformin on CAV9

Metformin is an oral biguanide and a first line treatment for type 2 diabetes. The principle of its antidiabetic action includes suppression of hepatic gluconeogenesis and lower of

glucose output. It also improves insulin resistance peripherally by enhancing cellular glucose uptake resulting in decrease in circular blood glucose (Rena *et al.*, 2017). These effects are mediated mainly through AMP activated protein kinase (AMPK) which stimulates the transport of glucose from the blood particularly into muscle cells. One of the additional potential advantages of this mechanism is to improve lipid profile and metformin has been found to significantly inhibit cholesterol content and decrease different cholesterol regulatory genes, as an AMPK is known to be a main controller of ACC activity which regulates fatty acid metabolism (Rena *et al.*, 2017).

Preliminary plaque reduction analysis (Figure 4.16) and viability assay (4.17) revealed a significant antiviral activity and an insignificant cellular toxicity of metformin. This drug has already been used for many years with strong evidence of being safe. A correlation between viral infection and insulin-glucose status have been reported for some viruses. For instance, infection with HCV was found to affect glucose metabolism, resulting in insulin resistance and predisposing to diabetes. Recovery from HCV infection improved glucose control and insulin resistance. Insulin resistance in turn was reported to impair anti-HCV response, which was improved when metformin added to peg/interferon and ribavirin. It was also found that some HCV proteins induced insulin resistance by damaging insulin-receptor substrates (Romero-Gómez *et al.*, 2009). In type 2 diabetic-HCV-cirrhosis patients who were treated with metformin notable reduction in liver-related carcinoma, transplantation and death was seen. These effects were mediated by inhibition of virus cis-acting elements and down-regulation of viral transcription (Chen *et al.*, 2018). Like HCV, HBV chronic infection has been also associated with insulin resistance. Metformin has been found to decrease HBV replication and viral antigen (HBsAg) expression and improve antiviral activity of interferon Alpha-2b and lamivudine when used in combination (Xun *et al.*, 2014). Metformin and other AMPK stimulating drugs have been shown to suppress virus infection including HIV and HCMV. In contrast, these viruses have also been shown to block AMPK activity (Moser *et al.*, 2012). In dengue virus, re-localisation of both AMPK and HMG-CoA was altered along with replication complex when the cells were treated with metformin and lovastatin (Soto-Acosta *et al.*, 2017). EVs, particularly CBVs, as well as rotavirus, rubella virus and mumps virus are also associated with diabetes (Filippi & Von Herrath, 2008). Therefore, metformin could be a potential approach for treating infections with these viruses, particularly in the individuals with a genetic-predisposition to development of type 1 diabetes.

To the best of our current knowledge, the effect of metformin has not been investigated on any of picornavirus members. Therefore, the further investigation of antiviral activity of metformin on CAV9 virus would be very novel and it would be very interesting to investigate its effects on other picornavirus and mechanism of its action on each one. Metformin is well tolerable with only some minor GI side effects that are in general transient, making it an excellent repurposed drug (Mccreight *et al.*, 2016; Krishnasamy & Abell, 2018).

Both CAV9 and HPeV1 manipulates LD levels and morphology during infection, we have investigated several drugs which interfere with LD formation. The results obtained indicate that the DGAT1 inhibitor A922500 could be a useful drug for treating infections by CAV9 and presumably other related viruses. The commonly used drugs aspirin and metformin could also be useful, and the further study of these drugs would be an important avenue of research.

Chapter 5: Natural Sources of Antiviral Drugs

5.1 Introduction

Natural products and their analogues contributed to about 80% of all drug production by 1990 and after there was a continuous decline on drug discovery from natural sources (Li & Vederas, 2009). Nonetheless, natural products remain a key potential source of new therapeutics and the work described in this chapter highlights naturally-occurring compounds sources as potential antiviral agents.

The *Ribes* genus from the family *Grossulariaceae* involves several species including redcurrant (*Ribes rubrum*) and black currant (*Ribes nigrum*) (Schulthes and Donoghue, 2004, Haasbach *et al.*, 2014, Saleem *et al.*, 2016). According to Haasbach *et al.*, a blackcurrant extract caused inhibition of influenza virus replication. It has been reported that extracts of some berries such as blackcurrant have significant antiviral activity (Ikuta *et al.*, 2013, Tiralongo *et al.*, 2016). Cranberry (*Vaccium macrocarpon*), an unrelated berry, has also been estimated to be effective against influenza virus (Weiss *et al.*, 2005). Redcurrant could be good source of therapeutic compounds, as most colourful fruits are known to be rich in phenolic compounds including carotenoids, flavonoids and anthocyanin (Sass-Kiss *et al.*, 2005), and some phenolic derivatives have been shown to have antiviral activity (Wang *et al.*, 2014).

Microalgae are a rich source of antimicrobial compounds with antiviral, antibacterial and antifungal properties. They have a high degree of diversity and the ability to produce secondary metabolites in response to different environmental conditions, in addition to a rapid rate of growth (they are capable of doubling every few h. during their peak growth period) and have a potential antioxidant features (Falaise *et al.*, 2016; Khan *et al.*, 2018). In the work described in this chapter, extracts from redcurrant (RC) and various microalgae (MA) were investigated in addition to quercetin which could be one consistent of RC extracts. As there is great evidence of antioxidant (AO) and fluorescence properties of natural products and their usefulness in antiviral approaches, some of investigated extracts have been examined for their AO and photodynamic inactivation properties.

5.2 Results

5.2.1 Comparison of the effects of RC samples from different extraction methods on the CAV9 viral infection

An RC extract was initially made by boiling the fruit with water and filtering and this gave promising results. To optimize the extraction methods for antiviral activity, RC was then extracted by 3 other procedures. These included extraction in water at room temperature (Rt), sonication-based extraction and solid-liquid phase extraction of the solid filtered off the room temperature residue, boiled residue and sonication residue. Interestingly, the methods of extraction yielded different antiviral efficacy profiles. The results showed that the extracted samples of the boiled RC crude materials caused significant inhibition at 4 mg/ml and almost complete inhibition to the viral growth when higher concentrations were used (Figure 5.1). The RC-Rt extract caused complete viral inhibition only at a concentration of 16 mg/ml and the sonicated RC extract led to some inhibition of virus at a concentration of 16 mg/ml. RC-Rt extract was visibly more toxic on cells than others followed by the sonicated sample. The boiled extract showed best antiviral activity and least cytotoxicity profiles and therefore was chosen among other extracts for further investigations.

5.2.2 Evaluation of the effects of RC crude extracts on CAV9 and HPeV1 viral infection

The effect of the boiled RC extract on CAV9 infection was then performed more quantitatively and in addition, the effect on a diverse picornavirus, HPeV1 (*Parechovirus* genus), was also assessed. The results are shown in figures 5.2 and 5.3. A range of concentrations between 2-8 mg/ml and 2-16 mg/ml of the boiled RC samples were investigated on CAV9 and HPeV1 in GMK and HT29 cell lines, respectively. The results showed dose-dependent inhibition of RC extracts on the infection caused by both CAV9 and HPeV1 viruses. The concentration of RC extract that conferred 50% of CAV9 infection inhibition was approximately around 1.8 mg/ml. Also, the total inhibition effect was achieved with 8 mg/ml. It required 6 mg/ml of RC extract to cause 50% inhibition of HPeV1 infection. The complete inhibition of infected cells by HPeV1 was accomplished with 16 mg/ml, double the concentration acquired for the infection with CAV9 virus. However, the experiment showed that members of two diverse *Picornaviridae* genera were inhibited by the extract.

5.2.3 The concentration dependent inhibitory effect of the boiled RC extract on different strains of Coxsackie virus B3

CBV3 is closely related to CAV9 but differs in receptor use. To further investigate the boiled RC extract, three CVB3 isolates, P55 (2), P6LK12 and P4 (75) were used (Figure 5.4). The boiled extract sample of RC exhibited a clear positive response with a range of concentrations applied. Both P6LK12 and P4 (75) were inhibited by over 95% at the 4 mg/ml concentration, while P55 (2) virus was completely inhibited at this concentration. Surprisingly, when the concentrations of RC sample were increased, P55 (2) virus showed some infection. However, the overall results showed that boiled RC extract is significantly active against CVB3 strains.

5.2.4 Effect of RC extract on fluoxetine drug resistant mutants

To further investigate the basis of the inhibition of CAV9 replication by the RC extract the fluoxetine DRMs were used (Figure 5.5). The RC extract caused a complete inhibition of original CAV9 and DRMs, which means that RC seems to act by a mechanism different from that of fluoxetine. This also suggests that combination therapy with the active RC component and fluoxetine could be useful to overcome the effects of DRM formation.

5.2.5 Effect of the RC extract on the CAV9 virus particle

To establish whether the ability of the RC extract to inhibit CAV9 infection is due to a direct effect on the virus particle, the virus was pre-treated for intervals of time between 20 minutes to 100 minutes in Eppendorf tube before applying to cells (Figure 5.6). The extract showed no significant inhibition differences on CAV9 infection after incubation for the above periods of time, compared to CAV9 infection without CAV9 treatment. Therefore, the antiviral effect of the RC extract does not seem to be due to a direct effect on the particle and is probably mediated intracellularly.

5.2.6 The effects of RC addition on replication during time-course of CAV9 pre-infection

Antiviral agents may interfere with viral replication at early and/or late stages of infection of the cell e.g. early during entry/uncoating/translation/RNA replication or later during assembly/ maturation/exit. Cells were treated with RC extract (8 mg/ml) at different time points, after infecting cells with CAV9. Also, cells were pre-treated with RC extract before

the addition of virus for comparison. According to the results shown (Figure 5.7), there was no viral growth when cells pre-treated with RC then inoculated with CAV9. The same is true when extract was added 2 and 4 hours after infection. From the 6 hours time point, however, some virus growth was observed and addition of the extract 10 hours after infection gave a result similar to no RC addition. As the infectious cycle of CAV9 is found in our laboratory typically to take 12 hours, the results suggest that RC extract might have an effect on early stages of viral replication, but not immediately post-entry. Probably, translation or RNA replication is affected.

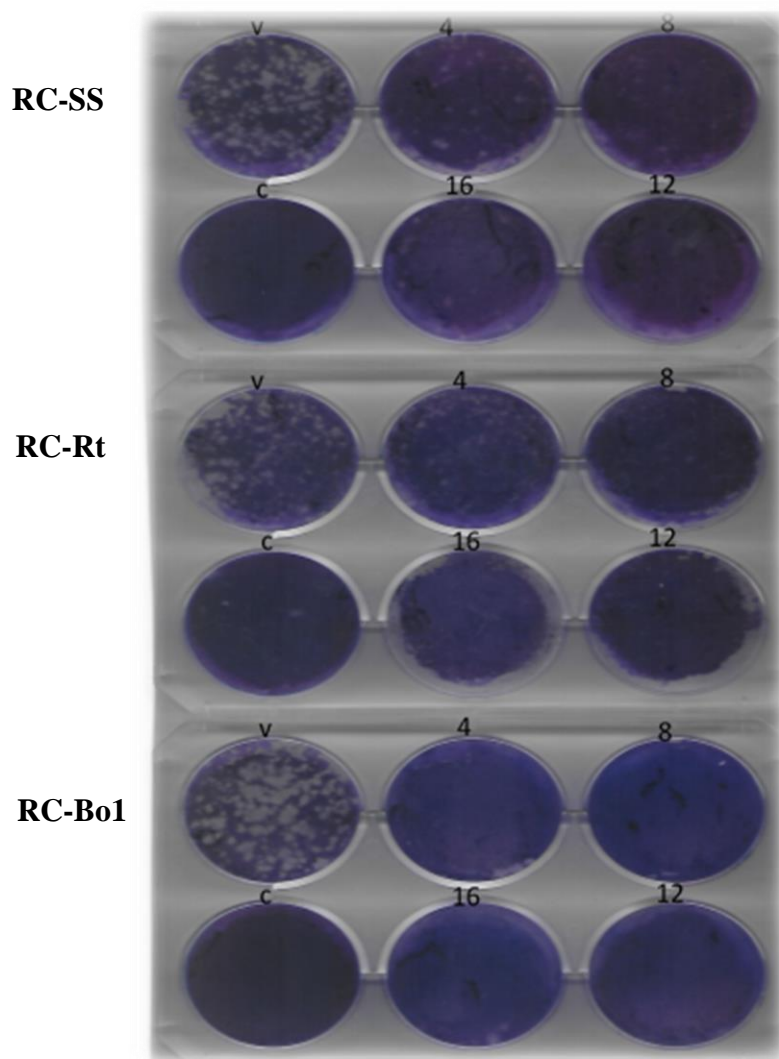


Figure 5-1. Inhibition of CAV9 infection by different crude RC extracts.

GMK monolayers in a 6 well plate were pre-treated with different concentrations of RC extract (4, 8, 12 and 16 mg/ml) in 0.5 ml of culture medium for 30 minutes. 370 PFU/ml of CAV9 were added and the cells were incubated on a rocking platform for 45 minutes at room temperature. 2 ml of a 2:1 mixture of culture medium and 2% CMC were added, and the plate was incubated for 3 days in a humidified CO₂ incubator at 37 °C. The media was discarded, and cells were washed and stained with crystal violet solution C: Cells only, V: Virus only, RC-SS: Sonicated extract, RC-Rt: Room temperature extract, RC-Bo1: Boiled crude extract.

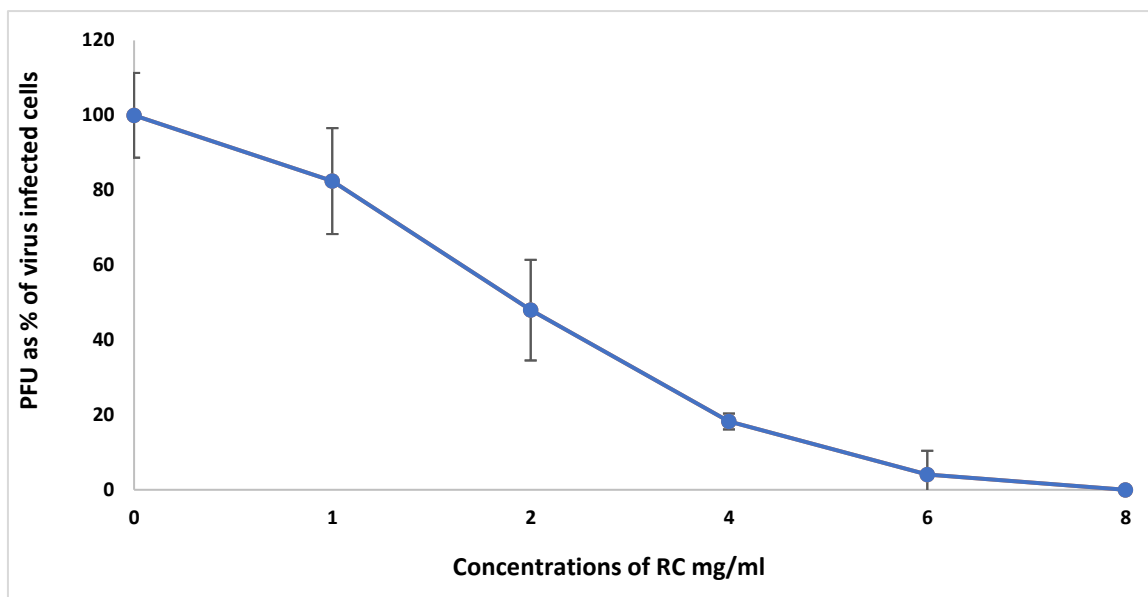


Figure 5-2. Inhibition of CAV9 infection by RC boiled extract.

GMK monolayers in 7.25 cm² (75 ml) flasks were pre-treated with a range of concentrations of boiled RC extract (0-8 mg/ml) in half ml of culture medium for 30 minutes. 370 PFU/ml of CAV9 were added and the cells were incubated on a rocking platform for 45 minutes at room temperature. 4 ml of a 2:1 mixture of culture medium and 2% CMC were added, and the flasks were incubated for 3 days in a humidified CO₂ incubator at 37 °C. The media was discarded, and cells were washed and stained with crystal violet solution and the number of plaques were counted. Error bars represent standard error from 3 independent experiments.

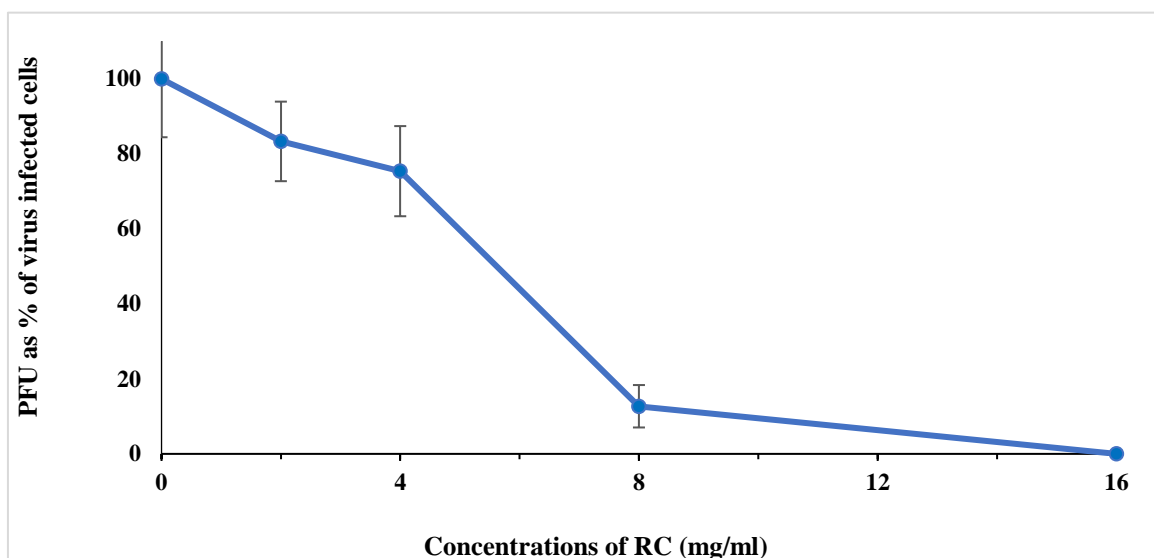


Figure 5-3. Inhibition of HPeV1 infection by RC boiled extract.

HT-29 cells monolayers in 6 well plate were pre-treated with a range of concentrations of boiled RC extract (0 - 16 mg/ml) in half ml of culture medium for 30 minutes. 370 PFU/ml of HPeV1 were added and the cells were incubated on a rocking platform for 45 minutes at room temperature. 2 ml of a 2:1 mixture of culture medium and 2% CMC were added, and the plate was incubated for 3 days in a humidified CO₂ incubator at 37 °C. The media was discarded, and cells were washed and stained with crystal violet solution and the number of plaques were counted. Error bars represent standard error from 3 independent experiments.

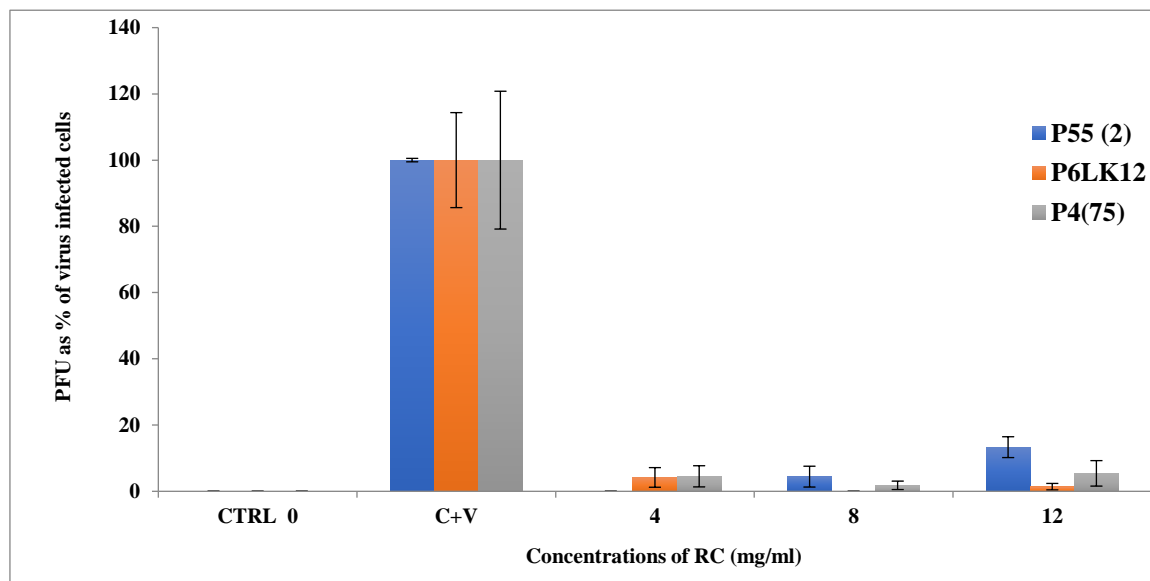


Figure 5-4. Inhibition of 3 different CBV3 isolates by boiled RC extract.

GMK monolayers in 6 well plate were pre-treated with a range of concentrations of RC extract (0 - 12 mg/ml) in 0.5 ml of culture medium for 30 minutes. 370 PFU/ml of three types of virus (P55 (2), P6LK12 and P4 (75)) were added and the cells were incubated on a rocking platform for 45 minutes at room temperature. 2 ml of a 2:1 mixture of culture medium and 2% CMC were added, and the plate was incubated for 3 days in a humidified CO₂ incubator at 37 °C. The media was discarded, and cells were washed and stained with crystal violet solution and the number of plaques were counted. CTRL 0: Cells only without virus or RC extracts, V: Virus. Error bars represent standard error from 3 independent experiments.

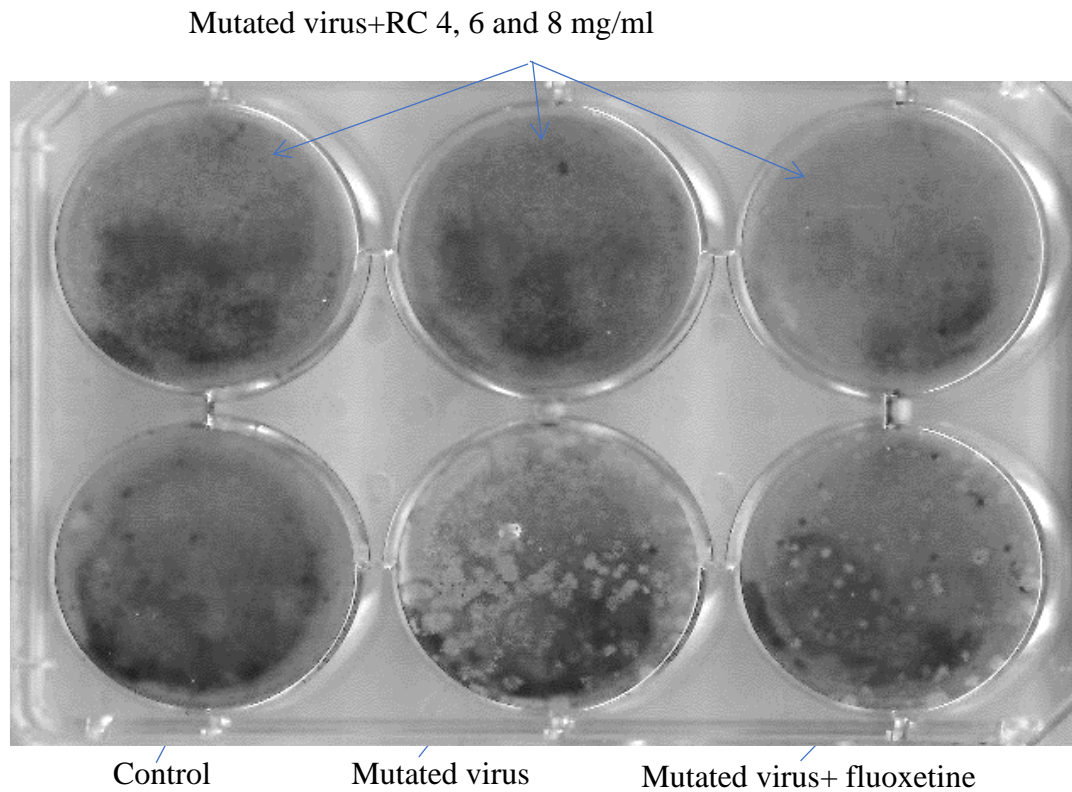


Figure 5-5. The effect of RC on CAV9 fluoxetine-resistant mutants in GMK cells.

Some of cells were pre-treated with RC 2 mg/ml, 4 mg/ml and 6 mg/l (top row) and others with fluoxetine 0.05 mM (bottom row) before adding the virus, then direct plaque assay was applied. The mutated viruses were resistant to fluoxetine, but not to RC.

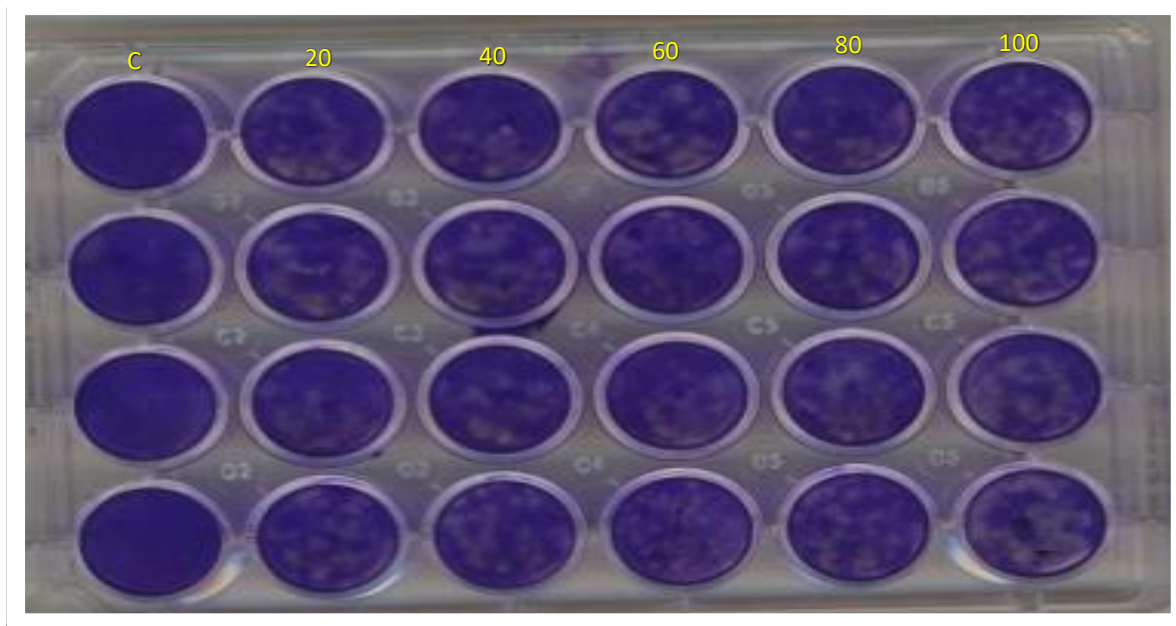


Figure 5-6. Analysis of the effect on infection of pre-treating CAV9 particles with boiled RC extract.

Each column represents a duplicate of the cells GMK monolayers in 24 well plate. CAV9 (370 PFU/ml) was pre-treated with RC boiled extract for the specific time (20 minutes to 100 minutes, shown in yellow) in a tube before addition to the cells. The cells were incubated on a rocking platform for 45 minutes at room temperature. 2 ml of a 2:1 mixture of culture medium and 2% CMC were added, and the plate were incubated for 3 days in a humidified CO₂ incubator at 37 °C. The media was discarded, and cells were washed and stained with crystal violet solution and the number of plaques were counted. CTRL: Cells only without virus or RC extracts, V: Virus.

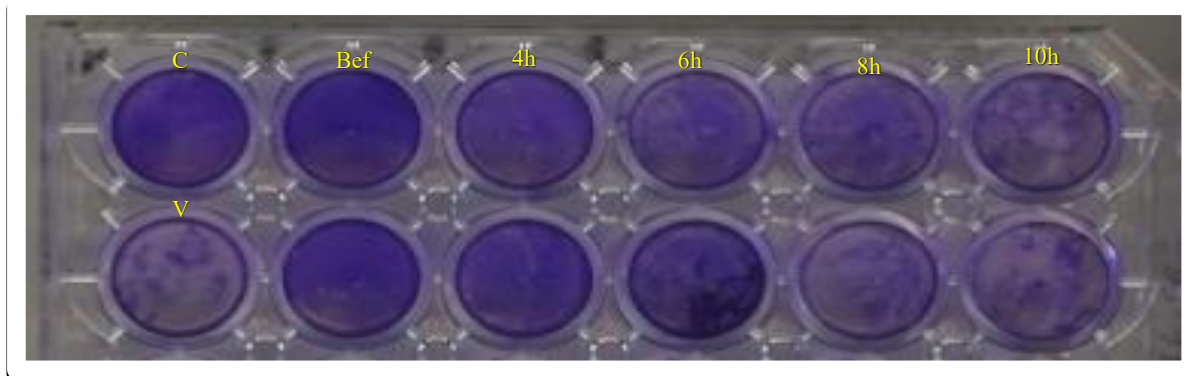


Figure 5-7. Comparison of the effects on infection of RC pre-treatment and addition of RC extract at different times after infection.

Some cells (Bef) were pre-treated with RC extract for 30 minutes. All the cells were then infected with 370 PFU/ml of CAV9 before treatment with 8 mg/ml of RC at the times shown. The cells were incubated on a rocking platform for 45 minutes at room temperature. 2.0 ml of a 2:1 mixture of culture medium and 2% CMC were added, and the plate incubated for 3 days in a humidified CO₂ incubator at 37 °C, media was discarded, and cells were washed, and stained with crystal violet solution. C in top row, cells [GMK] only, bottom row cells plus CAV9); V, Virus; h; hour. Bef; pre-treated with RC extract for 30 minutes before addition of virus.

5.2.7 Evaluation of the effects for the fractionated boiled RC on CAV9 viral infection/ plaque assay

To start to identify the active component(s) present in the boiled RC extract, fractionation was performed using automated flash chromatography as described in methods. Various fractions showed different effects on CAV9 using plaque assays (Figure 5.8 and Figure 5.9). The F3 fraction (Figure 5.8) had the most activity as no virus growth was seen even at lowest concentration of 0.25 mg/ml. F2 and F5 also had potent antiviral effects. F1 showed more moderate dose-dependent activity. Both F4 and F6 had no inhibitory effect on CAV9, in fact virus growth seemed to be enhanced slightly by F4 reaching up to 105% and substantially by F6 being 140% at 0.5 mg/ml, although there was a reduction of stimulation at higher concentrations. The antiviral activity of RC fractions in Figure 5.8 was estimated for once due to fractions deficiency.

To investigate the dose dependence of the highly active fractions, F2, F3 and F5 more fully, lower concentrations were used (Figure 5.9). This showed dose dependence and effective inhibition for each one, although none reached complete inhibition. F1 was used at the same concentration range as in Figure 5.8 and showed the same results. Increasing the concentration of F4 above that used previously achieved total inhibition of the infection. Increasing the concentration of the fractions F6 up to 2.0 mg/ml did not reduce viral growth further. The results suggest that there may be more than one active component present in the RC extract, as several fractions have an antiviral effect, or it may be that the imperfect fractionation method caused one active compound to be spread among the fractions.

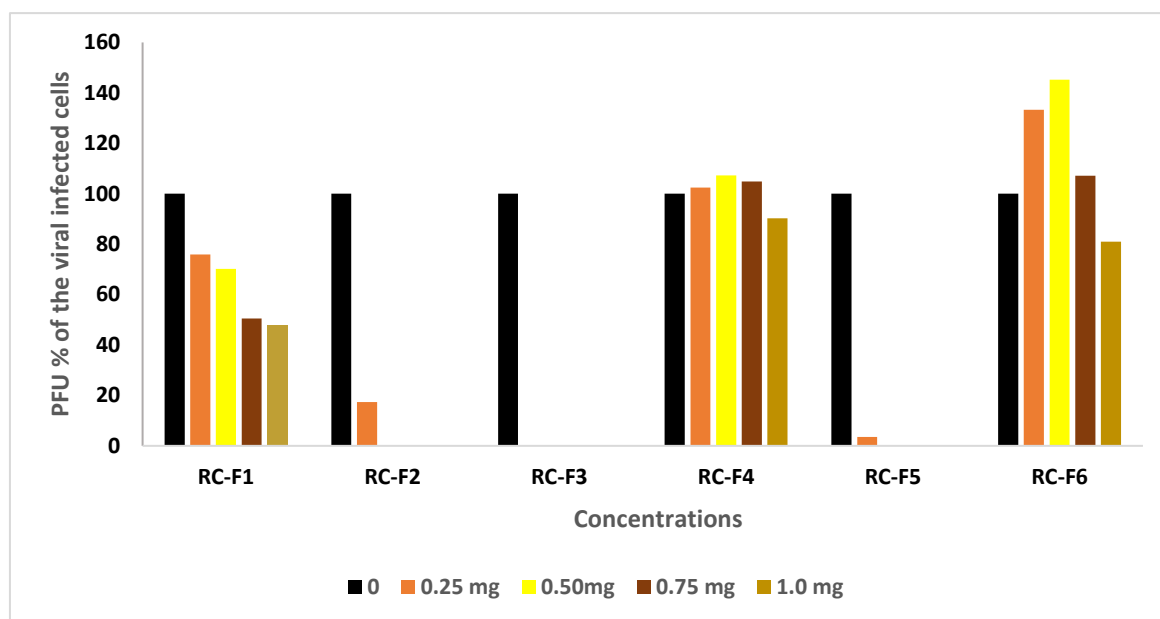


Figure 5-8. Effects of RC fractions on CAV9 infection.

Applying the direct plaque assay, GMK cells were infected with 370 PFU of CAV9 after pre-treatment with 4 concentrations of each RC fraction. Cells were incubated for 3 days in a humidified CO₂ incubator at 37 °C, the media was discarded and cells were washed, and stained with crystal violet solution. Plaques were counted and the number plotted as a % of the number seen in the absence of the RC fraction.

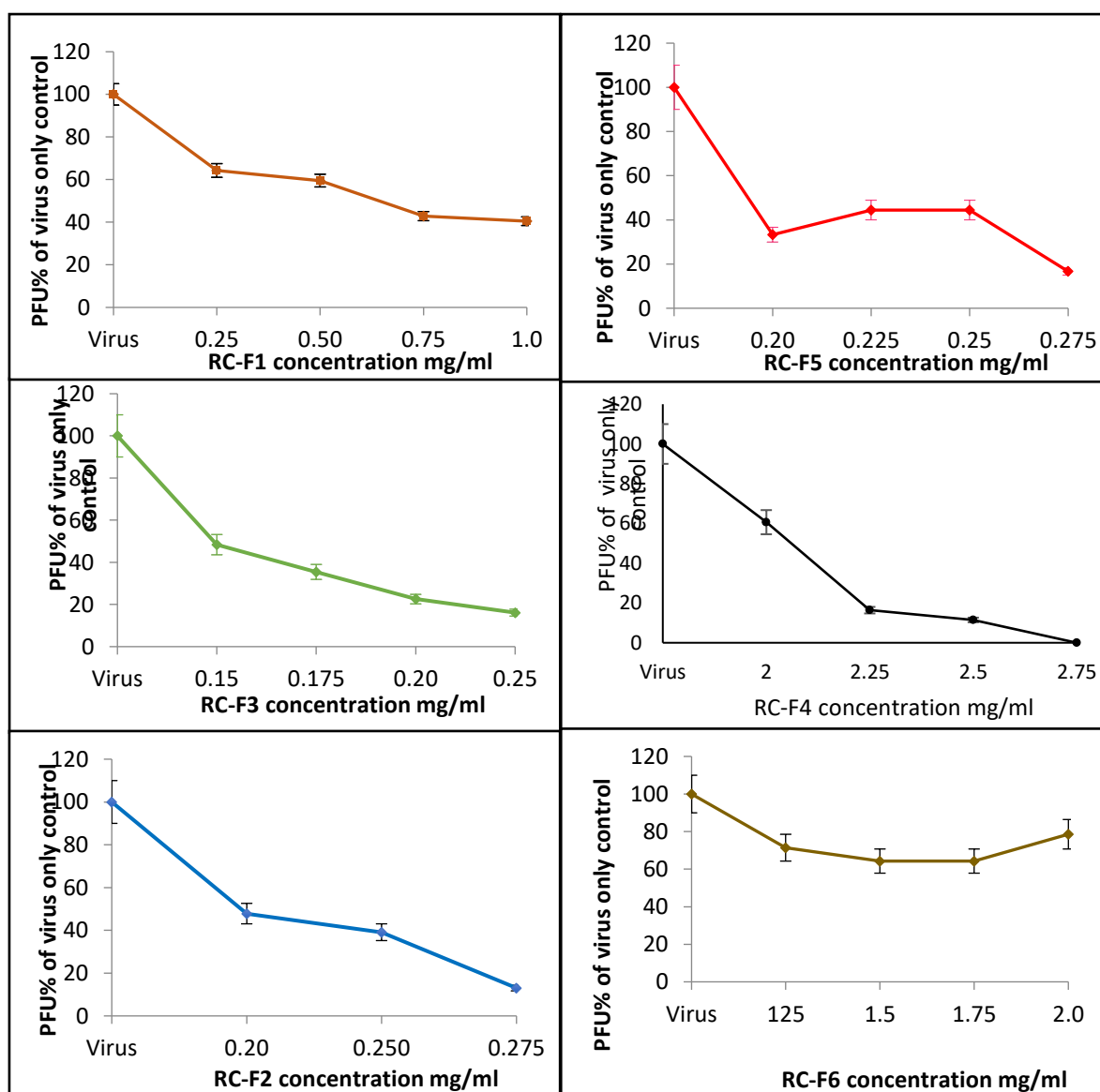


Figure 5-9. Effects of higher or lower concentrations of RC fractions against CAV9.

Applying a direct plaque assay, GMK cells were infected with 370 PFU of CAV9 after pre-treatment with higher or lower concentrations of boiled RC extracts (from F1 to F6) than those used in Figure 5.8. Cells then incubated for 3 days in a humidified CO₂ incubator at 37 °C, the media was discarded and cells were washed, and stained with crystal violet solution. Plaques were counted and the number plotted as a % of the number seen in the absence of the RC fraction.

5.2.8 Investigation of the effect of light on the activity of photosensitive constituents of RC extracts

The extracts of RC samples contain constituents that absorb light at different wavelengths and are activated to emit fluorescence at 310 nm and in the visible range at 615 nm (data not shown). They absorb at visible wavelength 620, 520, and 450 nm, and at 220, 280 nm in the uv range. Some fractions contain entities with no photosensitivity properties. It is known that fruit in general have many chemicals which act as antioxidant agents, nevertheless the absorbance properties suggest that some photosensitive constituents could be present and these may produce reactive oxygen species (ROS) or damage cells/viruses in other ways. Therefore, RC photosensitive constituents were exploited to assess the inhibition of viral growth. RC toxicity was examined first using a cell viability assay in 24-well plates (Figure 5.10) and the associated cell viability ranged between 80%-90% at all concentrations used.

5.2.9 The effect of different RC extracts on infection measured using MTT assays

The effect of RC extracts on cell viability and the inhibition of the viral activity in the dark were evaluated further using MTT assay. The experiment was carried out to compare the toxicity and the antiviral activity of different crude RC extracts without using plaque assays (Figure 5.11). All the extracts showed some toxicity, but the sample of boiled RC extract was the least toxic (Figure 5.11, A). Although, it showed 30% toxicity on the cells alone, nevertheless, the RC boiled extract increased the viability of the infected cells to nearly 100% compared to the control (cells without viruses) at the given concentration of 4 mg/ml. Both samples of the room temperature extraction (RC-Rt) and RC sonicated extraction samples (RC-SS) did not show any clear inhibition to the viral growth compared to the control with the virus only. Also, the solid-liquid phase extracted samples (RC-SBo2) showed only a slight inhibition of the viral infection of around 10%. The sample RC-Rt had the highest toxicity effect on the cells alone with approximately 75% in comparison to the control, while RC-SS extract and RC-Boi2) samples caused approximately 42% and 58% toxicity to the cells. Also, six fractions of RC sonicated extracts were tested and evaluated with the same method as the crude extracts (Figure 5.11B). The fraction RC1 was the only fraction that showed an improvement in cell viability in infected cells.

5.2.10 Effect of light exposure and RC extracts on the viral infection and cell viability

To determine the phototoxic effects of the crude extracts (the fluorescent constituents) on the virus activities indirectly, the confluent cells (GMK) in 96-well plate were exposed to either blue light (BL) or red light (RL) for 20 minutes after they were pre-treated with different RC extracts and then infected with CAV9 virus. This light exposure experiment was carried out on the same day and under the same conditions as the dark experiment. It was clearly seen that the antiviral inactivation effect of boiled RC sample was increased remarkably with BL, exceeding 130% of control (Figure 5.12 A). In addition, no cell toxicity was recorded upon incubation with the sonicated RC samples alone and exposure to BL, as compared to the control. However, there was no noticeable improvement with BL regarding other extracts in terms of toxicity or antiviral activity. The effect of the fractions of sonicated RC fractions (RC1– RC6) and the blue light were also investigated, (Figure 5.12 B). They impacted no remarkable viability improvement and the maximum viability increase was not more than 16% with RC5.

The infected cells pre-treated with the crude RC-Bo1 extract and exposed to RL had approximately 50 % increase in viability compared to the viability of infected cells alone. The other crude extracts and fractions gave little benefit (Figure 5.13).

In summary, there was some potential benefit of light treatment on cell viability in non-infected cells, but there was little consistent improvement in antiviral effect.

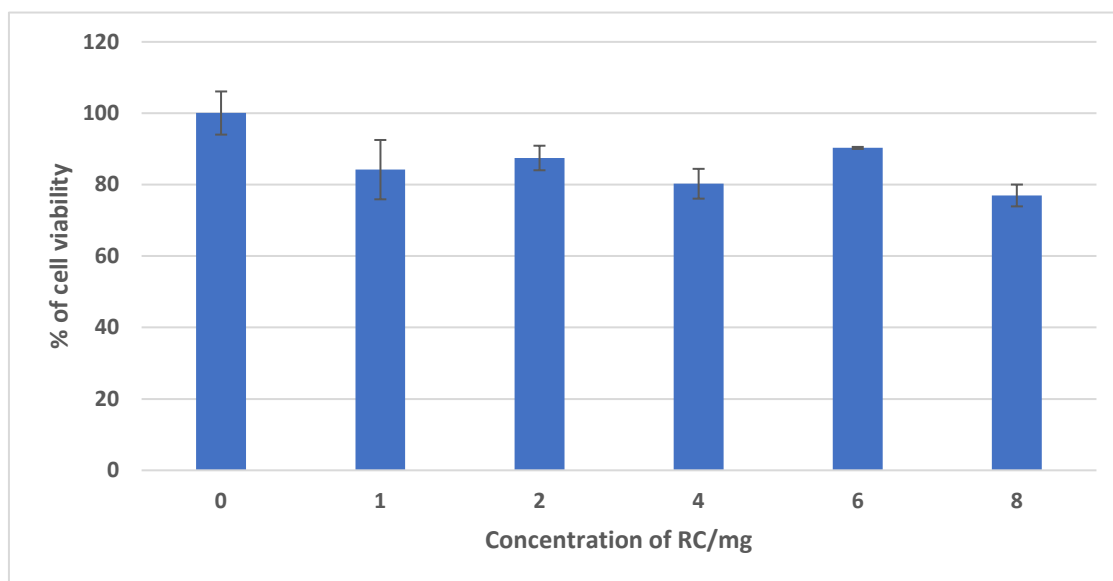


Figure 5-10. Cytotoxic effect of different boiled RC concentrations on A549 cells.

A549 monolayers in 24-well plate were pre-treated with different concentrations of RC in 0.5 ml of culture medium for 30 minutes and the cells were incubated on a rocking platform for 30 minutes at room temperature. 1 ml of a 2:1 mixture of culture medium and 2% CMC were added, and the plate was incubated for 2 days in a humidified CO₂ incubator at 37 °C. The medium was discarded, and cells were washed and 1 mg/ml of MTT in media were applied for 2 h, the resulting blue crystals were dissolved in DMSO and absorbance at λ_{550} was recorded. The cell viabilities were calculated as percentages of the control of cells alone.

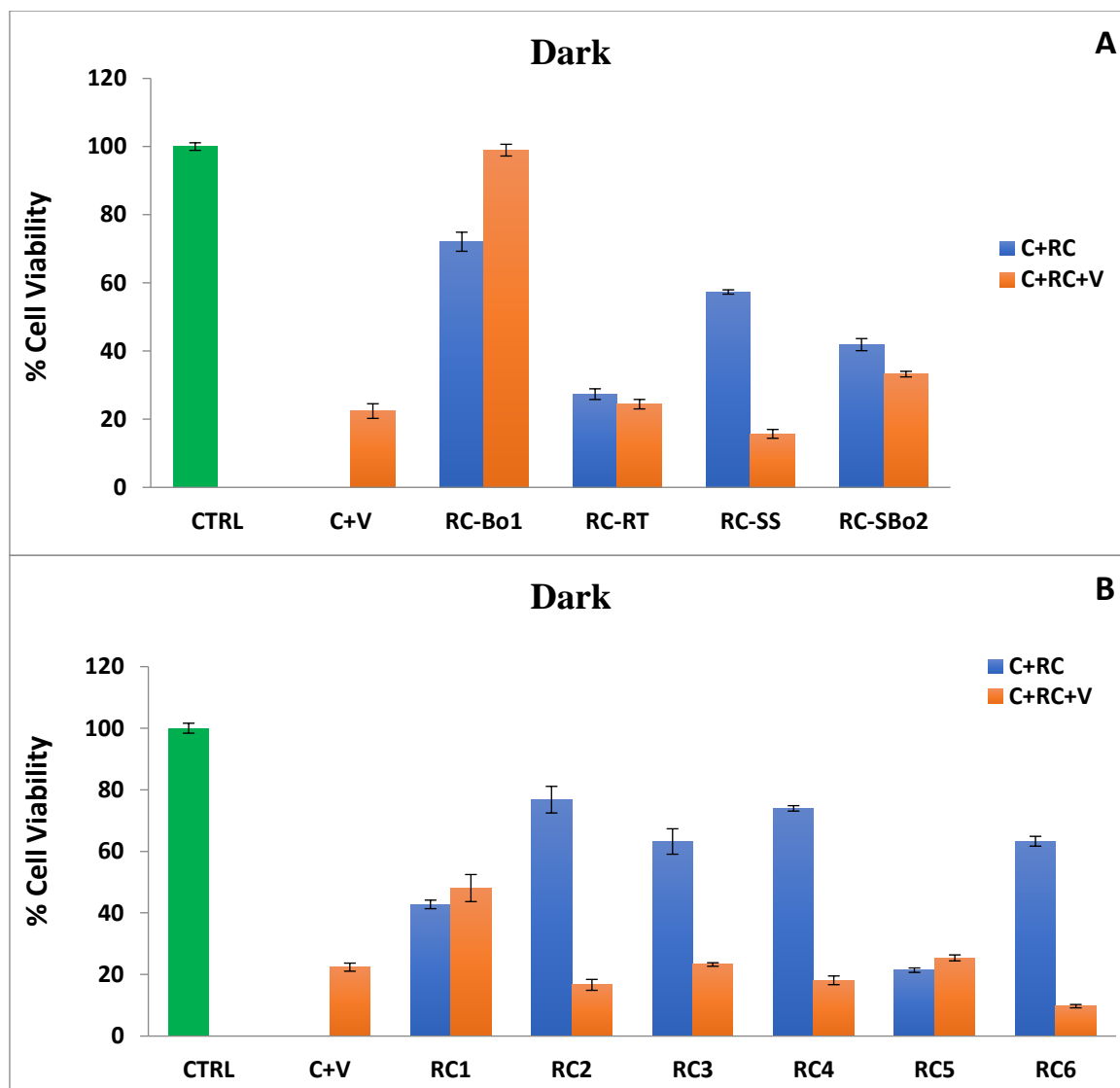


Figure 5-11. The effect of RC extracts and sonicated fraction samples on GMK cells with/ without CAV9 in the dark.

A: RC crude extracts (conc. 4 mg/ml). Cells were incubated with crude RC extracts produced by different extraction methods (blue bars), or CAV9 (C+V), or with RC extracts plus CAV9 and incubated for 3 days at 37 °C after a plate was wrapped with aluminium foil. CTRL, control with cells only, B: The fractionated samples of sonicated RC extract (RC1 to RC6, conc. 0.25 mg/ml). In both cases media were discarded and MTT in media were applied for 2 h, the resulting blue crystals were dissolved in DMSO and absorbance at λ_{550} was recorded. The cell's viabilities were calculated as percentages of the control of cells alone (green bar). RC-Bo1: Boiled extract. RC-Rt: Room temperature extract. RC SS: Sonicated extract. RC-SBO2: Solid-liquid phase extraction.

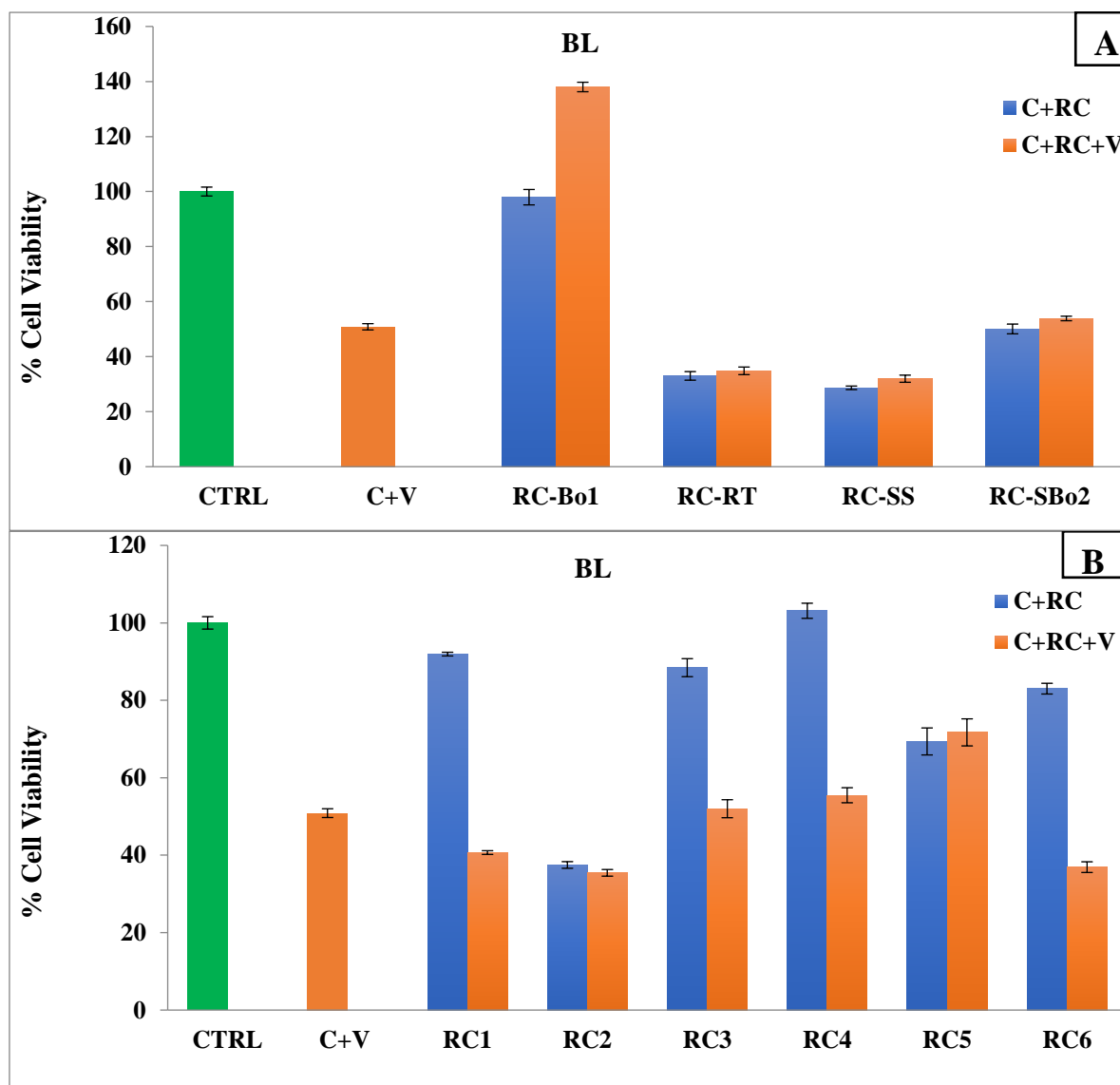


Figure 5-12. The effect of RC extracts and sonicated fraction samples on GMK cells with/ without CAV9 after exposure to blue light (BL) for 20 minutes. RC crude extracts (conc. 4 mg/ml).

A: Cells were incubated with crude RC extracts (conc. 4 mg/ml) produced by different extraction methods (blue bars), with CAV9, or with RC and virus, then exposed to blue light for 20 min. and incubated for 3 days at 37 °C after the plate was wrapped with aluminium foil. CTRL Control with cells only. B: Fractionated samples of sonicated RC extracts (conc. 0.25 mg/ml). In both cases media were discarded and MTT in media were applied for 2 h, the resulting blue crystals were dissolved in DMSO and absorbance at λ_{550} was recorded. The cell's viabilities were calculated as percentages of the control of cells alone (CTRL, green bar).

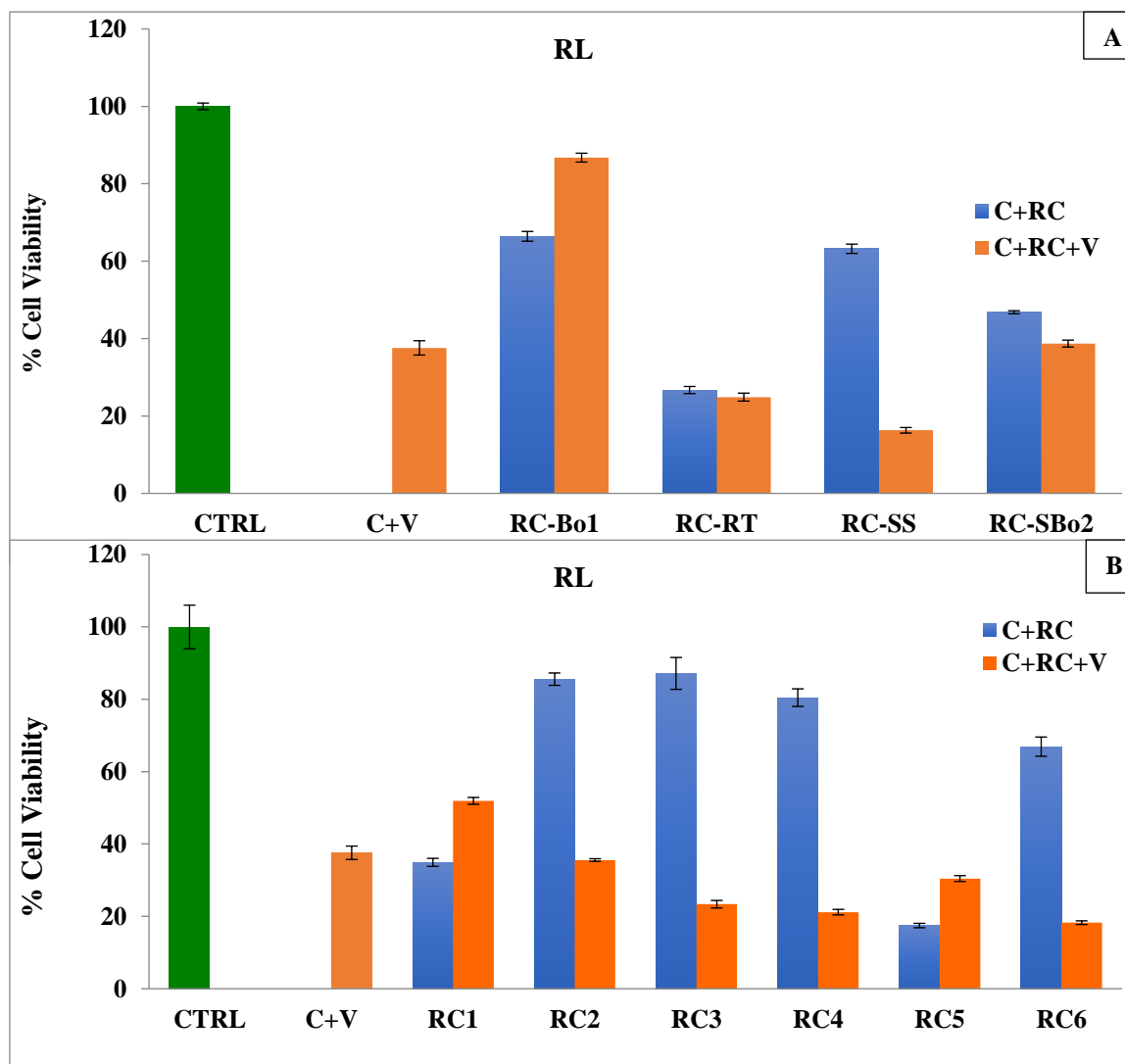


Figure 5-13. The effect of RC extracts and sonicated RC fraction samples on GMK cells with/ without CAV9 after exposure to red light (RL) for 20 minutes.

A: Crude RC extracts. Cells were incubated with crude RC extracts (conc. 4 mg/ml) produced by different extraction methods (blue bars), with CAV9, or with RC and virus, then exposed to red light for 10 min and incubated for 3 days at 37 °C after the plate was wrapped with aluminium foil. CTRL: Control with cells only (green bar), B: Fractionated samples of sonicated RC extracts (conc. 0.25 mg/ml). In both cases media were discarded and MTT in media were applied for 2 h, the resulting blue crystals were dissolved in DMSO and absorbance at λ_{550} was recorded. The cell's viabilities were calculated as percentages of the control of cells alone (CTRL, green bar).

5.2.11 The effect of microalgae extracts on CAV9 infectivity and cell viability in the absence and presence of light.

It has been found that microalgae (MA) contain several compounds with antiviral activities (Ahmadi *et al.*, 2015). Recent research has also found further applications of MA metabolites as fluorescent diagnostic tool (Chu, 2012). To establish if microalgae extracts could have a direct effect on the CAV9 particle, leading to inhibition of infection and whether light exposure would enhance antiviral activity, two series of MA were investigated for their antiviral activities against CAV9. Firstly, the virus was treated with several MA samples in the dark (Figure 5.14) then used to infect cells. Although MA extracts showed variable antiviral activity, they mostly had little toxicity to the cells. In fact, most of them increased the viability of cells in the absence of the virus. Most of the samples also had an antiviral effect in the dark. The sample MA-19 had a particularly efficient effect on CAV9.

The samples of MA (MA9, MA11, MA15, MA17 and MA19) were exposed to blue light (Figure 5.15A) which unexpectedly seemed to cause a general decrease in the antiviral activity in comparison to the dark experiment. The MA-19 that showed inhibition of more than 98% on the virus activity in the dark had negligible effect with the blue light (Figure 3.15 A). Also, all MA samples that were exposed to BL had no effect on cell viability. The sample of MA-F3 that was exposed to RL (Figure 3.15 B), also demonstrated moderate antiviral effects of around 55% viability compared to control but had no toxicity effect on cell's viability (control cells without virus). While MA1-F4 was ineffective (less than 5% viability) and had high cell toxicity.

Thus, although MA extracts showed some effect on CAV9, this was not enhanced by light treatment. Supply problems with MA extracts limited their further analysis.

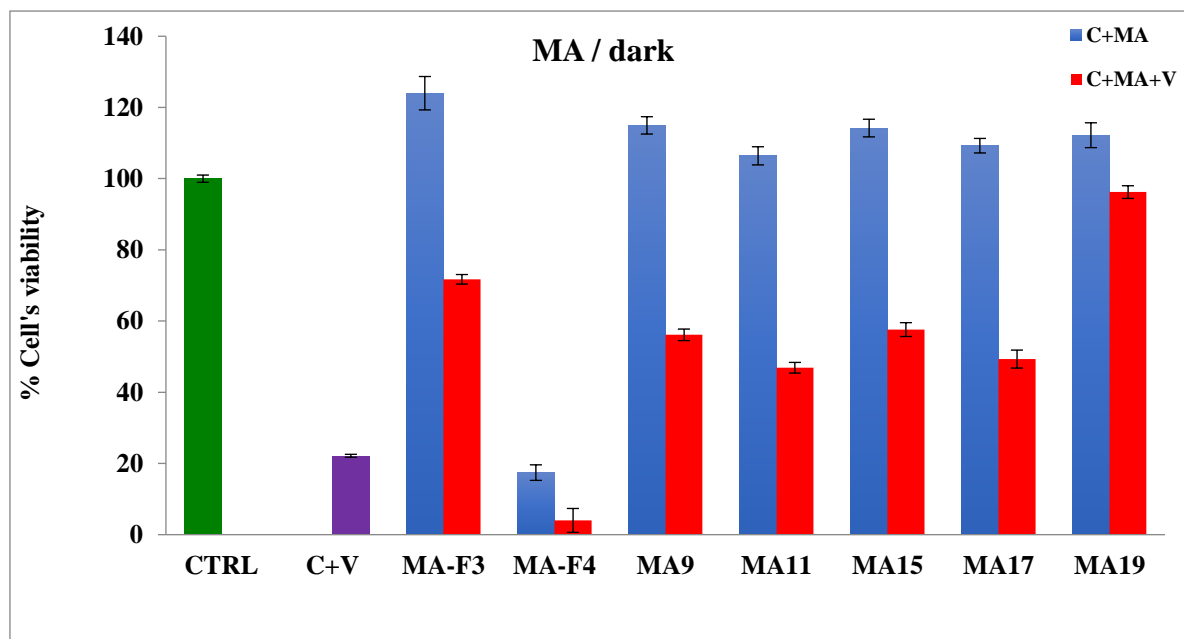


Figure 5-14. The effect of MA extracts on the viability of GMK cells and on CAV9 infectivity in the dark.

Control cells (CTRL) were incubated with the media only (green bar). Some cells were incubated with MA extracts with a concentration of 2.5 mg/ml (blue bars). Some cells were incubated with pre-incubated viruses with (red bars) or without MA extracts (purple bar). The plate was wrapped with aluminium foil. The cells were incubated for 3 days at 37 °C and the media was discarded, MTT in media were applied then for 2 h. The resulting blue crystals were dissolved in DMSO and absorbance at λ_{550} was recorded. The cell's viabilities were calculated as percentages of control (green bar).

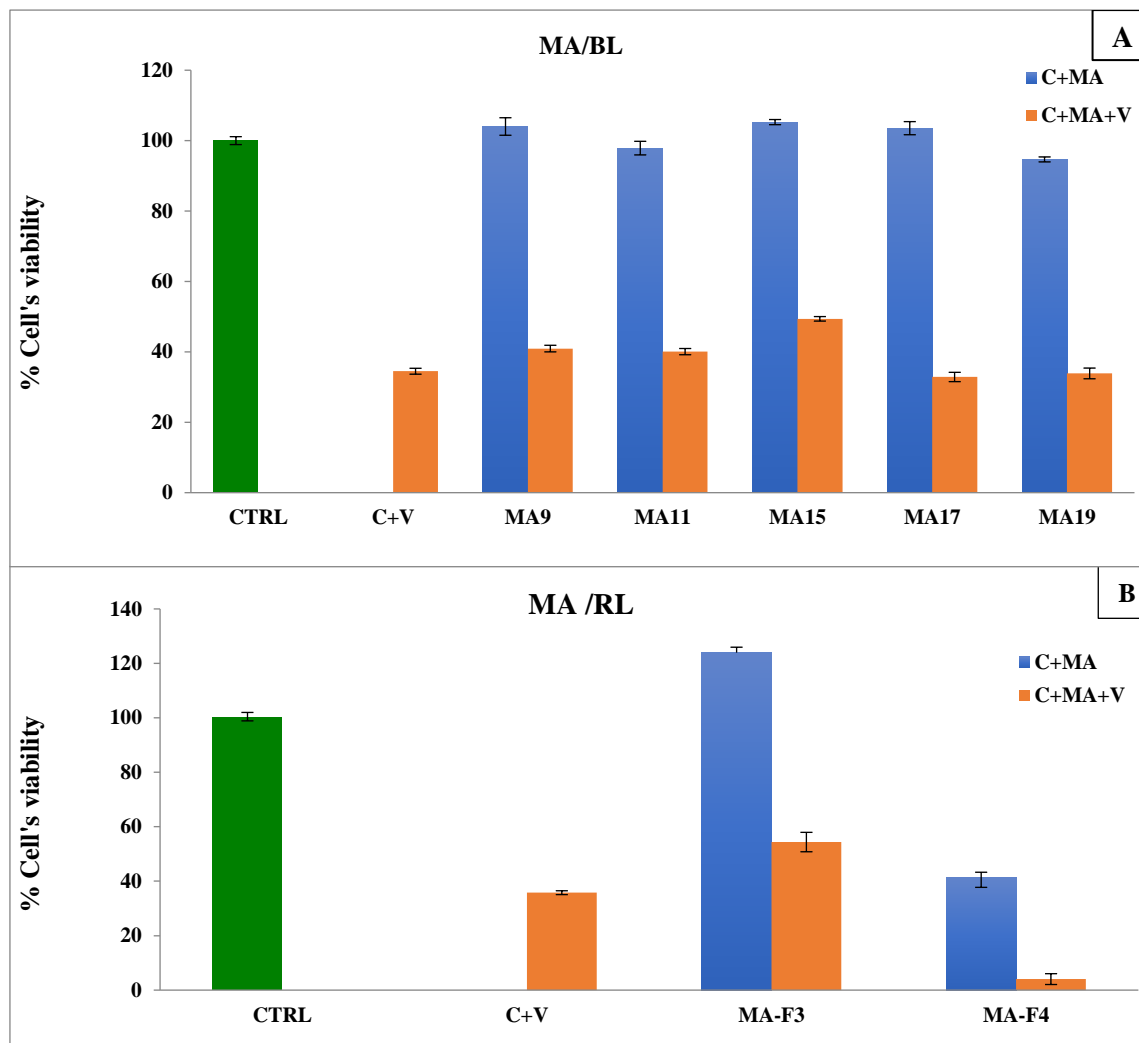


Figure 5-15. The effect of MA extracts on GMK cells with/ without CAV9 with exposure to A: Blue light (BL); B: Red light.

Control cells (CTRL) were incubated with the media only (green bar). Some cells were incubated with MA extracts with a concentration of 2.5 mg/ml (blue bars). Cells were incubated with CAV9 with or without pre-treatment with MA extracts, then exposed to the light for 30 min. The plate was wrapped with aluminium foil. The cells were incubated for 3 days at 37 °C and the media was discarded, MTT in media were applied then for 2 h. The resulting blue crystals were dissolved in DMSO and absorbance at λ_{550} was recorded. The cell's viabilities were calculated as percentages of control (green bar).

5.2.12 Quercetin antiviral activity in different cell lines

Quercetin is a naturally occurring compound present in several berries. It has been found to have an antiviral effect and could be an active component in the RC extract. Purified quercetin was therefore tested for activity against CAV9. In GMK cells quercetin caused a dose dependent decrease in CAV9 plaque formation when the concentrations increased from 0.10 to 0.75 mg/ml (Figure 5.16). The viral infection dropped sharply from 80% to approximately 7% of the value in the absence of the drug. However, total inhibition of the plaques was achieved with quercetin concentration of 2.0 mg/ml. A comparison of quercetin efficacy to inhibit the viral infection of CAV9 was made in two cell lines, A549 and GMK (Figure 5.17). In A549 cells, quercetin showed markable antiviral activity. This started at a concentration as low as 0.10 mg/ml to reach approximately 100% at only 0.50 mg/ml. As seen in Figure 5.16, the inhibition effect of quercetin was much lower in GMK cells. A concentration of 0.5 mg/ml caused only around 50% inhibition of GMK infected cells. Increasing quercetin further from 0.75 mg/ml to 2.0 mg/ml, resulted in much high inhibition of the infected cells from \approx 92% to 98%. It was concluded that the percentage of viral inhibition was significantly higher in A549 than GMK cells at low to moderate concentrations (0.10-0.50 mg/ml). Some of the apparent antiviral effect may be due to cell toxicity, as a 30% decrease in A549 viability is seen at a concentration of 0.50 mg/ml (Figure 5.18).

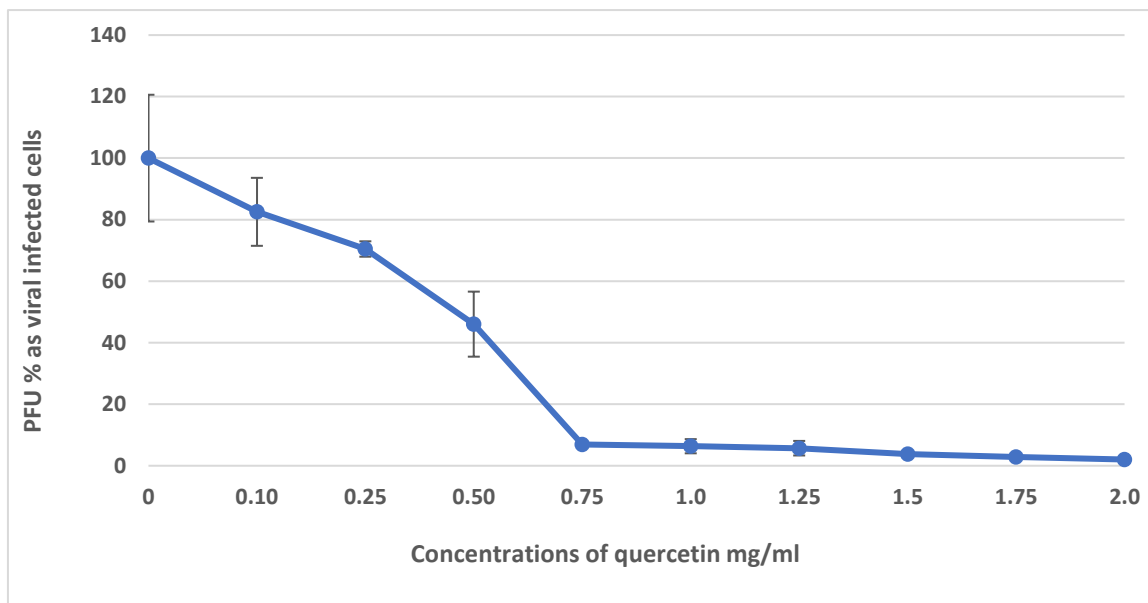


Figure 5-16. Effects of quercetin on CAV9 infection.

GMK cells were infected with 370 PFU of virus after pre-treatment with increasing concentrations of quercetin. The cells were incubated at 37 °C for 24 hours then lysed by freeze thawing three times. The amount of virus present was measured by plaque assay and expressed as a percentage of the value measured from virus-infected cells in the absence of drug.

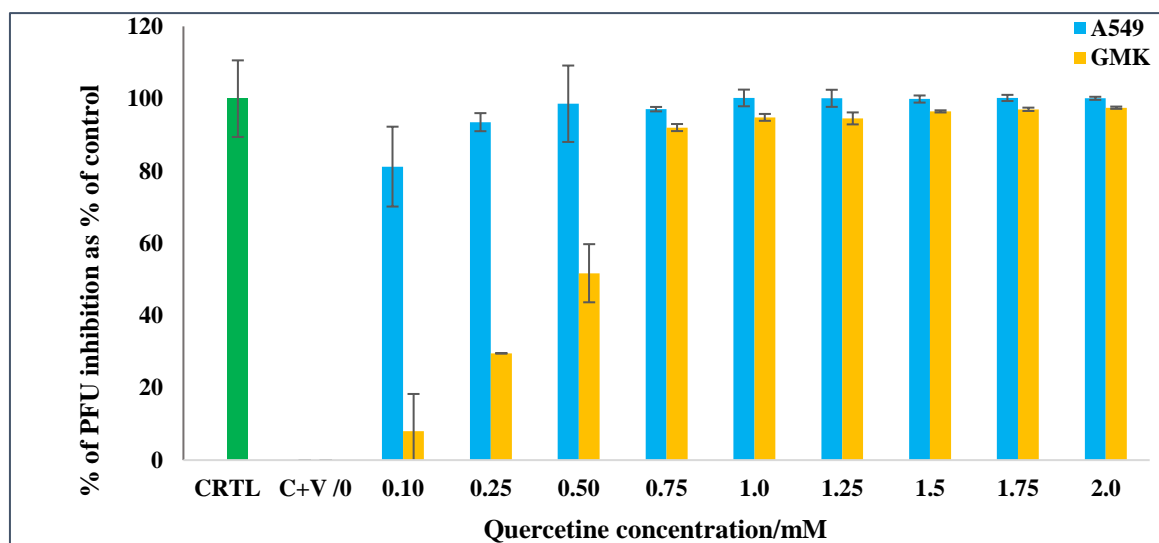


Figure 5-17. Comparison between CAV9 inhibition by quercetin in A549 and GMK cell lines.

A549 cells or GMK cells were infected with 370 PFU of CAV9 after pre-treatment with a range of concentrations of quercetin. The cells were incubated at 37 °C for 48 hours then lysed by freeze thawing three times. The amount of virus present was measured by plaque assay and expressed as a percentage of the value measured from virus-infected cells in the absence of drug. Percentage inhibition was then calculated by subtracting this value from 100 %.

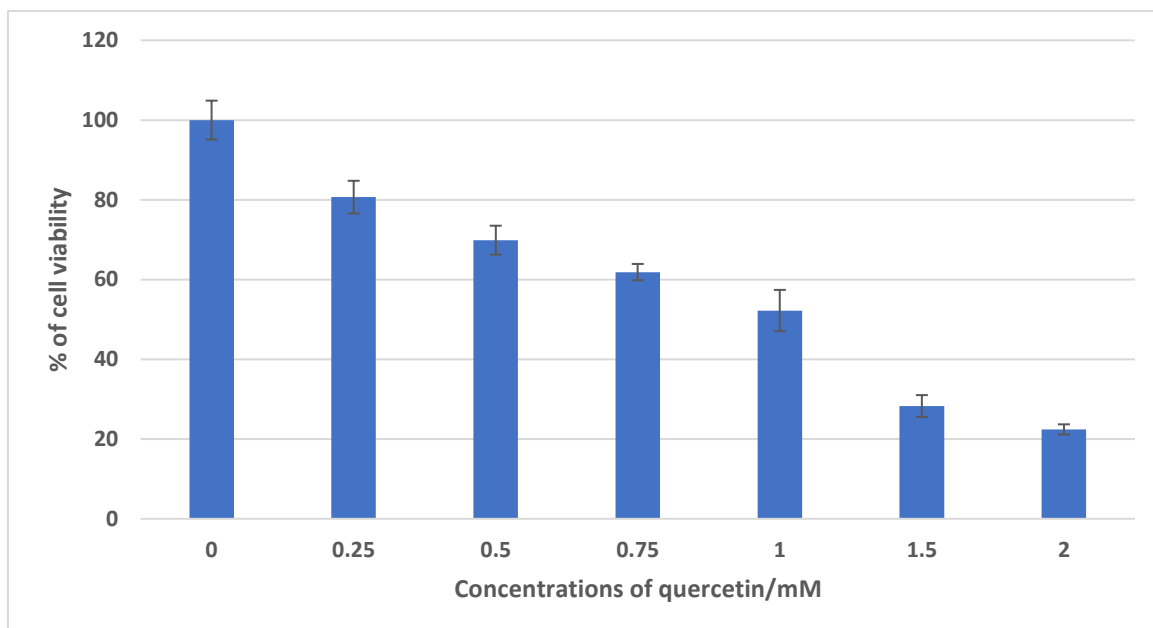


Figure 5-18. Cytotoxic effect of different quercetin concentrations on A549 cells.

A549 monolayers in 24-well plate were pre-treated with different concentrations of quercetin in 0.5 ml of culture medium for 30 minutes and the cells were incubated on a rocking platform for 30 minutes at room temperature. 1 ml of a 2:1 mixture of culture medium and 2% CMC were added, and the plate was incubated for 2 days in a humidified CO₂ incubator at 37 °C. The medium was discarded, and cells were washed and 1 mg/ml of MTT in media were applied for 2 h, the resulting blue crystals were dissolved in DMSO and absorbance at λ_{550} was recorded. The cell's viabilities were calculated as percentages of the control of cells alone.

5.2.13 Evaluation of antioxidant activities of the crude RC extracts and related fractions in cell free media

It has been reported that viral infection-induced free radical production reduces cellular AO levels and adversely affects cell function. On the other hand, various AO species were found to inhibit viral infection (Venkata *et al.*, 2013). To investigate if the antiviral effect of the RC extracts could be due to AO activity, we evaluated the AO activity of boiled RC extract using a myoglobin-based assay (Figure 5.19) and demonstrated reduction of myoglobin absorbance from 1.8 to 1.2. The end product of the reactions with RC samples showed significant antioxidant capabilities for all the extracts after nearly one hour from the start. Using myoglobin protective ratio percent (MPR) (Figure 5.20), the sample of liquid-solid extract (RC-SBo2) displayed the most powerful AO activity with its MPR above 110%. The MPR of RC boiled extract (RC-Bo1) was about 90% while that extracted at room temperature (RC-Rt) extract was just above 80%.

Using the myoglobin assay and gallic acid (GA) as a standard (Figure 5.21A), GA showed comparable AO activity with a concentration of only 7.5 $\mu\text{g/ml}$ to that concentration of RC-Bo1 extract with 250 $\mu\text{g/ml}$. The samples of the crude RC-Bo1 reactions at lower concentrations from (10 $\mu\text{g/ml}$ to 150 $\mu\text{g/ml}$) were much slower and didn't reach to a plateau within 50 min. The Rate of the AO (RC-Bo1) reaction with ferryl myoglobin (Rate (1/s) was calculated at the range of concentrations from 10 $\mu\text{g/ml}$ to 250 $\mu\text{g/ml}$ (Figure 5.21B). The calculated data demonstrated that the rate of the reactions for RC-Bo1 as AO is concentration dependant reaction at the initial period of the reaction time. RC-Bo1 exhibited remarkable AO activity with much faster rate to those figures of the other crude extracts. The reactions of RC-Bo1 fractions (Figure 5.22) with ferryl myoglobin were very fast and completed within few seconds. Therefore, it was difficult to record the kinetics of those fractions with this spectroscopic method.

The extracts clearly have AO activity, and this could contribute to the observed antiviral effect.

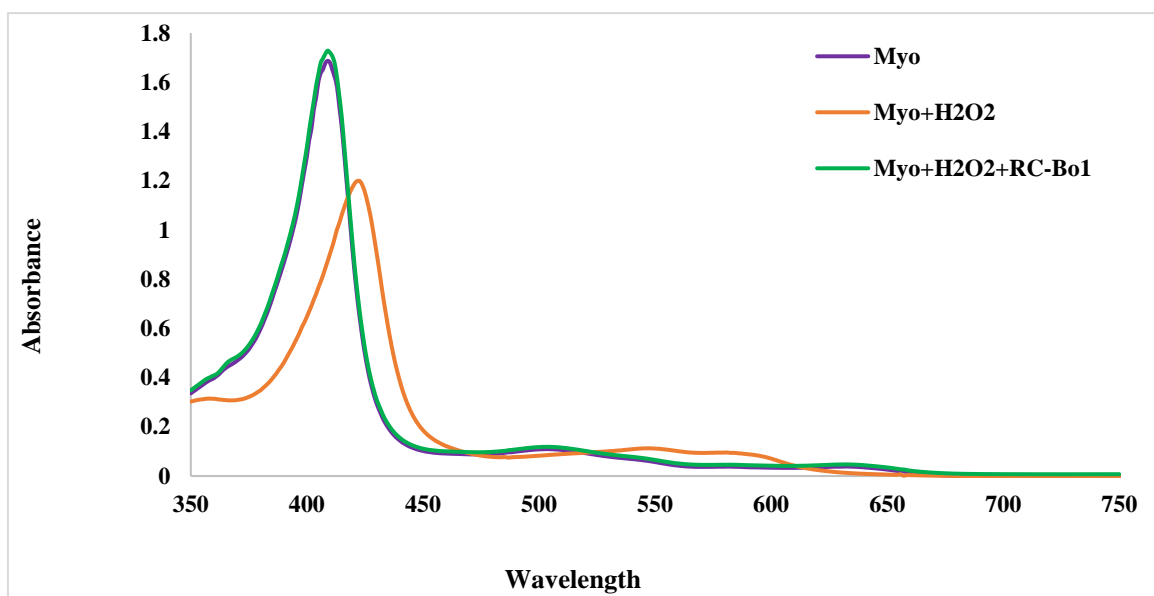


Figure 5-19. Antioxidant activity AO of boiled RC extract.

Myoglobin (Mb) alone ($13.5 \mu\text{M}$) was added to 2 ml of PBS at pH7.2 in cuvette and the absorbance was recorded at wavelength of 409 nm. Hydrogen peroxide (H_2O_2 , $140 \mu\text{M}$) was added at room temperature. The reaction was terminated after 10 min by adding $2 \mu\text{l}$ of catalase enzyme and the absorbance was recorded again after 2 min. The absorbance was also recorded at wavelength λ_{409} nm. RC samples with concentration of ($250 \mu\text{g/ml}$) were added and the absorbance was recorded at λ_{409} for the antioxidants.

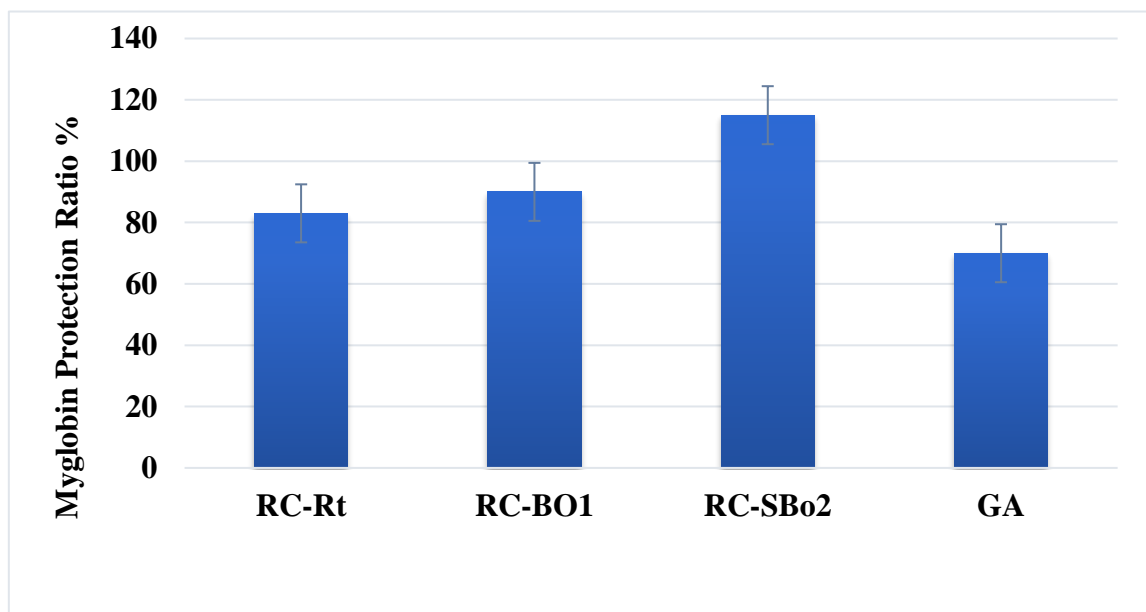


Figure 5-20. The myoglobin protective ratio (MPR) for AO activity of RC extract samples.

Myoglobin (Mb) alone ($13.5 \mu\text{M}$) was added to 2 ml of PBS at pH7.2 in cuvette and the absorbance was recorded at wavelength of 409. Hydrogen peroxide (H_2O_2 , $140 \mu\text{M}$) was added at room temperature. The reaction was terminated after 10 min by adding $2 \mu\text{l}$ of catalase enzyme and the absorbance was recorded again after 2 min. The absorbance was also recorded at wavelength $\lambda_{409} \text{ nm}$. RC samples with concentration of ($250 \mu\text{g/ml}$) or Gallic Acid (GA, $7.5 \mu\text{g/ml}$) were added and the absorbance was recorded again at λ_{409} for the antioxidants. RC-Rt: Room temperature extract. RC-Bo1: Boiled extract. RC-SBo2: Sample of solid-liquid extraction.

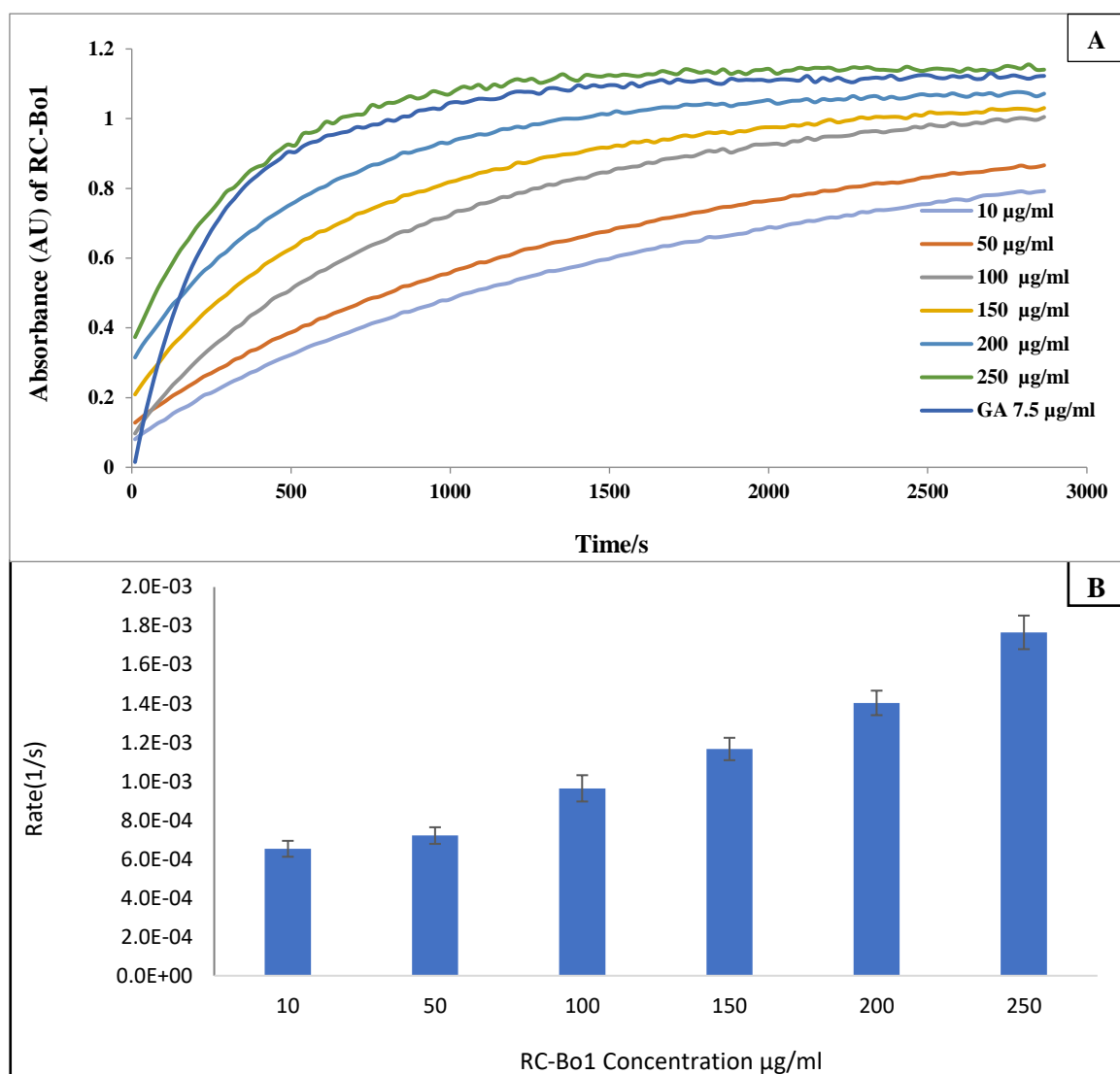


Figure 5-21. Kinetics and rate of reaction of antioxidant activity of boiled RC extract.

A: Kinetics of AO activity for crude RC boiled extract (RC-Bo1) samples against time. Myoglobin (Mb) alone (10 µM) was added to 2 ml of PBS at pH7.2 in cuvette and the absorbance was recorded at wavelength of 409. Hydrogen peroxide (H₂O₂, 100 µM) was added at room temperature. The reaction was terminated after 10 min by adding 1 µl of catalase enzyme. A range of concentrations of RC-Bo1 were added to each cell and the kinetics was recorded for 50 min (3000 s). **B: The calculated rate of reaction of AO with the ferryl of the myoglobin against time per second (s).**

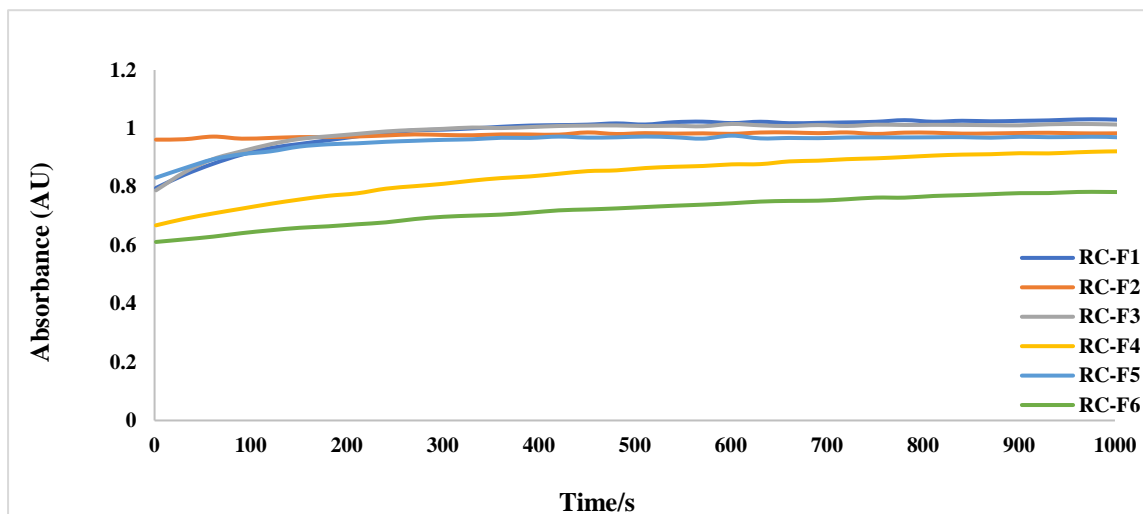


Figure 5-22. Kinetics of AO activity for crude RC fractionated of boiled extract (RC-F1-F6) samples against time.

Myoglobin (Mb) alone ($13.5 \mu\text{M}$) was added to 2 ml of PBS at pH7.2 in cuvette and the absorbance was recorded at wavelen μ th of 409. Hydrogen peroxide (H_2O_2 , $140 \mu\text{M}$) was added at room temperature. The reaction was terminated after 10 min by adding $2 \mu\text{l}$ of catalase enzyme. A concentration of $100 \mu\text{g/ml}$ from each RC fractions was added to each cell and the kinetics of the recorded for 1000 s.

5.2.14 LC-MS/MS analysis of RC fractions

To attempt to purify and identify active components from the boiled RC extract, it was fractionated by flash chromatography and the fractions were analysed with LC-MS/MS spectroscopy.

5.2.15 Methods of LC-MS/MS analysis

A mixture of gradient and isocratic program was employed after eluent's optimization. The diode array traces of each fraction (5 µg/ml) was recorded over 30 minutes and monitored at wavelengths between 200-800. The C18 reversed column based chromatographic separation along with trifluoroacetic acid (TFA) added to mobile phase was used in this work. The applied chromatographic technique is characterised by its good performance, high sensitivity and good selectivity (Chen *et al.*, 2014). TFA as ion-pairing agent was added to mobile phase to improve peak sharp and resolution. TFA was used at 0.1%. It has been reported that increased TFA concentration causes an improvement in peaks resolution and TFA of 1%, 5% and 10% were used with better separation and shorter elution time in some previous published works (Chen *et al.*, 2014). Therefore, higher TFA concentration may be suggested for future work. Positive ion mode was applied which has strong evidence of increasing response and sensitivity of tested compounds (Chen *et al.*, 2014).

The fractionation resulted in separation of the constituents into several bands containing mixtures of chemicals with similar polarities. The data obtained from LC-MS/MS, the UV spectra and MS confirmed the presence of two main types of compounds, the anthocyanins/anthocyanidins and flavonoids, alongside many other small molecules such as sugar, ascorbic acid, coumaric, cinnamic, etc. Several compounds in the separated fractions have molecular masses (ES/CI) of well-known compounds and documented extensively in the literature, but there were also unknown entities (Silva., 2007; Nakabayashi., 2009; Sasaki., 2014). Selected examples of analytical characterisation by a liquid chromatography system coupled to electrospray mass spectrometer LC-MS/MS for three fractions are presented in this section. The investigated fractions (F1 and F2) have similar elution pattern within a 60 min run (Figure 5.23 and 5.24, a-c). The first eluted peak was at retention time (t_R) of 0.89 min, the second peak eluted at t_R at 9.28 min with absorbance wavelengths of (230, 270 and 500 nm) with diode array. The peak at 16 min

was more pronounced in F2 than F1 fractions. The traces in figure 5.23 (d) and 5.24 (d) represent the total ion counting of the fractions after passing through MS spectrometer. It showed the peaks of ions that correspond to the constituents eluted and fractionated by LC system at small delay of about 0.5 min. The majority of constituent were between 1.47-9.8 min, then another major band between 45-50 min.

The elution of fraction F3 was optimised to run within 14 min (Figure 5.26, a-g). The Fraction F3 revealed most of its constituents with absorbance wavelength of 620 nm (Figure 5.25, a). It has peaks at t_R of 0.6-1.25 min, then major peaks at 5.12-5.40 min where it was also predominant in the other range of UV diode array traces at 220, 260, 360, 450, 520 nm (Figure 5.25, b-f). Those close peaks revealed a mixture of unresolved constituents eluted together. There were small peaks at 9.8 min but the largest peak it appeared at wavelength of 620 nm at t_R between 13.13-13.32 min. The trace in (Figure 5.25, g) displayed the total ion counting for the constituents of F3 passing through MS system, it seemed to be also a mixture of constituents. The absorbance spectra of couple of constituents in F3 fraction were recorded at t_R of 5.64 and 5.27 min, confirmed the differences of the constituent's spectra eluted at the time (Figure 5.26, a & b). The spectra in Figure 5.26a, showed aliphatic and aromatic types compounds around the visible range between wavelength 200-350 nm, while b trace displayed an extra peak appeared around 518 nm, which can indicate to the existence of poly-cyclic aromatic compounds, such as flavonoids anthocyanins, etc.

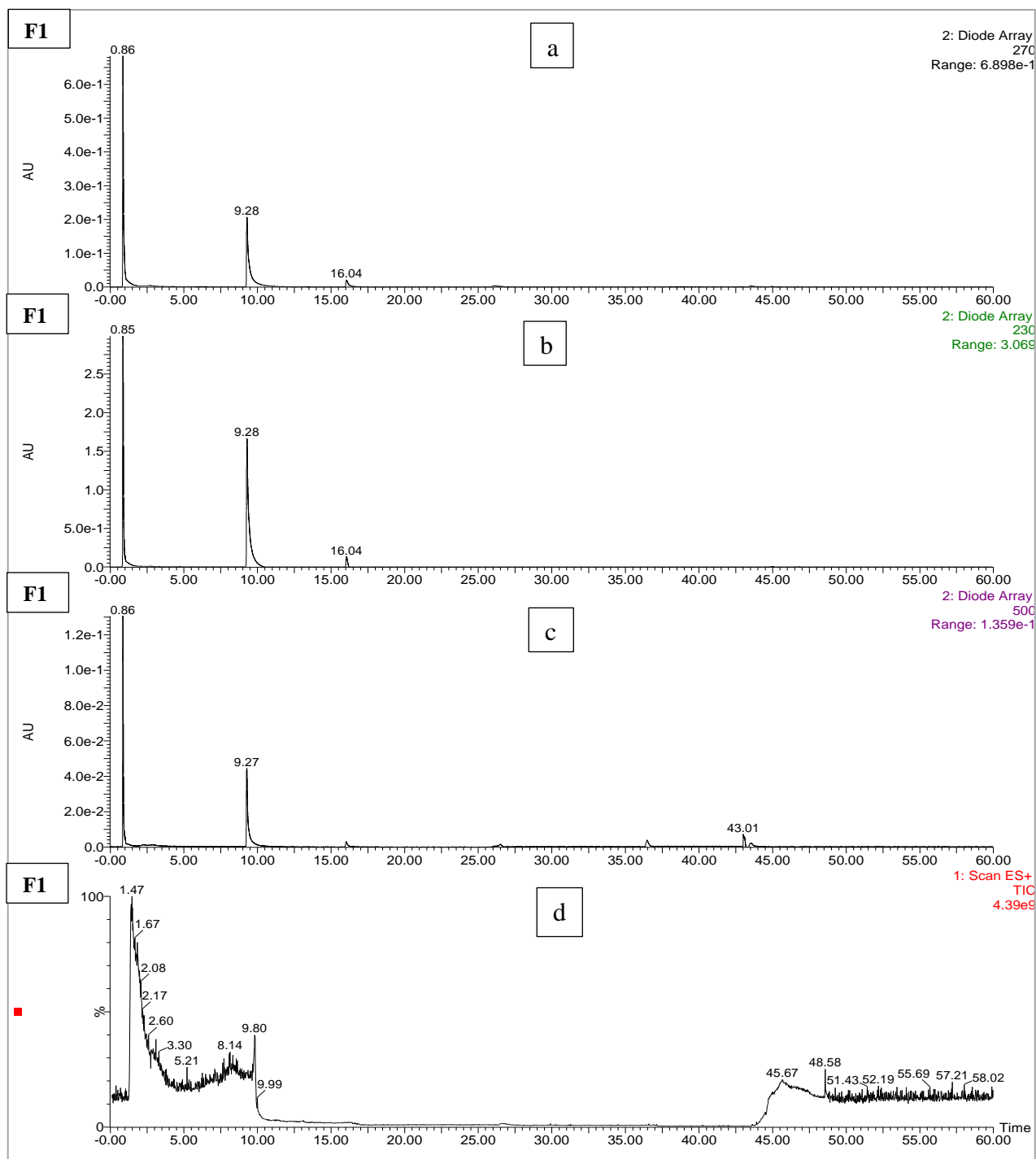


Figure 5-23. LC-MS elution of fraction F1.

a, b, and c are LC traces for 60 min elution time of F1 band at wavelength absorbance 270, 230, 500 nm. d: MS trace for total ion counting (TIC) in 60 min for F1 elution.

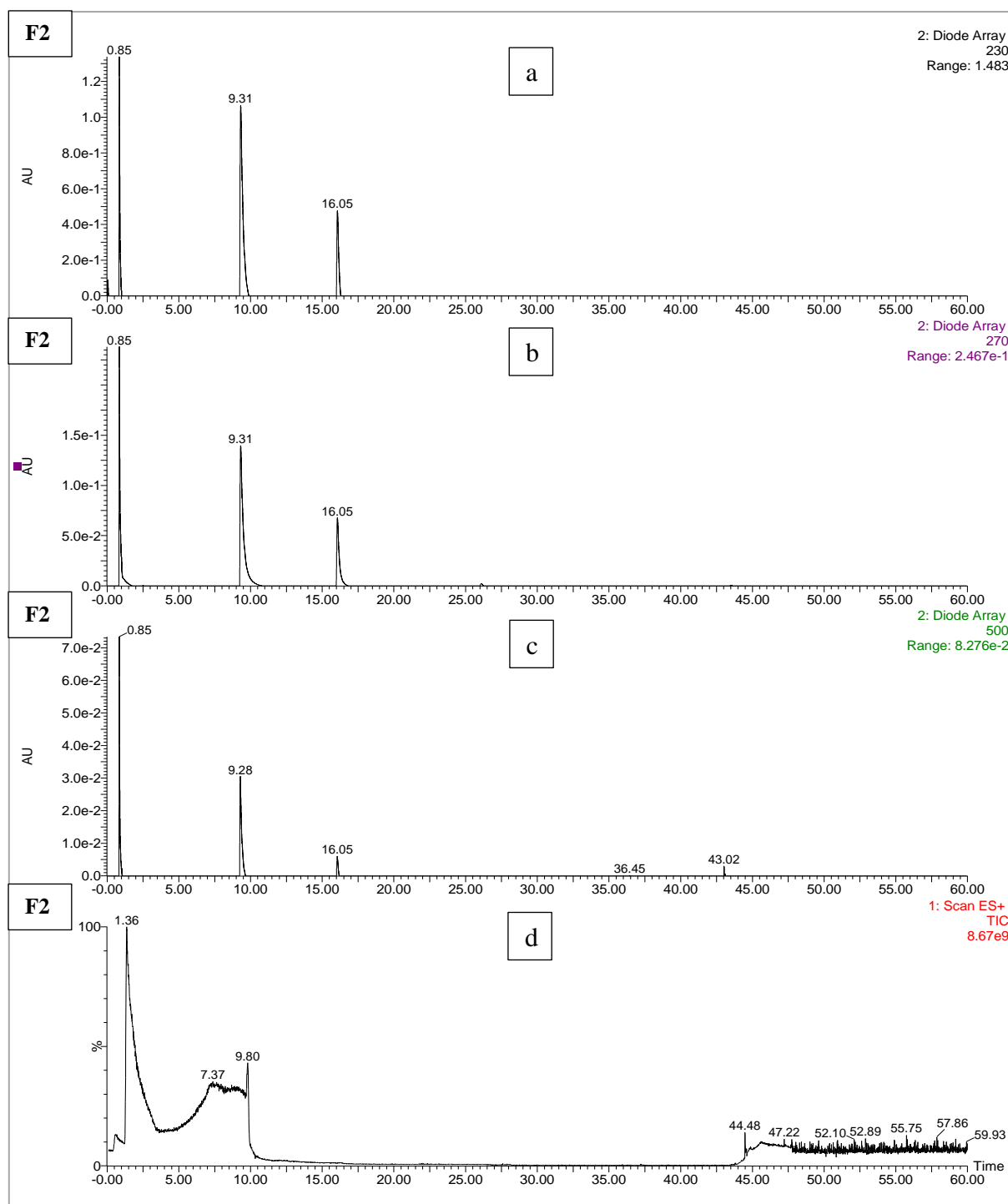


Figure 5-24. LC-MS elution of Fraction F2.

a, b, and c are LC traces for 60 min elution time of F1 band at wavelength absorbance 270, 230, 500 nm. d: MS trace for total ion counting (TIC) in 60 min for F2 elution.

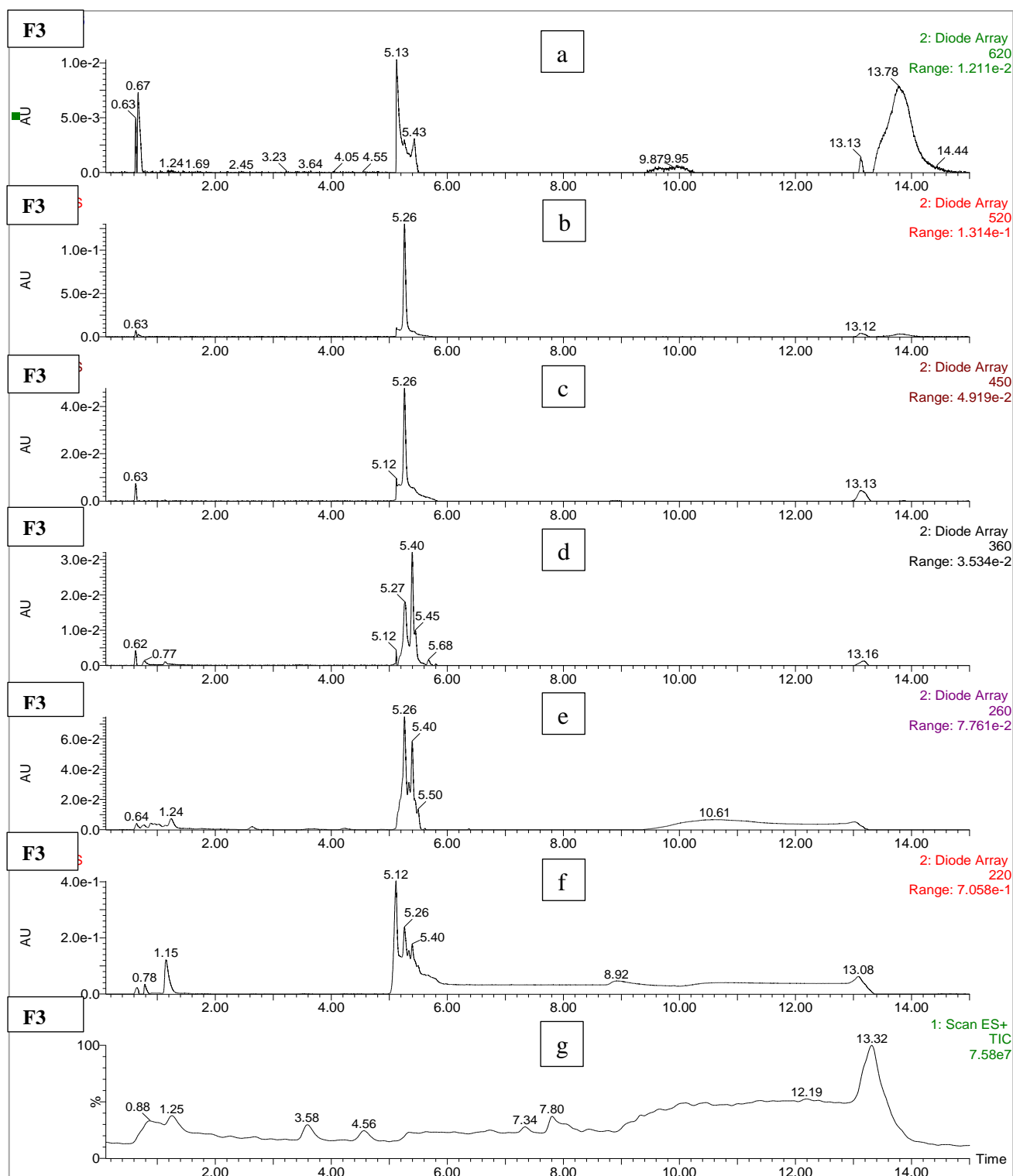


Figure 5-25. LC-MS elution of Fraction F3.

a, b, c, e, and f are LC traces for 14 min elution time of F3 band with diode array at wavelength absorbance 220, 260, 360, 450, 520, and 620 nm. g: MS trace for total ion counting (TIC) in 14 min for F3 elution. LC-MS was optimised with the sample's flow of 250 $\mu\text{l}/\text{min}$ from the DAD eluent was directed to the ESI interface using a flow-splitter.

The source block temperature was held at 120 °C and the desolvation gas (nitrogen gas) temperature was 350 °C. The flow rate of 650 l/h, and cone gas of 82 l/h was used. The capillary potential of 3.2 kV was used. MS spectra recorded between m/z range 100-950, in the positive mode cone voltages (CV) (25 V).

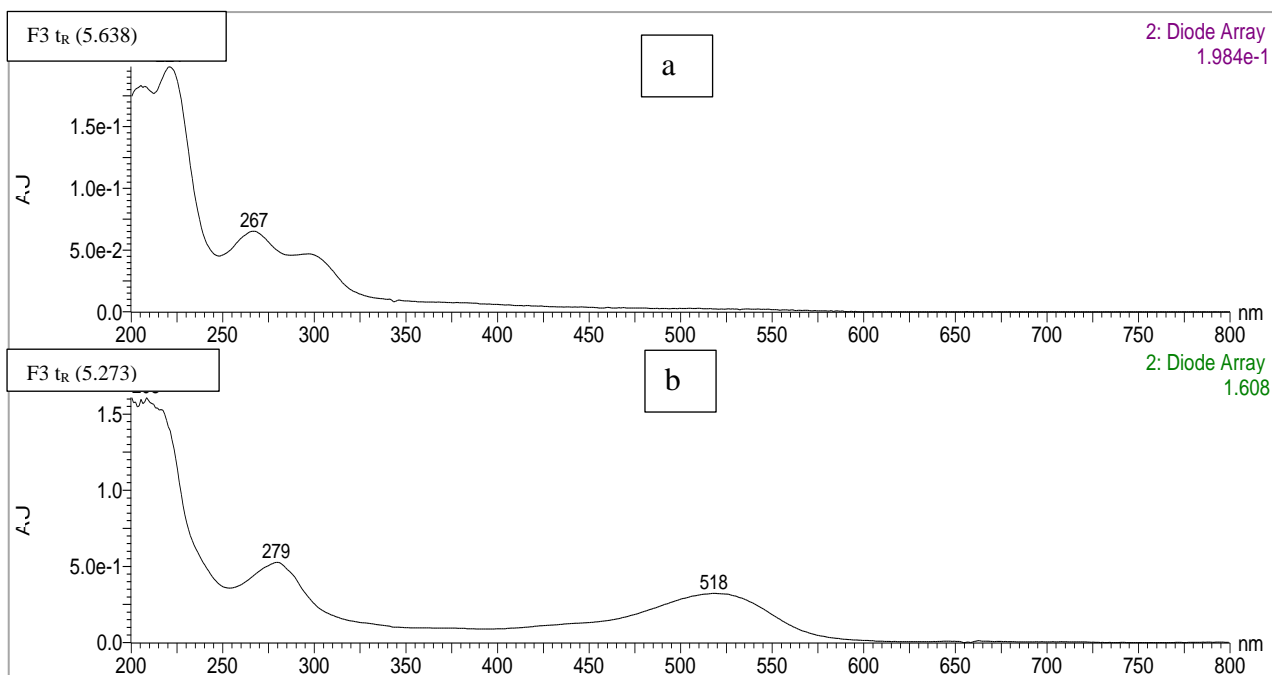


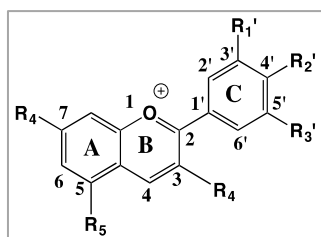
Figure 5-26. The diode array UV spectra of RC F3 constituent recorded from the wavelength 200-800 nm.

This was recorded for F3 during elution through LC-MS/MS; (a) at t_R of 5.638 min and (b) at 5.273 min below.

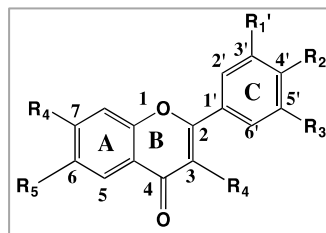
5.2.16 Analysis of MS and MS/MS spectroscopy

Selected MS spectra from F1, F2, and F3 at certain Retention times (t_R) were obtained and presented in this section according to their masses against charges (m/z). It was found from several LC-MS/MS analysis, the existence of anthocyanins/anthocyanidins and flavonoids moieties, Figure 5.27. Example of MS spectra gave dominant peaks with m/z 142-147, 610-612, 684 Daltons (D), they demonstrated the masses of m/z and their isotopes at 1.4 min t_R , Figure 5.28. The peak at 142-147 D could be a fragment of the compound belong to 610 D. The predicted proposed structures for the 610 D identified as cyanidin-3,5-di-*O*-glucoside = 611 or, also called (cyanidin sophoroside) according to other literatures (Cavaliere *et al.*, 2005; Abad-García *et al.*, 2009). Quercetin-3-*O*-digalactoside featured flavonoid moiety coupled to two glucoside groups either at the hydroxy group of ring B at hydroxy group of the ring B gave also m/z 610. The predominating detected peaks (Figure 5.29) for the constituents of F2 with 595 (cyanidin 3-galactoside) and 727 D, cyanidin 3-sambubioside-5-rhamnose (Kovinich, 2014) at around 9.8 min also predicted to contain anthocyanidin with glucosyl and galactosyl groups while an xylose group was added to the peak of 727 D. The MS spectra for F2 at t_R of 45.8 min (Figure 5.30) gave a peak with m/z of 885 D. Several proposed structures were displayed in Figure 5.30 based on the main unit for the predicted structure which was cyanidin or flavonoid group attached to galactosyl, malonyl, cinnamyl, coumaroyl, and feruloyl groups. The masses for the selected fractions and their constituents were suggested by two other techniques through MS/MS compartment. Utilizing MS/MS fragmentation pattern of the whole molecules (parent ions) to daughter ions (Figure 5.31), several parent ions were recorded for the daughter ion (m/z 287 D) in F1 at t_R around 1.4 min. There were fragmentation pattern of the parent ions with several fragments/daughter ions (m/z 370, 375, 427, 443, 461, 527, 596, 611, 731, 813, and 892). The recorded parents in F2 for m/z of 827 D detected at t_R 27 in Figure 5.32 could be corresponding to cyanidin molecule acylated with glucosyl and malonic. It gave parent ion of m/z 915 D (literature identification as prodelphinidin trimer = 915 (Liu *et al.*, 2009) while the peaks at t_R 22.2 and 23.1 with further coupling molecules to appear at m/z 1083 and 1108 D, respectively. The parent ions of one of F3 constituent (Figure 5.33) with t_R 9.3 was m/z 303 D which revealed parent ions at 415, 450, 466, 613, and 745. The obtained parent ions of m/z 145 (Figure 5.34) showed parent ions of m/z 186, 229, 307, and 804 D. Another analytic technique was applied called multiple reaction monitoring (MRM) which focus of the whole molecule and one fraction of the interest. An example of MRM

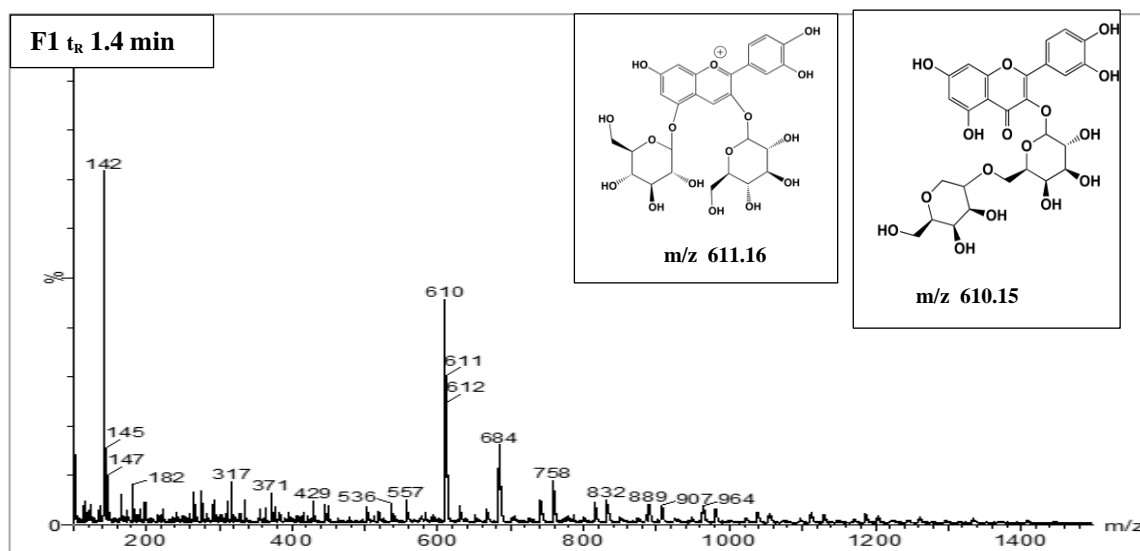
technique to provide more information about certain mass more information was displayed in figure 5.35.



Anthocyanin type



Flavonoid type

Figure 5-27. Basic structures of anthocyanin and flavonoid.**Figure 5-28. Mass spectra of F1 fraction and the predicted structure of some predominant peaks.**

Each peak in the mass spectra of F1 (A) was listed with its ion intensities and m/z ratio. The data were recorded at exact t_R of 1.415 min. The chemical structure for the predicted peaks at m/z 610 D. LC-MS sat up with the sample's flow of 250 $\mu\text{l}/\text{min}$ from the DAD eluent was directed to the ESI interface using a flow-splitter. The source block temperature was held at 120 $^{\circ}\text{C}$ and the desolvation gas (nitrogen gas) temperature was 350 $^{\circ}\text{C}$. The flow rate of 650 l/h, and cone gas of 82 l/h was used. The capillary potential of 3.2 kV was used. MS spectra recorded between m/z range 100-1500, in the positive mode with cone voltages (CV) 30 V.

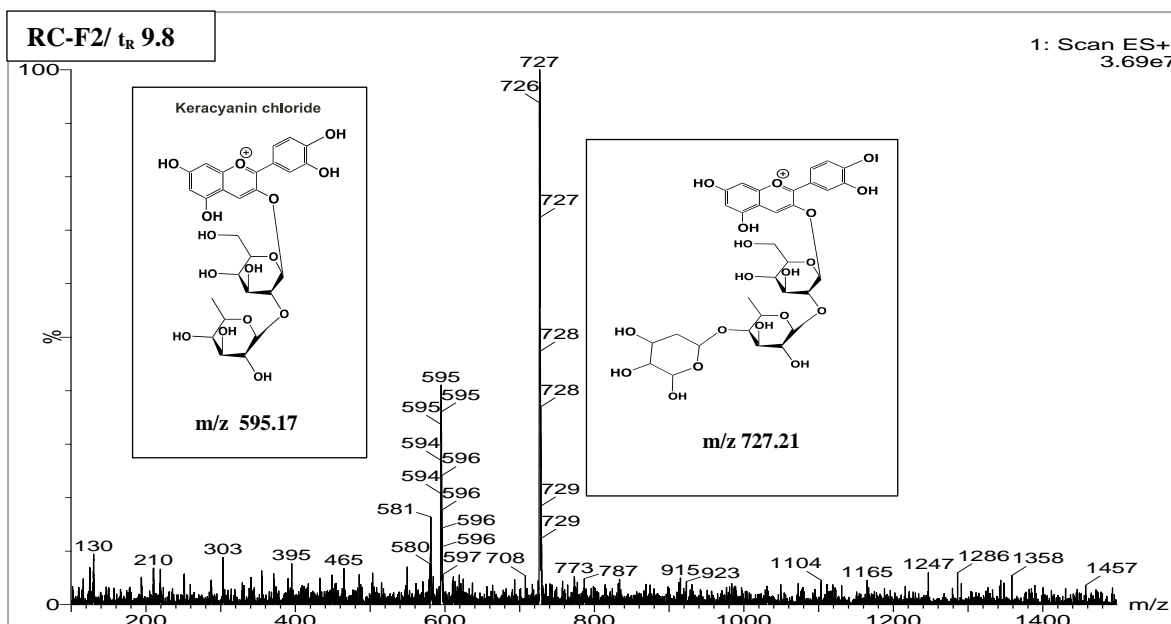


Figure 5-29. Mass spectra of F2 fraction and the predicted structure of some predominant peaks.

Each peak in the mass spectra of F2 (Cur 15) was listed with its ion intensities and m/z ratio 595 and 727 D. The data were recorded at the exact t_R of 9.8 min. LC-MS prepared with the sample's flow (250 $\mu\text{l}/\text{min}$) from the DAD eluent was directed to the ESI interface using a flow-splitter. The source block temperature was held at 120 $^{\circ}\text{C}$ and the desolvation gas (nitrogen gas) temperature was 350 $^{\circ}\text{C}$. The flow rate of 650 l/h, and cone gas of 82 l/h was used. The capillary potential of 3.5 kV was used. MS spectra recorded between m/z range 100-1500, in the positive mode with cone voltages (CV) 35 V.

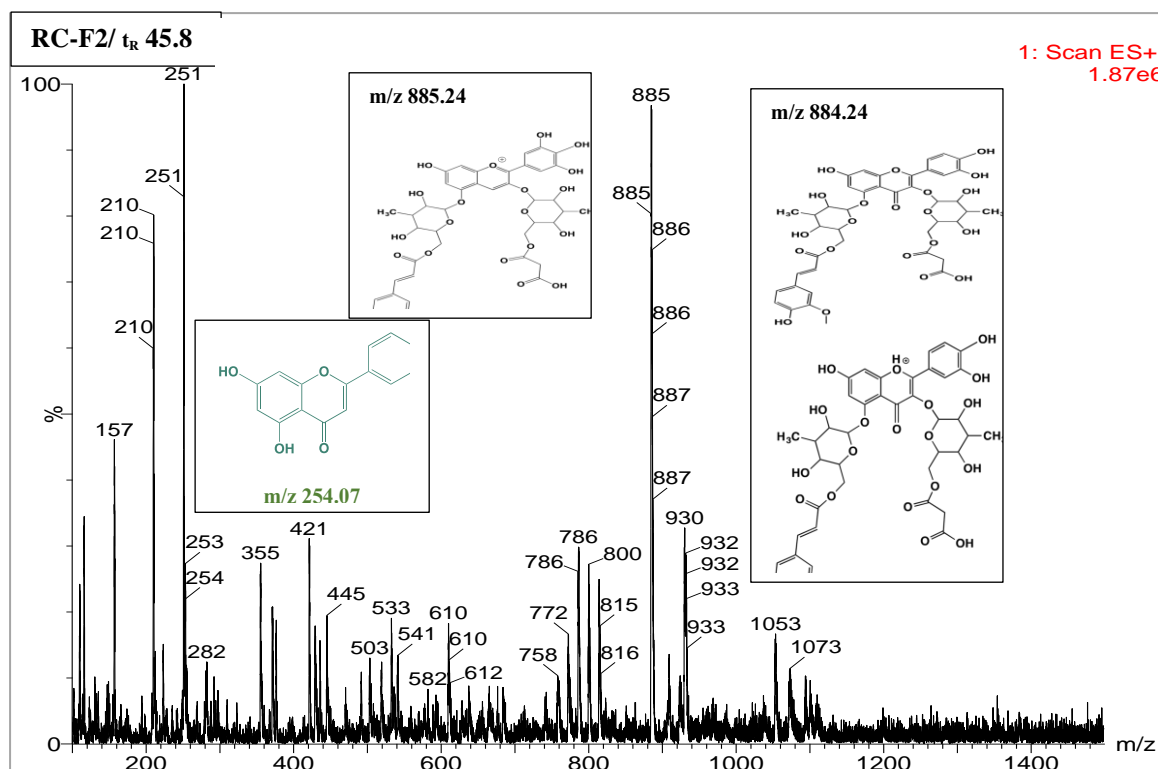


Figure 5-30. Mass spectra of F2 fraction and the predicted structure of some predominant peaks.

Each peak in the mass spectra of F2 (Cur 10) was listed with its ion intensities and m/z ratio 595 and 727 D. The data were recorded at the exact t_R of 45.8 min. LC-MS optimised the sample's flow (250 $\mu\text{l}/\text{min}$) from the DAD eluent was directed to the ESI interface using a flow-splitter. The source block temperature was held at 120 $^{\circ}\text{C}$ and the desolvation gas (nitrogen gas) temperature was 350 $^{\circ}\text{C}$. The flow rate of 650 l/h, and cone gas of 82 l/h was used. The capillary potential of 3.5 kV was used. MS spectra recorded between m/z range 100-1500, in the positive mode with cone voltages (CV) 42 V.

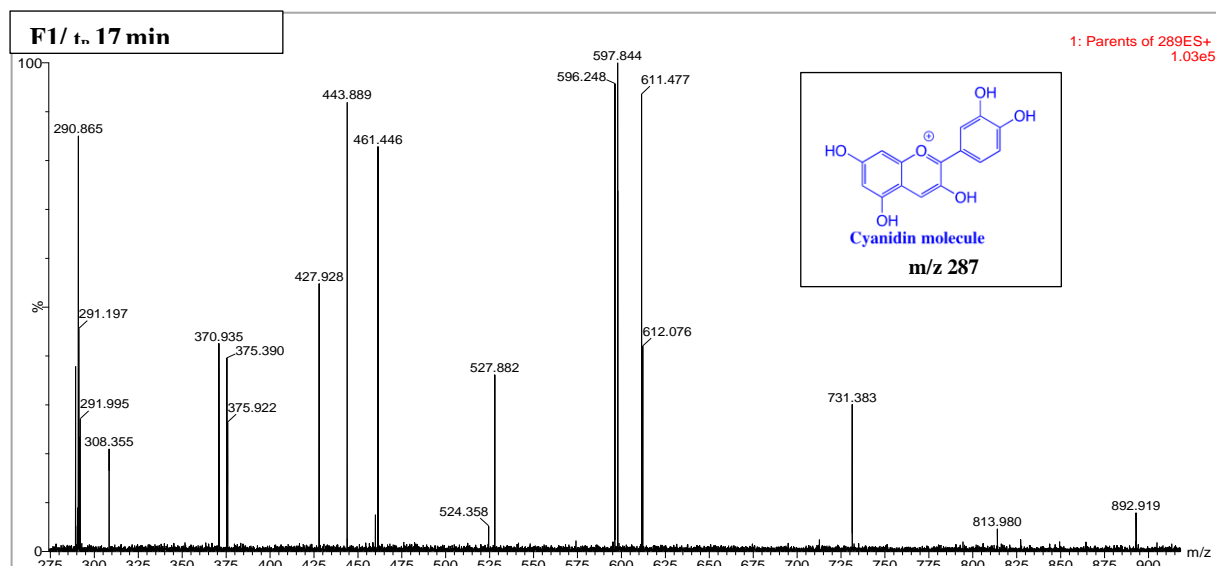


Figure 5-31. MS/MS parent ions of m/z 287 spectra from F1 constituent at t_R of 13 min.

LC-MS/MS was optimised with the sample's flow of 250 µl/min from the DAD eluent was directed to the ESI interface using a flow-splitter. The source block temperature was held at 120 °C and the desolvation gas (nitrogen gas) temperature was 350 °C. The flow rate of 650 l/h, and cone gas of 82 l/h was used. The capillary potential of 3.2 kV was used. MS spectra recorded between m/z range 100-950, in the positive mode cone voltages (CV) (45 V). Parent and daughter ions spectra were also recorded in positive mode using argon as collision gas at 1.5×10^{-3} mbar and different collision energies (CE) in the range 25 eV.

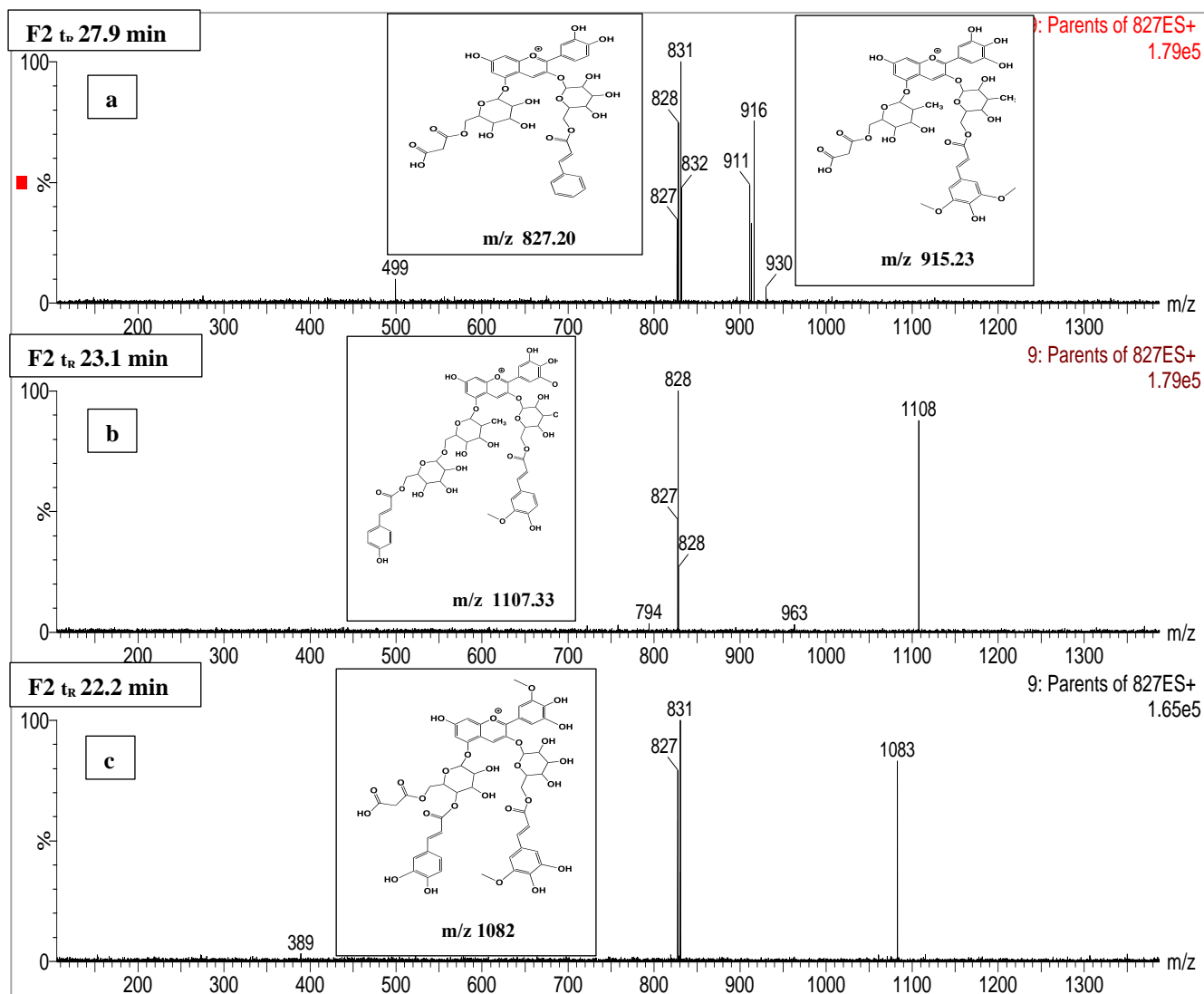


Figure 5-32. MS/MS Parent ions of m/z 827 spectra from F2 constituent at t_R of 22.2, 23.1, and 27.9 min.

LC-MS/MS was optimised with the sample's flow of 250 µl/min from the DAD eluent was directed to the ESI interface using a flow-splitter. The source block temperature was held at 120 °C and the desolvation gas (nitrogen gas) temperature was 350 °C. The flow rate of 650 l/h, and cone gas of 82 l/h was used. The capillary potential of 3.2 kV was used. MS spectra recorded between m/z range 100-950, in the positive mode cone voltages (CV) (35 V). Parent and daughter ions spectra were also recorded in positive mode using argon as collision gas at 1.5×10^{-3} mbar and different collision energies (CE) in the range 25 eV.

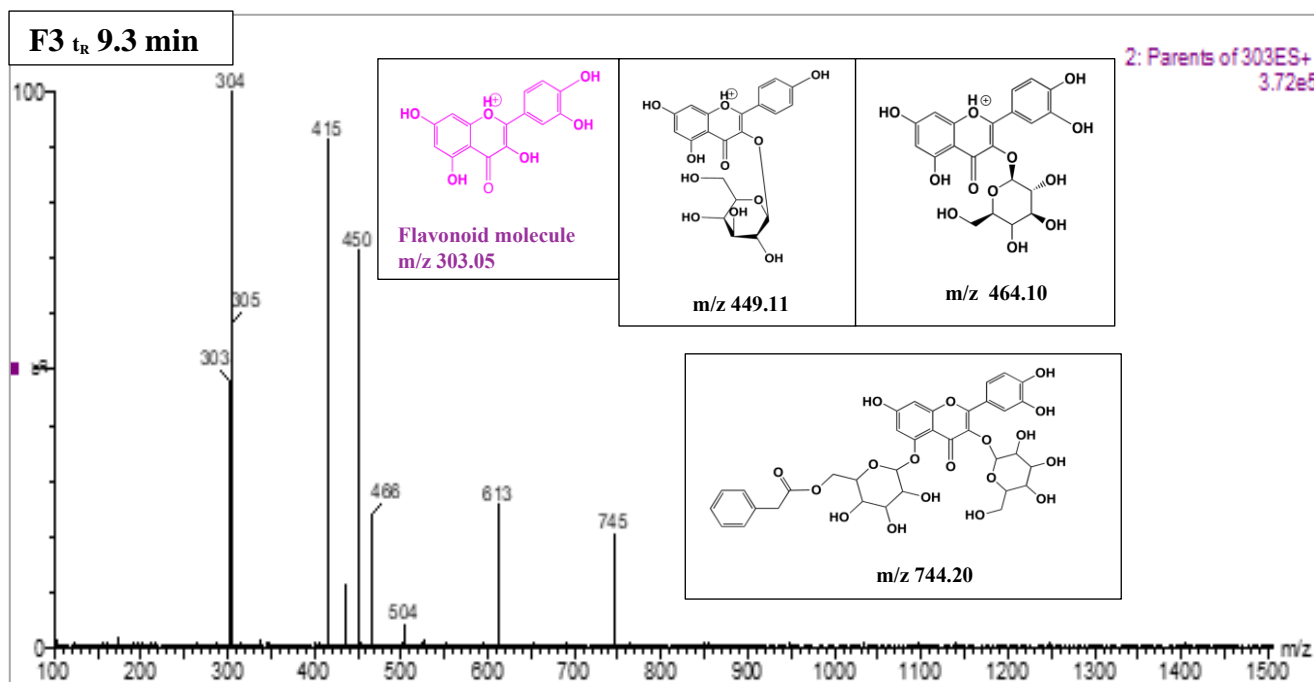


Figure 5-33. MS/MS parent ions of m/z 303 spectra from F3 constituent at t_R of 9.3 min.

LC-MS/MS with the sample's flow of 250 $\mu\text{l}/\text{min}$ from the DAD eluent was directed to the ESI interface using a flow-splitter. The source block temperature was held at 120 $^{\circ}\text{C}$ and the desolvation gas (nitrogen gas) temperature was 350 $^{\circ}\text{C}$. The flow rate of 650 l/h, and cone gas of 82 l/h was used. The capillary potential of 3.2 kV was used. MS spectra recorded between m/z range 100-950, in the positive mode cone voltages (CV) (35 V). Parent and daughter ions spectra were also recorded in positive mode using argon as collision gas at 1.5×10^{-3} mbar and different collision energies (CE) in the range 15 eV.

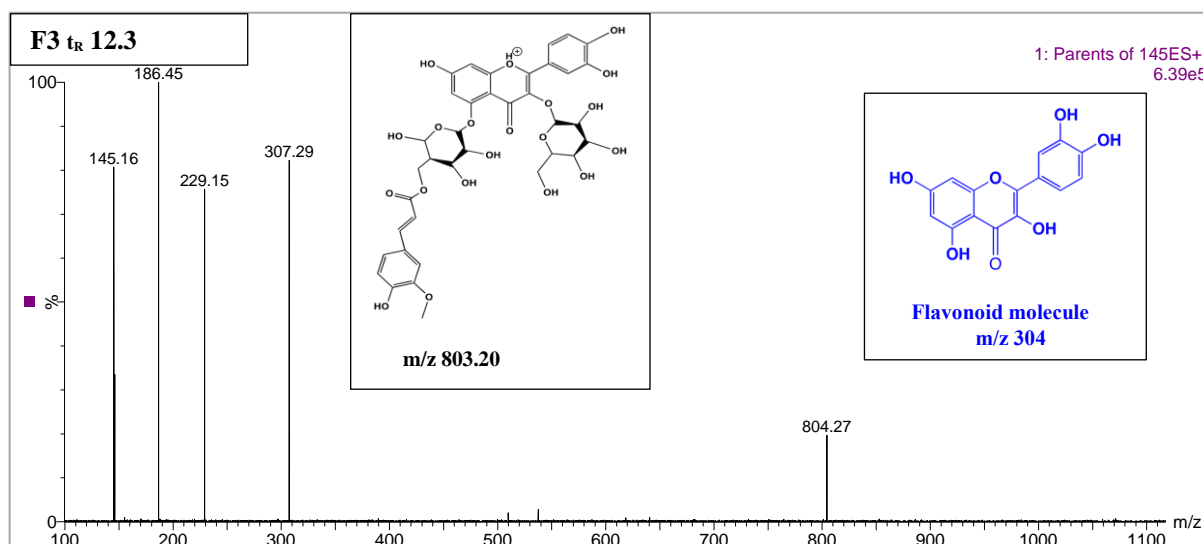


Figure 5-34. MS/MS parent ions of m/z 145 spectra from F3 constituent at t_R of 12.3 min.

LC-MS/MS was optimised with the sample's flow of 250 µl/min from the DAD eluent was directed to the ESI interface using a flow-splitter. The source block temperature was held at 120 °C and the desolvation gas (nitrogen gas) temperature was 350 °C. The flow rate of 650 l/h, and cone gas of 82 l/h was used. The capillary potential of 3.2 kV was used. MS spectra recorded between m/z range 100-950, in the positive mode cone voltages (CV) (25 V). Parent and daughter ions spectra were also recorded in positive mode using argon as collision gas at 1.5×10^{-3} mbar and different collision energies (CE) in the range 20 eV.

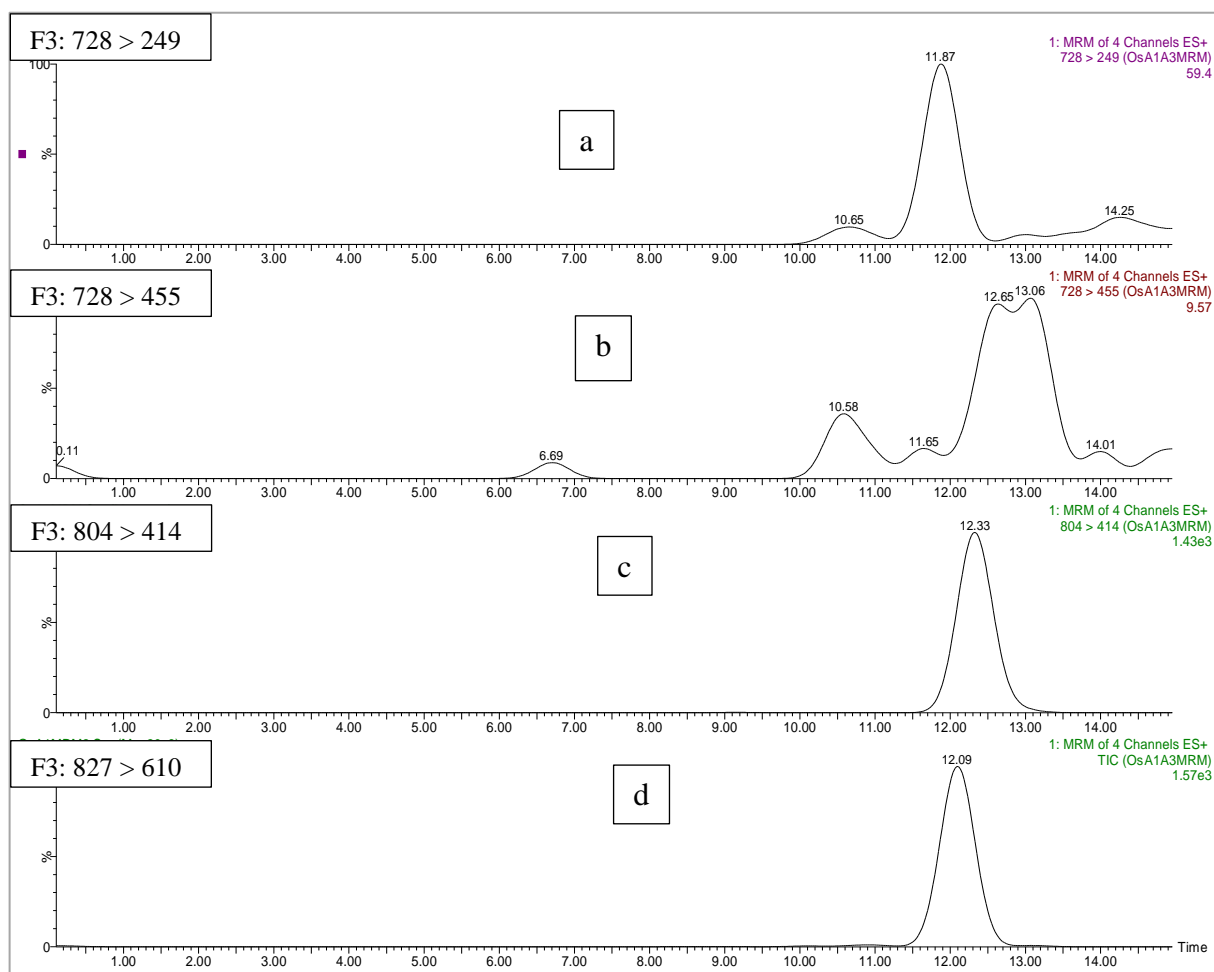


Figure 5-35. Multiple reaction monitoring (MRM) parent and daughter ions of a) m/z 728 > 249; b) 728 > 455; c) 804 > 414; d) 827 > 610 spectra for F3 constituents.

LC-MS/MS was optimised with the sample's flow of 250 $\mu\text{l}/\text{min}$ from the DAD eluent was directed to the ESI interface using a flow-splitter. The source block temperature was held at 120 $^{\circ}\text{C}$ and the desolvation gas (nitrogen gas) temperature was 350 $^{\circ}\text{C}$. The flow rate of 650 l/h, and cone gas of 82 l/h was used. The capillary potential of 3.2 kV was used. MS spectra recorded between m/z range 100-950, in the positive mode cone voltages (CV) (40 V). Parent and daughter ions spectra were also recorded in positive mode using argon as collision gas at 1.5×10^{-3} mbar and different collision energies (CE) in the range 20 eV.

5.3 Discussion

5.3.1 Redcurrant Extracts

5.3.1.1 Introduction

The work described in this chapter mainly describes an analysis of the possible antiviral effect of compounds contained within redcurrants. These were chosen as related berries have been shown to contain biologically active materials, including potential antiviral agents, but redcurrants have not been extensively studied.

5.3.1.2 Antiviral activity of RC extracts

Different RC extracts produced using different methods of extraction showed differences in cell toxicity profiles and variable antiviral activity. It was anticipated to find the extracts of redcurrant filtrates produced at room temperature (RC-Rt and RC-SS sonication) would be more potent than the filtrate of boiled extract, as there should be less degradation of labile compounds. However, the boiled extract showed in several experiments using plaque assays or cell viability measured by the MTT assay (Figures 5.1, 5.11-5.13), more significant antiviral activity and less toxicity to the cells than other tested extracts. In fact, it has been found that boiling of some plant material increases the biological activity and/or the levels of one or more of their components. For example, boiling of broccoli and green beans increases their phenolic levels (Turkmen *et al.*, 2005) and boiling of tomatoes raises free flavonol content (Stewart *et al.*, 2000). Therefore, boiling of RC might have increased the phenolic or other more potent compounds leading to an increase in the antiviral activity of the boiled RC extract. Another possible explanation is that during boiling, some of the chemical properties of heated compounds may change for example destroying chemical bonds, breaking down the complex compounds into their simple components, or it may even produce completely new chemical entities compounds with more or less activity than the original ones. Noteworthy, RCs have small solid seeds inside the berry. An increase in temperature during the boiling step might have extracted some active ingredients from seeds that were not released when the extraction was carried out at Rt (filtration at Rt and sonication).

The antiviral effect was mainly tested using CAV9, but the extract was also active against several isolates of CBV3, a closely related virus to CAV9, which nonetheless has differences in cell entry mechanisms, which could impact on antiviral therapy. However, the extract was equally effective against the CBV3 isolates. It was also effective against

HPeV1, which is quite different from CAV9, genetically. It is belonging to another *Picornaviridae* genus, *Parechovirus*, while CAV9 belongs to *Enterovirus*. There are many similarities between the HPeV1 genome and those of other picornaviruses, but there are several differences in molecular and biological properties. Unlike several other picornaviruses, HPeVs are partially resistant to guanidine hydrochloride and resistant to brefeldin A (Krogerus *et al.*, 2003). The membrane changes seen in HPeV-infected cells are not as extensive as those seen in EV-infected cells. HPeVs also do not appear to cause host-cell protein synthesis shut-off (Stanway *et al.*, 1994). There are unique features in terms of the biochemical properties of the HPeV proteins, for instance the maturation cleavage of VP0 to VP2 and VP4 does not occur (Stanway *et al.*, 1994) and 2A belongs to a distinctive protein class (Stanway & Hyypiä, 1999). Unlike the poliovirus (PV) 2C protein, for example, the 2C protein of HPeVs is not present in the replication complex (Krogerus *et al.*, 2003, 2007). The 2BC precursor is also not seen in infected cells (Krogerus *et al.*, 2003). As for other picornaviruses, HPeVs inhibit cellular secretion but this does not seem to be caused by 3A as in EVs, or 2BC or 3A/2BC as seen in other picornaviruses (Krogerus *et al.*, 2007). The antiviral spectrum seen suggest that phytochemicals present in RC can have broad activity against enteroviruses, or even picornaviruses as a whole and overcome the problems of the large number of virus types.

The direct contacts of the viruses with the RC extracts revealed no effect of the extract on the virus particle itself (Figure 5.6), indicating that RC extracts do not work, for instance, in the manner of pleconaril in binding to a pocket under the virus surface and inhibiting uncoating (Rossmann *et al.*, 2002) and so the effect is intracellular. The observed lack of a complete inhibitory effect when cells are treated with RC extract after 6 hours of infection indicates that a relatively early step in infection, but probably beyond the very early stages of attachment and uncoating, is the target (Figure 5.7).

5.3.2 The effect of microalgae extracts on the viruses and cells viability

All microalgae samples demonstrated variable inhibition patterns of viral growth. Some of them demonstrated the ability to enhance cell viability without the viruses at low concentration and probably stimulated cell growth. The majority of the samples of RC and MA are rich source of antioxidant and this may have a role in increasing cells viability. Additionally, another set of the investigated species of MA showed extreme toxicity on cells. These obtained diverse MA results (being active, inactive, stimulating cells' viability or being very toxic) reflect diversity between different MA species. Some of these samples

are from different species and even those of the same species are likely to contain different chemical and biomedical constituents. In addition, being toxic at certain concentration does not mean that the extract is toxic at all concentrations and all of its components are toxic, because in general each of MA species contains many ingredients and metabolites. Some of these ingredients may have beneficial effects, some may be independently harmful and other may be useless. By doing fractionation, useful fractions can be separated from those which caused adverse effects to probably obtain a pure antiviral agent or agents without harmful effects. For the investigated active compounds, it might be worth to be further purified and identified. However, owing to the cells were subjected to a length of time to the experimental conditions during the viability assays, the results might be deficient of constructive assessment.

The investigated MA samples belong to distinct MA members. *Chlorella* which contains MA17 and MA-30 is one of MA genus which has high nutritional content and is known to produce a wide range of carotenoids and contains phenolics that have been used for cardioprotective antioxidant, anticancer and anti-microbial disorders. Species from the *Chlorella* genus were reported to have antiviral activity. For example, *Chlorellaceae* was investigated to inhibit influenza A and B replication from not only strains that considered to be sensitive to oseltamivir but also resistant strains (Sathasivam & Ki, 2018; Silva *et al.*, 2018; Barkia *et al.*, 2019). *Chlamydomonas* is a green alga with unique flagellated single cell properties which has been used as a model organism and investigated for several biological and antimicrobial activities (Couso *et al.*, 2018; Sasso *et al.*, 2018).

MA are very primal plants (with size of approximately 3-20 μm). However, they are the most genetically varied, complex and polyphyletic organisms worldwide (Mustopa *et al.*, 2015; Barkia *et al.*, 2019). Therefore, the antiviral or other biological activities of certain MA may be not be very representative for all species within the family. Side effects have been reported for some MA specials. *Chlorella* for example may cause gastro intestine problems such as nausea and vomiting and some reported allergic reaction and more seriously renal failure due to acute tubulointerstitial nephritis.

Despite showing some promise in the antiviral assays, MA samples were available in very small quantities and this prevented them being studied further in the current work.

5.3.3 Photodynamic inactivation activity of RC and MA

The natural extracts of RC and MA contain entities with photosensitive chemicals when some of the extracts were fractionated. Although, it is known that fruit in general have many chemicals that act as antioxidants the ability of some RC photosensitive constituents to elevate and produce Reactive Oxygen Species (ROS), which can cause immediate damage to biological systems was assessed in terms of the inhibition of the viral growth.

The idea of using blue and red light sources with the RC and MA samples came from the previous use of several photosensitizer (PS) that occur naturally in many plants, such as psoralens, perylenequinonoid and hypericin pigments. These PS have been shown to have photo-destruction activity against HIV and several other viruses. (Wainwright, 1998). Pigments in colourful fruits like redcurrant may be photo-active and in recent research some microalgae metabolites were introduced as a fluorescent agent that could be used in PDI (Chu, 2012).

In this study, the preliminary fluorescence imaging from confocal microscope was carried out and confirmed the presence of highly photosensitive substituents within the RC samples (data not included). Although RL had no beneficial effects on RC or MA samples, the effects of BL vary between RC and MA. In the case of RC extracts, the antiviral activity and cells viability were almost equal to the healthy control cells, but the boiled RC extract showed unique antiviral activity and enhanced cell viability with BL. Surprisingly, the use of BL with MA-19 caused significant decrease in its antiviral activity comparing to its inhibition to the viral activity in the dark. It is worth mentioning there are many reports that documented the presence of several different constituents some of them photosensitisers, producing high quantum yield of reactive oxygen species (ROS) and in the same time contain quenchers as antioxidants. The types, numbers, quantum yield of ROS, quantities of the photosensitive and the quencher's constituents in RC and MA species, probably attributed to their variation responses to the BL light and RL exposure and their PDI efficacy. These different effects would only be resolved by purification of potential antiviral compounds.

Currently, PDI of viruses has some use in the medical field including disinfection and purification of blood products and treatment of local virus infection such as papilloma virus warts and herpes virus. Whether systemic application of PDI could be feasible is not clear. Noteworthy, PDI can affect all virus vital structure including nucleic acids, lipids and

proteins and inhibition of viral replication by PS has been shown. PDI has documented activity against many viruses such as poliovirus, influenza virus, HSV, arbovirus, encephalitis virus, phage and SV40 (Wiehe *et al.*, 2019).

Investigation of RC as a potential source of PS against one of picornavirus infection is novel and has a great probability to be involved to the library of effective PS. However, it needs first to be purified from other components and identified and preferably investigated against other types of virus.

5.3.4 Quercetin antiviral activity

In addition to strong evidence of antiviral activity of quercetin against EVs and other viruses (as is discussed below), our data from LC-MS/MS and HPLC indicated the availability of flavanol in the boiled RC extract and in some of its fractions that showed significant activity against infection. In the current work, quercetin has showed a significant anti-CAV9 activity although there was a considerable differences of quercetin potency between the 2 cell lines used, A549 and GMK.

Quercetin was shown to inhibit rhinovirus (RV) (which belongs to the *Enterovirus* species) infection in vitro and in vivo by multiple mechanisms. It was found to inhibit RV endocytosis and to decrease PI3-Kinase by competing for ATP binding and Akt phosphorylation and therefore decrease RV-induced chemokines and cytokines, including IFN and IL-8. Quercetin is also thought to decrease PI-4 kinase which is found to be very important for virus growth in lipid organelles (Ganesan *et al.*, 2013). Quercetin has anti-inflammatory and antioxidant properties and it is found to induce mitochondria antiviral signally response to increase rhinovirus clearance (Farazuddin *et al.*, 2018).

Interestingly, LY 294002, a potent PI-3 kinase inhibitor was designed accordingly to the quercetin structure (Vlahos *et al.*, 1994). In PV (another EV species within picornavirus), quercetin was found to inhibit viral 3D^{pol} (RNA polymerase) and so RNA synthesis (Castrillo & Carrasco, 1987).

In addition, quercetin has been found to decrease TAG synthesis and LD size in HCV (an RNA virus) and disorganise core protein localization around LDs and this was thought to be due to an inhibitory effect on DGAT activity. It has also been reported that 50 μ M quercetin can oppose an elevation of fatty acid synthase, diglyceride acyltransferase, low-density lipoprotein, acetyl-CoA carboxylase and microsomal triglyceride transfer protein

(Rojas *et al.*, 2016). Other quercetin-HCV findings suggested additional quercetin-related mechanisms of action including, inhibition of IRES and NS5A mediated-IRES translation, NS3 protease and HSP (Bachmetov *et al.*, 2012). Influenza virus another RNA virus has also been found to be inhibited by quercetin via interfering with attachment, endocytosis and viral cell fusion (Wu *et al.*, 2016).

Quercetin also inhibits viral replication of many other viruses including adenovirus, parainfluenza virus, respiratory syncytial virus, mouse hepatitis virus DENV-2, herpes simplex virus, human T-lymphotropic virus, Japanese encephalitis virus, porcine epidemic diarrhoea virus, pseudorabies virus, Sindbis virus and HBV (Ganesan *et al.*, 2013; Maalik *et al.*, 2014; Chiow *et al.*, 2016; Parvez *et al.*, 2019).

Many of the mentioned quercetin mechanisms are potentially applicable to CAV9 and the majority of picornaviruses. In addition, quercetin may inhibit viral infection by more than one mechanism, which means that there is little chance for viruses to develop resistance and it may target host factors and viral particles simultaneously. As quercetin has showed significant inhibition activity against several enteroviruses including rhinovirus, poliovirus and CAV9 (in the current work), in addition to non-picornaviruses such as HCV and influenza virus, there is a great probability that quercetin could be active against most or all picornavirus members.

Quercetin is cheap and abundantly available. Although antiviral activity of quercetin is usually achieved in the micromolar ranges *in vitro*, it has been reported that nanomolar plasma concentration is probably enough to prevent *in vivo* viral replication. In terms of reported side effects, quercetin has shown a high safety profile of up to 5g a day. Quercetin was reported to harm kidney at doses greater than 1g/day. However, human studies have showed quercetin usage for several months in doses of up to 1g/day without reported serious affects (Chiow *et al.*, 2016; Lu *et al.*, 2017; Andres *et al.*, 2018). Therefore, quercetin could have a wide range of antiviral activity and might not cause serious side effects.

5.3.5 Antioxidant activity of RC extracts and fractions

It is known that natural sources including fruits contain hundreds of antioxidants (Choe and Min, 2009). Antioxidants have been found to inhibit some enterovirus species like EV71 (Ho *et al.*, 2009). There are several antioxidant assays reported in the literatures

among them the myoglobin protection ratio (Terashima *et al.*, 2007, 2010, 2012, 2013; An *et al.*, 2014; Morikawa *et al.*, 2015). The reaction of myoglobin (Mb) in the II or met III form (i.e., in the heme) with H_2O_2 leads to oxidation of the hem to the (oxo) ferryl state $FeIV = O$ (ferrylmyoglobin) (Gibson *et al.*, 1958). Measuring antioxidant activity of RC samples was carried out based on UV-spectroscopic absorbance of myoglobin structural changes after reaction with hydrogen peroxide (H_2O_2) following the literature method (Terashima *et al.*, 2013). It is found that all RC extracts tested had high antioxidant activity (AO). The sample solid-liquid phase extract demonstrated the highest myoglobin protection MPR percentage and faster kinetics followed by boiled RC extract and then RC extract at room temperature. The fractionated samples were difficult to monitor due to the fast reactions of the ferryl ions with those fractions containing AO moieties (Figure 5.22).

The method of extraction may affect AO properties of each extract. For instance, during the solid-liquid phase extraction of the boiled RC it was refluxing with 60% of dichloromethane and 40% methanol. Organic compounds that are extracted with such solvents might have high antioxidant activity. Also, it has been found that boiling of natural compounds increase their polyphenol contents (Hes *et al.*, 2014), polyphenols are known naturally occurring AOs. Antioxidant capacity of the RC samples might have positive impact and contributed in their antiviral activity. For instance, the sample of boiled extract had higher percent of MPR and AO activity than the sample RC-Rt and also the former had higher antiviral (AV) activity than the latter sample.

Most fractions from the boiled RC sample also had good AO activity (Figure 5.22). However, the preliminary data showed; the antioxidant (AO)-antiviral activity of boiled RC fraction is related in some fractions and less relevant to other fractions. F1 showed the highest AO activity and considerable antiviral activity. The AO and antiviral activities were both significant for F1, F4 and F5. However, F6 had strong AO but weak antiviral activity. The antiviral activity of F2 and F3 was high despite less significant AO activity. The fraction F6 which has strong antioxidant activity but lacks antiviral activity may contain certain types of AO different from those contained in another active fraction. Accordingly, it is still early to decide if antiviral activity is directly related to the AO properties.

5.3.6 Analytical analysis of RC fractions

On the basis of flash chromatography and HPLC, retention time, choice of mobile phase, and gradient, the conditions for fractionation and purifications of phenolic compounds

could be optimized. There is extensive literature reporting the importance of these factors alongside the pH of the media that will provide adequate charges for accurate separations of the large numbers of the natural components with different polarities (Werner *et al.*, 2008).

Although, the prediction of the structures for the masses obtained at certain t_R should be alongside of other analysis such as NMR and elemental analysis. Nevertheless, the methodology of the current work was based on liquid chromatography with diode array detection (HPLC/DAD) coupled to electrospray ionization (ESI) and triple quadrupole mass spectrometry can provide preliminary prediction for the type of constituents and identify the structural characterization of phenolic compounds present in RC extracts. Also, comparing masses with published literatures can provide an insight to many of the polycyclic phenolic compound (Silva *et al.*, 2007; Vagiri *et al.*, 2012; Sasaki *et al.*, 2014). Recently, HPLC and LC-MS has been widely used in separation and identification of anthocyanins, and sometimes in partial quantification. Both HPLC with both diode array detector (DAD) and MS detectors are sensitive and efficient for the separation and detection of multiple components based on UV absorbance and MS fragmentation behavior (Kovinich *et al.*, 2014; Skrovankova *et al.*, 2015). In general, the investigated RC fractions showed certain peaks at similar t_R and other peaks at various t_R . They were mostly feature different components with predominant few major masses recorded by electrospray mass spectra (ES+, m/z) for the total ion counting (TIC) which of different fractions have many similar chemical constituents for various masses of well documented and also unknown chemical entities. The analysis of LC-MS/MS indicated the existence of polycyclic compound within the RC extracts. According to enormous published articles for many fruits and berries extracts, the polycyclic constituents identified anthocyanins, anthocyanidins, flavonoids, and coumarins as the main chemical units. A diverse type of modifications for the ring A, B, and C within the units of anthocyanin/anthocyanidin and flavonoids were found by attaching sugar or organic molecules, or combination of those variable groups. Further LC-MS/MS analysis by parents/daughters and Multi Reactions Monitoring (MRM) techniques identified pattern of variable modifications with organic groups. Among those groups were arabinoside, galactoside, glucoside, coumaroyl, feruloyl and/or malonyl groups. The major RC constituents of the investigated fractions were complying with the literature reported constituents from fruits, flowers, and some vegetable's extracts. The fragments of parents / daughter ions and neutral loss scanning

mode to observe the loss of dehydrated sugar moieties. By comparing the characteristic fragmentation patterns to those available in literature database, some of the flavonoids and anthocyanins were identified (Werner *et al.*, 2008). The glycol-conjugated and free polyphenols from diverse families (hydroxybenzoic acids, hydroxycinnamic acids, flavan-3-oles, procyanidins, coumarins, flavanones, flavones, dihydrochalcones, flavonols and anthocyanins) were detected in many fractionated samples after fragmentation patterns according to aglycone family, glycan sequence, interglycosidic linkages and attachment point of the substituents to the aglycone, allowing to interpret the mass spectra of no available phenolic compounds (Abad-García *et al.*, 2009). Methodological rules to make easier the identification of unknown polyphenols by LC-MS/MS and isotopic ionization of compounds in black currants and other fruits or natural plants extracts were established and reported before. Several anthocyanins in the extracts of skin from Syrah grapes were identified by HPLC with diode array detection, including 3-monoglucosides of delphinidin, cyanidin, petunidin, peonidin, and malvidin, and the acetylglucosides and p coumaryl glucosides of malvidin and peonidin. The elucidation of anthocyanins by MS/MS investigated the aglycon moiety and number and types of sugars even without standards (Abad-García *et al.*, 2009).

Flavonoids belong to polyphenols with various modified species and a basic structure of C6-C3-C6. They have multiple applications in nutrition and cosmetic fields but also in pharmaceutical and medicinal arena (Panche *et al.*, 2016). In terms of viruses, many of flavonoid subgroups have been investigated against viruses from different families such as enteroviruses, poliovirus, respiratory syncytial virus, influenza and parainfluenza viruses, immune deficiency viruses type 1 and type 2, herpesvirus and rabies virus (Kumar & Pandey, 2013; Dai *et al.*, 2019). Anthocyanins are glycosidic anthocyanidin and classified under phenolic compounds which are abundant in vegetables and fruits including berries and responsible for their red, blue and purple colours. Commercial standards of many anthocyanins are not sufficiently available, and this complicates their measurement by HPLC (Chen *et al.*, 2014). Therefore, structural prediction is sometimes indicated to be then subjected to other identifying methods. Cyanidin derivatives which are rich pigments belonging to anthocyanidins are also proposed as structures for some masses detected in MS spectra during this work including cyanin chloride and cyanidin-3-glucoside. Cyanidins like cyanidin-3-glucoside were reported previously as major analytes in several studies of natural extracts (Gouvêa *et al.*, 2012). Naturally occurring cyanidin derivatives

can be sources of antiviral compounds and/or photosensitizers which could be used for their photodynamic antiviral activities. Rich pigments especially from berries have been reported for their strong antioxidant activities (Khoo *et al.*, 2017). Therefore, the proposed detected cyanidin in the current work may contribute or be the origin of the antioxidant activities seen in RC extracts and their fractions. Groups such as cinnamyl, coumaroyl, feruloyl and malonyl are known for their antioxidant and anti-inflammatory properties and some of them like cinnamyl and coumaryl containing compounds have evidence for significant antiviral activity (Galabov *et al.*, 1998; de Oliveira Silva & Batista, 2017). Based on the current LC-MS/MS spectra and by comparing literatures, masses corresponded to cyanidin -3- glucose and keracyanine which is an analytical standard of cyanidin-3-rutinoside with antioxidant, anti-inflammatory activity and has been found to reduce absorption of carbohydrates and could be a potential agent for the treatment of diabetes mellitus. Interestingly, 595 was detected in previous published work with blackcurrant and 449 was found to be one of its major fragment ions and it was corresponded to the dissociation of a glucoside group with loss m/z of 146 (da Silva *et al.*, 2007). Parent ion scan not only reveals but also confirms masses of interested peaks. It gives explicit spectra at low concentrations and separate interfering MS/MS spectra and increases the sensitivity and accuracy of analysis (Liu *et al.*, 2014).

In practise, identification of a finally purified but otherwise unknown compound is difficult to achieve by one analytical system and usually combines LC-MS/MS with various ion sources, mass analysers and standard metabolite references with known molecular masses, and NMR. Other possible complementary methods include elemental analysis, crystallography, spectroscopic methods such as UV and IR detection with possible use of several recently introduced techniques such as computer-assisted structure elucidation (Abad-García *et al.*, 2009; Buevich & Elyashberg, 2016).

The final identification of active compounds will allow them to be made on a larger scale and so tested thoroughly in terms of antiviral effect and toxicity. Thus, the initial work done on RC extracts may lead eventually to useful drugs against picornavirus infections

Chapter 6: General Discussion

6.1 Discussion and suggestions

Picornaviruses are the largest and most diverse virus family that includes human pathogens in terms of the number of virus types, of which over 300 infect humans (ICTV, 2019). This makes vaccination against most picornaviruses impossible and so other interventions are required. Virus inhibition strategies are usually based on targeting viral conserved features (proteins or RNA structures in the picornavirus genome) or targeting host factors and organelles that viruses manipulate and exploit to favour their replication. As a virus in general and RNA virus in particular easily generate mutations, combination or incorporation of two suggested antivirals might greatly improve activity and decrease resistance at the expense of increasing side effects.

Currently, no an individual anti-picornaviral drug has been approved to treat or prevent diseases caused by these viruses at present, in picornaviral life-threatening infections there is only the option of supportive treatment that does not impact on the infection itself. These include treatment of respiratory failure, haemorrhage and seizures (Zou *et al.*, 2012). Finding effective anti-picornavirus drugs can prevent such infections and their serious consequences. Similarly, to limit virus replication in some cases, infected patients are provided with infusions of intravenous immunoglobulin from pooled donors (Zou *et al.*, 2012), and drug treatment if found would avoid the huge cost, danger and difficulties of such complex treatment. Therefore, there is a necessity for the development of new therapies and drugs against the wide range of infections and to overcome their high mutation rate. In this work, a number of new possible sources of natural extracts and repurposing of drugs of known uses have been explored and evaluated against virus replication and cell survival. These have been investigated against CAV9, a clinically important virus of the *Enterovirus* genus within *Picornaviridae*. Although repurposed drugs and natural extracts look distinct in terms of their origins, they share a very important common feature of being consumed (e.g. in berries) or used therapeutically for many years (e.g. fluoxetine) and having strong evidence of safety and tolerability profile.

Since the National Center for Advancing Translational Sciences (NCATS) initiative for drug repurposing, “Discovering new therapeutic uses for existing molecules”, major companies like Pfizer, AstraZeneca, Sanofi, Eli Lilly, Abbott, GlaxoSmithKline, Bristol-Myers Squibb and Janssen Pharmaceuticals have been active in this area (Allarakhia, 2013). The project is very appealing as brand-new drug development requires a long time and huge efforts and money. Only 0.01% of investigated new compounds succeeded to the market

with a rejection rate of 45% due to toxicity or inactivity (Ashburn & Thor, 2004). Drug repurposing has much in its favour in terms of these parameters, due to the presence of previous inclusive pharmacological information e.g. including principle mechanism of action, kinetic profile, toxicity and interaction with other drugs, in addition to structural and physicochemical properties. This knowledge potentially leads to rapid progress to phase I and phase II clinical trials, early FDA approval and a short route to the clinic, although there is still the hurdle of demonstrating a new mechanism, target, dosing and route of administration for the new purpose. Drug repurposing is quite a profitable approach. For instance, the repurposed antidepressant duloxetine (Ashburn & Thor, 2004), now used for urinary incontinence, made a sale profit of approximately US\$ 800 million within 4 years of its relaunch and Thalomid®, which is reprofiled thalidomide, and its derivative Revlimid® (Lenalidomide), made a profit of more than \$2.8 billion for Celgene (Cha *et al.*, 2018). In the USA, repurposed drugs made up approximately 30-40% of the drug market after 2007 (Agrawal, 2015).

One aim of the current study was to test the anti-picornaviral activity of a number of existing drugs which may target virus proteins (e.g. fluoxetine), or against host factors (specifically lipid droplets) which have been shown to be involved in picornavirus replication. Each strategy has its advantages and disadvantages. Targeting viral proteins is more frequently overcome by emergence of resistant viruses and host factors approaches may cause more side effects than blocking viral components.

Several antidepressant drugs such as fluoxetine, imipramine and promethazine, in addition to dibucaine, which is used as a topical anaesthetic have been investigated for their repurposing antiviral properties. Fluoxetine and dibucaine showed a significant inhibitory effect on CAV9. Imipramine also showed a significant antiviral activity but only when its concentration was much higher than needed for fluoxetine and dibucaine. Sequencing of selected fluoxetine mutants revealed a single consistent mutation in the 2C protein (I227V). Preliminary results from sequencing one dibucaine mutated virus revealed a mutation at the same position. If this is confirmed in future work by sequencing other mutants, this is consistent with the current proposed mechanism of action of fluoxetine, binding to a pocket in the 2C protein (Bauer *et al.*, 2019). These results are consistent with the previous findings using CBV3 DRMs originally selected against the drug TBEZ-029, which were also resistant to fluoxetine and dibucaine (de Palma *et al.*, 2008; Ulferts *et al.*, 2016). One

difference is that the TBEZ-029 DRMs had two nearby mutations (A224V) and A229V) in addition to I227V. I227V, is a key mutation in resistance to TBEZ-029, but none of the 3 mutations alone was sufficient to give drug resistance, in contrast to CAV9 resistance to fluoxetine and dibucaine. CBV3 studies on fluoxetine and dibucaine used the three mutation DRM and no attempt was made to select new DRMs, so this difference could be due to the different features of TBEZ-029 compared to fluoxetine/dibucaine, rather than differences between CAV9 and CBV3. This question may be answered using the modelled CBV3 2C structure (Bauer *et al.*, 2019) docked to TBEZ-029 and to fluoxetine. Similar modelling of the CAV9 2C structure would also be useful, particularly in designing new compounds that fit into the pocket and which may require more than one mutation to give resistance, as clinical use of fluoxetine may not be feasible if a single mutation is enough to give resistance.

In an attempt to improve fluoxetine and dibucaine antiviral activity to also inhibit the DRM, they were chemically combined to selected groups or compounds. Quinoline a core structure of dibucaine and a proposed source of its activity was linked to a butene group. The resultant compound QHB showed the opposite of the expectation and virus growth seemed to be stimulated by the compound. A fluoxetine-chlorambucil conjugate (F1-Ch) showed significant antiviral activity although was only seen at high concentration. This is possibly because there were still some impurities, shown by gas chromatography in spite of a purification procedure that was carried out by flash chromatography (Appendix II). Therefore, the first suggestion for F1-Ch is to purify it again by chromatography and test again against the virus. F1-Ch should also be investigated against fluoxetine and dibucaine DRMs. The quinoline core of dibucaine was also conjugate to chlorambucil and to a long chain linolenic acid in two separate chemical reaction procedures and these 2 novel compounds have not been examined with CAV9 nor with its resistant mutants. So, it would be very interesting to explore their antiviral activity. As discussed above, future drug modifications should be designed in the light of a modelled 2C structure. However, the accuracy of the CBV3 model (or a new CAV9 model), based on the EV71 (a different species of enterovirus) 2C structure, may not allow such detailed analysis, especially as the proposed fluoxetine binding site is in a region of 2C where CBV3 and EV71 sequences are relatively different and also EV71 is not itself inhibited by fluoxetine.

Anti-CAV9 activity of several existing drugs against a host factor, LDs which have been shown to be involved in picornavirus replication has also been investigated. Among investigated LD-interacting members, DGAT inhibitors including A922500 seemed to be the most acting compounds although toxicity accompanied its activity is a considerable issue that would need to be addressed. Simvastatin which is a 3-hydroxy-3-methylglutaryl (HMG) coenzyme A reductase (HMG-CoA reductase) inhibitor did not show activity and C75, a fatty acid synthase (FASN) inhibitor showed slight effect at a high concentration. Preliminary data on aspirin, a nonsteroidal anti-inflammatory drug (NSAID) and metformin a biguanide blood glucose lowering agent exhibited interesting, but not yet clear-cut antiviral activity and these primary results require further confirmation. In this regards it is worth mentioning that data investigated for one compound are not necessarily representing for the whole drug family members, and individual drug variation must always be considered. If the primary results of aspirin and metformin are confirmed, then propagation of DRM viruses against them could be very useful to determine the basis of their anti-CAV9 activity. LDs targeting compounds by definition are supposed to target LDs, the host factors. However, emergence of DRMs against A922500 means that actually a CAV9 protein may be targeted, rather than LDs themselves, in the same way that fluoxetine is a GPCR inhibitor, but anti-CAV9 activity may be due to binding to 2C, rather than to inhibition of a GPCR. On the other hand, the anti-enterovirus drug enviroxime inhibits virus replication by decreasing Golgi complex PI4P levels by directly inhibiting the enzyme PI4KIII β (van der Schaar *et al.*, 2012). Despite having a cellular target, CBV3 DRMs can be obtained and these have single mutations in the CBV3 3A protein, suggesting that these DRMs now use alternative pathways for replication. The CAV9 2C protein seems to interact with LDs but preliminary results from partially sequencing one A922500 DRM did not show a mutation in the part of 2C sequenced. This is not surprising as the region of 2C sequenced so far does not interact with LDs (Khridd, unpublished). The rest of 2C and the other viral proteins should be sequenced in the DRM to find the mutation responsible for resistance. It would be useful to have a clearer idea of which step in CAV9 replication involves LDs. Different reporter systems will be created for CAV9, to use EGFP or luciferin as reporter proteins to separately analyse steps such as translation and RNA replication, as done for CBV3 (Ulferts *et al.*, 2016).

Lipid droplets have been reported to fuel replication of some viruses (Zhang *et al.*, 2017). However, some reports have suggested indirect rather than direct involvement of LDs in

viral replication which might be equally important. In PV, the infection-related membranous structures are showed to be important for hiding the propagated viruses from the cellular immune system and host anti-virus response but was not very important for RNA replication. PV infection induces accumulation of lipases to LDs, increases neutral lipid lipolysis and phosphorylation of lipid and thus sustains infection-related phosphatidylcholine production which in turn supports expansion of the PV replication complex. As picornaviruses have the ability to quickly inhibit host transcription and translation processes, there would be a relatively short chance for a cell to avoid viral infection. Drug targeting of lipids may contribute to increase the time exposure and sensitivity of picornavirus to cellular immune system and improve the anti-virus response. As part of host organelles, targeting of LDs might adversely affect cell's homeostasis. However, interestingly and in some situations, cells can overcome pharmacological inhibition of lipids and perhaps other essential elements in favour of their survival by properly redistributing of these lipids in some ways that do not support virus life cycle (Perera *et al.*, 2012).

Plants and other natural sources are rich in bioactive compound and there is strong evidence of antiviral compounds, along with antibiotics and other useful chemicals. Boiled extracts from redcurrant showed a significant inhibitory effect on CAV9, closely related CBV3 and genetically distinct HPeV1. This means that RC could be active against other picornavirus groups. It also means that RC components may target certain proteins, domains or motifs which are common or conserved in many virus species, or it could target one or more of host factors that are essential for these viruses, or it might have multiple targets. Investigation of action modes requires purification of a single component/s which can then be identified and analysed by LC-MS/MS, NMR and elemental analysis. In this regard, partial fractionation has been done so far. Fractions obtained had different colours, suggesting different constituents, and various antiviral activities ranging from significant activity at relatively low concentrations to significantly active at moderate to high concentration or not active at all.

Differences in antioxidant activity were also observed through different RC extracts and various RC fractions. All RC extracts seemed to have significant although variant AO activity and fractions from boiled RC also showed some significant and some moderate AO activity. RC-related AO activity is promising not only for antiviral activity but also in other AO-associated diseases such as diabetes, cardiovascular diseases, kidney injuries and

cancer. RC extracts also seem to have noticeable photosensitive properties. All RC-investigated properties are very interesting, promising and novel, however, each component (antiviral compounds, AO components and PS) needs to be isolated, purified and analysed to be useful for application.

There were several fractions that were observed to inhibit CAV9 and therefore, RC could be a source for more than one active compound for treatment of picornavirus and these compounds could be used solely or in combination to decrease the occurrence of virus resistance. A boiled extract of RC was also active against fluoxetine resistant mutant virus (and A922500) and so its purified compounds are potential candidates to combine with other drugs to overcome the possibility of drug resistance.

Quercetin and/or its derivatives could be contained within the RC extract, based on preliminary characterisation of the components. When it was investigated against CAV9, pure quercetin was significantly active. It has also been reported to be active on other RNA and DNA viruses. In addition, quercetin has been demonstrated to inhibit viruses by variant modes of action from entry to release. These include attachment, endocytosis, translation, RNA replication, anti-inflammatory effects, LD inhibition and heat shock protein interactions. Accordingly, quercetin has the potential to have a multi-virus, multi-mechanisms action. The antioxidant activity of quercetin has been previously documented, and it is interesting in the future to investigate its PDI activity.

Microalgae are very diverse, just like the results obtained in this work. Some MA extracts were very active, and others were not. Some caused stimulation of cell viability. The MA results indicate that this source could be significantly rich in anti-picornavirus compounds and more work is required on this field. Unexpectedly, using light on MA extracts had a negative effect on at least M19. The reasons for this MA activity loss need to be explored. It could be due to loss of AO activity or structural changes.

Since the first compound was successfully purified from opium 200 years ago, the number of naturally produced or derived (analogues) drugs has been significantly increased to reach approximately 80% around 1990. However, during 1990 and thereafter there has been a big expansion of chemistry-related synthetic drugs, and this has been at the expense of the investment in natural sources. This may be due to laborious procedures and technical limitations in purifying and identification of new natural compounds including supply reliability, seasonal change, source loss and extinction and structure complexity. It is also

because of the general attitudes of large pharmaceutical companies to invest in libraries of synthetic compounds.

However, plants and other natural remain a very rich resources of not only antibiotics such as penicillin, erythromycin and tetracycline, anti-malarials like quinine and anti-parasitics e.g. ivermectin, but also medicines of different family groups including lipids lowering agents (by astatine) analgesics (aspirin), cardiovascular agents (digitoxin) and even immunosuppressed (cyclosporine) and anticancer agents (doxorubicin). Therefore, underestimation of these rich resources means missing a huge number of biologically active molecules. In any case, it has been reported that only 15% or even less of natural sources are explored and these have given all the approved known naturally derived medicines. The remaining 85% could contain huge numbers of antiviral and other bioactive molecules. The conclusion is not that naturals are more important than chemistry-based products, but it rather means that both ways are very important in novel antiviral approaches and one general aim of this study is to highlight their equally important approaches.

One drawback of the current work is that the GMK cell line was used to investigate the antiviral activity of many of the compounds and extracts and A549 cells were used to measure the toxicity of the investigated agents. In principle, the same cells should always be used for both toxicity and antiviral activity of compounds. However, due to the unforeseen situation of losing GMK cells at the end of the study, there was no option except to finish the work with the available A549 cells. Data from viability assay with A549 gave some unexpected results, as with A922500 and dibucaine, which did not show visible toxicity with GMK cells in plaque assay but then showed significant toxicity with A549 on viability assay. However, in general and for the majority of tested compounds, it was useful, and the results were with expectation with that of GMK cells-plaque assay in most cases. For future work, viability assay or other toxicity sensitive assay would be recommended to be carried out on GMK cells for the investigated compounds. Given that there were some cell type differences in antiviral effect of some compounds, for instance quercetin, it would also be interesting to test all compounds on multiple cell lines. This might reveal activity missed on one cell line where differences in cell biochemistry or structure may mean that a drug has no effect.

In general, all the included work of this study has been done by myself, except the GS work which was totally done by Dr Sinan Battah, and the LC-MS/MS analysis which was a

shared work between Dr Sinan Battah and myself. The chemical syntheses were devised by Dr Sinan Battah and the practical work was carried out by myself.

6.2 Conclusion

In this study, many chemically-derived compounds were studied for potential repurposing as antivirus agents and natural materials were explored for their potential as sources of compounds for the development of antiviral agents. Several assays were used to evaluate toxicity and antiviral activity of these agents and all the employed methods provided valuable data about the natural compounds and chemicals under investigation. Some repurposed active compounds seem to have a similar within CAV9 target (2C protein). However, they might be used in different ways. i.e. fluoxetine systemically and dibucaine locally. Both imipramine and the novel structurally modified F1-Ch showed significant antiviral activity at high doses, but their proposed mechanisms are yet to be known. Finding that fluoxetine and dibucaine have antiviral activity against CAV9 just like their activity on CBV3 and that they are acting on the same region the 2C protein support the well-known close relationship between CAV9 and CBV3.

Variant pathways involved in lipid and LDs production and metabolism have been investigated, using distinct agents in order to screen different LD biosynthetic pathways and find which are involved in viral replication, and so could be useful antiviral targets. The DGAT1 inhibitor A922500 looks to be more active than all other agents, although it showed cellular toxicity, and this might give false antiviral activity and therefore its antiviral activity needs further investigation. As some of investigated lipid-interacting compounds have different mechanism of action than other such as A922500 and fluoxetine, they are possible candidates for combination therapy which is sometimes suggested for virus infection. Naturals are rich sources of anti-picornavirus activity, RC extract and quercetin showed significant antiviral activity against CAV9 and in the case of RC, against CBV3 and HPeV1 as well. Several microalgae species were significantly active as well. Natural products could also be very useful for combination therapy. For example, RC extracts inhibited fluoxetine drug resistant mutant at an even lower concentration required to inhibit the parent virus. In addition, natural products, as shown with RC, are also a substantial source of antioxidant compounds that could be exploited clinically and industrially. RC is also a source of photosensitizers which have started to enter the medical application world. As through this study both repurposed chemicals and naturals have

exhibited a significant antiviral activity, it is recommended that there should be a balance between two sources in terms of research and investment.

Declaration

In general, all the included work of this study has been done by myself, except the GS work which was totally done by Dr Sinan Battah, and the LC-MS/MS analysis which was a shared work between Dr Sinan Battah and myself. The chemical syntheses were devised by Dr Sinan Battah and the practical work was carried out by myself.

References

- Abad-García B, Berrueta LA, Garmón-Lobato S, Gallo B, Vicente F (2009) A general analytical strategy for the characterization of phenolic compounds in fruit juices by high-performance liquid chromatography with diode array detection coupled to electrospray ionization and triple quadrupole mass spectrometry. *Journal of Chromatography A*, **1216**, 5398–5415.
- Abdul-Quader AS, Collins C (2011) Identification of structural interventions for HIV/AIDS prevention: the concept mapping exercise. *Public Health Reports*, **126**, 777–788.
- Abraham OSJ, Miguel TS, Inocencio HC, Blondy CC (2017) A quick and effective in-house method of DNA purification from agarose gel, suitable for sequencing. *3 Biotech*, **7**, 7–12.
- Accioly MT, Pacheco P, Maya-Monteiro CM *et al.* (2008) Lipid bodies are reservoirs of cyclooxygenase-2 and sites of prostaglandin-E2 synthesis in colon cancer cells. *Cancer Research*, **68**, 1732–1740.
- Afonso CL, Amarasinghe GK, Bánya K *et al.* (2016) Taxonomy of the order Menonegavirales: update 2016. *Archives of Virology*, **161**, 2351–2360.
- Afrose T (2017) Coxsackie virus: the hand, foot, mouth disease (HFMD). *Juniper Online Journal of Public Health*, **1**, 1–5.
- Agrawal P (2015) Advantages and challenges in drug re-profiling. *Journal of Pharmacovigilance*, **S2**, 2–3.
- Ahmadi A, Moghadamtousi SZ, Abubakar S, Zandi K (2015) Antiviral potential of algae polysaccharides isolated from marine sources: A Review. *BioMed Research International*, **2015**, doi.org/10.1155/2015/825203.
- Aizawa, Y., Izumita, R., Saitoh, A. (2017). Human parechovirus type 3 infection: An emerging infection in neonates and young infants. *Journal of Infection and Chemotherapy*, **23**, 419-426.

- Albulescu L, Wubbolts R, Kuppeveld FJM Van, Strating JRPM (2015) Cholesterol shuttling is important for RNA replication of coxsackievirus B3 and encephalomyocarditis virus. *Cellular Microbiology*, **17**, 1144–1156.
- Aldabe R, Barco A, Carrasco L (1996) Membrane permeabilization by poliovirus proteins 2B and 2BC. *Journal of Biological Chemistry*, **271**, 23134–23137.
- Alho A, Marttila J, Ilonen J, Hyypiä T, Hyypia T (2003) Diagnostic potential of parechovirus capsid proteins diagnostic potential of parechovirus capsid proteins. *Journal of clinical microbiology*, **41**, 2294–2299.
- Alidjinou EK, Sané F, Trauet J, Copin M (2015) Coxsackievirus B4 can infect human peripheral blood-derived macrophages. *Viruses*, **7**, 6067–6079.
- Allarakhia M (2013) Open-source approaches for the repurposing of existing or failed candidate drugs: Learning from and applying the lessons across diseases. *Drug Design, Development and Therapy*, **7**, 753–766.
- Althof N, Whitton JL (2013) Coxsackievirus B3 infects the bone marrow and diminishes the restorative capacity of erythroid and lymphoid progenitors. *Journal of Virology*, **87**, 2823–2834.
- Al-Zuhair S, Ashraf S, Hisaindee S *et al.* (2006) Enzymatic pre-treatment of microalgae cells for enhanced extraction of protein. *Engineering in Life Sciences*, doi. 10.1002/elsc.201600127.
- Amaro HM, Guedes AC, Malcata FX (2011) Antimicrobial activities of microalgae: an invited review. In “Science against microbial pathogens: communicating current research and technological advances” Méndez-Vilas A. (ed) Formatex, pp. 1272–1280.
- Amorim R, Costa SM, Cavaleiro NP, Da Silva EE, Da Costa LJ (2014) HIV-1 transcripts use ires-initiation under conditions where cap-dependent translation is restricted by poliovirus 2A protease. *PLoS ONE*, **9**, 1–13.
- An S, Park HS, Kim GH (2014) Evaluation of the antioxidant activity of cooked gomchwi (*Ligularia fischeri*) using the myoglobin methods. *Preventive Nutrition and Food Science*, **19**, 34–39.

- Andino R, Rieckhof GE, Achacoso PL, Baltimore D (1993) Poliovirus RNA synthesis utilizes an RNP complex formed around the 5'-end of viral RNA. *The EMBO journal*, **12**, 3587–98.
- Andreev DE, Fernandez-Miragall O, Ramajo J, Dmitriev SE, Terenin IM, Martinez-Salas E, Shatsky IN (2007) Differential factor requirement to assemble translation initiation complexes at the alternative start codons of foot-and-mouth disease virus RNA. *Rna*, **13**, 1366–1374.
- Andreoni AR, Colton AS (2017) Coxsackievirus B5 associated with hand-foot-mouth disease in a healthy adult. *JAAD Case Reports*, **3**, 165–168.
- Andres S, Pevny S, Ziegenhagen R, Bakhiya N, Schäfer B, Hirsch-Ernst KI, Lampen A (2018) Safety aspects of the use of quercetin as a dietary supplement. *Molecular Nutrition and Food Research*, **62**, doi.10.1002/mnfr.201700447.
- Annamalay AA, Lanaspá M, Khoo SK *et al.* (2016) Rhinovirus species and clinical features in children hospitalised with pneumonia from Mozambique. *Tropical Medicine and International Health*, **21**, 1171–1180.
- Anticoli S, Amatore D, Matarrese P, Angelis M De, Palamara AT, Nencioni L, Ruggieri A (2019) Counteraction of HCV-induced oxidative stress concurs to establish chronic infection in liver cell cultures. *Oxidative Medicine and Cellular Longevity*, doi.org/10.1155/2019/6452390.
- Aoki-Utsubo C, Chen M, Hotta H (2018) Time-of-addition and temperature-shift assays to determine particular step(s) in the viral life cycle that is blocked by antiviral substance(s). *Bio-Protocol*, **8**, 1–12.
- Arakawa M, Okamoto-Nakagawa R, Toda S *et al.* (2012) Molecular epidemiological study of human rhinovirus species A, B and C from patients with acute respiratory illnesses in Japan. *Journal of Medical Microbiology*, **61**, 410–419.
- Arzt J, Juleff N, Zhang Z, Rodriguez LL (2011) The pathogenesis of foot-and-mouth disease I: viral pathways in cattle. *Transboundary and Emerging Diseases*, **58**, 291–304.
- Ashburn TT, Thor KB (2004) Drug repositioning: identifying and developing new uses for existing drugs. *Nature Reviews Drug Discovery*, **3**, 673–683.

- Bachmetov L, Gal-Tanamy M, Shapira A *et al.* (2012) Suppression of hepatitis C virus by the flavonoid quercetin is mediated by inhibition of NS3 protease activity. *Journal of Viral Hepatitis*, **19**, e81–e88.
- Back SH, Kim YK, Kim WJ, Cho S, Oh HR, Kim J-E, Jang SK (2002) Translation of polioviral mRNA is inhibited by cleavage of polypyrimidine tract-binding proteins executed by polioviral 3C(pro). *Journal of Virology*, **76**, 2529–2542.
- Baer A, Kehn-Hall K (2014) Viral concentration determination through plaque assays: using traditional and novel overlay systems. *Journal of Visualized Experiments*, **93**, e52065.
- Bahuguna A, Khan I, Bajpai VK, Kang SC (2017) MTT assay to evaluate the cytotoxic potential of a drug. *Bangladesh Journal of Pharmacology*, **12**, 115–118.
- Baicus A (2012) History of polio vaccination. *World Journal of Virology*, **1**, 108–114.
- Bailey JM, Tappich WE (2007) Structure of the 5′ nontranslated region of the coxsackievirus B3 genome: chemical modification and comparative sequence analysis. *Journal of Virology*, **81**, 650–668.
- Bargagli E, Olivieri C, Bennett D, Prasse A, Muller-Quernheim J, Rottoli P (2009) Oxidative stress in the pathogenesis of diffuse lung diseases: A review. *Respiratory Medicine*, **103**, 1245–1256.
- Barkia I, Saari N, Manning SR (2019) Microalgae for high-value products towards human health and nutrition. *Marine Drugs*, **17**, doi:10.3390/md17050304.
- Barr JN, Fearn R (2010) How RNA viruses maintain their genome integrity. *Journal of General Virology*, **91**, 1373–1387.
- Barton DJ, O'Donnell BJ, Flanagan JB (2001) 5′ cloverleaf cloverleaf in poliovirus RNA is a cis-acting replication element required for negative-strand synthesis. *EMBO Journal*, **20**, 1439–1448.
- Bartz R, Li W-H, Venables B *et al.* (2007) Lipidomics reveals that adiposomes store ether lipids and mediate phospholipid traffic. *Journal of Lipid Research*, **48**, 837–847.

- Bauer L, Lyoo H, van der Schaar HM, Strating JR, van Kuppeveld FJ (2017) Direct-acting antivirals and host-targeting strategies to combat enterovirus infections. *Current Opinion in Virology*, **24**, doi. org/10.1016/j.coviro.2017.03.009.
- Bauer L, Manganaro R, Zonsics B et al (2019) Fluoxetine inhibits enterovirus replication by targeting the viral 2C protein in a stereospecific manner. *ACS Infectious Diseases*, **5**, 1609–1623.
- Beisser P, Verzijl D (2005) The Epstein-Barr virus BILF1 gene encodes a G protein-coupled receptor that inhibits phosphorylation of RNA-dependent protein kinase. *Journal of Virology*, **79**, 441–449.
- Belov GA, Altan-Bonnet N, Kovtunovych G, Jackson CL, Lippincott-Schwartz J, Ehrenfeld E (2007) Hijacking components of the cellular secretory pathway for replication of poliovirus RNA. *Journal of Virology*, **81**, 558–567.
- Belov GA, Fogg MH, Ehrenfeld E (2005) Poliovirus proteins induce membrane association of GTPase ADP-ribosylation factor. *Journal of Virology*, **79**, 7207–7216.
- Belov GA, Lidsky P V, Mikitas O V, Egger D, Lukyanov KA, Bienz K, Agol VI (2004) Bidirectional increase in permeability of nuclear envelope upon poliovirus infection and accompanying alterations of nuclear pores. *Journal of Virology*, **78**, 10166–10177.
- Benschop K, Wildenbeest J (2004) Human parechoviruses, new players in the pathogenesis of viral meningitis. *Meningitis*. **12**. 145–162.
- Benschop KSM, Schinkel J, Minnaar RP *et al.* (2006) Human parechovirus infections in dutch children and the association between serotype and disease severity. *Clinical Infectious Diseases*, **42**, 204–210.
- Bergamini G, Preiss T, Hentze MW (2000) Picornavirus IRESes and the poly(A) tail jointly promote cap-independent translation in a mammalian cell-free system. *Rna*, **6**, 1781–1790.
- Bergelson JM, Chan M, Solomon KR, John NFS, Lin H, Finberg RW (1994) Decay-accelerating factor (CD55), a glycosylphosphatidylinositol-anchored complement regulatory protein, is a receptor for several echoviruses. *Proceedings of the National Academy of Sciences*, **91**, 6245–6248.

- Berryman S, Moffat K, Harak C, Lohmann V, Jackson T (2016) Foot-and-mouth disease virus replicates independently of phosphatidylinositol 4-phosphate and type III phosphatidylinositol 4-kinases. *Journal of General Virology*, **97**, 1841–1852.
- Bienz K, Egger D, Pasamontes L (1987) Association of polioviral proteins of the P2 genomic region with the viral replication complex and virus-induced membrane synthesis as visualized by electron microscopic immunocytochemistry and autoradiography. *Virology*, **160**, 220–226.
- Binns D, Januszewski T, Chen Y *et al.* (2006) An intimate collaboration between peroxisomes and lipid bodies. *The Journal of Cell Biology*, **173**, 719–731.
- Bird AG, Britton S (1979) A New Approach to the study of human B lymphocyte function using an indirect plaque assay and a direct B cell activator. *Immunological Reviews*, **45**, 41–67.
- Bird SW, Kirkegaard K (2015) Escape of non-enveloped virus from intact cells. *Virology*, **479–480**, 444–449.
- Birtley JR, Knox SR, Jaulent AM, Brick P, Leatherbarrow RJ, Curry S (2005) Crystal structure of foot-and-mouth disease virus 3C protease: New insights into catalytic mechanism and cleavage specificity. *Journal of Biological Chemistry*, **280**, 11520–11527.
- Blaas D (2016) Viral entry pathways: the example of common cold viruses. *Wiener Medizinische Wochenschrift*, **166**, 211–226.
- Blaas D, Fuchs R (2016) Mechanism of human rhinovirus infections. *Molecular and Cellular Pediatrics*, **3**, **21**. doi.10.1186/s40348-016-0049-3
- Blake IM, Pons-Salort M, Molodecky NA *et al.* (2018) Type 2 poliovirus detection after global withdrawal of trivalent oral vaccine. *New England Journal of Medicine*, **379**, 834–845.
- Blanco-Colio LM, Tuñón J, Martín-Ventura JL, Egido J (2003) Anti-inflammatory and immunomodulatory effects of statins. *Kidney International*, **63**, 12–23.

- Blaner WS, O'Byrne SM, Wongsiriroj N *et al.* (2009) Hepatic stellate cell lipid droplets: a specialized lipid droplet for reinoid storage. *Biochim Biophys Acta.*, **1791**, 467–473.
- Blomqvist S, Savolainen C, Raman L, Roivainen M, Hovi T (2002) Human rhinovirus 87 and enterovirus 68 represent a unique serotype with rhinovirus and enterovirus features. *Journal of clinical microbiology*, **40**, 4218–4223.
- Boldescu V, Behnam MAM, Vasilakis N, Klein CD, Diseases T (2017) Broad-spectrum agents for flaviviral infections: Dengue, Zika and beyond. *Nature Reviews Drug Discovery*, **16**, 565–586.
- Boonyakiat Y, Hughes PJ, Ghazi F, Stanway G (2001) Arginine-Glycine-Aspartic acid motif is critical for human Parechovirus 1 entry. *Journal of Virology*, **75**, 10000–10004.
- Borman AM, Deliat FG, Kean KM (1994) Sequences within the poliovirus internal ribosome entry segment control viral RNA synthesis. *The EMBO Journal*, **13**, 3149–3157.
- Borrajo A, Ranazzi A, Pollicita M *et al.* (2017) Effects of amprenavir on HIV-1 maturation, production and infectivity following drug withdrawal in chronically-infected monocytes/macrophages. *Viruses*, **9**, doi:10.3390/v9100277.
- Boson B, Denolly S, Turlure F, Chamot C, Dreux M, Cosset FL (2017) Daclatasvir prevents hepatitis C virus infectivity by blocking transfer of the viral genome to assembly sites. *Gastroenterology*, **152**, 895–907.
- Boulant S, Stanifer M, Lozach PY (2015) Dynamics of virus-receptor interactions in virus binding, signaling, and endocytosis. *Viruses*, **7**, 2794–2815.
- Bozza P, Avila HD, Almeida P *et al.* (2017) Lipid droplets in host – pathogen interactions. *Clinical Lipidology*, **4299**, 791–807.
- Britton PN, Jones CA, Macartney K, Cheng AC (2018a). Parechovirus: an important emerging infection in young infants. *The Medical Journal of Australia*, **208**, 365-369.

- Britton PN, Khandaker G, Khatami A, *et al.* (2018b). High prevalence of developmental concern amongst infants at 12 months following hospitalised parechovirus infection. *Journal of Paediatrics and Child Health*, **54**, 289-295.
- Brock TG, McNish RW, Peters-Golden M (1999) Arachidonic acid is preferentially metabolized by cyclooxygenase-2 to prostacyclin and prostaglandin E2. *Journal of Biological Chemistry*, **274**, 11660–11666.
- Brown CH (2008) Overview of drug–drug interactions with SSRIs. *US Pharm*, 33, HS-3-HS-19.
- Buchen-Osmond C (2007) Taxonomy and classification of viruses. *Virology*, **76**, 1217–1225.
- Buevich A V, Elyashberg ME (2016) Synergistic combination of CASE algorithms and DFT chemical shift predictions: A powerful approach for structure elucidation, verification, and revision. *Journal of Natural Products*, **79**, 3105–3116.
- Buhman KK, Chen HC, Farese R V. (2001) The enzymes of neutral lipid synthesis. *Journal of Biological Chemistry*, **276**, 40369–40372.
- Bukh J (2016) The history of hepatitis C virus (HCV): Basic research reveals unique features in phylogeny, evolution and the viral life cycle with new perspectives for epidemic control. *Journal of Hepatology*, **65**, S2–S21.
- Bulankina A V, Deggerich A, Wenzel D *et al.* (2009) TIP47 functions in the biogenesis of lipid droplets. *Journal of Cell Biology*, **185**, 641–655.
- Burckhardt CJ, Greber UF (2009) Virus movements on the plasma membrane support infection and transmission between cells. *PLoS Pathogens*, **5**, e1000621.
- Cabrerizo M, De Miguel T, Armada A, Martínez-Risco R, Pousa A, Trallero G (2010) Onychomadesis after a hand, foot, and mouth disease outbreak in Spain, 2009. *Epidemiology and Infection*, **138**, 1775–1778.
- Cai J, Chen Y, Seth S, Furukawa S, Compans RW, P. JD (2003) Inhibition of influenza inhibition by glutathione. *Free Radical Biology & Medicine*, **34**, 928–936.

- Cameron CE, Suk Oh H, Moustafa IM (2010) Expanding knowledge of P3 proteins in the poliovirus lifecycle. *Future Microbiology*, **5**, 867–881.
- Campagnola G, McDonald S, Beaucourt S, Vignuzzi M, Peersen OB (2015) Structure-function relationships underlying the replication fidelity of viral RNA-dependent RNA polymerases. *Journal of Virology*, **89**, 275–286.
- Campbell ID, Humphries MJ (2011) Integrin structure, activation, and interactions. *Cold Spring Harbor Perspectives in Biology*, **3**, doi.10.1101/cshperspect.a004994.
- Cann A.J (2001) Principles of molecular virology. 3rd ed. *Academic Press*, eBook ISBN: 9780080886909.
- Cardosa MJ, Perera D, Brown BA *et al.* (2003) Molecular epidemiology of human enterovirus 71 strains and recent outbreaks in the Asia-Pacific region: comparative analysis of the VP1 and VP4 genes. *Emerging Infectious Diseases*, **9**, 461–468.
- Cassidy CM, Tunney MM, Mccarron PA, Donnelly RF (2009) Drug delivery strategies for photodynamic antimicrobial chemotherapy: From benchtop to clinical practice. *Journal of Photochemistry & Photobiology, B: Biology*, **95**, 71–80.
- Castello A, Álvarez E, Carrasco L (2011) The multifaceted poliovirus 2A protease: Regulation of gene expression by picornavirus proteases. *Journal of Biomedicine and Biotechnology*, **2011**, doi.10.1155/2011/369648.
- Castrillo JL, Carrasco L (1987) Action of 3-methylquercetin on poliovirus RNA replication. *Journal of Virology*, **61**, 3319–3321.
- Cathcart AL, Baggs EL, Semler BL (2015) Picornavirus: Pathogenesis and molecular biology, 3 ed. Elsevier, pp 1-11.
- Cavaliere C, Foglia P, Pastorini E, Samperi R, Laganà A (2005) Identification and mass spectrometric characterization of glycosylated flavonoids in *Triticum durum* plants by high-performance liquid chromatography with tandem mass spectrometry. *Rapid Communications in Mass Spectrometry*, **19**, 3143–3158.
- Cermelli S, Guo Y, Gross SP, Welte MA (2006) The lipid-droplet proteome reveals that droplets are a protein-storage depot. *Current Biology*, **16**, 1783–1795.

- Cha Y, Erez T, Reynolds IJ *et al.* (2018) Drug repurposing from the perspective of pharmaceutical companies. *British Journal of Pharmacology*, **175**, 168–180.
- Chang KH, Auvinen P, Hyypiä T, Stanway G (1989) The nucleotide sequence of Coxsackievirus A9; implications for receptor binding and enterovirus classification. *Journal of General Virology*, **70**, 3269–3280.
- Chang K-S, Jo H-J (2011) HMG CoA reductase inhibitors inhibit HCV RNA replication of HCV genotype 1b but not 2a. *Journal of Bacteriology and Virology*, **41**, 99–108.
- Chang PC, Chen SC, Chen KT (2016) The current status of the disease caused by enterovirus 71 infections: Epidemiology, pathogenesis, molecular epidemiology, and vaccine development. *International Journal of Environmental Research and Public Health*, **13**, 29–34.
- Chang Y, Chen K, Chen K (2018) Hand, foot and mouth disease and herpangina caused by enterovirus A71 infections: a review of enterovirus A71 molecular epidemiology, pathogenesis, and current vaccine development. *The Revista do Instituto de Medicina Tropical de São Paulo*, **60**, e70.
- Chansaenroj J, Tuanthap S, Thanusuwannasak T *et al.* (2017) Human enteroviruses associated with and without diarrhea in Thailand between 2010 and 2016. *PLoS ONE*, **12**, doi.org/10.1371/journal.pone.0182078.
- Chase AJ, Daijogo S, Semler BL (2014) Inhibition of poliovirus-induced cleavage of cellular protein PCBP2 reduces the levels of viral RNA replication. *Journal of Virology*, **88**, 3192–3201.
- Chen C, Han X, Zou X *et al.* (2014) C75, an inhibitor of fatty acid synthase, suppresses the mitochondrial fatty acid synthesis pathway and impairs mitochondrial function. *Journal of Biological Chemistry*, **289**, 17184–17194.
- Chen TC, Weng KF, Chang SC, Lin JY, Huang PN, Shih SR (2008a) Development of antiviral agents for enteroviruses. *Journal of Antimicrobial Chemotherapy*, **62**, 1169–1173.

- Chen X, Parker J, Krueger CG, Shanmuganayagam D, Reed JD (2014) Validation of HPLC assay for the identification and quantification of anthocyanins in black currants. *Analytical Methods*, **6**, 8141–8147.
- Chen Y, Gu F, Guan J (2018) Metformin might inhibit virus through increasing insulin sensitivity. *Chinese Medical Journal*, **131**, 376–377.
- Chen Y, Zeng S, Hsu JT *et al.* (2008b) Amantadine as a regulator of internal ribosome entry site. *Acta Pharmacologica Sinica*, **29**, 1327–1333.
- Cheng F, Murray JL, Zhao J, Sheng J, Zhao Z, Rubin DH (2016) Systems biology-based investigation of cellular antiviral drug targets identified by gene-trap insertional mutagenesis. *PLoS Computational Biology*, **12**, doi.10.1371/journal.pcbi.1005074.
- Cheng H, Lear-Rooney CM, Johansen L, Varhegyi E, Chen ZW, Olinger GG, Rong L (2015) Inhibition of Ebola and Marburg virus entry by G Protein-Coupled Receptor Antagonists. *Journal of Virology*, **89**, 9932–9938.
- Chinsembu KC (2019) Chemical diversity and activity profiles of HIV-1 reverse transcriptase inhibitors from plants. *Revista Brasileira de Farmacognosia*, **572**, doi.org/10.1016/j.bjp.2018.10.006.
- Chioh KH, Phoon MC, Putti T, Tan BKH, Chow VT (2016) Evaluation of antiviral activities of *Houttuynia cordata* Thunb. extract, quercetin, quercetrin and cinanserin on murine coronavirus and dengue virus infection. *Asian Pacific Journal of Tropical Medicine*, **9**, doi. 10.1016/j.apjtm.2015.12.002.
- Chitraju C, Mejhert N, Haas JT *et al.* (2017) Triglyceride synthesis by DGAT1 protects adipocytes from lipid-induced ER stress during lipolysis. *Cell Metabolism*, **26**, 407–418.e3.
- Cho MW, Teterina N, Egger D, Bienz K, Ehrenfeld E (1994) Membrane rearrangement and vesicle induction by recombinant poliovirus 2C and 2BC in human cells. *Virology*, **202**, 129–145.
- Choe E, Min DB (2009) Mechanisms of antioxidants in the oxidation of foods. *Comprehensive Reviews in Food Science and Food Safety*, **8**, 345–358.

- Choi HJ, Song JH, Park KS, Baek SH (2010) In vitro anti-enterovirus 71 activity of gallic acid from *Woodfordia fruticosa* flowers. *Letters in Applied Microbiology*, **50**, 438–440.
- Cichewicz R H, Kouzi S A (2004) Chemistry, biological activity, and chemotherapeutic potential of betulinic acid for the prevention and treatment of cancer and HIV infection. *Medicinal Research Reviews*, **24**, 90-114. doi.10.1002/m.
- Ciomperlik JJ, Basta HA, Palmenberg AC (2016) Cardiovirus Leader proteins bind exportins: implications for virus replication and nucleocytoplasmic trafficking inhibition. *Virology*, **487**, 19–26.
- Clercq E De, Férir G, Kaptein S, Neyts J (2010) Antiviral treatment of chronic Hepatitis B virus (HBV) infections. *Viruses*, **2**, 1279–1305.
- Colebc NB, Murphy DD, Grider T, Rueter S, Brasaemle D, Nussbaum RL (2002) Lipid droplet binding and oligomerization properties of the Parkinson's disease protein α -synuclein. *Journal of Biological Chemistry*, **277**, 6344–6352.
- Collier B, Goobar-Larsson L, Sokolowski M, Schwartz S (1998) Translational inhibition in vitro of human papillomavirus type 16 L2 mRNA mediated through interaction with heterogenous ribonucleoprotein K and poly(rC)-binding proteins 1 and 2. *Journal of Biological Chemistry*, **273**, 22648–22656.
- Cordey S, Gerlach D, Junier T, Zdobnov EM, Kaiser L, Tapparel C (2008) The cis-acting replication elements define human enterovirus and rhinovirus species. *Rna*, **14**, 1568–1578.
- Cornelis JJ, Su ZZ, Rommelaere J (1982) Direct and indirect effects of ultraviolet light on the mutagenesis of parvovirus H-1 in human cells. *The EMBO Journal*, **1**, 693–699.
- Cornelissen M, Gall A, Vink M *et al.* (2017) From clinical sample to complete genome: Comparing methods for the extraction of HIV-1 RNA for high-throughput deep sequencing. *Virus Research*, **239**, 10–16.
- Corsetto PA, Colombo I, Kopecka J, Rizzo AM, Riganti C (2017) Ω -3 long chain polyunsaturated fatty acids as sensitizing agents and multidrug sesistance

- revertants in cancer therapy. *International Journal of Molecular Sciences*, **18**, doi.10.3390/ijms18122770.
- Costa L, Faustino MAF, Almeida A (2012) Photodynamic inactivation of mammalian viruses and bacteriophages. *Viruses*, **2012**, 1034–1074.
- Costantini D, Rowe M, Butler MW, McGraw KJ (2010) From molecules to living systems: historical and contemporary issues in oxidative stress and antioxidant ecology. *Functional Ecology*, **24**, 950–959.
- Cottam EM, Wadsworth J, Shaw AE *et al.* (2008) Transmission pathways of foot-and-mouth disease virus in the United Kingdom in 2007. *PLoS Pathogens*, **4**, e1000050.
- Couso I, Pérez-Pérez ME, Martínez-Force E, Kim HS, He Y, Umen JG, Crespo JL (2018) Autophagic flux is required for the synthesis of triacylglycerols and ribosomal protein turnover in *Chlamydomonas*. *Journal of Experimental Botany*, **69**, 1355–1367.
- Cox DW, Bizzintino J, Ferrari G *et al.* (2013) Human rhinovirus species C infection in young children with acute wheeze is associated with increased acute respiratory hospital admissions. *American Journal of Respiratory and Critical Care Medicine*, **188**, 1358–1364.
- Cox DW, Khoo SK, Zhang G *et al.* (2018) Rhinovirus is the most common virus and rhinovirus-C is the most common species in paediatric intensive care respiratory admissions. *European Respiratory Journal*, **52**. doi.10.1183/13993003.00207-2018.
- Crawford SE, Desselberger U (2017) Lipid droplets form complexes with viroplasms and are crucial for rotavirus replication. *Current Opinion in Virology*, **11–15**, doi.10.1016/j.coviro.2016.05.008.
- Crotty S, Hix L, Sigal LJ, Andino R (2002) Poliovirus pathogenesis in a new poliovirus receptor transgenic mouse model: Age-dependent paralysis and a mucosal route of infection. *Journal of General Virology*, **83**, 1707–1720.
- Crow TJ (1978) Viral causes of psychiatric disease. *Postgraduate Medical Journal*, **54**, 763–767.

- Crump CE, Rollins BS, Hayden FG (2015) In vitro antiviral activity and cytotoxicity of aspirin: lack of selective activity against influenza A virus or rhinovirus. *Antiviral Chemistry and Chemotherapy*, **1**, 217–221.
- Czabany T, Wagner A, Zweytick D, Lohner K, Leitner E, Ingolic E, Daum G (2008) Structural and biochemical properties of lipid particles from the yeast *Saccharomyces cerevisiae*. *Journal of Biological Chemistry*, **283**, 17065–17074.
- da Silva FL, Escribano-Bailón MT, Pérez Alonso JJ, Rivas-Gonzalo JC, Santos-Buelga C (2007) Anthocyanin pigments in strawberry. *LWT - Food Science and Technology*, **40**, 374–382.
- Daelemans D, Pauwels R, De Clercq E, Pannecouque C (2011) A time-of-drug addition approach to target identification of antiviral compounds. *Nature Protocols*, **6**, 925–933.
- Dagan R, Leventhal A, Anis E, Slater P, Ashur Y, Shouval D (2005) Incidence of hepatitis A in Israel following universal immunization of toddlers. *Journal of the American Medical Association*, **294**, 202–210.
- Dai W, Bi J, Li F *et al.* (2019) Antiviral efficacy of flavonoids against enterovirus 71 infection in vitro and in newborn mice. *Viruses*, **11**, 625. doi.10.3390/v11070625
- Daneschvar HL, Aronson MD, Smetana GW (2016) FDA-approved anti-obesity drugs in the United States. *American Journal of Medicine*, **129**, e871–e876.
- de Chassey B, Meyniel-Schicklin L, Vonderscher J, André P, Lotteau V (2014) Virus-host interactomics: new insights and opportunities for antiviral drug discovery. *Genome Medicine*, **6**, <http://genomemedicine.com/content/6/11/115>.
- de Crom SCM, Rossen JWA, van Furth AM, Obihara CC (2016) Enterovirus and parechovirus infection in children: a brief overview. *European Journal of Pediatrics*, **175**, 1023–1029.
- de Jong AS, Melchers WJG, Glaudemans DH, Willems PH, van Kuppeveld FJ (2004) Mutational Analysis of Different Regions in the Coxsackievirus 2B Protein. *Journal of Biological Chemistry*, **279**, 19924–19935.

- de Jong AS, Melchers WJG, Van Dommelen MM, de Mattia F Willems PHGM, van Kuppeveld FJM, Lanke K (2008) Functional Analysis of Picornavirus 2B Proteins: Effects on Calcium Homeostasis and Intracellular Protein Trafficking. *Journal of Virology*, **82**, 3782–3790.
- de Oliveira Silva E, Batista R (2017) Ferulic acid and naturally occurring compounds bearing a feruloyl moiety: A review on their structures, occurrence, and potential health benefits. *Comprehensive Reviews in Food Science and Food Safety*, **16**, 580–616.
- De Palma AM, Heggermont W, Lanke K et al (2008) The Thiazolobenzimidazole TBZE-029 Inhibits Enterovirus Replication by Targeting a Short Region Immediately Downstream from Motif C in the Nonstructural Protein 2C. *Journal of Virology*, **82**, 4720–4730.
- Debing Y, Neyts J, Delang L (2015) The future of antivirals: Broad-spectrum inhibitors. *Current Opinion in Infectious Diseases*, **28**, 596–602.
- Del Campo JA, García-Valdecasas M, Gil-Gómez A *et al.* (2018) Simvastatin and metformin inhibit cell growth in hepatitis C virus infected cells via mTOR increasing PTEN and autophagy. *PLoS ONE*, **13**, doi.org/10.1371/journal.pone.0191805.
- del Real G, Jiménez-Baranda S, Mira E *et al.* (2004) Statins inhibit HIV-1 infection by down-regulating Rho activity. *The Journal of Experimental Medicine*, **200**, 541–547.
- Dempsey CM, Mackenzie SM, Gargus A, Blanco G, Sze JY (2005) Serotonin (5HT), fluoxetine, imipramine and dopamine target distinct 5HT receptor signaling to modulate *Caenorhabditis elegans* egg-laying behavior. *Genetics*, **1436**, 1425–1436.
- Denis TGS, Hamblin MR (2011). An introduction to photoantimicrobial: photodynamic therapy as a novel method of microbial pathogen eradication. In “Science against microbial pathogen: communicating current research and technological advances” Mendez-Vils(ed) Formax. pp 675-683.

- DeStefano JJ, Titilope O (2006) Poliovirus protein 3AB displays nucleic acid chaperone and helix-destabilizing activities. *Journal of Virology*, **80**, 1662–1671.
- Dobrikova EY, Grisham RN, Kaiser C, Lin J, Gromeier M (2006) Competitive translation efficiency at the picornavirus type 1 internal ribosome entry site facilitated by viral cis and trans factors. *Journal of virology*, **80**, 3310–3321.
- Doedens JR, Giddings Jr. TH, Kirkegaard K (1997) Inhibition of endoplasmic reticulum-to-Golgi traffic by poliovirus protein 3A: genetic and ultrastructural analysis. *Journal of Virology*, **71**, 9054–9064.
- Domingo E, Sheldon J, Perales C (2012) Viral quasispecies evolution. *Microbiology and Molecular Biology Reviews*, **76**, 159–216.
- Donaldson AI, Alexandersen S (2002) Predicting the spread of foot and mouth disease by airborne virus. *Scientific and Technical Review*, **21**, 569–575.
- Dong Y, Liu Y, Jiang W, Smith TJ, Xu Z, Rossmann MG (2017) Antibody-induced uncoating of human rhinovirus B14. *Proceedings of the National Academy of Sciences*, **14**, 8017–8022.
- Donnelly MLL, Luke G, Mehrotra A, Li X, Hughes LE, Gani D, Ryan MD (2001) Analysis of the aphthovirus 2A/2B polyprotein “cleavage” mechanism indicates not a proteolytic reaction, but a novel translational effect: A putative ribosomal “skip”. *Journal of General Virology*, **82**, 1013–1025.
- Dorner AA (2005) Coxsackievirus-adenovirus receptor (CAR) is essential for early embryonic cardiac development. *Journal of Cell Science*, **118**, 3509–3521.
- Dotta F, Censini S, Halteren AGS Van *et al.* (2007) Coxsackie B4 virus infection of cells and natural killer cell insulinitis in recent-onset type 1 diabetic patients. *PNAS*, **104**, 5115–5120
- Drescher KM, Kono K, Bopegamage S, Carson SD, Tracy S (2004) Coxsackievirus B3 infection and type 1 diabetes development in NOD mice: insulinitis determines susceptibility of pancreatic islets to virus infection. *Virology*, **329**, 381–394.
- Drexler JF, Baumgarte S, Eschbach-bludau M, Simon A, Kemen C, Bode U (2011) Human meningitis, and cardioviruses, death syndrome sudden infant in children. *Emerging infectious diseases*, **17**, 2313–2315.

- Drexler JF, Kleber L, Luna DS *et al.* (2008) Circulation of 3 lineages of a novel Saffold Coronavirus in humans. *Emerging Infectious Diseases*, **14**, 1398–1405.
- Drummond CG, Bolock AM, Ma C, Luke CJ, Good M, Coyne CB (2017) Enteroviruses infect human enteroids and induce antiviral signaling in a cell lineage-specific manner. *Proceedings of the National Academy of Sciences*, **114**, 1672–1677.
- Duke GM, Hoffman MA, Palmenberg AC (1992) Sequence and structural elements that contribute to efficient encephalomyocarditis virus RNA translation. *Journal of Virology*. **66**, 1602–1609.
- Duncan AL, Reddy T, Koldsø H, Hélie J, Fowler PW, Chavent M, Sansom MSP (2017) Protein crowding and lipid complexity influence the nanoscale dynamic organization of ion channels in cell membranes. *Scientific Reports*, **7**, 16647. doi.10.1038/s41598-017-16865-6.
- Duque H, Palmenberg AC (2001) Phenotypic Characterization of Three Phylogenetically Conserved Stem-Loop Motifs in the Mengovirus 3J Untranslated Region. *Society*, **75**, 3111–3120.
- Ekins S, Freundlich JS, Coffee M (2015) A common feature pharmacophore for FDA-approved drugs inhibiting the Ebola virus [version 1; peer review: 2 approved]. *F1000 Research*, **3**, 277. doi.org/10.12688/f1000research.5741.1).
- Elamin B (2003) Dibucaine inhibition of serum cholinesterase. *Journal of biochemistry and molecular biology*, **36**, 149–53.
- Eldaghayes I, Dayhum A, Kammon A *et al.* (2017) Exploiting serological data to understand the epidemiology of foot-and-mouth disease virus serotypes circulating in Libya. *Open Veterinary Journal*, **7**, doi.10.4314/ovj.v7i1.1.
- El-Shehabi F, Taman A, Moali LS, El-Sakkary N, Ribeiro P (2012) A novel g protein-coupled receptor of schistosoma mansoni (smgpr-3) is activated by dopamine and is widely expressed in the nervous system. *PLoS Neglected Tropical Diseases*, **6**, e1523.
- Eriksson S, Schmidt EE, Prigge JR, Talago EA, Arne ESJ (2015) homeostasis in the mouse liver. *Nature Communications*, **1038**, doi.10.1038/ncomms7479.

- Esposito S, Bosis S, Niesters H, Principi N (2015) Enterovirus D68 infection. *Viruses*, **7**, 6021–6028.
- Falaise C, François C, Travers MA *et al.* (2016) Antimicrobial compounds from eukaryotic microalgae against human pathogens and diseases in aquaculture. *Marine Drugs*, **14**, doi.10.3390/md14090159.
- Falkenhagen A, Joshi S (2018) HIV Entry and Its Inhibition by Bifunctional Antiviral Proteins. *Molecular Therapy - Nucleic Acids*, **13**, 347–364.
- Farazuddin M, Mishra R, Jing Y, Srivastava V, Comstock AT, Sajjan US (2018) Quercetin prevents rhinovirus-induced progression of lung disease in mice with COPD phenotype. *PLoS ONE*, **13**, doi.org/10.1371/journal.pone.0199612.
- Farese RVF Jr, Walther TC (2009) Lipid droplets finally get a little R-E-S-P-E-C-T. *Cell*, **139**, 855–860.
- Faria NR, De Vries M, Van Hemert FJ, Benschop K, Van Der Hoek L (2009) Rooting human parechovirus evolution in time. *BMC Evolutionary Biology*, **9**, doi.10.1186/1471-2148-9-164.
- Fauquet CM, 1994. Taxonomy and classification general. In: Webster RG, Granoff, A. (Eds.), *Encyclopedia of Virology*. Academic Press, London, pp. 1396–1410.
- Murphy EA, Fauquet CM, Bishop DHL, Ghabrial SA, Jarvis AW, Martelli GP, Mayo MA, Summers M D, 1995. Classification and Nomenclature of Viruses. In: *Virus Taxonomy*. Springer-Verlag Wien GmbH. pp. 1-8.
- Fawkner-Corbett D, Khoo S, Duarte M *et al.* (2016) Rhinovirus-C detection in children presenting with acute respiratory infection to hospital in Brazil. *Journal of Medical Virology*, **88**, 58–63.
- Fenn S, Du Z, Lee JK, Tjhen R, Stroud RM, James TL (2007) Crystal structure of the third KH domain of human poly(C)-binding protein-2 in complex with a C-rich strand of human telomeric DNA at 1.6Å resolution. *Nucleic Acids Research*, **35**, 2651–2660.
- Ferguson JM, Ferguson JM (2001) SSRI antidepressant medications: adverse effects and tolerability. *Primary Care Companion Journal of Clinical Psychiatry*, **3**, 22–27.

- Fernandez-Garcia MD, Volle R, Joffret ML *et al.* (2018) Genetic characterization of enterovirus A71 circulating in Africa. *Emerging Infectious Diseases*, **24**, 754–757.
- Fernández-Oliva A, Ortega-González P, Risco C (2019) Targeting host lipid flows: exploring new antiviral and antibiotic strategies. *Cellular Microbiology*, **21**, e12996.
- Ferré P, Le Lay S, Blouin CM *et al.* (2009) Lipid droplet analysis in caveolin-deficient adipocytes: alterations in surface phospholipid composition and maturation defects. *Journal of Lipid Research*, **51**, 945–956.
- Ferrer-Orta C, Arias A, Perez-Luque R, Escarmís C, Domingo E, Verdaguer N (2004) Structure of foot-and-mouth disease virus RNA-dependent RNA polymerase and its complex with a template-primer RNA. *Journal of Biological Chemistry*, **279**, 47212–47221.
- Ferrer-Orta C, Ferrero D, Verdaguer N (2015) RNA-dependent RNA polymerases of picornaviruses: From the structure to regulatory mechanisms. *Viruses*, **7**, 4438–4460.
- Feuer R, Ruller CM, An N *et al.* (2009) Viral Persistence and Chronic Immunopathology in the Adult Central Nervous System following Coxsackievirus Infection during the Neonatal Period. *Journal of Virology*, **83**, 9356–9369.
- Filippi CM, Von Herrath MG (2008) Viral trigger for type 1 diabetes: *Pros and cons*. *Diabetes*, **57**, 2863–2871.
- Fine PE., Carneiro IA. (1999) Transmissibility and persistence of oral polio vaccine viruses: Implications for the global poliomyelitis eradication initiative. *American Journal of Epidemiology*, **150**, 1001–1021.
- Flather D, Semler BL (2015) Picornaviruses and nuclear functions: Targeting a cellular compartment distinct from the replication site of a positive-strand RNA virus. *Frontiers in Microbiology*, **6**, doi.10.3389/fmicb.2015.00594.
- Forman S, Le Gall F, Belton D *et al.* (2009) Animal health division, food safety and consumer affairs Bureau, Ministry of Agriculture. *Scientific and Technical Review of the Office International des Epizooties*, **28**, 1–2.

- Fuentes C, Bosch A, Pintó RM, Fuentes C, Bosch A, Pintó RM, Guix S (2012) Identification of human astrovirus genome-linked protein (VPg) essential for virus infectivity. *Journal of Virology*, **86**,10070-8, doi: 10.1128/JVI.00797-12.
- Fujimoto T, Parton RG (2011) Not just fat: The structure and function of the lipid droplet. *Cold Spring Harbor Perspectives in Biology*, **3**, doi.10.1101/cshperspect.a004838.
- Galabov AS, Nikolaeva L, Todorovab D, Tsenka M (1998) Antiviral activity of cholesteryl esters of cinnamic acid derivatives. *Zeitschrift für Natur forschung A*, **53c**, 883–887.
- Gamble TR, Vajdos FF, Yoo S, Worthylake DK, Houseweart M, Sundquist WI, Hill CP (1996) Crystal structure of human cyclophilin A bound to the amino-terminal domain of HIV-1 capsid. *Cell*, **87**, 1285–1294.
- Gan XL, Zhang T De (2017) Onychomadesis after hand-foot-and-mouth disease. *Canadian Medical Association Journal*, **189**, E279.
- Ganesan S, Faris AN, Comstock AT, Wang Q, Hershenson MB, Sajjan US (2013) Quercetin inhibits rhinovirus replication in vitro and in vivo. *Antiviral research*, **94**, 258–271.
- Ganjian H, Zietz C, Mechtcheriakova D, Blaas D, Fuchs R (2017) ICAM-1 binding rhinoviruses enter Hela cells via multiple pathways and travel to distinct intracellular compartments for uncoating. *Viruses*, **9**, doi.10.3390/v9040068.
- Garmaroudi FS, Marchant D, Hendry R *et al.* (2015) Coxsackievirus B3 replication and pathogenesis. *Future Microbiology*, **10**, 629–653.
- Gebhard LG, Filomatori CV, Gamarnik AV (2011) Functional RNA elements in the dengue virus genome. *Viruses*, **3**, 1739–1756.
- Geller R, Taguwa S, Frydman J (2012) Broad action of Hsp90 as a host chaperone required for viral replication. *Biochimica et Biophysica Acta - Molecular Cell Research*, **1823**, 698–706.
- Gibson, J F, Ingram, J E, Nicholls, P (1958) Free radical produced in the reaction of metmyoglobin with hydrogen peroxide. *Nature*, **181**, 13982- 1399.

- Glatthaar-Saalmüller B, Mair KH, Saalmüller A (2017) Antiviral activity of aspirin against RNA viruses of the respiratory tract—an in vitro study. *Influenza and other Respiratory. Viruses*, **11**, 85–92.
- Glikson M, Galun E, Oren R, Tur-Kaspa R, Shouval D (1992) Relapsing Hepatitis A review of 14 cases and literature survey. *Medicine*, **71**, 14–23.
- Glisovic T, Bachorik JL, Yong J, Dreyfuss G (2008) RNA-binding proteins and post-transcriptional gene regulation. *FEBS letters*, **582**, 1977–86.
- Global Polio Eradication Initiative (GPEI) (2020). <http://polioeradication.org/where-we-work/>. Accessed on 29/3/2020.
- Gofshteyn J, Cárdenas AM, Bearden D (2016) Treatment of chronic enterovirus encephalitis with fluoxetine in a patient with X-linked agammaglobulinemia. *Pediatric Neurology*, **64**, 94–98.
- Goiffon J P, Mouly P P, Gaydou E M (1999) Anthocyanic pigment determination in red fruit juices, concentrated juices and syrups using liquid chromatography. *Analytica Chimica Acta*, **382**, 39–50.
- Gong P, Kortus MG, Nix JC, Davis RE, Peersen OB (2013) Structures of coxsackievirus, rhinovirus, and poliovirus polymerase elongation complexes solved by engineering RNA mediated crystal contacts. *PLoS ONE*, **8**, e60272.
- Goodfellow I, Chaudhry Y, Richardson A, Meredith J, Almond JW, Barclay W, Evans DJ (2000) Identification of a cis-acting replication element within the poliovirus coding region. *Journal of virology*, **74**, 4590–4600.
- Goodfellow IG, Polacek C, Andino R, Evans DJ (2003) Physical load imposed on soccer players during small-sided training games. *Journal of General Virology*, **84**, 166–171.
- Gorbalenya AE, Krupovic M, Mushegian A, Kropinski AM, Varsani A, Kuhn JH (2017) Increasing the number of ranks available in virus taxonomy, <https://www.researchgate.net/publication/322101007> (Accessed on 20/12/2020).
- Gouvêa ACMS, Araujo MCP de, Schulz DF, Pacheco S, Godoy RL de O, Cabral LMC (2012) Anthocyanins standards (cyanidin-3-O-glucoside and cyanidin-3-O-

- rutinoside) isolation from freeze-dried açai (Euterpe oleraceae Mart.) by HPLC. *Food Science and Technology*, **32**, 43–46.
- Gower TL, Graham BS (2001) Antiviral activity of lovastatin against respiratory syncytial virus in vivo and in vitro. *Antimicrobial Agents and Chemotherapy*, **45**, 1231–1237.
- Grassmé H, Riehle A, Wilker B, Gulbins E (2005) Rhinoviruses infect human epithelial cells via ceramide-enriched membrane platforms. *The Journal of Biological Chemistry*, **280**, 26256–26262.
- Grove J, Marsh M (2011) The cell biology of receptor-mediated virus entry. *Journal of Cell Biology*, **195**, 1071–1082.
- Guan H, Tian J, Qin B *et al.* (2017) Crystal structure of 2C helicase from enterovirus 71. *Science Advances*, **3**, e1602573.
- Guedes AC, Amaro HM, Malcata FX (2011) Microalgae as sources of carotenoids. *Marine Drugs*, **9**, 625–644.
- Guiry MD (2012) How many species of algae are there? *Journal of Phycology*. **48**, 1057–1063.
- Guo H, Huang M, Yuan Q *et al.* (2017) The important role of lipid raft-mediated attachment in the infection of cultured cells by coronavirus infectious bronchitis virus beaudette strain. *PLoS ONE*, **12**, doi.10.1371/journal.pone.0170123.
- Haasbach E, Hartmayer C, Hettler A, Sarnecka A, Wulle U, Ehrhardt C, Ludwig S, Planz O (2014) Antiviral activity of Ladania067, an extract from wild black currant leaves against influenza A virus in vitro and in vivo. *Frontier in Microbiology*, **5**, doi.10.3389/fmicb.2014.00171.
- Han S, Hu L, Quach T, Simpson JS, Trevaskis NL, Porter CJH (2015) Profiling the Role of Deacylation-Reacylation in the Lymphatic Transport of a Triglyceride-Mimetic Prodrug. *Pharmaceutical Research*, **32**, 1830–1844.
- Han Z, Boshra H, Sunyer JO, Zwiers SH, Paragas J, Harty RN (2003) Biochemical and functional characterization of the Ebola virus VP24 protein: Implications for a role in virus assembly and budding. *Journal of Virology*, **77**, 1793-1800.

- Haque A, Hober D, Blondiaux J (2015) Addressing Therapeutic Options for Ebola Virus Infection in Current and Future Outbreaks. *Antimicrobial Agents and Chemotherapy*, **59**, 5892–5902.
- Hardy MJ, Kuczera G, Coombes PJ (2005) Integrated urban water cycle management: The urbancycle model. *Water Science and Technology*, **52**, <https://iwaponline.com/wst/article-pdf/52/9/1/434499/1>.
- Harris JR, Racaniello VR (2005) Amino acid changes in proteins 2B and 3A mediate rhinovirus type 39 growth in mouse cells amino acid changes in proteins 2B and 3A mediate rhinovirus type 39 growth in mouse cells. *Society*, **79**, 5363–5373.
- Hartigh LJ Den, Connolly-rohrbach JE, Fore S, Thomas R (2010) Fatty acids from VLDL lipolysis products induce lipid droplet accumulation in human monocytes. *Journal of Immunology*, **184**, 3927–3936.
- Harvala H, Kalimo H, Dahllund L, Santti J, Hughes P, Hyypiä T, Stanway G (2002) Mapping of tissue tropism determinants in coxsackievirus genomes. *Journal of General Virology*, **83**, 1697–1706.
- Harvala H, Robertson I, Chieochansin T, McWilliam Leitch EC, Templeton K, Simmonds P. 2009. Specific association of human parechovirus type 3 with sepsis and fever in young infants, as identified by direct typing of cerebrospinal fluid samples. *Journal of Infectious Diseases*. 199:1753–1760. doi:10.1086/599094.
- Headey SJ, Huang H, Claridge JK *et al.* (2007) NMR structure of stem-loop D from human rhinovirus-14. *Rna*, **13**, 351–360.
- Heaton NS, Perera R, Berger KL, Khadka S, LaCount DJ, Kuhn RJ, Randall G (2010b) Dengue virus nonstructural protein 3 redistributes fatty acid synthase to sites of viral replication and increases cellular fatty acid synthesis. *Proceedings of the National Academy of Sciences*, **107**, 17345–17350.
- Heaton NS, Perera R, Berger KL, Khadka S, LaCount DJ, Randall G, Kuhn RJ (2010a) Dengue virus nonstructural protein 3 redistributes fatty acid synthase to sites

- of viral replication and increases cellular fatty acid synthesis. *Proceedings of the National Academy of Sciences*, **107**, 17345–17350.
- Herold J, Andino R, Francisco S (2001) Poliovirus RNA replication requires genome circularization through a protein–protein bridge. *Molecular cell*, **7**, 581–591.
- Hershenson MB (2013) Rhinovirus-induced exacerbations of asthma and COPD. *Scientifica*, **2013**, 405876. doi.10.1155/2013/405876.
- Himeda T, Ohara Y (2012) Saffold virus, a novel human cardiovirus with unknown pathogenicity. *Journal of Virology*, **86**, 1292–1296.
- Hinson ER, Cresswell P (2009) The antiviral protein, viperin, localizes to lipid droplets via its N-terminal amphipathic-helix. *Proceedings of the National Academy of Sciences*, **106**, 20452–20457.
- Ho H, Cheng M, Weng S, Chang L, Yeh T, Shih S, Chiu DT (2008) Glucose-6-phosphate dehydrogenase deficiency enhances enterovirus 71 infection. *Journal of General Virology*, **89**, 2080–2089.
- Hodges BDM, Wu CC (2009) Proteomic insights into an expanded cellular role for cytoplasmic lipid droplets. *Journal of Lipid Research*, **51**, 262–273.
- Hodik M, Anagandula M, Fuxe J *et al.* (2016) Coxsackie-adenovirus receptor expression is enhanced in pancreas from patients with type 1 diabetes. *BMJ Open Diabetes Research and Care*, **4**, doi.10.1136/bmjdr-2016-000219.
- Horton JD, Goldstein JL, Brown MS (2002) SREBPs: activators of the complete pr/ of cholesterol and fatty acid synthesis in the liver. *The Journal of Clinical Investigation*, **109**, 1125–1131.
- Howard RS (2005) Clinical review poliomyelitis and the postpolio syndrome. *British Medical Journal*, **330**, doi.org/10.1136/bmj.330.7503.1314.
- Hsu N, Ilnytska O, Belov G *et al.* (2010) Viral reorganization of the secretory pathway generates distinct organelles for RNA replication. *Cell*, **141**, 799–811.
- Huang H, Shih S (2015) Neurotropic enterovirus infections in the central nervous system. *Viruses*, **7**, 6051–6066.

- Huang YC, Chu YH, Yen TY *et al.* (2013) Clinical features and phylogenetic analysis of Coxsackievirus A9 in Northern Taiwan in 2011. *BMC Infectious Diseases*, **13**, doi.10.1186/1471-2334-13-33.
- Hughes PJ, Horsnell C, Hyypiä T, Stanway G (1995) The coxsackievirus A9 RGD motif is not essential for virus viability. *Journal of virology*, **69**, 8035–8040.
- Hughes PJ, Stanway G (2000) The 2A proteins of three diverse picornaviruses are related to each other and to the H-rev107 family of proteins involved in the control of cell proliferation. *Journal of General Virology*, **81**, 201–207.
- Hung HC, Chen TC, Fang MY, Yen KJ, Shih SR, Hsu JTA, Tseng CP (2010) Inhibition of enterovirus 71 replication and the viral 3D polymerase by aurointricarboxylic acid. *Journal of Antimicrobial Chemotherapy*, **65**, 676–683.
- Huotari J, Helenius A (2011) Endosome maturation. *EMBO Journal*, **30**, 3481–3500.
- Hynynen R, Suchanek M, Spandl J, Bäck N, Thiele C, Olkkonen VM (2009) OSBP-related protein 2 is a sterol receptor on lipid droplets that regulates the metabolism of neutral lipids. *Journal of Lipid Research*, **50**, 1305–1315.
- Hyslop St. NG (1973) Transmission of the virus of foot and mouth disease between animals and man. *Bulletin of the World Health Organization*, **49**, 577–585.
- Hyypiä T, Hovi T, Knowles NJ, Stanway G (1997) Classification of enteroviruses based on molecular and biological properties. *Journal of General Virology*, **78**, doi.10.1099/0022-1317-78-1-1.
- Hyypiä T, Kallajoki M, Maaronen M, Stanway G, Kandolf R, Auvinen P, Kalimo H (1993) Pathogenetic differences between coxsackie A and B virus infections in newborn mice. *Virus Research*, **27**, 71–78.
- Ikuta K, Mizuta K, Suzutani T (2013) Anti-influenza virus activity of two extracts of the blackcurrant (*Ribes nigrum* L.) from New Zealand and Poland. *Fukushima journal of medical science*, **59**, 35–38.
- Ilnytska O, Santiana M, Hsu N *et al.* (2013) Enteroviruses harness the cellular endocytic machinery to remodel the host cell cholesterol landscape for effective viral replication. *Cell Host Microbe*, **14**, 281–293.

- Ingle H, Peterson S, Baldrige M (2018) Distinct effects of type I and III interferons on enteric viruses. *Viruses*, **10**, doi:10.3390/v10010046.
- Inglot AD (1969) Comparison of the antiviral activity in vitro of some non-steroidal anti-inflammatory drugs. *The Journal of general virology*, **4**, 203–214.
- International Committee on Taxonomy of Viruses (2019). *Archives of Virology*, **164**, 2417–2429.
- Ishikawa-Sasaki K, Nagashima S, Taniguchi K, Sasaki J (2018) Model of OSBP-mediated cholesterol supply to Aichi Virus RNA replication sites involving protein-protein interactions among viral proteins, ACBD3, OSBP, VAP-A/B, and SAC1. *Journal of Virology*, **92**, doi:10.1128/JVI.01952-17.
- Ishikawa-Sasaki K, Sasaki J, Taniguchi K (2014a) A complex comprising phosphatidylinositol 4-kinase III, ACBD3, and Aichi virus proteins enhances phosphatidylinositol 4-phosphate synthesis and is critical for formation of the viral replication complex. *Journal of Virology*, **88**, 6586–6598.
- Itta KC, Patil T, Kalal S, Ghargi KV, Roy S (2016) Salivirus in children with diarrhoea, western India. *International Journal of Infectious Diseases*, **52**, 14–15.
- Iwakawa H, Kaido M, Mise K, Okuno T (2007) cis-Acting core RNA elements required for negative-strand RNA synthesis and cap-independent translation are separated in the 3'-untranslated region of Red clover necrotic mosaic virus RNA1. *Virology*, **369**, 168–181.
- Jacobs SE, Lamson DM, George K St., Walsh TJ (2013) Human rhinoviruses. *Clinical Microbiology Reviews*, **26**, 135–162.
- Jacobson JR, Barnard JW, Grigoryev DN, Ma S-F, Tuder RM, Garcia JGN (2005) Simvastatin attenuates vascular leak and inflammation in murine inflammatory lung injury. *American Journal of Physiology-Lung Cellular and Molecular Physiology*, **288**, L1026–L1032.
- James AD, Rushton J (2002) The economics of foot and mouth disease. *Scientific and Technical Review of the Office International des Epizooties*, **21**, 637–644.

- Jecht M, Probst C, Gauss-Müller V (1998) Membrane permeability induced by hepatitis A virus proteins 2B and 2BC and proteolytic processing of HAV 2BC. *Virology*, **252**, 218–227.
- Jeppesen J, Kiens B (2012) Regulation and limitations to fatty acid oxidation during exercise. *Journal of Physiology*, **590**, 1059–1068.
- Jha NK, Latinovic O, Martin E *et al.* (2011) Imaging single retrovirus entry through alternative receptor isoforms and intermediates of virus-endosome fusion. *PLoS Pathogens*, **7**, e1001260.
- Jiang P, Liu Y, Ma H-C, Paul A V., Wimmer E (2014) Picornavirus morphogenesis. *Microbiology and Molecular Biology Reviews*, **78**, 418–437.
- Jin Y, McFie PJ, Banman SL, Brandt C, Stone SJ (2014) Diacylglycerol acyltransferase-2 (DGAT2) and monoacylglycerol acyltransferase-2 (MGAT2) interact to promote triacylglycerol synthesis. *Journal of Biological Chemistry*, **289**, 28237–28248.
- Kalynych S, Pálková L, Plevka P (2016) The structure of human Parechovirus 1 reveals an association of the RNA genome with the capsid. *Journal of Virology*, **90**, 1377–1386.
- Kam PCA, Chang GWM (1997) Selective serotonin reuptake inhibitors Pharmacology and clinical implications in anaesthesia and critical care medicine. *Anaesthesia*, **52**, 982–988.
- Kato K, Ishiwa A (2015) The role of carbohydrates in infection strategies of enteric pathogens. *Tropical Medicine and Health*, **43**, 41–52.
- Katritch V, Cherezov V, Stevens RC (2013) Structure-function of the G protein-coupled receptor superfamily. *Annual Review of Pharmacology and Toxicology*, **53**, 531–556.
- Kearney MT (2001) Viral myocarditis and dilated cardiomyopathy: mechanisms, manifestations, and management. *Postgraduate Medical Journal*, **77**, 4–10.
- Kempf BJ, Barton DJ (2016) Picornavirus RNA polyadenylation by 3Dpol, the viral RNA-dependent RNA polymerase. *Virus Research.*, **206**, doi.10.1016/j.virusres.2014.12.030.

- Kempf BJ, Kelly MM, Springer CL, Peersen OB, Barton DJ (2013) Structural features of a picornavirus polymerase involved in the polyadenylation of viral RNA. *Journal of Virology*, **87**, 5629–5644.
- Kennedy JL, Turner RB, Braciale T, Heymann W, Borish L (2012) Pathogenesis of rhinovirus infection Joshua. *Current Opinion in Virology*, **2**, 287–293.
- Kessler N, Ferraris O, Palmer K, Marsh W, Steel A (2004) Use of the DNA Flow-Thru Chip, a three-dimensional biochip, for typing and subtyping of influenza viruses. *Journal of Clinical Microbiology*, **42**, 2173–2185.
- Khamrin P, Maneekarn N (2014a) Detection and genetic characterization of cosavirus in a pediatric patient with diarrhea. *Archives of virology*, **159**, 2485–2489.
- Khamrin P, Maneekarn N, Okitsu S, Ushijima H (2014b) Epidemiology of human and animal kobuviruses. *Virus Disease*, **25**, 195–200.
- Khan MI, Shin JH, Kim JD (2018) The promising future of microalgae: Current status, challenges, and optimization of a sustainable and renewable industry for biofuels, feed, and other products. *Microbial Cell Factories*, **17**, doi.org/10.1186/s12934-018-0879-x Microbial.
- Khan S, Toyoda H, Linehan M *et al.* (2014) Poliomyelitis in transgenic mice expressing CD155 under the control of the Tage4 promoter after oral and parenteral poliovirus inoculation. *Journal of General Virology*, **95**, 1668–1676.
- Khandge NV, Pradhan S, Doshi Y, Kulkarni A, Dhruva I (2013) Photodynamic therapy (Part 1: Applications in dentistry). *International Journal of Laser Dentistry*, **3**, 7–13.
- Khelifa N, Brik M, Tessedre AC, De Rocquigny H, Roques BP, Courtieu J, Rimbault A (1999) Cleavage of L-leucine-containing dipeptides by *Clostridium butyricum*. *Bioorganic and Medicinal Chemistry Letters*, **9**, 109–112.
- Khetsuriani N, LaMonte-Fowlkes A, Oberste S, Pallansch MA (2006) Enterovirus Surveillance -United States, 1970–2005. Morbidity and Mortality Weekly Report. *Surveillance Summaries*, **55**, 10, doi.10.3390/v8010010.
- Khoo HE, Azlan A, Tang ST, Lim SM (2017) Anthocyanidins and anthocyanins: colored pigments as food, pharmaceutical ingredients, and the potential health

- benefits. *Food & Nutrition Research*, **61**, 1361779. doi.10.1080/16546628.2017.1361779.
- Kim D, Goo J Il, Kim M Il *et al.* (2018) Suppression of hepatitis c virus genome replication and particle production by a novel diacylglycerol acyltransferases inhibitor. *Molecules*, **23**, doi.10.3390/molecules23082083.
- Kim JH, Singh A, Del Poeta M, Brown DA, London E (2017) The effect of sterol structure upon clathrin-mediated and clathrin-independent endocytosis. *Journal of Cell Science*, **130**, 2682–2695.
- Kim MS, Racaniello VR (2007) Enterovirus 70 receptor utilization is controlled by capsid residues that also regulate host range and cytopathogenicity. *Journal of Virology*, **81**, 8648–8655.
- Kim Y, George D, Prior AM *et al.* (2012) Novel Triacsin C analogs as potential antivirals against rotavirus infections. *European Journal of Medicinal Chemistry*, **71**, 233–236.
- Kirkegaard K (2017) Unconventional secretion of hepatitis A virus. *Proceedings of the National Academy of Sciences*, **114**, 6653–6655.
- Kitajima M, Gerba C (2015) Aichi virus 1: Environmental occurrence and behaviour. *Pathogens*, **4**, 256–268.
- Klaiber N (2018) The role of rhinovirus in the pathogenesis and acute exacerbation of asthma. *Clinical Pulmonary Medicine*, **25**, 12–19.
- Klein KA, Jackson WT (2011) Picornavirus subversion of the autophagy pathway. *Viruses*, **3**, 1549–1561.
- Kloc A, Rai DK, Rieder E (2018) The roles of picornavirus untranslated regions in infection and innate immunity. *Frontiers in Microbiology*, **9**, doi.org/10.3389/fmicb.2018.00485.
- Knight-Jones TJD, Rushton J (2013) The economic impacts of foot and mouth disease - What are they, how big are they and where do they occur? *Preventive Veterinary Medicine*, **112**, 162–173.

- Kolehmainen P, Jaaskelainen A, Blomqvist S, Kallio-Kokko H, Nuolivirta K, Helminen M, Roivainen M, Lappalainen M, Tauriainen S (2014). Human parechovirus type 3 and 4 associated with severe infections in young children. *Pediatric Infectious Disease Journal*. **33**, 1109–1113.
- Kolehmainen, P, Siponen, A, Smura, T, Kallio-Kokko, H, Vapalahti, O, Jääskeläinen, A, & Tauriainen, S (2017). Intertypic recombination of human parechovirus 4 isolated from infants with sepsis-like disease. *Journal of Clinical Virology*, **88**, 1-7. doi.org/10.1016/j.jcv.2017.01.001
- Kotecha A, Wang Q, Dong X *et al.* (2017) Rules of engagement between $\alpha\beta 6$ integrin and foot-and-mouth disease virus. *Nature Communications*, **8**, doi.10.1038/ncomms15408.
- Kovinich N, Kayanja G, Chanoca A, Riedl K, Otegui MS, Grotewold E (2014) Not all anthocyanins are born equal: distinct patterns induced by stress in *Arabidopsis*. *Planta*, **240**, 931–940.
- Krishnasamy S, Abell TL (2018) Diabetic gastroparesis: Principles and current trends in management. *Diabetes Therapy*, **9**, doi.10.1007/s13300-018-0454-9.
- Krogerus C, Egger D, Samuilova O, Hyypiä T, Bienz K (2003) Replication complex of human parechovirus 1. *Journal of virology*, **77**, 8512–23.
- Krogerus C, Samuilova O, Pöyry T, Jokitalo E, Hyypiä T (2007) Intracellular localization and effects of individually expressed human parechovirus 1 non-structural proteins. *Journal of General Virology*, **88**, 831–841.
- Kuan MM (1997) Detection and rapid differentiation of human enteroviruses following genomic amplification. *Journal of Clinical Microbiology*, **35**, 2598–2601.
- Kumar S, Pandey AK (2013) Chemistry and biological activities of flavonoids: An overview. *The Scientific World Journal*, **73**, doi.org/10.1155/2013/162750.
- Kurokawa M, Shimizu T, Watanabe W, Shiraki K (2010) Development of new antiviral agents from natural products. *The Open Antimicrobial Agents Journal*, **2**, 49–57.

- Kusov YY, Gauss-Muller V (1997) In vitro RNA binding of the hepatitis A virus proteinase 3C (HAV) to secondary structure elements within the 5' terminus of the HAV genome. *RNA Society Journal*, **3**, 291–302.
- Kwo PY, Cohen SM, Lim JK (2017) ACG clinical guideline: Evaluation of abnormal liver chemistries. *American Journal of Gastroenterology*, **112**, 18–35.
- L'Huillier AG, Kaiser L, Petty TJ *et al.* (2015) Molecular epidemiology of human rhinoviruses and enteroviruses highlights their diversity in sub-saharan Africa. *Viruses*, **7**, 6412–6423.
- Lai JKF, Sam IC, Verlhac P, Baguet J, Eskelinen EL, Faure M, Chan YF (2017) 2BC non-structural protein of enterovirus A71 interacts with SNARE proteins to trigger autolysosome formation. *Viruses*, **9**, doi.10.3390/v9070169.
- Lama J, Paul A V., Harris KS, Wimmer E (1994) Properties of purified recombinant poliovirus protein 3AB as substrate for viral proteinases and as co-factor for RNA polymerase 3Dpol. *Journal of Biological Chemistry*, **269**, 66–70.
- Lancaster AM, Jan E, Sarnow P (2006) Initiation factor-independent translation mediated by the hepatitis C virus internal ribosome entry site. *Rna*, **12**, 894–902.
- Langford MP, Yin-Murphy M, Barber JC, Heard HK, Stanton GJ (1986) Conjunctivitis in rabbits caused by enterovirus type 70 (EV70). *Investigative Ophthalmology and Visual Science*, **27**, 915–920.
- Lau SKP, Woo PCY, Li KSM *et al.* (2016b) Identification of novel rosavirus species that infects diverse rodent species and causes multisystemic dissemination in mouse model. *PLoS Pathogens*, **12**, doi.10.1371/journal.ppat.1005911.
- Lau SKP, Yip CCY, Zhao PSH *et al.* (2016a) Enterovirus D68 Infections Associated with Severe Respiratory Illness in Elderly Patients and Emergence of a Novel Clade in Hong Kong. *Scientific Reports*, **6**, doi.10.1038/srep2514.
- Launes C, Armero G, Anton A *et al.* (2015) Molecular epidemiology of severe respiratory disease by human rhinoviruses and enteroviruses at a tertiary paediatric hospital in Barcelona, Spain. *Clinical Microbiology and Infection*, **21**, 799.e5-799.e7.

- Lee KY (2016) Enterovirus 71 infection and neurological complications. *Korean Journal of Pediatrics*, **59**, 395–401.
- Lee WM, Lemanske RF, Evans MD *et al.* (2012) Human rhinovirus species and season of infection determine illness severity. *American Journal of Respiratory and Critical Care Medicine*, **186**, 886–891.
- Lefkowitz EJ, Dempsey DM, Hendrickson RC, Orton RJ, Siddell SG, Smith DB (2018) Virus taxonomy: The database of the International Committee on Taxonomy of viruses (ICTV). *Nucleic Acids Research*, **46**, D708–D717.
- Lemon SM, Ott JJ, Van Damme P, Shouval D (2018) Type A viral hepatitis: A summary and update on the molecular virology, epidemiology, pathogenesis and prevention. *Journal of Hepatology*, **68**, 167–184.
- Leotte J, Trombetta H, Faggion HZ, Almeida BM, Nogueira MB, Vidal LR, Raboni SM (2017) Impact and seasonality of human rhinovirus infection in hospitalized patients for two consecutive years. *Jornal de Pediatria*, **93**, 294–300.
- Li JS, Dong XG, Qin M *et al.* (2015) Outbreak of febrile illness caused by coxsackievirus A4 in a nursery school in Beijing, China. *Virology Journal*, **12**, doi.10.1186/s12985-015-0325-1.
- Li JWH, Vederas JC (2009) Drug discovery and natural products: End of an era or an endless frontier? *Science*, **325**, 161–165.
- Li M, Hsu T, Chen T *et al.* (2002) The 3C protease activity of enterovirus 71 induces human neural cell apoptosis. *Virology*, **293**, 386–395.
- Li Z, Liu X, Wang S *et al.* (2016) Identification of a nucleotide in 5' untranslated region contributing to virus replication and virulence of coxsackievirus A16. *Scientific Reports*, **6**, doi.10.1038/srep20839.
- Li Zhihong, Fan Youpeng, Wei Junhong, Mei Xionge, He Qiang, Zhang Yonghua, Li Tian, Long Mengxian, Chen Jie, Bao Jialing, Pan Guoqing, Li Chunfeng, Zhou Zeyang (2018) Baculovirus utilizes cholesterol transporter Niemann – Pick C1 for host cell entry. *Frontier in Microbiology*, **10**, doi: org/10.1101/312744.
- Liang TJ (2009) Hepatitis B: The virus and disease T. *Hepatology*, **49**, S13–S21.

- Liang Z, Mao Q, Wang Y, Li C, Gao K, Wang J (2014) Regulatory science accelerates the development of biotechnology drugs and vaccines by NIFDC. *Emerging Microbes and Infections*, **3**, e67.
- Lin C, Chen KH, Tong Chen K (2018a) Update on enterovirus 71 infections: Epidemiology, molecular epidemiology, and vaccine development. *Journal of Infectious Diseases & Therapy*, **6**, doi.10.4172/2332-0877.1000370.
- Lin G-L, McGinley JP, Drysdale SB, Pollard AJ (2018b) Epidemiology and immune pathogenesis of viral sepsis. *Frontiers in Immunology*, **9**, doi.10.3389/fimmu.2018.02147.
- Lin JY, Chen TC, Weng KF, Chang SC, Chen LL, Shih SR (2009) Viral and host proteins involved in picornavirus life cycle. *Journal of Biomedical Science*, **16**, doi.10.1186/1423-0127-16-103.
- Lin JY, Li ML, Huang PN, Chien KY, Horng JT, Shih SR (2008) Heterogeneous nuclear ribonuclear protein K interacts with the enterovirus 71 5' untranslated region and participates in virus replication. *Journal of General Virology*, **89**, 2540–2549.
- Lin L-T, Hsu W-C, Lin C-C (2014) Antiviral natural products and herbal medicines. *Journal of Traditional and Complementary Medicine*, **4**, 24–35.
- Lindenbach BD (2013) Virion assembly and release. *Current Topics in Microbiology and Immunology*, **369**, 289–320.
- Linsuwanon P, Puenpa J, Huang S-W, Wang Y-F, Mauleekoonphairoj J, Wang J-R, Poovorawan Y (2014) Epidemiology and seroepidemiology of human enterovirus 71 among Thai populations. *Journal of Biomedical Science*, **21**, doi.10.1186/1423-0127-21-16.
- Liu J, Gorski JN, Gold SJ *et al.* (2013) Pharmacological inhibition of diacylglycerol acyltransferase 1 reduces body weight and modulates gut peptide release - Potential insight into mechanism of action. *Obesity*, **21**, 1406–1415.
- Liu P, Bartz R, Zehmer JK, Ying Y, Zhu M, Anderson RGW (2007) Rab-regulated interaction of early endosomes with lipid droplets. *Biochim Biophys Acta*, **1773**, 784–793.

- Liu P, Kallio H, Yang B (2014) Flavonol glycosides and other phenolic compounds in buds and leaves of different varieties of black currant (*Ribes nigrum* L.) and changes during growing season. *Food Chemistry*, **160**, 180–189.
- Liu S, Rodriguez A V., Tosteson MT (2006) Role of simvastatin and methyl- β -cyclodextrin on inhibition of poliovirus infection. *Biochemical and Biophysical Research Communications*, **347**, 51–59.
- Liu Y, Wimmer E, Paul A V. (2009) Cis-acting RNA elements in human and animal plus-strand RNA viruses. *Biochim Biophys Acta.*, **1789**, 495–517.
- Liu Y, Zhu Z, Zhang M, Zheng H (2015) Multifunctional roles of leader protein of foot-and-mouth disease viruses in suppressing host antiviral responses. *Veterinary Research*, **46**, doi.10.1186/s13567-015-0273-1.
- Lloyd RE (2015) Nuclear proteins hijacked by mammalian cytoplasmic plus strand RNA viruses. *Virology*, **479–480**, 457–474.
- Lodeiro MF, Filomatori C V., Gamarnik A V. (2009) Structural and functional studies of the promoter element for Dengue virus RNA replication. *Journal of Virology*, **83**, 993–1008.
- Lu L, Van Dung N, Ivens A *et al.* (2018) Genetic diversity and cross-species transmission of kobuviruses in Vietnam. *Virus Evolution*, **4**, doi.10.1093/ve/vey002.
- Lu Q Bin, Wo Y, Wang LY *et al.* (2014) Molecular epidemiology of human rhinovirus in children with acute respiratory diseases in Chongqing, China. *Scientific Reports*, **4**, doi.10.1038/srep06686.
- Lu UnT, Crespi CM, Liu NM *et al.* (2017) A Phase I dose escalation study demonstrates quercetin safety and explores potential for bioflavonoid antivirals in patients with chronic hepatitis C. *Phytotherapy Research*, **176**, 139–148.
- Ludi A, Ahmed Z, Pomeroy L *et al.* (2016) Serotype diversity of foot-and-mouth-disease virus in livestock without history of vaccination in the far North Region of Cameroon. *Transboundary and Emerging Diseases*, **63**, e27-38.
- Ludi AB, Horton DL, Mahapatra M *et al.* (2013) Antigenic variation of foot-and-mouth disease virus serotype A. *Journal of General Virology*, **95**, 384–392.

- Lunde BM, Moore C, Varani G (2017) RNA-binding proteins: modular design for efficient function. *Nature Reviews Molecular Cell Biology*, **8**, 479–490.
- Lyons T, Murray KE, Roberts AW, Barton DJ (2001) Poliovirus 5'-terminal cloverleaf RNA is required in cis for VPg uridylylation and the initiation of negative-strand RNA synthesis. *Journal of Virology*, **75**, 10696–10708.
- Maalik A, Khan FA, Mumtaz A *et al.* (2014) Pharmacological applications of quercetin and its derivatives: A short review. *Tropical Journal of Pharmaceutical Research*, **13**, 1561–1566.
- Mackenzie JM, Khromykh AA, Parton RG (2007) Cholesterol manipulation by West Nile Virus perturbs the cellular immune response. *Cell Host and Microbe*, **2**, 229–239.
- Maitreyi RS, Dar L, Muthukumar A *et al.* (1999) Acute hemorrhagic conjunctivitis due to enterovirus 70 in India. *Emerging Infectious Diseases*, **5**, 267–269.
- Malakouti M, Kataria A, Ali SK, Schenker S (2017) Elevated liver enzymes in asymptomatic patients – What should I do? *Journal of Clinical and Translational Hepatology*, **5**, 394–403.
- Mandary MB, Poh CL (2018) Changes in the EV-A71 genome through recombination and spontaneous mutations: Impact on virulence. *Viruses*, **10**, doi.10.3390/v10060320.
- Marken PA, Munro JS (2000) Selecting a Selective Serotonin Reuptake Inhibitor: Clinically Important Distinguishing Features. *Primary care companion to the Journal of clinical psychiatry*, **2**, 205–210.
- Marsh M, Helenius A (2006) Virus entry: Open sesame. *Cell*, **124**, 729–740.
- Martín-Acebes MA, Blázquez AB, Jiménez de Oya N, Escribano-Romero E, Saiz JC (2011) West Nile virus replication requires fatty acid synthesis but is independent on phosphatidylinositol-4-phosphate lipids. *PLoS ONE*, **6**, e24970.
- Martín-Acebes MA, Gabandé-Rodríguez E, García-Cabrero AM, Sánchez MP, Ledesma MD, Sobrino F, Saiz J-C (2016) Host sphingomyelin increases West Nile virus infection in vivo. *Journal of Lipid Research*, **57**, 422–432.

- Martín-Acebes MA, Vázquez-Calvo A, Caridi F, Saiz J-C, Sobrino F (2013) Lipid involvement in viral infections: Present and future perspectives for the design of antiviral strategies. In *Lipid Metabolism*, Valenzuela R (ed). InTech, pp 291–322.
- Martínez-A. C, Lucas P, Gómez-Moutón C *et al.* (2002) Blocking of HIV-1 infection by targeting CD4 to non raft membrane domains. *The Journal of Experimental Medicine*, **196**, 293–301.
- Martínez-Gutierrez M, Castellanos JE, Gallego-Gómez JC (2011) Statins reduce dengue virus production via decreased virion assembly. *Intervirology*, **54**, 202–216.
- Martinez-Salas E, Fernandez-Miragall O (2018) Picornavirus IRES: Structure function relationship. *Current Pharmaceutical Design*, **10**, 3757–3767.
- Martins AS, Martins IC, Santos NC (2018) Methods for lipid droplet biophysical characterization in flaviviridae infections. *Frontiers in Microbiology*, **9**, doi.10.3389/fmicb.2018.01951.
- Mason PW, Bezborodova S V., Henry TM (2002) A novel approach to test Data compression for BIST and its implementation. *Journal of Virology*, **76**, 9686–9694.
- Mavrouli MD, Spanakis N, Levidiotou S *et al.* (2007) Serologic prevalence of coxsackievirus group B in Greece. *Viral Immunology*, **20**, 11–18.
- Mazur I, Wurzer WJ, Ehrhardt C *et al.* (2007) Acetylsalicylic acid (ASA) blocks influenza virus propagation via its NF- κ B-inhibiting activity. *Cellular Microbiology*, **9**, 1683–1694.
- McCarty MF, Block KI (2006) Preadministration of high-dose salicylates, suppressors of NF- κ B activation, may increase the chemosensitivity of many cancers: An example of proapoptotic signal modulation therapy. *Integrative Cancer Therapies*, **5**, 252–268.
- Mccreight LJ, Bailey CJ, Pearson ER (2016) Metformin and the gastrointestinal tract. *Diabetologia*, **2016**, 426–435.
- Mckimm-Breschkin JL (2013) Influenza neuraminidase inhibitors: Antiviral action and mechanisms of resistance. *Influenza and other Respiratory Viruses*, **7**, 25–36.

- McLaughlin-Drubin ME, Munger K (2008) Viruses associated with human cancer. *Biochimica et Biophysica Acta (BBA) - Molecular Basis of Disease*, **1782**, 127–150.
- McMinn PC (2002) An overview of the evolution of enterovirus 71 and its clinical and public health significance. *FEMS Microbiology Reviews*, **26**, 91–107.
- Medigeshi GR, Kumar R, Dhamija E, Agrawal T (2016) N-Desmethylozapine, Fluoxetine, and Salmeterol Inhibit Postentry Stages of the Dengue Virus Life Cycle. *Antimicrobial Agents and Chemotherapy*, **60**, 6709–6718.
- Medina NH, Haro-Munoz E, Pellini AC, Machado BC, Russo DH, Timenetsky M do C, Carmona R de CC (2016) Acute hemorrhagic conjunctivitis epidemic in Sao Paulo State, Brazil, 2011. *Revista Panamericana de Salud Publica/Pan American Journal of Public Health*, **39**, 137–141.
- Mehndiratta MM, Mehndiratta P, Pande R (2014) Poliomyelitis: Historical facts, epidemiology, and current challenges in eradication. *The Neurohospitalist*, **4**, 223–229.
- Mehrbod P, Omar AR, Hair-Bejo M, Haghani A, Ideris A (2014) Mechanisms of action and efficacy of statins against influenza. *BioMed Research International*, **2014**, 11–14.
- Mehta A, Larson K, Ganapathineedi BS, Villegas E, Dande S, Ahmed W, Sebro N (2018) An out-of-season case of coxsackie B myocarditis with severe rhabdomyolysis. *Case Reports in Infectious Diseases*, **2018**, doi:org/10.1155/2018/4258296.
- Mekaj A, Mekaj Y, Daci F (2015) New insights into the mechanisms of action of aspirin and its use in the prevention and treatment of arterial and venous thromboembolism. *Therapeutics and Clinical Risk Management*, **11**, 1449–1456.
- Melnick JL (1996) Current status of poliovirus infections. *Clinical Microbiology Reviews*, **9**, 293–300.

- Merilahti P, Koskinen S, Heikkilä O, Karelehto E, Susi P (2012) Endocytosis of integrin-binding human picornaviruses. *Advances in Virology*, **2012**, doi.10.1155/2012/547530.
- Merilahti P, Tauriainen S, Susi P (2016) Human parechovirus 1 infection occurs via α V β 1 integrin. *PLoS ONE*, **10**, doi.10.1371/journal.pone.0154769.
- Michel YM, Borman AM, Paulous S, Kean KM (2001) Eukaryotic initiation factor 4G-poly(A) binding protein interaction is required for poly(A) tail-mediated stimulation of picornavirus internal ribosome entry segment-driven translation but not for X-mediated stimulation of hepatitis C virus translation. *Molecular and cellular biology*, **21**, 4097–109.
- Midgley CM, Jackson MA, Selvarangan R *et al.* (2014) Severe respiratory illness associated with enterovirus 68- Missouri and Illinois, 2014. *Morbidity and Mortality Weekly Report*, **63**, 798–799.
- Mirand A, Henquell C, Archimbaud C, Ughetto S, Antona D, Bailly JL, Peigue-Lafeuille H (2012) Outbreak of hand, foot and mouth disease/herpangina associated with coxsackievirus A6 and A10 infections in 2010, France: A large citywide, prospective observational study. *Clinical Microbiology and Infection*, **18**, E110–E118.
- Mirkovic RR, Kono R, Yin-Murphy M, Sohler R, Schmidt NJ, Melnick JL (1973) Enterovirus type 70: the etiologic agent of pandemic acute haemorrhagic conjunctivitis. *Bulletin of the World Health Organization*, **49**, 341–346.
- Mirmomeni MH, Hughes PJ, Stanway G (1997) An RNA tertiary structure in the 3'-untranslated region of enteroviruses is necessary for efficient replication. *Journal of virology*, **71**, 2363–2370.
- Moldavski O, Amen T, Levin-Zaidman S *et al.* (2015) Lipid droplets are essential for efficient clearance of cytosolic inclusion bodies. *Developmental Cell*, **33**, 603–610.
- Molenaar MR, Vaandrager AB, Helms JB (2017) Some lipid droplets are more equal than others: Different metabolic lipid droplet pools in hepatic stellate cells. *Lipid Insights*, **10**, doi.10.1177/1178635317747281 <https://doi.org/10.1>.

- Monge-fuentes V, Muehlmann LA, Azevedo RB De (2015) Perspectives on the application of nanotechnology in photodynamic therapy for the treatment of melanoma. *Nano Reviews*, **5**, doi.10.3402/nano.v5.24381.
- Monleau M, Montavon C, Laurent C *et al.* (2009) Evaluation of different RNA extraction methods and storage conditions of dried plasma or blood spots for human immunodeficiency virus type 1 RNA quantification and PCR amplification for drug resistance testing. *Journal of Clinical Microbiology*, **47**, 1107–1118.
- Moore RA, Derry S, Wiffen PJ, Straube S (2015) Effects of food on pharmacokinetics of immediate release oral formulations of aspirin, dipyrrone, paracetamol and NSAIDs - A systematic review. *British Journal of Clinical Pharmacology*, **80**, 381–388.
- Moreau B, Bastedo C, Michel RP, Ghali P (2011) Hepatitis and encephalitis due to Coxsackie virus A9 in an adult. *Case Reports in Gastroenterology*, **5**, 617–622.
- Moreira V, Peres S, Steyaert J, Bigan E, Paulevé L, Nogueira ML, Schwartz L (2015) Cell cycle progression is regulated by intertwined redox oscillators. *Theoretical Biology and Medical Modelling*, **12**, doi.10.1186/s12976-015-0005-2.
- Morikawa M, Ando Y, Kita A, Sugita M, Matsumura S, Terashima M (2015) Comprehensive Evaluation of the Antioxidant Activity of Miso by the Myoglobin Method. *Food Science and Technology Research*, **20**, 1221–1228.
- Moser TS, Schieffer D, Cherry S (2012) AMP-activated kinase restricts rift valley fever virus infection by inhibiting fatty acid synthesis. *PLoS Pathogens*, **8**, e1002661.
- Mosmann T (1983) Rapid colorimetric assay for cellular growth and survival: Application to proliferation and cytotoxicity assays. *Journal of Immunological Methods*, **65**, 55–63.
- Mothes W, Sherer NM, Jin J, Zhong P (2010) Minireview virus cell-to-cell transmission. *Journal of Virology*, **84**, 8360–8368.
- Mukherjee S, Majumdar S, Vipat VC, Mishra AC, Chakrabarti AK (2012) Non structural protein of avian influenza A (H1N1) virus is a weaker suppressor of immune

- responses but capable of inducing apoptosis in host cells. *Virology Journal*, **9**, doi.10.1186/1743-422X-9-149.
- Munger J, Bennett BD, Parikh A, Feng X, Rabitz H a, Shenk T, Rabinowitz JD (2008) Synthesis as a target for antiviral therapy. *Nature biotechnology*, **26**, 1179–1186.
- Murat P, Tellam J (2015) Effects of messenger RNA structure and other translational control mechanisms on major histocompatibility complex-I mediated antigen presentation. *Wiley Interdisciplinary Reviews: RNA*, **6**, 157–171.
- Murray KE, Barton DJ (2003) Poliovirus CRE-Dependent VPg Uridylylation is required for positive-strand RNA synthesis but not for negative-strand RNA synthesis. *Society*, **77**, 4739–4750.
- Murray KE, Steil BP, Roberts AW, Barton DJ (2004) Replication of poliovirus RNA with complete internal ribosome entry site deletions. *Journal of Virology*, **78**, 1393–1402.
- Mustopa AZ, Umami RN, Putri PH (2015) Identification of bioactive compound from microalga BTM 11 as Hepatitis C virus RNA helicase inhibitor. *Jurnal Biologi Indonesia*, **11**, 243–251.
- Nainan O V, Xia G, Vaughan G, Margolis HS (2014) Diagnosis of Hepatitis A virus infection: a Molecular approach. *Clinical Microbiology Reviews*, **19**, 63–79.
- Nakabayashi R, Kusano M, Kobayashi M et al (2009) Metabolomics-oriented isolation and structure elucidation of 37 compounds including two anthocyanins from *Arabidopsis thaliana*. *Phytochemistry*, **70**, 1017–1029.
- Narayanan A, Amaya M, Voss K *et al.* (2014) Reactive oxygen species activate NFκB (p65) and p53 and induce apoptosis in RVFV infected liver cells. *Virology*, **449**, 270–286.
- Nateri AS, Hughes PJ, Stanway G (2000) In vivo and in vitro identification of structural and sequence elements of the human parechovirus 5' untranslated region required for internal initiation. *Journal of Virology*, **74**, 6269–6277.

- Nathanson N, Kew OM (2010) From emergence to eradication: The epidemiology of poliomyelitis deconstructed. *American Journal of Epidemiology*, **172**, 1213–1229.
- Neitlich HW (1966) Increased plasma cholinesterase activity and succinyl- choline resistance: A genetic variant. *Journal of Clinical Investigation*, **45**, 380–387.
- Nelson TM, Vuillermin P, Hodge J, Druce J, Williams DT, Jasrotia R, Alexandersen S (2017) An outbreak of severe infections among Australian infants caused by a novel recombinant strain of human parechovirus type 3. **Scientific Reports**, **7**, 1–12.
- Newcombe NG, Andersson P, Johansson ES, Au GG, Lindberg AM, Barry RD, Shafren DR (2003) Cellular receptor interactions of C-cluster human group A coxsackieviruses. *Journal of General Virology*, **84**, 3041–3050.
- Nishimoto Y, Tamori Y (2017) CIDE family-mediated unique lipid droplet morphology in white adipose tissue and brown adipose tissue determines the adipocyte energy metabolism. *Journal of Atherosclerosis and Thrombosis*, **24**, 989–998.
- Nishino N, Tamori Y, Tateya S *et al.* (2008) FSP27 contributes to efficient energy storage in murine white adipocytes by promoting the formation of unilocular lipid droplets. *The Journal of Clinical Investigation*, **118**, 2808–2821.
- Nix WA, Maher K, Johansson ES, Niklasson B, Lindberg AM, Pallansch MA, Oberste MS (2008) Detection of all known parechoviruses by real-time PCR. *Journal of Clinical Microbiology*, **46**, 2519–2524.
- Nomoto A (2007) Molecular aspects of poliovirus pathogenesis. *Proceedings of the Japan Academy, Series B*, **83**, 266–275.
- Norder H, De Palma AM, Selisko B *et al.* (2011) Picornavirus non-structural proteins as targets for new anti-virals with broad activity. *Antiviral research*, **89**, 204–18.
- Oberste MS, Maher K, Schnurr D *et al.* (2004) Enterovirus 68 is associated with respiratory illness and shares biological features with both the enteroviruses and the rhinoviruses. *Journal of General Virology*, **85**, 2577–2584.

- Ochs K, Zeller A, Saleh L, Bassili G, Song Y, Sonntag A, Niepmann M (2003) Impaired binding of standard initiation factors mediates poliovirus translation attenuation. *Journal of Virology*, **77**, 115–122.
- Oermann CM, Schuster JE, Connors GP, Newland JG, Selvarangan R, Jackson MA (2015) Enterovirus D68: A focused review and clinical highlights from the 2014 U.S. outbreak. *Annals of the American Thoracic Society*, **12**, 775–781.
- Ogawa K, Hishiki T, Shimizu Y, Funami K, Sugiyama K, Miyanari Y, Shimotohno K (2009) Hepatitis C virus utilizes lipid droplet for production of infectious virus. *Proceedings of the Japan Academy. Series B, Physical and biological sciences*, **85**, 217–228.
- Ogram SA, Boone CD, McKenna R, Flanagan JB (2014) Amiloride inhibits the initiation of Coxsackievirus and poliovirus RNA replication by inhibiting VPg uridylylation. *Virology*, **464–465**, 87–97.
- Oh M, Park S, Choi Y *et al.* (2003) Acute hemorrhagic conjunctivitis caused by coxsackievirus A24 variant, South Korea, 2002. *Emerging Infectious Diseases*, **9**, 1010–1012.
- OIE (2009) Foot and mouth disease: Chapter 2.1.5. http://www.oie.int/eng/A_FMD2012/docs/2.01.05
- Okitsu S, Khamrin P, Hanaoka N *et al.* (2016) Cosavirus (family Picornaviridae) in pigs in Thailand and Japan. *Archives of Virology*, **161**, 159–163.
- Olijve L, Jennings L, Walls T (2018) Human Parechovirus: an increasingly recognized cause of sepsis-like illness in young infants. *Clinical Microbiology Reviews*, **31**, e00047-17.
- Olivera A, Rivera J (2005) Sphingolipids and the balancing of immune cell function: Lessons from the mast cell. *The Journal of Immunology*, **174**, 1153–1158.
- Olzmann JA, Kopito RR (2011) Lipid droplet formation is dispensable for endoplasmic reticulum-associated degradation. *Journal of Biological Chemistry*, **286**, 27872–27874.
- Onal G, Kutlu O, Gozuacik D, Dokmeci Emre S (2017) Lipid droplets in health and disease. *Lipids in Health and Disease*, **16**, doi.10.1186/s12944-017-0521-7.

- Orban T, Palczewska G, Palczewski K (2011) Retinyl ester storage particles (retinosomes) from the retinal pigmented epithelium resemble lipid droplets in other tissues. *Journal of Biological Chemistry*, **286**, 17248–17258.
- Ornoy A, Tenenbaum A (2006) Pregnancy outcome following infections by coxsackie, echo, measles, mumps, hepatitis, polio and encephalitis viruses. *Reproductive Toxicology*, **21**, 446–457.
- Otto GA, Puglisi JD (2004) 1: The pathway of HCV IRES-mediated translation initiation. *Cell*, **119**, 369–380.
- Ouimet M, Franklin V, Mak E, Liao X, Tabas I, Marcel YL (2011) Autophagy regulates cholesterol efflux from macrophage foam cells via lysosomal acid lipase. *Cell Metabolism*, **13**, 30–42.
- Ozeki S, Cheng J, Tauchi-Sato K, Hatano N, Taniguchi H, Fujimoto T (2005) Rab18 localizes to lipid droplets and induces their close apposition to the endoplasmic reticulum-derived membrane. *Journal of Cell Science*, **118**, 2601–2611.
- Pal M (2018) Foot and mouth disease: A highly infectious viral zoonosis of global importance. *Journal of Applied Microbiology and Biochemistry*, **2**, doi.10.21767/2576-1412.100028.
- Palmenberg AC, Gern JE (2015) Classification and Evolution of Human Rhinoviruses. *Methods Molecular Biology*, **1221**, doi.10.1007/978-1-4939-1571-2_1.
- Pan J, Narayanan B, Shah S, Yoder JD, Cifuentes JO, Hafenstein S, Bergelson JM (2011) Single amino acid changes in the virus capsid permit Coxsackievirus B3 to bind decay-accelerating factor. *Journal of Virology*, **85**, 7436–7443.
- Panche AN, Diwan AD, Chandra SR (2016) Flavonoids: An overview. *Journal of Nutritional Science*, **5**, e47.
- Pannunzio A, Coluccia M (2018) Cyclooxygenase-1 (COX-1) and COX-1 inhibitors in cancer: A review of oncology and medicinal chemistry literature. *Pharmaceuticals*, **11**, doi.10.3390/ph11040101.

- Papageorgiou AP, Heggermont W, Rienks M *et al.* (2015) Liver X receptor activation enhances CVB3 viral replication during myocarditis by stimulating lipogenesis. *Cardiovascular Research*, **107**, 78–88.
- Parsley TB, Towner JS, Blyn LB, Ehrenfeld E, Semler BL (1997) Poly (rC) binding protein 2 forms a ternary complex with the 5'-terminal sequences of poliovirus RNA and the viral 3CD proteinase. *Rna*, **3**, 1124–1134.
- Parvez MK, Tabish Rehman M, Alam P, Al-Dosari MS, Alqasoumi SI, Alajmi MF (2019) Plant-derived antiviral drugs as novel hepatitis B virus inhibitors: Cell culture and molecular docking study. *Saudi Pharmaceutical Journal*, **27**, 389–400.
- Pathak HB, Arnold JJ, Wiegand PN, Hargittai MRS, Craig E (2007) Picornavirus genome replication: Assembly and organization of the vpg uridylylation ribonucleoprotein (initiation) complex. *Journal of Biological Chemistry*, **282**, 16202–16213.
- Patočka J (2003) Biologically active pentacyclic triterpenes and their current medicine signification. *Journal of Applied Biomedicine*, **1**, 7–12.
- Paton DJ, Gubbins S, King DP (2018) Understanding the transmission of foot-and-mouth disease virus at different scales. *Current Opinion in Virology*, **28**, 85–91.
- Pau AK, George JM (2014) Antiretroviral therapy: Current drugs. *Infectious Disease Clinics of North America*, **28**, 371–402.
- Paul A V, Peters J, Mugavero J, Yin J, van Boom JH, Wimmer E (2003) Biochemical and genetic studies of the VPg uridylylation reaction catalyzed by the RNA polymerase of poliovirus. *Journal of Virology*, **77**, 891–904.
- Paul A V., Wimmer E (2016) Initiation of protein-primed picornavirus RNA synthesis. *Virus Research*, **15**, 477–491.
- Paul-Clark MJ, van Cao T, Moradi-Bidhendi N, Cooper D, Gilroy DW (2004) 15-epi-lipoxin A 4 –mediated induction of nitric oxide explains how aspirin inhibits acute inflammation. *The Journal of Experimental Medicine*, **200**, 69–78.
- Paulsen SJ, Rosenkilde MA, Eugen-Olsen J, Kledal TN (2005) Epstein-Barr virus-encoded BILF1 is a constitutively active G protein-coupled receptor. *Journal of Virology*, **79**, 536–546.

- Peersen OB (2017) Picornaviral polymerase structure, function, and fidelity modulation. *Virus Research*, **15**, doi.10.1016/j.virusres.2017.01.026.
- Peesa JP, Yalavarthi PR, Rasheed A, Mandava VBR (2016) A perspective review on role of novel NSAID prodrugs in the management of acute inflammation. *Journal of Acute Disease*, **5**, 364–381.
- Peng LF, Schaefer E a K, Maloof N *et al.* (2011) Ceestatin, a novel small molecule inhibitor of hepatitis C virus replication, inhibits 3-hydroxy-3-methylglutaryl-coenzyme A synthase. *The Journal of infectious diseases*, **204**, 609–616.
- Perera R, Daijogo S, Walter BL, Nguyen JHC, Semler BL (2007) Cellular protein modification by poliovirus: The two faces of poly(rC)-binding protein. *Journal of Virology*, **81**, 8919–8932.
- Perera R, Riley C, Isaac G *et al.* (2012) Dengue virus infection perturbs lipid homeostasis in infected mosquito cells. *PLoS Pathogens*, **8**, e1002584.
- Perez-caballero L, Torres-sanchez S, Bravo L, Mico JA, Berrocoso E (2014) Drug discovery case history fluoxetine: a case history of its discovery and preclinical development. *Informa healthcare*, **9**, doi.10.1517/17460441.2014.907790.
- Pfeiffer HC, Bragstad K, Skram MK *et al.* (2015) Two cases of acute severe flaccid myelitis associated with enterovirus D68 infection in children, Norway, autumn 2014. *Eurosurveillance*, **20**, doi.10.2807/1560-7917.es2015.20.10.21062.
- Pfister T, Jones KW, Wimmer E (2000) A cysteine-rich motif in poliovirus protein 2C ATPase is involved in RNA replication and binds zinc in vitro. *Journal of virology*, **74**, 334–343.
- Phillips J, Phillips I, Enya B, Zhao H, Nitta T (2018) Effect of betulinic acid and its ionic derivatives on M-MuLV replication Jasmine. *Biochem Biophys Research Community*, **500**, doi.10.1016/j.bbrc.2018.04.080.
- Pickering BM, Mitchell SA, Evans JR, Willis AE (2003) Polypyrimidine tract binding protein and poly r(C) binding protein 1 interact with the BAG-1 IRES and stimulates its activity in vitro and in vivo. *Nucleic Acids Research*, **31**, 639–646.

- Picornavirus home page (2019) Virus Taxonomy: 2019 Release.
<http://www.picornaviridae.com>
- Pilipenko E V., Pestova T V., Kolupaeva VG, Khitrina E V., Poperechnaya AN, Agol VI, Hellen CUT (2000) A cell cycle-dependent protein serves as a template-specific translation initiation factor. *Genes and Development*, **14**, 2028–2045.
- Piret J, Boivin G (2011) Resistance of Herpes Simplex viruses to nucleoside analogues: mechanisms, prevalence, and management. *Antimicrobial Agents And Chemotherapy*, **55**, 459–472.
- Plotch SJ, Palant O (1995) Poliovirus protein 3AB forms a complex with and stimulates the activity of the viral RNA polymerase, 3Dpol. *Journal of Virology*, **69**, 7169–7179.
- Pohjala L, Alakurtti S, Ahola T, Yli-Kauhaluoma J, Tammela P (2009) Betulin-derived compounds as inhibitors of alphavirus replication. *Journal of Natural Products*, **72**, 1917–1926.
- Pol A, Gross SP, Parton RG (2014) Biogenesis of the multifunctional lipid droplet: Lipids, proteins, and sites. *Journal of Cell Biology*, **204**, 635–646.
- Ponnuraj EM, John TJ, Levin MJ, Simoes EAF (1998) Cell-to-cell spread of poliovirus in the spinal cord of bonnet monkeys (*Macaca radiata*). *Journal of General Virology*, **79**, 2393–2403.
- Porter FW, Bochkov YA, Albee AJ, Wiese C, Palmenberg AC (2006) A picornavirus protein interacts with Ran-GTPase and disrupts nucleocytoplasmic transport. *Proceedings of the National Academy of Sciences*, **103**, 12417–12422.
- Porter FW, Palmenberg AC (2009) Leader-induced phosphorylation of nucleoporins correlates with nuclear trafficking inhibition by cardioviruses. *Journal of Virology*, **83**, 1941–1951.
- Poste G, Reeve P (1972) Inhibition of virus-induced cell fusion by local anaesthetics and phenothiazine tranquilizers. *The Journal of general virology*, **16**, 21–28.
- Potena L, Frascaroli G, Grigioni F *et al.* (2004) hydroxymethyl-glutaryl coenzyme a reductase inhibition limits cytomegalovirus infection in human endothelial cells. *Circulation*, **109**, 532–536.

- Power O, Jakeman P, Fitzgerald RJ (2013) Antioxidative peptides: Enzymatic production, in vitro and in vivo antioxidant activity and potential applications of milk-derived antioxidative peptides. *Amino Acids*, **44**, 797–820.
- Primache V, Binda S, De Benedittis G, Barbi M (1998) In vitro activity of acetylsalicylic acid on replication of varicella-zoster virus. *New Microbiologica*, **21**, 397–401.
- Puenpa J, Vongpunsawad S, Österback R *et al.* (2016) Molecular epidemiology and the evolution of human coxsackievirus A6. *Journal of General Virology*, **97**, 3225–3231.
- Racaniello VR (2006) One hundred years of poliovirus pathogenesis. *Virology*, **344**, 9–16.
- Racaniello VR, Baltimore D, Hi B (1981) Molecular cloning of poliovirus cDNA and determination of the complete nucleotide sequence of the viral genome. *Proceedings of the National Academy of Sciences of the United States of America*. **78**, 4887–4891.
- Raja A, Venturi M, Kwong P, Sodroski J (2003) CD4 binding site antibodies inhibit human immunodeficiency virus gp120 envelope glycoprotein interaction with CCR5. *Journal of Virology*, **77**, 713–718.
- Rappuoli R, Del Giudice G (2019) Inhibiting neuraminidase can make the difference. *The Journal of Experimental Medicine*, **216**, 251–252.
- Reddy VN, K RR, Chandana G, Sehrawat S (2009) Photodynamic therapy. *Indian Journal of Dental Advancements*, **1**, 46–50.
- Reid CR, Airo AM, Hobman TC (2015) The virus-host interplay: biogenesis of +RNA replication complexes. *Viruses*, **7**, 4385–4413.
- Reithmayer M, Reischl A, Snyers L, Blaas D (2002) Species-specific receptor recognition by a minor-group human rhinovirus (HRV): HRV serotype 1A distinguishes between the murine and the human low-density lipoprotein receptor. *Journal of virology*, **76**, 6957–6965.
- Ren R, Racaniello VR (1992) Human poliovirus receptor gene expression and poliovirus tissue tropism in transgenic mice. *Journal of virology*, **66**, 296–304.

- Rena G, Hardie DG, Pearson ER (2017) The mechanisms of action of metformin. *Diabetologia*, **60**, 1577–1585.
- Rendina AR, Cheng D (2005) Characterization of the inactivation of rat fatty acid synthase by C75: inhibition of partial reactions and protection by substrates. *Biochemical Journal*, **388**, 895–903.
- Reuter G, Boros Á, Pankovics P (2011) Kobuviruses - a comprehensive review. *Reviews in Medical Virology*, **21**, 32–41.
- Reuter G, Nemes C, Boros Á, Kapusinszky B, Delwart E, Pankovics P (2013) Porcine kobuvirus in wild boars (*Sus scrofa*). *Archives of Virology*, **158**, 233–245.
- Rezkalla S, Khatib G, Khatib R (1986) Coxsackievirus B3 murine myocarditis: deleterious effects of nonsteroidal anti-inflammatory agents. *Journal of Laboratory and Clinical Medicine*, **107**, 393–395.
- Rhoades RE, Tabor-Godwin JM, Tsueng G, Feuer R (2011) Enterovirus infections of the central nervous system. *Virology*, **411**, 288–305.
- Richards OC, Spagnolo JF, Lyle JM, Vleck SE, Kuchta RD, Kirkegaard K (2006) Intramolecular and intermolecular uridylylation by poliovirus RNA-dependent RNA polymerase. *Journal of Virology*, **80**, 7405–7415.
- Richardson CD, Vance DE (1978) The effect of colchicine and dibucaine on the morphogenesis of semliki forest virus. *Journal of Biological Chemistry*, **253**, 4584–4589.
- Rieder E, Xiang W, Paul A, Wimmer E (2003) Analysis of the cloverleaf element in a human rhinovirus type 14/poliovirus chimera: Correlation of subdomain D structure, ternary protein complex formation and virus replication. *Journal of General Virology*, **84**, 2203–2216.
- Robenek H, Hofnagel O, Buers I, Robenek MJ, Troyer D, Severs NJ (2006) Adipophilin-enriched domains in the ER membrane are sites of lipid droplet biogenesis. *Journal of Cell Science*, **119**, 4215–4224.
- Rocha-Pereira J, Nascimento MSJ, Ma Q, Hilgenfeld R, Neyts J, Jochmans D (2014) The enterovirus protease inhibitor rupintrivir exerts cross-genotypic anti-

- norovirus activity and clears cells from the norovirus replicon. *Antimicrobial Agents and Chemotherapy*, **58**, 4675–4681.
- Rohll JB, Percy N, Ley R, Evans DJ, Almond JW, Barclay WS (1994) The 5′-untranslated regions of picornavirus RNAs contain independent functional domains essential for RNA replication and translation. *Journal of Virology*, **68**, 4384–4391.
- Rojas N, Del Campo JA, Clement S *et al.* (2016) Effect of quercetin on Hepatitis C virus life cycle: From viral to host targets. *Scientific Reports*, **6**, doi.10.1038/srep31777.
- Romero-Gómez M, Diago M, Andrade RJ *et al.* (2009) Treatment of insulin resistance with metformin in naïve genotype 1 chronic hepatitis C patients receiving peginterferon alfa-2a plus ribavirin. *Hepatology*, **50**, 1702–1708.
- Romero-López C, Barroso-DelJesus A, García-Sacristán A, Briones C, Berzal-Herranz A (2012) The folding of the hepatitis C virus internal ribosome entry site depends on the 3′-end of the viral genome. *Nucleic Acids Research*, **40**, 11697–11713.
- Ross C, Knox C, Tastan Bishop Ö (2017) Interacting motif networks located in hotspots associated with RNA release are conserved in Enterovirus capsids. *FEBS Letters*, **591**, 1687–1701.
- Rossmann MG, He Y, Kuhn RJ (2002) Picornavirus – receptor interactions. *Cell Press*, **10**, 324–331.
- Rozovics JM, Chase AJ, Cathcart AL *et al.* (2012) Picornavirus modification of a host mRNA decay protein. *mBio*, **3**, doi.10.1128/mBio.00431-12.
- Rweyemamu M, Roeder P, MacKay D *et al.* (2008) Epidemiological patterns of foot-and-mouth disease worldwide. *Transboundary and Emerging Diseases*, **55**, 57–72.
- Samsa MM, Mondotte JA, Iglesias NG *et al.* (2009) Dengue virus capsid protein usurps lipid droplets for viral particle formation. *PLoS Pathogens*, **5**, e1000632. www.plospathogens.org.

- Sacre S, Medghalchi M, Gregory B, Brennan F, Williams R (2010) Fluoxetine and citalopram exhibit potent antiinflammatory activity in human and murine models of rheumatoid arthritis and inhibit toll-like receptors. *Arthritis and Rheumatism*, **62**, 683–693.
- Sadowy E, Miłner M, Haenni A-L (2001) Proteins attached to viral genomes are multifunctional. *Advances in Virus Research*, **57**, 185–262.
- Saeidnia S, Abdollahi M (2014) Role of micronutrients and natural antioxidants in fighting against HIV; a quick mini-review. *Research Journal of Pharmacognosy*, **1**, 49–55.
- Said ZN, Abdelwahab KS (2013) Antiviral replication agents. *Intech open*, **2**, 127–144.
- Saleem Dar M, Oak P, Chidley H, Deshpande A, Giri A, Gupta V (2016) Nutrient and flavor content of mango (*Mangifera indica* L.) cultivars: an appurtenance to the list of staple foods. *Nutritional Composition of Fruit Cultivars*, **2016**, 445–467.
- Sasaki J, Nagashima S, Taniguchi K (2003) Aichi Virus Leader protein is involved in viral RNA replication and encapsidation. *Journal of virology*, **77**, 10799–10807.
- Sasaki N, Nishizaki Y, Ozeki Y, Miyahara T (2014) The role of acyl-glucose in anthocyanin modifications. *Molecules*, **19**, 18747–18766.
- Sass-Kiss A, Kiss J, Milotay P, Kerek MM, Toth-Markus M (2005) Differences in anthocyanin and carotenoid content of fruits and vegetables. *Food Research International*, **38**, 1023–1029.
- Sasso S, Stibor H, Mittag M, Grossman AR (2018) From molecular manipulation of domesticated *Chlamydomonas reinhardtii* to survival in nature. *eLife*, **7**, e39233. doi.10.7554/eLife.39233.
- Sathasivam R, Ki JS (2018) A review of the biological activities of microalgal carotenoids and their potential use in healthcare and cosmetic industries. *Marine Drugs*, **16**, doi.10.3390/md16010026.
- Sattar S a, Jason T, Bidawid S, Farber J (2000) Foodborne spread of hepatitis A: Recent studies on virus survival, transfer and inactivation. *The Canadian journal of infectious diseases*, **11**, 159–63.

- Schachter M (2005) Chemical, pharmacokinetic and pharmacodynamic properties of statins: An update. *Fundamental and Clinical Pharmacology*, **19**, 117–125.
- Schlegel A, Giddings TH, Ladinsky MS, Kirkegaard K (1996) Cellular origin and ultrastructure of membranes induced during poliovirus infection. *Journal of virology*, **70**, 6576–88.
- Schmidt NJ, Lennette EH, Ho HH (1974) An apparently new enterovirus isolated from patients with disease of the central nervous system. *Journal of Infectious Diseases*, **129**, 304–309.
- Schneider-Schaulies J (2000) Cellular receptors for viruses: Links to tropism and pathogenesis. *Journal of General Virology*, **81**, 1413–1429.
- Schultheis L M, Donoghue M J (2004) Molecular phylogeny and biogeography of ribes (grossulariaceae), with an emphasis on gooseberries (subg. Grossularia). *Systematic Botany*, **29**, 77-96.
- Schuermans RM, Alphen P Van, Schuurmans JM, Matthijs HCP (2015) Comparison of the photosynthetic yield of cyanobacteria and green algae: Different Methods Give Different Answers. *PLoS ONE*, doi.10.1371/journal.pone.0139061.
- Sena L, Chandel N (2012) Physiological roles of mitochondrial reactive oxygen species. *Molecular cell*, **48**, 158–167.
- Shakeel S, Seitsonen JJT, Kajander T, Laurinmaki P, Hyypiä T, Susi P, Butcher SJ (2013) Structural and functional analysis of coxsackievirus A9 integrin v 6 binding and uncoating. *Journal of Virology*, **87**, 3943–3951.
- Sharma N, Ogram SA, Morasco BJ, Spear A, Chapman NM, Flanagan JB (2009) Functional role of the 5' terminal cloverleaf in Cocksackievirus RNA replication. *Virology*, **393**, 238–249.
- Sharma P, Jha AB, Dubey RS, Pessaraki M (2012) Reactive oxygen species, oxidative damage, and antioxidative defense mechanism in plants under stressful conditions. *Journal of Botany*, **2012**, doi.10.1155/2012/217037.
- Shi R, Lewis RS, Panthee DR (2018) Filter paper-based spin column method for cost-efficient DNA or RNA purification. *PLoS ONE*, **13**, e0203011.

- Shin JU, Oh SH, Lee JH (2010) A case of hand-foot-mouth disease in an immunocompetent adult. *Annals of Dermatology*, **22**, 216–218.
- Shin JY, Cho BK, Park HJ (2014) A clinical study of nail changes occurring secondary to hand-foot-mouth disease: Onychomadesis and beau's lines. *Annals of Dermatology*, **26**, 280–283.
- Shingler KL, Cifuentes JO, Ashley RE, Makhov AM, Conway JF, Hafenstein S (2015) The enterovirus 71 procapsid binds neutralizing antibodies and rescues virus infection in vitro. *Journal of virology*, **89**, 1900–1908.
- Shukla SD, Mahmood MQ, Weston S, Latham R, Muller HK, Sohal SS, Walters EH (2017) The main rhinovirus respiratory tract adhesion site (ICAM-1) is upregulated in smokers and patients with chronic airflow limitation (CAL). *Respiratory Research*, **18**, doi.10.1186/s12931-016-0483-8.
- Silva T, S. Salomon P, Hamerski L *et al.* (2018) Inhibitory effect of microalgae and cyanobacteria extracts on influenza virus replication and neuraminidase activity. *Peer Journal*, **6**, e5716.
- Silvestri LS, Parilla JM, Morasco BJ, Ogram SA, Flanagan JB (2006) Relationship between poliovirus negative-strand RNA synthesis and the length of the 3'-poly tail. *Virology*, **345**, 509-519.
- Simmonds P, Adams MJ, Benko M (2017) Virus taxonomy in the age of metagenomics. *Nature Reviews*, **15**, 161–168.
- Simons K, Ehehalt R (2002) Cholesterol, lipid rafts, and disease Find the latest version: Cholesterol, lipid rafts, and disease. *Biology and biochemistry of cholesterol*, **110**, 597–603.
- Sin J, Mangale V, Thienphrapa W, Gottlieb RA, Feuer R (2015) Recent progress in understanding coxsackievirus replication, dissemination, and pathogenesis. *Virology*, **484**, 288–304.
- Singh R, Cuervo AM (2012) Lipophagy: Connecting Autophagy and Lipid Metabolism. *International Journal of Cell Biology*, **2012**, doi.org/10.1155/2012/282041.
- Skinner JR, Shew TM, Schwartz DM, Tzekov A, Lepus CM, Abumrad NA, Wolins NE (2009) Diacylglycerol enrichment of endoplasmic reticulum or lipid droplets

- recruits perilipin 3/TIP47 during lipid storage and mobilization. *Journal of Biological Chemistry*, **284**, 30941–30948.
- Skrovankova S, Sumczynski D, Mlcek J, Jurikova T, Sochor J (2015) Bioactive compounds and antioxidant activity in different types of berries. *International Journal of Molecular Sciences*, **16**, 24673–24706.
- Smith AE, Helenius A (2004) How viruses enter animal cells. *Science*, **304**, 237–242.
- Smith DB, Bukh J, Kuiken C, A. Scott M, Rice CM, Stapleton JT, Simmonds P (2017) HCV Classification. Flaviviridae Study Group. https://talk.ictvonline.org/ictv_wikis/flaviviridae/w/sg_flavi/56/hcv-classification
- Smyth MS, Martin JH (2002) Picornavirus uncoating. *Journal of Clinical Pathology - Molecular Pathology*, **55**, 214–219.
- Sołtysik K, Ohsaki Y, Tatematsu T, Cheng J, Fujimoto T (2019) Nuclear lipid droplets derive from a lipoprotein precursor and regulate phosphatidylcholine synthesis. *Nature Communications*, **10**, doi.org/10.1038/s41467-019-08411.
- Somasundaram S, Sigthorsson G, Simpson RJ *et al.* (2000) Uncoupling of intestinal mitochondrial oxidative phosphorylation and inhibition of cyclooxygenase are required for the development of NSAID-enteropathy in the rat. *Alimentary Pharmacology and Therapeutics*, **14**, 639–650.
- Soto-Acosta R, Bautista-Carbajal P, Cervantes-Salazar M, Angel-Ambrocio AH, del Angel RM (2017) DENV up-regulates the HMG-CoA reductase activity through the impairment of AMPK phosphorylation: A potential antiviral target. *PLoS Pathogens*, **13**, doi.10.1371/journal.ppat.1006257.
- Spear A, Sharma N, Flanagan JB (2008) Protein-RNA tethering: The role of poly(C) binding protein 2 in poliovirus RNA replication. *Virology*, **374**, 280–291.
- Speir E, Yu Z, Ferrans VJ, Huang E, Epstein SE (1998) Aspirin Attenuates Cytomegalovirus Infectivity and Gene Artery Smooth Muscle Cells. *Circulation Research*, **83**, 210–217.

- Stanway G (2013) Molecular Biology and Classification of Enterovirus. In: Taylor K, Hyöty H, Toniolo A, Zuckerman A (eds) *Diabetes and Viruses*. Springer, New York, NY, pp. 109–115.
- Stanway G, Hyypiä T (1999) Parechoviruses. *Journal of virology*, **73**, 5249–5254.
- Stanway G, Kalkkinen N, Roivainen M *et al.* (1994) Molecular and biological characteristics of echovirus 22, a representative of a new picornavirus group. *Journal of Virology*, **68**, 8232–8238.
- Steil BP, Barton DJ (2009) Conversion of VPg into VPgpUpUOH before and during Poliovirus Negative-Strand RNA Synthesis. *Journal of Virology*, **83**, 12660–12670.
- Steil BP, Kempf BJ, Barton DJ (2010) Poly(A) at the 3′end of positive-strand RNA and VPg-linked poly(U) at the 5′end of negative-strand RNA are reciprocal templates during replication of poliovirus RNA. *Journal of Virology*, **84**, 2843–2858.
- Stewart A J, Bozonnet S, Mullen W, Jenkins G I, Michael E J, Crozier A (2000) Occurrence of flavonols in tomatoes and tomato-based products. *Journal of Agricultural and Food Chemistry*, **48**, 2663-2669.
- Stiver G (2003) The treatment of influenza with antiviral drugs. *Canadian Medical Association Journal*, **168**, 49–57.
- Strating JRPM, van der Linden L, Albuлесcu L *et al.* (2015) Itraconazole inhibits enterovirus replication by targeting the oxysterol-binding protein. *Cell Reports*, **10**, 600–615.
- Strauss DM, Glustrom LW, Wuttke DS (2003) Towards an understanding of the poliovirus replication complex: The solution structure of the soluble domain of the poliovirus 3A protein. *Journal of Molecular Biology*, **330**, 225–234.
- Su YS, Tsai AH, Ho YF, Huang SY, Liu YC, Hwang LH (2018) Stimulation of the internal ribosome entry site (IRES)-dependent translation of enterovirus 71 by DDX3X RNA helicase and viral 2A and 3C proteases. *Frontiers in Microbiology*, **9**, doi.10.3389/fmicb.2018.01324.

- Sun D, Chen S, Cheng A, Wang M (2016b) Roles of the picornaviral 3c proteinase in the viral life cycle and host cells. *Viruses*, **8**, doi.10.3390/v8030082.
- Sun H, Sun Q, Jiang W *et al.* (2016a) Prevalence of rhinovirus in wheezing children: A comparison with respiratory syncytial virus wheezing. *Brazilian Journal of Infectious Diseases*, **20**, 179–183.
- Sun X, Whittaker GR (2003) Role for Influenza Virus Envelope Cholesterol in Virus Entry and Infection. *Journal of Virology*, **77**, 12543–12551.
- Sun Y, Wang Y, Shan C *et al.* (2012) Enterovirus 71 VPg Uridylation Uses a Two-Molecular Mechanism of 3D Polymerase. *Journal of Virology*, **86**, 13662–13671.
- Sutmoller P, Barteling SS, Olascoaga RC, Sumption KJ (2003) Control and eradication of foot-and-mouth disease. *Virus Research*, **91**, 101–144.
- Suvisaari J, Mautemps N, Haukka J, Hovi T, Lönnqvist J (2003) Childhood central nervous system viral infections and adult schizophrenia. *American Journal of Psychiatry*, **160**, 1183–1185.
- Svitkin Y V, Imataka H, Khaleghpour K, Kahvejian A, Liebig HD, Sonenberg N (2001) Poly(A)-binding protein interaction with eIF4G stimulates picornavirus IRES-dependent translation. *RNA*, **12**, 1743–1752.
- Svitkin Y V., Costa-Mattioli M, Herdy B, Perreault S, Sonenberg N (2007) Stimulation of picornavirus replication by the poly(A) tail in a cell-free extract is largely independent of the poly(A) binding protein (PABP). *Rna*, **13**, 2330–2340.
- Sweeney TR, Abaeva IS, Pestova T V., Hellen CUT (2014) The mechanism of translation initiation on type 1 picornavirus IRESs. *EMBO Journal*, **33**, 76–92.
- Takeda N, Tanimura M, Miyamura K (1994) Molecular evolution of the major capsid protein VP1 of enterovirus 70. *Journal of Virology*, **68**, 854–862.
- Talsma M, Vegting M, Hess J (1984) Generalised Coxsackie A9 infection in a neonate presenting with pericarditis. *British Heart Journal*, **52**, 683–685.
- Tamm Ti, Truve E (2000) Sobemoviruses. *Journal of Virology*, **74**, 6231–6241.

- Tan CW, Lai JKF, Sam IC, Chan YF (2014) Recent developments in antiviral agents against enterovirus 71 infection. *Journal of Biomedical Science*, **21**, <http://www.jbiomedsci.com/content/21/1/14>.
- Tang JJ, Li JG, Qi W, Qiu WW, Li PS, Li BL, Song BL (2011) Inhibition of SREBP by a small molecule, betulin, improves hyperlipidemia and insulin resistance and reduces atherosclerotic plaques. *Cell Metabolism*, **13**, 44–56.
- Tang JW, Holmes CW (2017) Acute and chronic disease caused by enteroviruses. *Virulence*, **8**, 1062–1065.
- Tang WF, Yang SY, Wu BW *et al.* (2007) Reticulon 3 binds the 2C protein of enterovirus 71 and is required for viral replication. *Journal of Biological Chemistry*, **282**, 5888–5898.
- Tapparel C, Sobo K, Constant S, Huang S, Van Belle S, Kaiser L (2013) Growth and characterization of different human rhinovirus C types in three-dimensional human airway epithelia reconstituted in vitro. *Virology*, **446**, doi.10.1016/j.virol.2013.06.031. Epub 2013 Aug 7.
- Targett-Adams P, Boulant S, Douglas MW, McLauchlan J (2010) Lipid metabolism and HCV infection. *Viruses*, **2**, 1195–1217.
- Tarnopolsky MA, Rennie CD, Robertshaw HA, Fedak-Tarnopolsky SN, Devries MC, Hamadeh MJ (2006) Influence of endurance exercise training and sex on intramyocellular lipid and mitochondrial ultrastructure, substrate use, and mitochondrial enzyme activity. *American Journal of Physiology-Regulatory, Integrative and Comparative Physiology*, **292**, R1271–R1278.
- Tauchi-Sato K, Ozeki S, Houjou T, Taguchi R, Fujimoto T (2002) The surface of lipid droplets is a phospholipid monolayer with a unique fatty acid composition. *Journal of Biological Chemistry*, **277**, 44507–44512.
- Tauriainen S, Oikarinen S, Taimen K, Laranne J, Sipila M, Lonnrot M, Ilonen J, Simell O, Knip M, Hyoty H. (2008) Temporal relationship between human parechovirus 1 infection and otitis media in young children. *International Journal of Infectious Diseases*, **198**, 35–40.

- Taylor MP, Kirkegaard K (2007) Modification of cellular autophagy protein LC3 by poliovirus. *Journal of Virology*, **81**, 12543–12553.
- Tee KK, Lam TT-Y, Chan YF *et al.* (2010) Evolutionary genetics of human enterovirus 71: Origin, population dynamics, natural selection, and seasonal periodicity of the VP1 gene. *Journal of Virology*, **84**, 3339–3350.
- Terashima M, Fukukita A, Kodama R *et al.* (2013) Evaluation of antioxidant activity of leafy vegetables and beans with myoglobin method. *Plant Cell Reports*, **32**, 349–357.
- Terashima M, Kakuno Y, Kitano N *et al.* (2012) Antioxidant activity of flavonoids evaluated with myoglobin method. *Plant Cell Reports*, **31**, 291–298.
- Terashima M, Nakatani I, Harima A, Nakamura S, Shiiba M (2007) New method to evaluate water-soluble antioxidant activity based on protein structural change. *Journal of Agricultural and Food Chemistry*, **55**, 165–169.
- Terashima M, Watanabe R, Ueki M, Matsumura S (2010) Comprehensive evaluation of antioxidant activity for various substances with 5-axe cobweb chart. *Food Chemistry*, **120**, 150–155.
- Teterina NL, Gorbalenya AE, Egger D, Bienz K, Ehrenfeld E (1997) Poliovirus 2C protein determinants of membrane binding and rearrangements in mammalian cells. *Journal of Virology*, **71**, 8962–8972.
- Teterina NL, Levenson E, Rinaudo MS, Egger D, Bienz K, Gorbalenya AE, Ehrenfeld E (2006) Evidence for functional protein interactions required for poliovirus RNA replication. *Journal of Virology*, **80**, 5327–5337.
- Teterina NL, Levenson EA, Ehrenfeld E (2010) Viable polioviruses that encode 2A proteins with fluorescent protein tags. *Journal of Virology*, **84**, 1477–1488.
- Tevar AD, Clarke C, Wang J, Rudich SM, Woodle S, Lentsch AB, Edwards ML (2010) Clinical review of nonalcoholic steatohepatitis in liver surgery and transplantation. *Journal of the American College of Surgeons*, **210**, 1252–1260.
- Thiam AR, Farese RVF Jr, Walther TC (2013) The Biophysics and Cell Biology of Lipid Droplets. *Nature Reviews Molecular Cell Biology*, **14**, 775–786.

- Thierry E, Deprez E, Delelis O (2017) Different pathways leading to integrase inhibitors resistance. *Frontiers in Microbiology*, **7**, doi. 10.3389/fmicb.2016.02165 Edited.
- Thompson KM, Duintjer Tebbens RJ, Pallansch MA *et al.* (2008) The risks, costs, and benefits of possible future global policies for managing polioviruses. *American Journal of Public Health*, **98**, 1322–1330.
- Tiralongo E, Wee SS, Lea RA (2016) Elderberry supplementation reduces cold duration and symptoms in air-travellers: A randomized, double-blind placebo-controlled clinical trial. *Nutrients*, **8**, doi.10.3390/nu8040182.
- Tirinato L, Pagliari F, Limongi T *et al.* (2017) An overview of lipid droplets in cancer and cancer stem cells. *Stem Cells International*, **2017**, doi.org/10.1155/2017/1656053.
- Tuthill TJ, Gropelli E, Hogle JM, Rowlands DJ (2010) Picornaviruses. *Current Topics in Microbiology and Immunology*, **343**, 43–89.
- Tokarz R, Firth C, Madhi SA *et al.* (2012) Worldwide emergence of multiple clades of enterovirus 68. *Journal of General Virology*, **93**, 1952–1958.
- Torrens F, Castellano G (2006) Periodic classification of local anaesthetics (procaine analogues). *International Journal of Molecular Sciences*, **7**, 12–34.
- Toyoda H, Franco D, Fujita K, Paul A V, Wimmer E (2007) Replication of poliovirus requires binding of the poly (rC) binding protein to the cloverleaf as well as to the adjacent C-rich spacer sequence between the cloverleaf and the internal ribosomal entry site. *Journal of Virology*, **81**, 10017–10028.
- Triantafilou K, Fradelizi D, Wilson K, Triantafilou M (2002) GRP78, a coreceptor for coxsackievirus A9, interacts with major histocompatibility complex class I molecules which mediate virus internalization. *Journal of Virology*, **76**, 633–643.
- Triggiani BM, Oriente A, Seeds MC, Bass DA, Marone SG, Chilton FH, Carolina N (1995) Migration of human inflammatory cells into the lung results in the remodeling of arachidonic acid into a triglyceride pool. *Journal of Experimental Medicine*, **182**, 1181–1190.

- Truong DB, Goutard FL, Bertagnoli S, Delabouglise A, Grosbois V, Peyre M (2018) Benefit–cost analysis of foot-and-mouth disease vaccination at the farm-level in south vietnam. *Frontiers in Veterinary Science*, **5**, doi.10.3389/fvets.2018.00026.
- Tsatsral S, Xiang Z, Fuji N *et al.* (2015) Molecular epidemiology of the human rhinovirus infection in mongolia during 2008–2013. *Japanese Journal of Infectious Diseases*, **68**, 280–287.
- Tschapalda K, Zhang YQ, Liu L *et al.* (2016) A class of diacylglycerol acyltransferase 1 inhibitors identified by a combination of phenotypic high-throughput screening, genomics, and genetics. *EBio Medicine*, **8**, 49–59.
- Tu YK, Hong YY, Chen YC (2009) Finite element modeling of kirschner pin and bone thermal contact during drilling. *Life Science Journal*, **6**, 23–27.
- Turchetto-Zolet AC, Maraschin FS, de Morais GL, Cagliari A, Andrade CMB, Margis-Pinheiro M, Margis R (2011) Evolutionary view of acyl-CoA diacylglycerol acyltransferase (DGAT), a key enzyme in neutral lipid biosynthesis. *BMC Evolutionary Biology*, **11**, doi.10.1186/1471-2148-11-263.
- Turkmen N, Sari F, Velioglu S Y (2005) The effect of cooking methods on total phenolics and antioxidant activity of selected green vegetables. *Food Chemistry*. **93**, 713-718.
- Ulferts R, De Boer SM, Van Der Linden L *et al.* (2016) Screening of a library of FDA-approved drugs identifies several enterovirus replication inhibitors that target viral protein 2C. *Antimicrobial Agents and Chemotherapy*, **60**, 2627–2638.
- Ulferts R, Van Der Linden L, Thibaut HJ *et al.* (2013) Selective serotonin reuptake inhibitor fluoxetine inhibits replication of human enteroviruses B and D by targeting viral protein 2C. *Antimicrobial Agents and Chemotherapy*, **57**, 1952–1956.
- Vagiri M, Ekholm A, Andersson SC, Johansson E, Rumpunen K (2012) An optimized method for analysis of phenolic compounds in buds, leaves, and fruits of black currant (*ribes nigrum* l.). *Journal of Agricultural and Food Chemistry*, **60**, 10501–10510.

- Vagner S, Galy B, Pyronnet S (2001) Irresistible IRES. Attracting the translation machinery to internal ribosome entry sites. *EMBO Reports*, **2**, 893–898.
- Valle L, Hernández R, Ávila J (2013) Oxidative stress associated to disease progression and toxicity during antiretroviral therapy in human immunodeficiency virus infection. *Journal of Virology & Microbiology*, **2013**, 1–15.
- Vallochi AL, Teixeira L, Oliveira K da S, Maya-Monteiro CM, Bozza PT (2018) Lipid droplet, a key player in host-parasite interactions. *Frontiers in Immunology*, **9**. 1022. doi.10.3389/fimmu.2018.01022.
- van der Linden L, Wolthers KC, van Kuppeveld FJM (2015) Replication and inhibitors of enteroviruses and parechoviruses. *Viruses*, **7**, 4529–4562.
- van der Schaar HM, Dorobantu CM, Albulescu L, Strating JRPM, van Kuppeveld FJM (2016) Fat(al) attraction: Picornaviruses usurp lipid transfer at membrane contact sites to create replication organelles. *Trends in Microbiology*, **24**, 535–546.
- Van Der Schaar HM, Van Der Linden L, Lanke KHW *et al.* (2012) Coxsackievirus mutants that can bypass host factor PI4KIII β and the need for high levels of PI4P lipids for replication. *Cell Research*, **22**, 1576–1592.
- Van Der Want JPH, Dijkstra J (2006) A history of plant virology. *Archives of Virology*, **151**, 1467–1498.
- Van Kuppeveld FJM, Hoenderop JGJ, Smeets RLL, Willems PHGM, Dijkman HBPM, Galama JMD, Melchers WJG (1997a) Coxsackievirus protein 2B modifies endoplasmic reticulum membrane and plasma membrane permeability and facilitates virus release. *EMBO Journal*, **16**, 3519–3532.
- Van Kuppeveld FJM, Melchers WJG, Kirkegaard K, Doedens JR (1997b) Structure-function analysis of coxsackie B3 virus protein 2B. *Virology*, **227**, 111–118.
- van Ooij MJM, Polacek C, Glaudemans DHRF *et al.* (2006a) Polyadenylation of genomic RNA and initiation of antigenomic RNA in a positive-strand RNA virus are controlled by the same cis-element. *Nucleic Acids Research*, **34**, 2953–2965.

- van Ooij MJM, Vogt DA, Paul A *et al.* (2006b) Structural and functional characterization of the coxsackievirus B3 CRE(2C): Role of CRE(2C) in negative- and positive-strand RNA synthesis. *Journal of General Virology*, **87**, 103–113.
- Van Regenmortel MH V, Mahy BWJ (2004) emerging issues in virus taxonomy. *Emerging Infectious Diseases*, **10**, 8–13.
- Vanni S (2017) Intracellular lipid droplets: From structure to function. *Lipid Insights*, **10**, 14–16.
- Varma NRS, Janic B, Ali MM, Iskander ASM, Arbab AS (2011) Simvastatin potentiates the anti-hepatitis B virus activity of FDA- approved nucleoside analogue inhibitors in vitro. *Journal of Stem Cells and Regenerative Medicine*, **7**, 41–53.
- Vasilyeva LN, Stephenson SL (2008) The Linnaean Hierarchy and ‘Extensional Thinking.’ *The Open Evolution Journal*, **2**, 55–65.
- Venkata KC, Wudayagiri R, Valluru L (2013) Free Radicals and Antioxidants Newcastle disease virus (NDV) modulates pro/antioxidant status in different brain regions of chicken. *Free Radicals and Antioxidants*, **3**, 81–86.
- Verma AK, Kumar A, Mahima, Sahzad (2012) Epidemiology and diagnosis of foot-and-mouth disease: A review. *Indian Journal of Animal Sciences*, **82**, 543–551.
- Vidricaire G, Tremblay MJ (2007) A Clathrin, caveolae, and dynamin-independent endocytic pathway requiring free membrane cholesterol drives HIV-1 internalization and infection in polarized trophoblastic cells. *Journal of Molecular Biology*, **368**, 1267–1283.
- Viktorova EG, Nchoutmboube JA, Ford-Siltz LA, Iverson E, Belov GA (2018) Phospholipid synthesis fueled by lipid droplets drives the structural development of poliovirus replication organelles, *PLoS Pathogens*, **14**, doi.org/10.1371/journal.ppat.1007280 August p.
- Villanueva CJ, Monetti M, Shih M, Zhou P, Watkins SM, Bhanot S, Farese R V. (2009) Specific role for acyl CoA: diacylglycerol acyltransferase 1 (Dgat1) in hepatic steatosis due to exogenous fatty acids. *Hepatology*, **50**, 434–442.

- Vistica DT, Monks A, Pittman A, Boyd MR (1991) Tetrazolium-based assays for cellular viability: a critical examination of selected parameters affecting formazan production. *Cancer Research*, **51**, 2515–2520.
- Vlahos CJ, William F, Kwan Y, Raymond F (1994) A Specific inhibitor of phosphatidylinositol 3-kinase, 2-(4-morpholinyl)-8-phenyl-4h-1-benzopyran-4-one (LY294002). *The Journal of Biological Chemistry*, **269**, 5241–5248.
- Vleck SE, Oliver SL, Brady JJ, Blau HM, Rajamani J, Sommer MH (2011) Structure – function analysis of varicella-zoster virus glycoprotein H identifies domain-specific roles for fusion and skin tropism. *Proceedings of the National Academy of Sciences of the United State of America*, **108**, 2–7.
- Voumvourakis KI, Kitsos DK, Tsiodras S, Petrikkos G, Stamboulis E (2010) Human herpesvirus 6 infection as a trigger of multiple sclerosis. *Mayo Clinic proceedings. Mayo Clinic*, **85**, 1023–1030.
- Wade M, Li Y-C, Wahl G (2013) Poliovirus cell entry: Common structural themes in viral cell entry pathways. *Nature Reviews Cancer*, **13**, 83–96.
- Wadia NH, Wadia PN, Katrak SM, Misra VP (1983) A study of the neurological disorder associated with acute haemorrhagic conjunctivitis due to enterovirus 70. *Journal of Neurology, Neurosurgery and Psychiatry*, **46**, 599–610.
- Wainwright M (1998) Photodynamic antimicrobial chemotherapy (PACT). *Journal of Antimicrobial Chemotherapy*, **42**, 13–28.
- Wakabayashi H, Oda H, Yamauchi K, Abe F (2014) Lactoferrin for prevention of common viral infections. *Journal of Infection and Chemotherapy*, **20**, 666–671.
- Walker PJ, Siddell SG, Lefkowitz EJ *et al.* (2019) Changes to virus taxonomy and the International Code of Virus Classification and Nomenclature ratified by the International Committee on Taxonomy of Viruses (2019). *Archives of Virology*, **164**, 2417–2429.
- Walsh D, Mathews MB, Mohr I (2013) Tinkering with translation: protein synthesis in virus-infected cells. *Cold Spring Harbor Perspectives in Biology*, **5**, a012351. doi.10.1101/cshperspect.a012351.

- Walter BL, Parsley TB, Ehrenfeld E, Semler BL (2002) Distinct poly (rC) binding protein KH domain determinants for poliovirus translation initiation and viral RNA replication. *Journal of Virology*, **76**, 12008–12022.
- Walther TC, Farese RVF Jr (2009) The life of lipid droplets. *Biochimica et Biophysica Acta*, **1791**, 459–466.
- Walther TC, Farese RVF Jr (2012) Lipid droplets and cellular lipid metabolism. *Annual Review of Biochemistry*, **81**, 687–714.
- Ward NC, Watts GF, Eckel RH (2019) Statin toxicity mechanistic insights and clinical implications. *Circulation Research*, **124**, 328–350.
- Watters K, Palmenberg AC (2011) Differential processing of nuclear pore complex proteins by rhinovirus 2A proteases from different species and serotypes. *Journal of Virology*, **85**, 10874–10883.
- Wawrzyńska M, Kałas W, Biały D, Ziolo E, Arkowski J, Mazurek W, Strzdała L (2010) In vitro photodynamic therapy with chlorin e6 leads to apoptosis of human vascular smooth muscle cells. *Archivum Immunologiae et Therapiae Experimentalis*, **58**, 67–75.
- Wayne LG (1967) Selection of characters for an Adansonian analysis of mycobacterial taxonomy. *Journal of Bacteriology*, **93**, 1382–1391.
- Weber FS, Heilmann A, Hahn G, Rüdiger M, Dinger J (2016) A preterm neonate with coxsackievirus infection, supraventricular arrhythmia and cerebral sinus venous thrombosis. *Clinical Medical Reviews and Case Reports*, **3**, doi.10.23937/2378-3656/1410115.
- Wei W, Sodroski J, Tager A *et al.* (2019) Blocking HIV-1 infection by chromosomal integrative expression of human CD4 on the surface of *Lactobacillus helveticus* R0052. *Journal of Virology*, **93**. doi.10.1128/JVI.01830-18.
- Weinstein J (1980) Synovial fluid leukocytosis associated with intracellular lipid inclusions. *Archives of Internal Medicine*, **140**, 560–561.

- Weiss EI, Hourri-Haddad Y, Greenbaum E, Hochman N, Ofek I, Zakay-Rones Z (2005) Cranberry juice constituents affect influenza virus adhesion and infectivity. *Antiviral Research*, **66**, 9–12.
- Weitz-Schmidt G, Welzenbach K, Brinkmann V *et al.* (2001) Statins selectively inhibit leukocyte function antigen-1 by binding to a novel regulatory integrin site. *Nature Medicine*, **7**, 687–692.
- Welch SL (2000) Local anesthetic toxicosis. *Veterinary Medicine*, **95**, 6–9.
- Wells AI, Coyne CB (2019) Enteroviruses: A gut-wrenching game of entry, detection, and evasion. *Viruses*, **11**, doi.10.3390/v11050460.
- Weng K, Li M, Hung C, Shih S (2009) Enterovirus 71 3C protease cleaves a novel target CstF-64 and inhibits cellular polyadenylation. *PLoS Pathogens*, **5**, e1000593.
- Werner E, Heilier JF, Ducruix C, Ezan E, Junot C, Tabet JC (2008) Mass spectrometry for the identification of the discriminating signals from metabolomics: Current status and future trends. *Journal of Chromatography B*, **871**, 143–163.
- Westerhuis B, Kolehmainen P, Benschop K, Nurminen N, Koen G, Koskiniemi M, Simell O, Knip M, Hyoty H, Wolthers K, Tauriainen S (2013) Human parechovirus seroprevalence in Finland and The Netherlands. *Journal of Clinical Virology*, **58**, 211–215.
- White EJJ, Wilson GM (2018) AUF1 regulation of coding and noncoding RNA Elizabeth. *Wiley Interdisciplinary Reviews: RNA*, **8**, doi.10.1002/wrna.1393.
- White SH, Brisson CD, Andrew RD (2012) Examining protection from anoxic depolarization by the drugs dibucaine and carbetapentane using whole cell recording from CA1 neurons. *Journal of Neurophysiology*, **107**, 2083–2095.
- WHO (2012) WHO position paper on hepatitis a vaccines – June 2012. *Weekly epidemiological record*. **87**, 261–276. https://www.who.int/wer/2012/wer8728_29.p.
- WHO (2015) WHO Model list of essential medicines. <http://www.who.int/medicines/publications/essentia>.

- Wideman TH, Zautra AJ, Edwards RR (2009) Lipodystrophies: Disorders of adipose tissue biology Abhimanyu. *Biochim Biophys Acta.*, **1791**, 507–513.
- Wiehe A, O'Brien JM, Senge MO (2019) Trends and targets in antiviral phototherapy. *Photochemical & Photobiological Sciences*, **10**, doi.10.1039/c9pp00211a.
- Wildenbeest JG (2014) Human enteroviruses and parechoviruses: disease spectrum and need for treatment in young children. Digital Academic Repository. 202-221, www.intechopen.com/books/meningitis/human-parecho p.
- Wildenbeest JG, Van Den Broek PJ, Benschop KSM *et al.* (2012) Pleconaril revisited: Clinical course of chronic enteroviral meningoencephalitis after treatment correlates with in vitro susceptibility. *Antiviral Therapy*, **17**, 459–466.
- Wildenbeest JG, van der Schee MP, Hashimoto S *et al.* (2016) Prevalence of rhinoviruses in young children of an unselected birth cohort from the Netherlands. *Clinical Microbiology and Infection*, **22**, 736.e9-736.e15.
- Wilén CB, Tilton JC, Doms RW *et al.* (2012) HIV: Cell Binding and Entry. *Cold Spring Harbor Perspectives in Medicine*, **2**, 1–14.
- Willcocks MM, Zaini S, Chamond N *et al.* (2017) Distinct roles for the III_{d2} sub-domain in pestivirus and picornavirus internal ribosome entry sites. *Nucleic Acids Research*, **45**, 13016–13028.
- Winther B, Arruda E, Witek TJ, Marlin SD, Tsianco MM, Innes DJ, Hayden FG (2002) Expression of ICAM-1 in nasal epithelium and levels of soluble ICAM-1 in nasal lavage fluid during human experimental rhinovirus infection. *Archives of otolaryngology--head & neck surgery*, **128**, 131–136.
- Wlodkovic D, Skommer J, Darzynkiewicz Z (2009) Flow cytometry-based apoptosis detection. *Methods in Molecular Biology*, **559**, doi:10.1007/978-1-60327-017-5_2.
- Wong RSY (2019) Role of nonsteroidal anti-inflammatory drugs (NSAIDs) in cancer prevention and cancer promotion. *Advances in Pharmacological Sciences*, **9**, doi. org/10.1155/2019/3418975.
- Woo PCY, Lau SKP, Huang Y *et al.* (2010) Comparative analysis of six genome sequences of three novel picornaviruses, turdiviruses 1, 2 and 3, in dead wild birds, and

- proposal of two novel genera, Orthoturdivirus and Paraturdivirus, in the family Picornaviridae. *Journal of General Virology*, **91**, 2433–2448.
- Wright PW, Strauss GH, Langford MP (1992) Acute hemorrhagic conjunctivitis. *American Family Physician*, **45**, 173–178.
- Wu W, Li R, Li X, He J, Jiang S, Liu S, Yang J (2016) Quercetin as an antiviral agent inhibits influenza A virus (IAV) entry. *Viruses*, **8**, doi.10.3390/v8010006.
- Wu Y, Lou Z, Miao Y *et al.* (2010) Structures of EV71 RNA-dependent RNA polymerase in complex with substrate and analogue provide a drug target against the hand-foot-and-mouth disease pandemic in China. *Protein and Cell*, **1**, 491–500.
- Wurie HR, Buckett L, Zammit VA (2012) Diacylglycerol acyltransferase 2 acts upstream of diacylglycerol acyltransferase 1 and utilizes nascent diglycerides and de novo synthesized fatty acids in HepG2 cells. *FEBS Journal*, **279**, 3033–3047.
- Xia H, Wang P, Wang GC *et al.* (2015) Human enterovirus nonstructural protein 2CATPase functions as both an RNA helicase and ATP-independent RNA chaperone. *PLoS Pathogens*, **11**, 1–29.
- Xiang W, Cuconati A, Hope D, Kirkegaard K, Wimmer E (1998a) Complete protein linkage map of poliovirus P3 proteins: interaction of polymerase 3Dpol with VPg and with genetic variants of 3AB. *Journal of virology*, **72**, 6732–41.
- Xiang W, Harris KS, Alexander L, Wimmer E (1995) Interaction between the 5' -Terminal Cloverleaf and 3AB / 3CD pro of Poliovirus Is Essential for RNA Replication. *Journal of Virology*, **69**, 3658–3667.
- Xiang Z, Gonzalez R, Wang Z *et al.* (2012) Coxsackievirus A21, Acute Respiratory Tract Infection, China. *Emerging Infectious Diseases*, **18**, 821–824.
- Xing L, Huhtala M, Pietiäinen V *et al.* (2004) Structural and Functional Analysis of Integrin α 2I Domain Interaction with Echovirus 1. *Journal of Biological Chemistry*, **279**, 11632–11638.
- Xu L, Zhang X, Cheng W, Wang Y, Yi K, Wang Z, Zhang Y (2019) Hypericin photodynamic therapy inhibits the growth of adult T cell leukemia cells through induction of apoptosis and suppression of viral transcription. *Retrovirology*, **16**, doi.org/10.1186/s12977-019-0467-0 *Retrovirology*.

- Xun YH, Zhang YJ, Pan QC *et al.* (2014) Metformin inhibits hepatitis B virus protein production and replication in human hepatoma cells. *Journal of Viral Hepatitis*, **21**, 597–603.
- Y, Wang C, Mueller S, Paul AV, Wimmer E, Jiang P (2010) Direct interaction between two viral proteins, the nonstructural protein 2C and the capsid protein VP3, is required for enterovirus morphogenesis. *PLoS Pathogenesis*, **6**, e1001066.
- Yacoubian S (2017) Changes in cardiac index during labour analgesia: A double-blind randomised controlled trial of epidural versus combined spinal epidural analgesia - A preliminary study Stephanie. *Indian Journal of Anaesthesia*, **61**, 295–301.
- Yamamoto K, Takahara K, Oyadomari S, Okada T, Sato T, Harada A, Mori K (2010) Induction of Liver Steatosis and Lipid Droplet Formation in ATF6 α -Knockout Mice Burdened with Pharmacological Endoplasmic Reticulum Stress. *Molecular Biology of the Cell*, **21**, 1546–1555.
- Yamauchi Y, Helenius A (2013) Virus entry at a glance. *Journal of Cell Science*, **126**, 1289–1295.
- Yamayoshi S, Fujii K, Koike S (2014) Receptors for enterovirus 71. *Emerging Microbes and Infections*, **3**, e53;doi.10.1038/emi.
- Yang W, Hood BL, Chadwick SL *et al.* (2008) Fatty acid synthase is up-regulated during hepatitis C virus infection and regulates hepatitis C virus entry and production. *Hepatology*, **48**, 1396–1403.
- Yang X, Hu Z, Fan S *et al.* (2018) Picornavirus 2A protease regulates stress granule formation to facilitate viral translation. *PLoS Pathogens*, **14**, e1006901.
- Yang Y, Rijnbrand R, Mcknight KL, Paul A, Martin A, Lemon SM, Wimmer E (2002) Sequence Requirements for Viral RNA Replication and VPg Uridylylation Directed by the Internal cis -Acting Replication Element (cre) of Human Rhinovirus Type 14 Sequence Requirements for Viral RNA Replication and VPg Uridylylation Directed by the Intern. *Society*, **76**, 7485–7494.
- Yen C-LE, Stone SJ, Koliwad S, Harris C, Farese R V. (2008) DGAT enzymes and triacylglycerol biosynthesis. *Journal of Lipid Research*, **49**, 2283–2301.

- Yogeeswari P, Sriram D (2005) Betulinic Acid and Its Derivatives: A Review on their Biological Properties. *Current Medicinal Chemistry*, **12**, 657–666.
- Yogo Y, Wimmer E (1972) Polyadenylic acid at the 3'-terminus of poliovirus RNA. *Proceedings of the National Academy of Sciences of the United States of America*, **69**, 1877–82.
- Young KC, Bai CH, Su HC et al (2014) Fluoxetine a novel anti-hepatitis C virus agent via ROS-, JNK-, and PPAR β/γ -dependent pathways. *Antiviral Research*, **110**, 158–167.
- Yu J, Ao Y, Liu N, Li L, Duan Z (2015) Salivirus in Children and Its Association with Childhood Acute Gastroenteritis: A Paired Case-Control Study. *PLoS ONE*, **10**, doi.10.1371/journal.pone.0130977.
- Zandi K, Teoh B, Sam S, Wong P, Mustafa MR (2012) Antiviral Activity of Bioflavonoid against Dengue Virus Type-2. *BMC Complementary and Alternative Medicine*, **12**, <http://www.biomedcentral.com/1472-6882/12/214>.
- Zanghellini J, Wodlei F, von Grünberg HH (2010) Phospholipid demixing and the birth of a lipid droplet. *Journal of Theoretical Biology*, **264**, 952–961.
- Zavagno G, Jaffe B, Esteban M (1987) Role of prostaglandins and non-steroid anti-inflammatory drugs in the pathogenicity of vaccinia virus. *Journal of General Virology*, **68**, 593–600.
- Zell R, Delwart E, Gorbalenya AE et al (2018) ICTV Virus Taxonomy Profile: Picornaviridae. *General Virology*, **98**, 2421–2422.
- Zell R, Delwart E, Gorbalenya AE, Hovi T, King AMQ, Knowles, NJ, Lindberg, AM, Pallansch, MA, Palmenberg, AC, Reuter, G, Simmonds, P, Skern, T, Stanway, G, Yamashita, T and ICTV Report Consortium (2017). ICTV Virus Taxonomy Profile: Picornaviridae. *Journal of General Virology*, **98**. Doi. 10.1099/jgv.0.000911.
- Zeng H, Lu J, Zheng H et al. (2015) The epidemiological study of Coxsackievirus A6 revealing hand, foot and mouth disease epidemic patterns in Guangdong, China. *Scientific Reports*, **5**, 1–8.

- Zhang D, Lou X, Yan H *et al.* (2018) Metagenomic analysis of viral nucleic acid extraction methods in respiratory clinical samples. *BMC Genomics*, **19**, 1–8.
- Zhang J, Diaz A, Mao L, Ahlquist P, Wang X (2012) Host Acyl Coenzyme A Binding Protein Regulates Replication Complex Assembly and Activity of a Positive-Strand RNA Virus. *Journal of Virology*, **86**, 5110–5121.
- Zhang J, Lan Y, Sanyal S (2017) Modulation of lipid droplet metabolism-A potential target for therapeutic intervention in Flaviviridae Infections. *Frontiers in Microbiology*, **8**, doi: 10.3389/fmicb.2017.02286.
- Zhang X, Lu Q, Wo Y *et al.* (2015) Prevalence and genetic characteristics of Saffold cardiovirus in China from 2009 to 2012. *Scientific Reports*, **5**, doi. 10.1038/srep07704.
- Zhao G, Souers AJ, Voorbach M *et al.* (2008) Validation of diacyl glycerolacyltransferase I as a novel target for the treatment of obesity and dyslipidemia using a potent and selective small molecule inhibitor. *Journal of Medicinal Chemistry*, **51**, 380–383.
- Zheng N, Dai J, Cao H *et al.* (2013) Current understanding on antihepatocarcinoma effects of xiao Chai Hu Tang and its constituents. *Evidence-based Complementary and Alternative Medicine*, **2013**, doi.org/10.1155/2013/529458.
- Zhou G, Goodyear LJ, Moller DE *et al.* (2001) Role of AMP-activated protein kinase in mechanism of metformin action Find the latest version: Role of AMP-activated protein kinase in mechanism of metformin action. *The Journal of Clinical Investigation*, **108**, 1167–1174.
- Zhou G, Goodyear LJ, Moller DE *et al.* (2001) Role of AMP-activated protein kinase in mechanism of metformin action find the latest version: Role of AMP-activated protein kinase in mechanism of metformin action. *The Journal of Clinical Investigation*, **108**, 1167–1174.
- Zlotnick A (2005) Theoretical aspects of virus capsid assembly. *Journal of Molecular Recognition*, **18**, 479–490.

Zoll J, Hulshof SE, Lanke K, Lunel FV, Melchers WJG (2009) Saffold virus, a human Theiler's-like cardiovirus, is ubiquitous and causes infection early in life. *PLoS Pathogens*, **5**, e1000416.

Zuo J, Quinn KK, Kye S, Cooper P, Damoiseaux R, Krogstad P (2012) Fluoxetine is a potent inhibitor of coxsackievirus replication. *Antimicrobial Agents and Chemotherapy*, **56**, 4838–4844.

Appendices

Appendix 1 Materials used in this work and the sources

A. Materials for cell culture

- Accutase solution (Sigma-Aldrich).
- Trypsin-EDTA (0.25 %) (Gibco, by Life Technologies).
- Dimethyl sulfoxide minimum (DMSO) ≥ 99.5 % (Sigma-Aldrich).
- Dulbecco's Modified Eagle's Medium high glucose (DMEM) (Sigma-Aldrich).
- McCoy's 5A Medium (Life Technologies).
- Fetal bovine serum (FBS) (Sigma-Aldrich).
- MEM non-essential amino acid 100x Solution (Sigma-Aldrich).
- Penicillin-streptomycin with 10,000 units penicillin and 10 mg streptomycin per ml (Sigma-Aldrich).
- HEPES 4-(2-hydroxyethyl)-1-piperazineethanesulfonic acid (Sigma-Aldrich).

B. Materials for virology

- Carboxymethylcellulose sodium (CMC) (Sigma-Aldrich).
- Crystal violet, pure, indicator (ACROS Organics).
- Triton X-100 (Sigma-Aldrich).
- Formaldehyde, 37 % by weight (Fisher Chemical).
- Ethanol, absolute (Fisher BioReagents).

C. Drugs

- Fluoxetine HCl (LKT laboratories, Inc.).
- Imipramine (Sigma-Aldrich).
- Promethazine (Sigma-Aldrich).
- Quercetin ≥ 95 % (HPLC) (Sigma-Aldrich).
- C75 (Cayman Chemical).

- Simvastatin ≥ 97 % (HPLC) (Sigma-Aldrich).
- Betulinic acid ≥ 98 % (HPLC) (Sigma-Aldrich).
- A922500 (Sigma-Aldrich).
- Metformin (Sigma-Aldrich).
- Acetylsalicylic acid (Sigma-Aldrich).

D. **Biological materials**

- Redcurrants (RCs, *Ribes rubrum*) were grown in Wivenhoe, Essex, UK and harvested when ripe; 2 kg of red currant fruit was obtained and used after storing at -20 °C.
- Microalgae (MA): Samples of microalgae (MA) extracts (labelled MA9, MA11, MA15, MA17, M19, MA-S1, MA-S2, MA-S3, MA-S4, CO2, Ceb, CO6 and NO8) were provided by the School of Chemical Engineering (United Arab Emirates University) after extraction by the method previously described (Al-Zuhair *et al.*, 2006).

E. **Materials for molecular biology**

- Agarose (Electrophoresis Grade) (Fisher BioReagents).
- Isopropanol (Fisher BioReagents).
- QIAamp Viral RNA Mini Kit (Qiagen).
- QIAquick gel extraction kit (Qiagen).
- SafeView nucleic acid stain (NBS biologicals).
- Tris base (Fisher BioReagents).
- Water, nuclease-free (Thermo Scientific).

Primers (Sigma-Aldrich);

- CAV92C5d (AGCCCTCATCGGTTGCACCTCGT).
- CAV92Cmf (TGCTCCTACATGGGAGTCCAGGT).
- CAV92C3r (GAGTAGATCAGCGATGACAGGTGGT).

- CAV92Cmr (TCCATCAGGGTTCTGGCATAGGTC).

F. **Materials for extraction and fractionation of RC and for chemical modification**

- 1-Hydroxybenzotriazole hydrate (HOBT) ≥ 97 % (Aldrich Chemistry).
- 2-Hydroxyquinoline-4-carboxylic acid 97 % (Sigma-Aldrich).
- 2-Bromoethylamine hydrobromide 99 % (Alfa Aesar).
- 1-Butyl-3-methylimidazolium bromide > 97.0 % (Fluka).
- N,N'-Dicyclohexylcarbodiimide (DCC) ≥ 99 % (Fluka).
- 1-Butyl-3-methylimidazolium bromide > 97 % (Sigma-Aldrich).
- N,N-Dimethylformamide (DMF) anhydrous, 99.8 % . (Sigma-Aldrich).
- Dichloromethane (DCM) ≥ 99.8 % (VWR Chemicals).
- N,N-Diisopropylethylamine (DIPEA) ≥ 99 % (Sigma-Aldrich).
- Phthalimide, potassium derivative 99 % (Acros Organics).
- Hydrazine acetate 97 % (Sigma-Aldrich).
- Tetrahydrofuran ≥ 99.9 % (Sigma-Aldrich).
- Chlorambucil (Sigma-Aldrich).
- 4-Bromo-1-butene, 97 % (Aldrich Chemistry).
- Di-*tert*-butyl dicarbonate 99 % (Acros Organics).
- Acetonitrile (Fisher Chemical).
- Fluoxetine HCl (LKT laboratories, Inc).
- *tert*-Butyl (2-bromoethyl) carbamate ≥ 98 % (Sigma-Aldrich).
- H₂CO₃ (Sigma-Aldrich).
- Trifluoroacetic acid ≥ 99 % (Sigma-Aldrich).

- Ethyl acetate ≥ 99.5 % (VWR Chemicals).
- Mono (1-butyl-3-methyl-1h-imidazol-1-3-dium) monobromide (PubChem).
- Acetone ≥ 99 % (VWR Chemicals).
- Ethanol, absolute (Fisher Chemical).
- Methanol (Fisher Chemical).
- Toluene (Fisher Chemicals).

G. Solutions and buffers

- Phosphate buffered saline buffer:

Seven tablets of PBS were added to 700 ml of deionized water to prepare 1X PBS buffer. The solution then was autoclaved.

- HEPES buffer:

To prepare a HEPES solution of 250 mM, 12 g of HEPES was dissolved in 100 ml of de-ionized distilled water and then adjusted to pH 7.4 with 10 M NaOH, and then autoclaved.

- Carboxy methyl cellulose 2 % (CMC):

CMC (2 g) was dissolved in 100 ml of distilled water and then autoclaved.

- Crystal violet solution 0.5 % (CV):

Crystal violet (0.5 g) was added to 495 ml of distilled water and 5 ml of ethanol.

- Fixing solution:

For a fixing solution of 4 % formaldehyde, 5 ml of 37% formaldehyde was added to 50 ml of 1X PBS buffer.

- Permeabilization solution:

Triton X-100 (125 μ l) was added to 50 ml of 1X PBS buffer and 65 μ l of Tween 20 to give a final concentration of Triton of 0.25%.

- DNA electrophoresis buffer (Tris-EDTA or ELFO)

First, 50X Tris-EDTA stock was prepared by adding 242 g of Tris and 100 ml of 0.5 M EDTA (pH 8.0) to 600 ml of deionized water. The pH was adjusted to 7.7 with glacial acetic acid then the solution was made up to 1 l. Then, the dilution of 1X Tris-EDTA was used to make agarose gels and running buffer.

- Clear loading dye for agarose gels

Glycerol (50 ml) was added to 200 μ l of 0.5 M EDTA (pH 8.0) and 49.8 ml deionized water.

- Gene Ruler 1kb ladder (ThermoFisher Scientific)

This was used as a size-marker for DNA electrophoresis and was prepared for use by mixing the marker (5 μ l) with deionized water (20 μ l) and the provided 6x loading buffer (5 μ l). Usually, 5 μ l of the mixture was loaded per well.

H. Cell lines

- African Green Monkey Kidney epithelial (GMK) cell line, originally provided by Dr Merja Roivainen.
- The Lung Carcinoma cell line (A549), provided by Dr Muslim Idan Mohsin.
- The Human Colon Adenocarcinoma (HT29) cell line, provided by Dr Andrea Mohr.

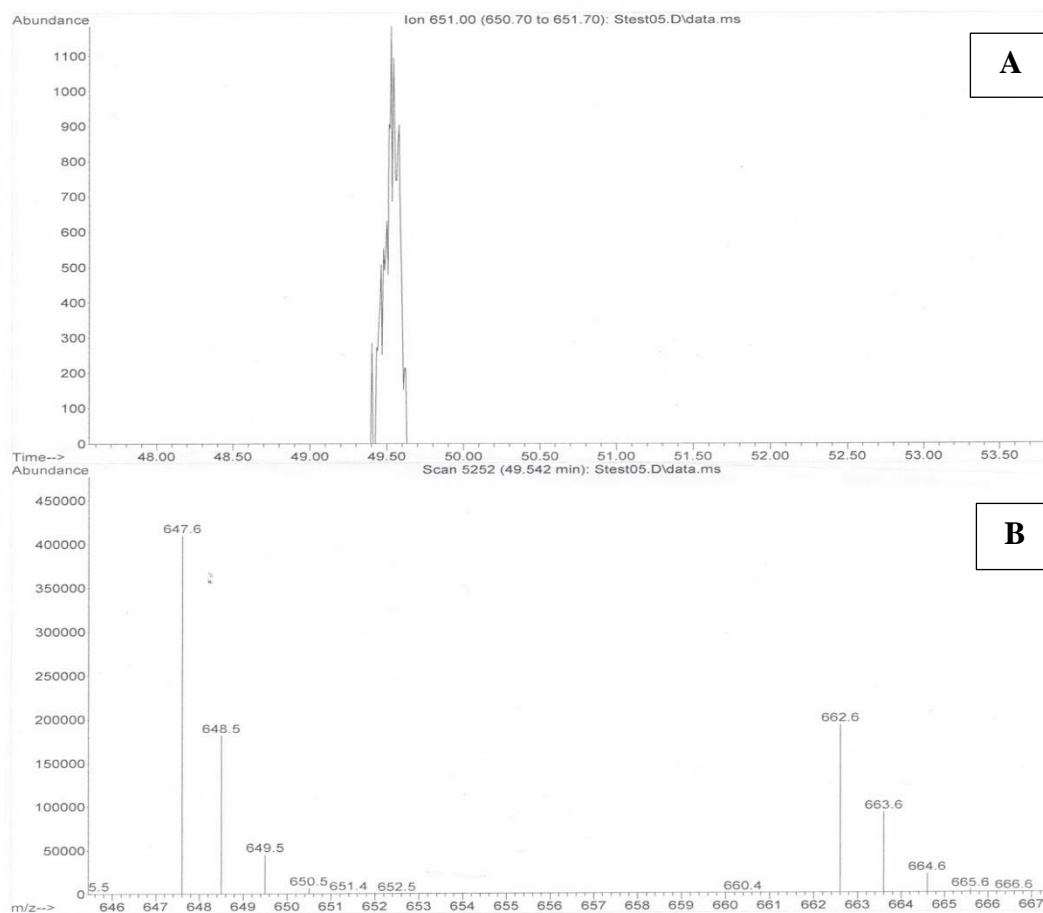
I. Viruses

- Coxsackievirus A9 (CAV-9), Griggs strain, was recovered from the cDNA clone pCAV9 (Hughes *et al.*, 1995).
- Human parechovirus (HPeV1), Harris strain, was recovered from the cDNA clone pHPeV1 (Nateri *et al.*, 2000).
- Coxsackie B viruses (CBV): Three CBV3 isolates, P55 (2), P6LK12 and P4 (75) were provided by Professor Heikki Hyöty.

Fresh stocks of these viruses were produced by adding 10 μ l of the original virus stock to cell monolayers (GMK for CAV9 and CBV3; HT29 for HPeV1) in 25 cm² flasks and incubating in a 5% CO₂ incubator at 37 °C until all cells were detached. Flasks were freeze-thawed three times and the liquid was centrifuged (12,000 rpm in a microcentrifuge, 2 min) and the supernatant was divided into aliquots and stored at -80 °C.

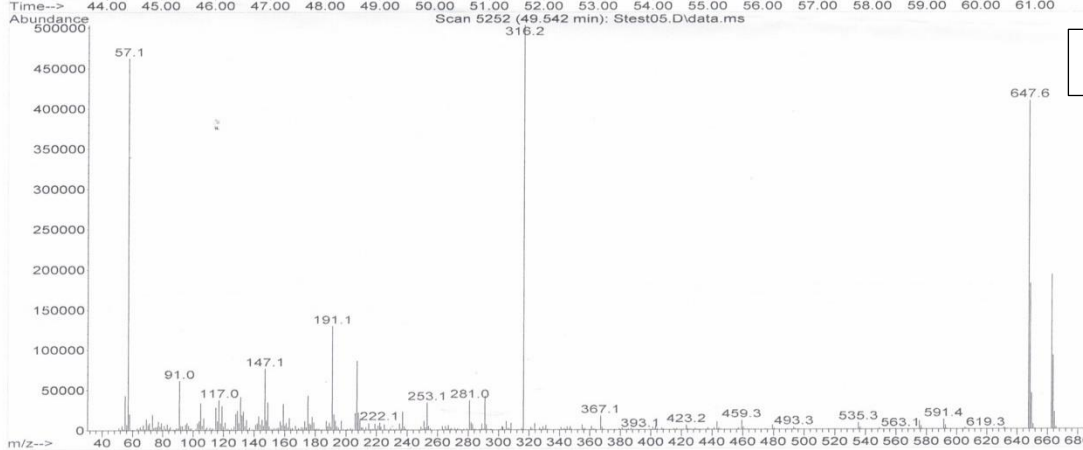
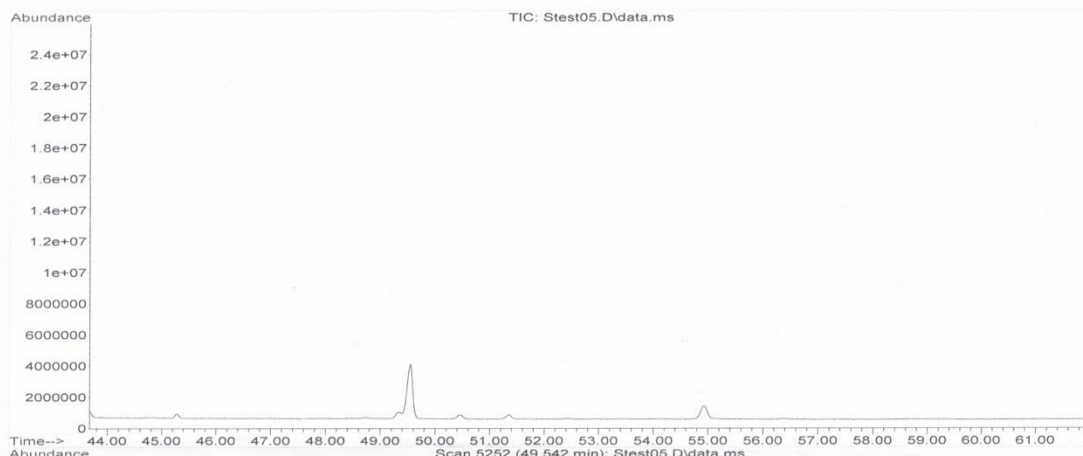
Appendix 2 Spectroscopies and masses of the fluoxetine-chlorambucil conjugate.

File :C:\msdchem\1\sequence\John G\Stest05.D
Operator : JG
Acquired : 26 Apr 2018 13:39 using AcqMethod SUNTESTO_700NM_BAKFLUSH1.M
Instrument : msd
Sample Name: SB8
Misc Info :
Vial Number: 47



(M^+-3 , 647.6 D), (M^+-2 , 648.5 D), (M^+-1 , 649.5 D), ($M^+-3 + \text{CH}_3$, 662.6 D), (M^+-2 , + CH_3 , 663.6 D), (M^+-1 , + CH_3 , 664.6 D).

File : C:\msdchem\1\sequence\John G\Stest05.D
Operator : JG
Acquired : 26 Apr 2018 13:39 using AcqMethod SUNTEST0_700NM_BAKFLUSH1.M
Instrument : msd
Sample Name: SB8
Misc Info :
Vial Number: 47

A1**B1**

A1: Total ion counting (TIC) peaks at elution time 49.5 min. B1: The peak with 316 D is impurity (excess of chlorambucil).